



Université Catholique de Louvain

Faculté des Sciences

Département de Physique

Bound State Description in Quantum Electrodynamics and Chromodynamics

Binding Energy Effects on Annihilation Rates and Spectra

Christopher Smith

Dissertation présentée en vue
de l'obtention du grade de
Docteur en Sciences
(Groupe des Sciences Physiques)

Louvain-la-Neuve

Mai 2002

Remerciements

Je voudrais tout d'abord remercier mon promoteur, Jean Pestieau, pour toutes ces années de soutiens et de collaborations efficaces, ainsi que pour les innombrables discussions sur la physique des particules en général. C'est bien sûr sous son impulsion que cette thèse a vu le jour, et, tout au long du travail, son soutien fut très important pour faire face aux nombreuses difficultés tant techniques que conceptuelles, et pour persévérer malgré les vicissitudes de la communication scientifique.

Je remercie également les professeurs Jean-Marc Gérard et Jacques Weyers pour leur aide dans ce long apprentissage de la théorie des champs. Les différents aspects de cette théorie qu'ils m'ont fait découvrir durant mes premières années de thèse furent essentiels à l'aboutissement de ce travail.

Merci à tous les lecteurs de cette thèse, qui ont accepté de faire partie du Jury, les professeurs J.-P. Antoine, R. Gastmans, J. Govaerts et L. Sehgale.

Finalement, je remercie bien entendu toute ma famille et tous les amis, et en particulier Stéphanie Trine pour son soutien patient, pour son aide aux premiers stades de ce travail, et sa lecture critique du présent manuscrit.

Contents

Introduction	v
1 Overview of Positronium Physics	1
1.1 History	1
1.1.1 Theoretical Expectations (1934-1952)	1
1.1.2 Discovery and First Measurements (1951)	5
1.2 Current Situation (2002)	6
1.2.1 Experimental Achievements	6
1.2.2 Theoretical Achievements	8
1.3 Theoretical Description of Positronium Decay	10
1.3.1 Pirenne-Wheeler Formula	11
1.3.2 Convolution Formula	12
1.3.3 Bethe-Salpeter Loop	14
2 A New Basis for QED Bound States	17
2.1 Critical Analysis of Standard Approach Decay Formula	17
2.1.1 Problematic Properties of the Convolution Formula	18
2.1.2 Dispersion Analysis of the BS Loop	20
2.2 Lowest Order Decay Amplitudes	22
2.2.1 A Simple Formula	23
2.2.2 First Example: Parapositronium to Two Photons	24
2.2.3 Second Example: Paradimuonium and Low's Theorem	26

ii Contents

2.2.4	Conclusion	29
2.3	Orthopositronium Decay	30
2.3.1	Ore-Powell Spectrum	30
2.3.2	Point-like Amplitude	32
2.3.3	Coulomb Form factor and Ore-Powell Spectrum	33
2.3.4	A Simple Ansatz	36
2.3.5	A Scalar and Pseudoscalar Resonance Model	39
2.4	Application to Other Processes	41
2.4.1	Orthodimuonium and Photon Vacuum Polarization	42
2.4.2	Pion Decay to Orthopositronium and Radial Excitations	46
2.4.3	Hyperfine Splitting and Mass Renormalization	47
2.4.4	Possible Extensions	49
2.4.5	Higher Orders	50
2.5	Conclusion	53
3	Overview of Quarkonium Theory	55
3.1	Quarkonium Physics Observables	55
3.1.1	Heavy Quarkonium Spectroscopy	55
3.1.2	Heavy Quarkonium Decay	58
3.1.3	Other Quarkonium Physics Observables	61
3.2	Quarkonium Annihilation Rates	62
3.2.1	Decay Rate Formula and Selection Rules	62
3.2.2	Pseudoscalar Quarkonium Decay	65
3.2.3	Vector Quarkonium Decays	69
3.3	Analysis of Inclusive Charmonium Decay	70
3.3.1	Pseudoscalar Charmonium Decay	70

3.3.2	Vector Charmonium Decay	71
3.3.3	Ratios of Wavefunctions	74
3.3.4	Conclusion: Fit to the Charmonium Data	75
3.3.5	Vector Bottomonium Decay	76
4	Binding Energy Effects on Quarkonium Annihilation Rates	79
4.1	Binding Energy Effects on Quarkonium Physics	80
4.1.1	QCD Quarkonium Wavefunctions	80
4.1.2	Strong Coupling Extraction	81
4.1.3	Rho-pi Puzzle	83
4.1.4	Photon Spectrum in Quarkonium Inclusive Radiative Decays	85
4.1.5	Transitions among Quarkonium States	87
4.2	Conclusion	88
	Conclusions and Perspectives	89
A	Resources for QED Bound states	95
A.1	Parapositronium	95
A.1.1	Details of the Dispersion Study	95
A.1.2	Sommerfeld Factor and Form Factors	97
A.1.3	Radiative Corrections to Parapositronium Decay	100
A.1.4	Dispersion Relations and Kaon Decay	108
A.2	Orthopositronium	113
A.2.1	Phase-space Structure	113
A.2.2	Euler-Heisenberg Lagrangian	116
A.2.3	The Photon Two-point Function	118
A.2.4	The Photon Four-point Function	120

A.2.5	The Ansatz.....	123
B	Resources for QCD Bound States.....	125
B.1	Running of the Strong Coupling Constant.....	125
B.1.1	One-Loop Running.....	125
B.1.2	Running Beyond One-Loop.....	128
B.2	Standard Annihilation Rate Computations.....	130
B.2.1	Pseudoscalar Quarkonium Decays.....	130
B.2.2	Vector Quarkonium Decays.....	133
C	Useful formulae.....	137
C.1	Wavefunction for Hydrogen-like Atoms.....	137
C.1.1	Momentum Space Wavefunctions.....	138
C.2	Loop Integrals, Gamma Functions and Related.....	139
C.2.1	Dirac Matrix Algebra.....	139
C.2.2	Feynman Parameters.....	139
C.2.3	Complex logarithms.....	139
C.2.4	D-Dimensional Integrals.....	140
C.2.5	Digamma, Polylogarithms and Riemann Functions.....	141
C.2.6	Hypergeometric Functions.....	143
C.3	Cross Section, Phase Space.....	145
C.3.1	Two-Body Phase Space.....	145
C.3.2	Three-Body Phase Space.....	146
C.3.3	Recursive Calculation of Phase-Space.....	146
	Bibliography.....	147

Introduction

Positronium is the bound state made of an electron with a positron, in a sea of virtual particles (photons and electron-positron pairs). The electromagnetic interaction is responsible for the binding; hence positronium shares many properties with the hydrogen atom. An important difference, however, is the possibility of annihilation of the electron when it meets the positron, giving gamma rays. Positronium is a short-lived system. Another specificity is the absence of strong interaction effects: the proton in the hydrogen atom is not an elementary particle, but is a complicated aggregate of quarks, antiquarks and gluons. Positronium is purely electromagnetic; QED is sufficient, in principle, to predict all its properties to a very high accuracy. Both the weak and strong interactions are present, but through highly suppressed corrections, and do not enter at the present level of experimental or theoretical precision.

There are two motivations for studying the positronium system: because it is a standard test for QED, and because it is a first approach to the more complicated problem of the quark structure of hadrons, and confinement in QCD.

QED Standard Tests

The Standard tests for QED, or alternatively the domains in which QED has been very successfully applied, are of two types: elementary particle processes and low-energy bound state properties. For elementary particles, one can distinguish:

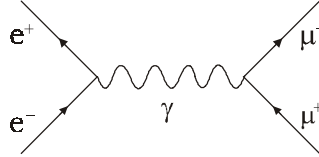
- 1- High energy processes, like $e^+e^- \rightarrow \gamma\gamma$, $e^+e^- \rightarrow l^+l^-$ with l any lepton (e, μ, τ). Such processes typically test QED at several GeV , at facilities like *LEP*, *SLC*, ... which proceed by colliding positron with electron beams. At such an energy scale, QED must be supplemented by strong and weak interaction effects. No disagreement has been reported.
- 2- The electron and muon anomalous moments a_e and a_μ . By this is understood the deviation of the magnetic moment g from its value of 2 as predicted by the Dirac theory. The current achievements, both theoretically and experimentally are impressive. On the theoretical side, the computation of thousands of multi-loop diagrams has been done. The agreement between theory and experiment is a great success of QED. However, beyond the present level of precision, the anomalous moments can no longer be used as pure tests for QED because strong interaction effects will dominate.

Our main concern will be bound state-type QED tests. Again, we distinguish two types:

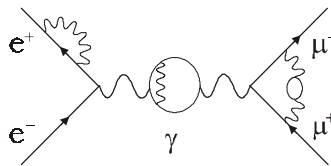
- 3- Spectroscopic properties of atom-like systems. The various spacings between the energy levels of hydrogen have been both theoretically and experimentally very well studied. The most famous historically is the Lamb shift: the spacing $2S_{1/2} - 2P_{1/2}$ of the hydrogen levels. The fine and hyperfine structure of the hydrogen, helium and muonium (the hydrogen atom with a muon in place of the proton) also provide very accurate tests.
- 4- Positronium spectroscopy and lifetime.

For a more detailed presentation of all those tests, we refer to [16]. The distinction made between elementary particle and bound state tests is profound. One of the most natural frameworks of quantum field theory is perturbation theory: the Feynman graphs with their associated rules. For example, to describe the process

$e^+e^- \rightarrow \mu^+\mu^-$, one starts with a simple lowest order approximation

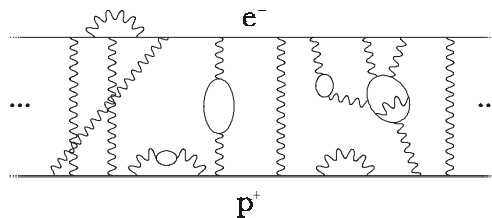


to which corrections are then calculated, like for example



The theoretical computation is then ordered as a series in the fine-structure constant $\alpha \approx 1/137$: each coupling between a photon and a charged particle line brings in a factor of $e = \sqrt{4\pi\alpha}$, with e the electric charge. Because the constant α is much smaller than one, the whole computation method is under control. The only difficulty is the various divergences occurring in some graphs. Renormalizability of QED ensures that a meaningful answer can be obtained. Also, infrared divergences have been shown to exponentiate. At the end of the day, the agreement between theory and experiment is a very stringent test of QED in its perturbative regime, and of the associated theoretical tools.

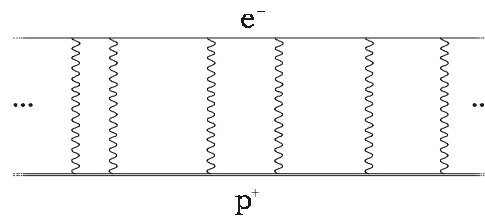
On the other hand, a bound state is intrinsically non-perturbative. It is the permanent exchange of photons between the constituents that binds them together



The ordering of processes in increasing orders of α collapses. Perturbative quantum field theory is rather devoid in front of such problems. Many standard theoretical methods explicitly assume the non-existence of bound states.

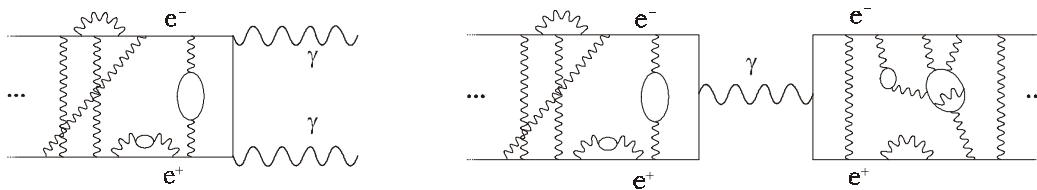
Fortunately, there is a way out. The idea is to change the basis on which perturbation theory is built, i.e. the lowest order, and to consider alternative expansion parameters. For all spectroscopic observables, a natural small parameter is the ratio of the binding energy over the masses of the constituents. For the hydrogen atom, it is $E_B/m_{e^-} \approx 13.6 \text{ eV}/511 \text{ keV} \approx 3 \times 10^{-5}$. In other words, the natural energy scale of any process inside the hydrogen atom is at the atomic level, a few eV . Equivalently, for such loosely bound systems, the constituent velocities are small, $v/c \ll 1$, which is the expansion parameter used in practice. Since the system is essentially non-relativistic, to first order in the new expansion parameter, one recovers the non-relativistic Schrödinger equation with a Coulomb potential. That simpler problem can be solved exactly (i.e., non-perturbatively), and will serve as a new basis for a perturbation theory. Graphically, the lowest order is the so-called ladder approx-

imation (technically, crossed ladders are neglected, and only Coulomb photon exchanges are considered in the non-relativistic limit)



Both radiative and relativistic corrections to this first approximation are then computed, in increasing order of the small parameters (α and v/c say). These are the very successful techniques used for the spectroscopic tests.¹

Positronium is also a bound state, and the same techniques have been used. The small binding energy and v/c are the expansion parameters: the system is treated non-relativistically to lowest order, and radiative and relativistic corrections are then computed perturbatively. All this would be fine, except for one point. The positronium annihilates into photons. That process is intrinsically relativistic. The Schrödinger equation cannot describe the disappearance of positronium into photons. Further, the atomic energy scale of a few eV is no longer natural, because of processes like



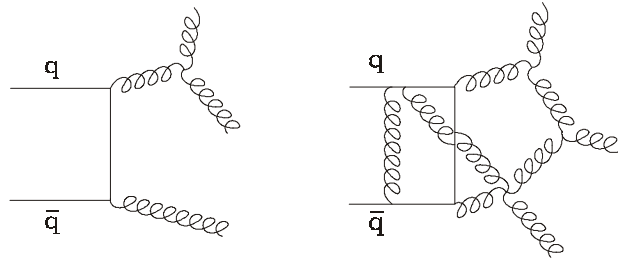
where the photons carry energies of the order of the electron mass. The photons can serve as probes, giving information on the internal structure of the bound state. When they are hard, they essentially see a slowly moving electron-positron pair, while when they are soft, they are sensitive to the non-perturbative binding of the pair. In this respect, positronium is a unique system. It requires a full understanding of bound states in the relativistic quantum field theory framework. Most theoretical approaches rely on the same type of approximations (mainly a factorization of the bound state wavefunction and the annihilation mechanism). The subject of the present thesis is to test the theoretical consistency of those models.

QCD and Confinement

Quarks are subject to the strong interaction. There are three types of strong charges, called colors. Quantum chromodynamics is the theory describing the interactions between quarks, antiquark and gluons. This theory is similar to QED, except that gluons do carry a strong charge and therefore can interact among themselves. Technically, QCD is a gauge theory with the non-abelian $SU(3)$ as gauge group. The eight gluons belong to the adjoint representation, while the three colored quarks belong to the fundamental representation.

¹ For the hydrogen atom physics, yet another small expansion parameter has proven to be useful: $m_{e^-}/m_{p^+} \approx 1/2000$. This parameter is important in the treatment of the proton recoil effects.

In principle, the consequences of the gluon charge lead to a small increase of complexity: compared to QED, one only has to consider new diagrams like



Unfortunately, the main characteristic of the strong interaction is, evidently, of being strong. In other words, the coupling constant of QCD is much greater than one at ordinary energies, and perturbation theory breaks down: the two diagrams shown above cannot be ordered in decreasing magnitude.

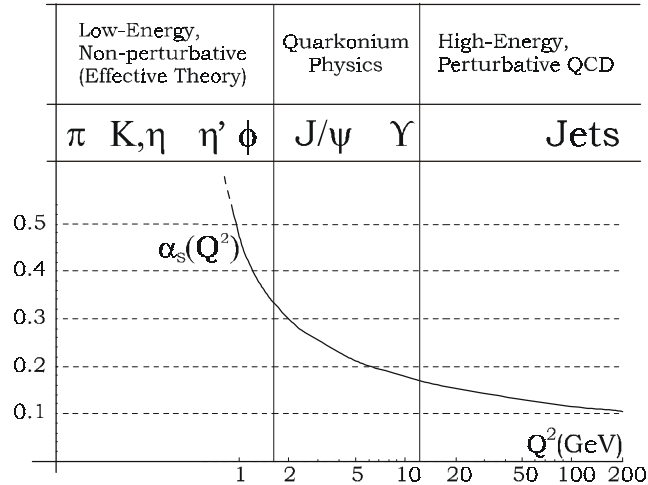
This picture of the strong interaction is supported by two main facts:

- 1- There is another consequence of the gluon charge. As the energy increases, the strong charge decreases. At sufficiently high energy, above a few GeV, QCD is perturbative, and can be directly tested. Various processes at high energy are consistently described within the context of QCD, and this is a great success. The measured coupling constant, when extrapolated to low-energy, is indeed greater than unity.
- 2- Quarks and gluons have never been observed as free particles. Instead, one always sees aggregates of quarks and gluons, the baryons (like protons, pions,...). This phenomenon is called confinement. This is understood as follows. If the interaction is very strong, a colorful particle cannot exist freely, its stable state will always be inside a colorless aggregate. For a group like $SU(3)$, the most trivial aggregates are the quark-antiquark and the three-quark bound states. This nicely fits the observed spectrum of particles.

It should be emphasized that no rigorous proof that the stable states of QCD are indeed the observed hadrons exists. Nobody has ever been able to compute the mass of the pion or the proton in terms of the quark masses and QCD coupling constant. Further, low-energy reactions (below 1GeV) among hadrons are not quantitatively described in terms of the underlying quark processes. This is a serious limitation. By comparison, the most stringent tests on QED do involve low-energy bound states. For QCD, quantitative tests are only possible at high energy. The most promising tests of QCD at low energy seem to be lattice calculations, but they are still very far from the precision achieved in QED.

The study of bound states in Quantum Field Theory is already a very difficult non-perturbative problem. Confinement adds to this complexity, and most methods used in QED are just no longer applicable. There is one exception: heavy quarkonia. Such states are made of a heavy quark c or b with its corresponding antiquark. Being very heavy (of a few GeV), one can hope that a first order non-relativistic approximation is reliable. Of course, the quarkonium wavefunctions are not known, since non-relativistically, QCD cannot just be a Coulomb-like interaction (such a potential does not lead to confinement). By studying quarkonium states, one gets information

on the QCD potential. Quarkonium is therefore a crucial intermediate step to understand low-energy QCD.



The physics of quarkonium is very similar to that of positronium. The spectroscopy is analogous, while quarkonium decays through the annihilation of its constituents, like positronium. The techniques used for quarkonium are inspired from the positronium ones. In particular, the same factorization hypothesis is used in both problems to disentangle the perturbative and non-perturbative parts of the dynamics. The applicability of the positronium models to quarkonium will be analyzed in the present thesis.

Brief Outline of the Thesis

The goal is to address the relevance and consistency of the positronium models. We will show that a basic requirement of Quantum Field Theory is violated in the current computations of positronium decay rates. The probability amplitudes for positronium decay are not analytical. This is rather technical, but far reaching; a modification of the model is unavoidable. In fact, we will see that the perturbation method designed for spectroscopic studies cannot be used for decay processes. The binding energy expansion is in contradiction with quantum field theory analyticity requirements. A natural solution is then to construct a new basis for an alternative perturbation theory. This has to be done non-perturbatively in the binding energy. There is an additional motivation for this. In quarkonium physics, typical binding energies are much greater. Being able to treat them exactly will unavoidably lead to interesting advances.

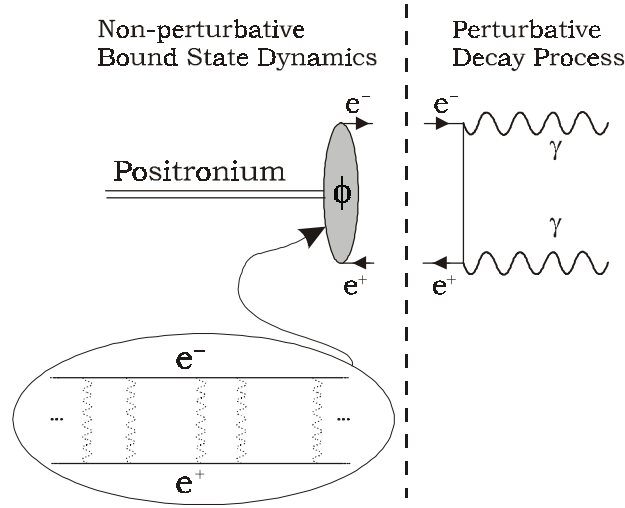
The thesis is organized in four chapters, with the structure

Chapter 1	Positronium	General Introduction and Standard Approaches
Chapter 2		Original Contributions
Chapter 3	Quarkonium	General Introduction and Standard Approaches
Chapter 4		Original Contributions

The original discussions in chapter 2 and 4 have been made as self-contained as possible. Chapter 1 and 3 serve to set the stage, and introduce the standard material needed for our presentation.

Chapter 1 begins with a brief historical overview of positronium physics. Then, the present status of both experiment and theory is shortly reviewed. The final section describes the evolution of the theoretical models designed to describe the annihilation of positronium. By models is meant a scheme of computation: the definition of a lowest order approximation, exactly calculable, and of the perturbation theory. All those models introduce

some kind of factorization of the bound state dynamics from the decay process



For instance, the simplest of all formulas is

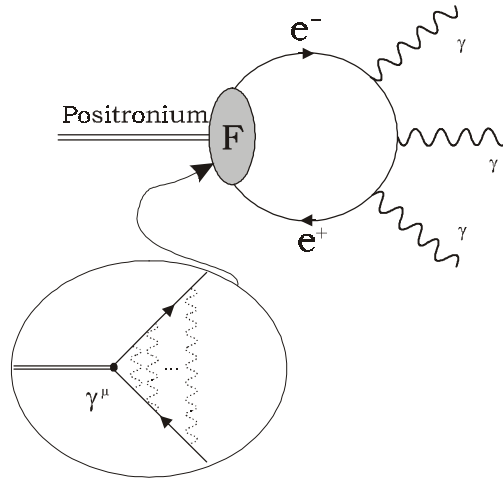
$$\Gamma(Ps \rightarrow n\gamma) = \frac{1}{2J+1} |\phi(0)|^2 (4v_{rel}\sigma(e^-e^+ \rightarrow n\gamma))_{v_{rel} \rightarrow 0} \quad (1)$$

with ϕ the Schrödinger wavefunction encoding the non-perturbative bound state dynamics, and $\sigma(e^-e^+ \rightarrow n\gamma)$ is the scattering cross section representing the perturbative decay process. More advanced techniques will be described, and their factorization hypothesis emphasized.

Chapter 2 begins with a clarification of the physics of the approximation done in defining the lowest order amplitude in standard approaches. In doing so, it will be seen immediately that this basis is in contradiction with analyticity. By factorizing the process as pictured above, the photons are always emitted from charged particles. If the photon is very soft, however, it should behave as emitted from a neutral boson (i.e. the positronium) instead. It cannot discern the charged content of the bound state if its wavelength is much larger than the typical e^+e^- separation. The binding of the electron and positron into a neutral boson becomes very important for a soft photon, or in other words, when the energy of the photon is of the order of the binding energy.

The goal is therefore to construct amplitudes so that the photons are always aware of the binding of the charged particles. We propose such an alternative construction for the lowest order amplitude, with no factoriza-

tion. Graphically, it is



The decay amplitudes are constructed as closed loops. The bound state dynamics is introduced via a form factor which is related to the Schrödinger wavefunction, hence contains the effects of Coulomb photon exchanges. Technically, by closing the loop (i.e. without factorization), the resummation of the Coulomb photon is no longer independent of the decay process. As a result, the final state photons do "feel" the binding, and behave as if emitted from a true neutral bound state.

For this construction to be a well-defined lowest order amplitude, it has to be calculable. To this end, we found a very simple procedure, in which our new lowest order amplitudes are obtained from standard QED ones. We then show that indeed, our approach correctly describes soft photons. Many other interesting, but more technical, properties of our approach will also be discussed.

The chapter ends with a systematic study of various decay processes. The implication for spectroscopic studies is also sketched. Finally, some possible extensions are reviewed.

Chapter 3 is a very short introduction to the physics of the $c\bar{c}$ (charmonium) and the $b\bar{b}$ (bottomonium) heavy quark bound states. It begins with the spectroscopy of charmonium and bottomonium as established experimentally. Then, the description of decay processes is presented. Most studies rely on the extension of the positronium decay formula (1) to the quarkonium case. The predictions for the decay rates of 1S_0 and 3S_1 quarkonium states are systematically studied. Comparison with experimental branchings, along with the extraction of α_S , closes the chapter.

The last chapter presents the many problems and puzzles of quarkonium physics. It is shown that binding energy effects can explain most of them. A definite quantitative study has not been performed though, because of the lack of information on the QCD potential. However, the results obtained are qualitatively independent of the detailed form of it.

Three appendices supplement the text with calculation details, proofs and numerical studies. The first appendix contains additional information and detailed studies relevant for the chapter 2, while the second appendix is related to chapter 3 and 4. The final appendix contains useful formulas like special functions, dimensional regularization formulas, phase-space analysis,...

Finally, the thesis ends with a bibliography. The references are ordered in sections (with no direct relation to the sections of the text), and in each section, in chronological order. This bibliography is intended to be more or less complete for positronium (but some omissions are unavoidable). For quarkonium, a complete reference list would be too long, and only the papers directly related to our studies are quoted.

Chapter 1

Overview of Positronium Physics

This chapter presents the basic observables of positronium physics. This chapter sets the stage for more elaborated studies. For this presentation, we have chosen a more or less historical flow.

The first section begins with the exposition of the theoretical status at the end of the forties, just before the experimental evidence. Then, the first confrontation of QED theory in positronium physics is presented. In the second section, the most recent theoretical and experimental results are given and compared for both spectroscopic and lifetime observables.

In the final section, the evolution of the theoretical description of positronium decay is reviewed. The hypotheses done are described. Their relevance will be discussed in the next chapter.

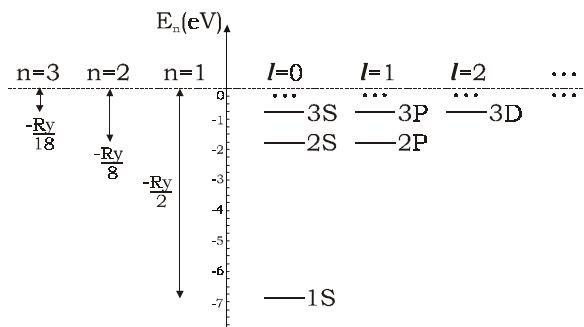
1.1 History

Historically, it was first postulated in 1934 by Mohorovicic [59] that an electron and its associated antimatter particle could form a quasi-stable atom, one year after the experimental discovery of the positron by Anderson. That state was first called positronium by Ruark in 1945 [33], who was unsuccessfully trying to observe it.

The properties of positronium, both spectroscopic and lifetime, were studied theoretically for about 20 years. The first experimental observation finally came in 1951, in agreement with the expectations.

1.1.1 Theoretical Expectations (1934-1952)

The first approach to the positronium bound state is non-relativistic. The quantum mechanical treatment of it is exactly the same as that of the hydrogen atom, except for a change of reduced mass. For instance, the energy levels



and corresponding wavefunctions can be specified by the same set of quantum numbers n, l, m_l , with $l = 0, \dots, n - 1$ and $m_l = -l, \dots, l$. The energy levels exhibit the well-known degeneracy in l and m_l :

$$E_{n,l,m_l} = -\frac{\mu\alpha^2}{2n^2}$$

where $\mu = m/2$, m the electron mass. The ground state energy is therefore $E_{0,0,0} = -m\alpha^2/4 \equiv -Ry/2 \approx -6.8$ eV (half that of the hydrogen).

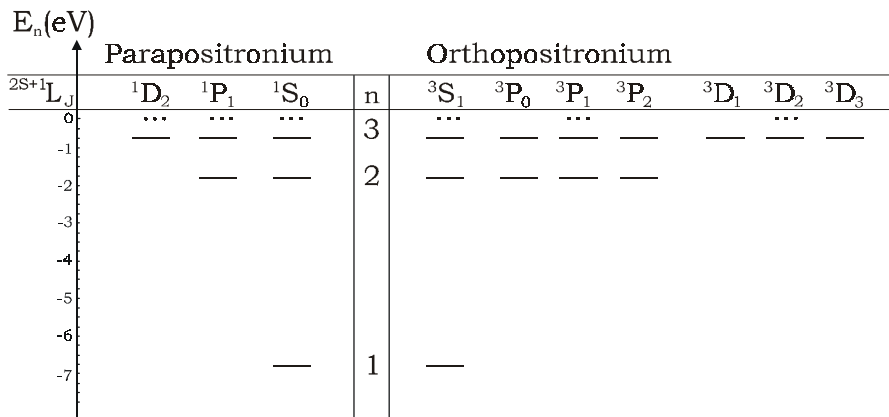
To the above quantum numbers, one has to add that of the spin. Two particles of spin $1/2$ can give a total spin angular momentum of 0 or 1. The spin four-fold degeneracy of each of the levels drawn on the figure is split into a singlet spin 0 state (parapositronium, p - Ps) and a triplet spin 1 state (orthopositronium, o - Ps)²

$$\begin{aligned} \text{Singlet} & \quad \frac{1}{\sqrt{2}} (|\uparrow\downarrow\rangle - |\downarrow\uparrow\rangle) \\ \text{Triplet} & \quad |\uparrow\uparrow\rangle, \frac{1}{\sqrt{2}} (|\uparrow\downarrow\rangle + |\downarrow\uparrow\rangle), |\downarrow\downarrow\rangle \end{aligned}$$

The spin then combines with the orbital angular momentum to give the final total angular momentum. For example, using the spectroscopic notation $n^{2S+1}L_J$ with $L = S, P, D, F, \dots$, the twelve $2P$ states arrange as

$$2P \text{ (12 states)} \rightarrow \begin{cases} \text{Parapositronium} & 2^1P_1 & 3 \text{ states} \\ \text{Orthopositronium} & 2^3P_0 & 1 \text{ state} \\ & 2^3P_1 & 3 \text{ states} \\ & 2^3P_2 & 5 \text{ states} \end{cases}$$

Graphically,



Fine and Hyperfine Structure

At the lowest order, there is a high degeneracy. This does not survive at higher orders. Pirenne (1947) [61] and Berestetski (1949) [62] were the first to compute the fine and hyperfine structure of the positronium energy levels. Their results were later corrected by Ferrell (1951) ([64], see also [26]), who found

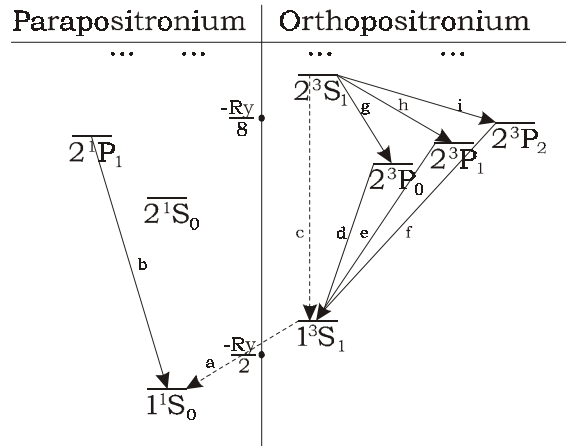
$$E_{n,l,(j)} = -\frac{m\alpha^2}{4n^2} + \Delta E_{n,l,(j)}^{(s(t))} \quad \text{with} \quad \Delta E_{n,l,(j)}^{(s(t))} = \left(\frac{11}{64n^4} + \frac{\varepsilon_{l,(j)}^{(s(t))}}{n^3} \right) m\alpha^4$$

² For the hydrogen atom, this classification is not relevant because of the very small proton magnetic moment $\mu_n = \frac{q\hbar}{2M_p} \ll \mu_e = \frac{e\hbar}{2m_e}$. For positronium, the magnetic moment is the same (in magnitude) for both constituents.

where

$$\varepsilon_l^{(s)} = -\frac{1}{2} \frac{1}{2l+1} \quad \varepsilon_{l,j}^{(t)} = \varepsilon_l^{(s)} + \frac{7}{12} \delta_{0l} + \frac{(1-\delta_{0l})}{8(l+1/2)} \times \begin{cases} \frac{3l+4}{(l+1)(2l+3)}, j = l+1 \\ -\frac{1}{l(l+1)}, j = l \\ -\frac{3l-1}{l(2l-1)}, j = l-1 \end{cases} \quad (1.1)$$

Hence, we can modify our spectral representation



with the transition frequencies (in GHz),

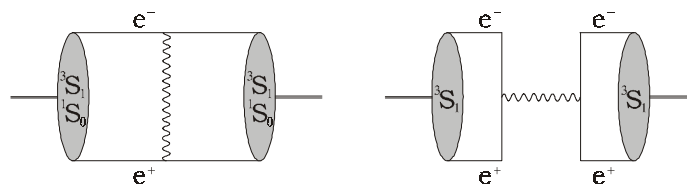
a	204.387	Hyperfine Splitting
b(≈ c, d, e, f)	1.234 × 10 ⁶	Lyman α
g	18.2	
h	12.8	
i	8.39	Lamb Shift

We have also indicated the commonly used names for the most remarkable transitions. Physically, one has the following selection rule for the dominant radiative transitions:

$$E1 \begin{cases} \Delta L = \pm 1 \\ \Delta J = \pm 1, 0 \\ \Delta m_J = \pm 1, 0 \end{cases} \gg M1 \begin{cases} \Delta L = 0 \\ \Delta J = \pm 1, 0 \\ \Delta m_J = \pm 1, 0 \end{cases}$$

where E1 are the electric dipole (or allowed) transitions (plain lines on the picture), by far the strongest transitions. The forbidden transitions are the M1 magnetic dipole transitions (dashed lines).

The most interesting splitting is the $1^1S_0 - 1^3S_1$ hyperfine splitting of positronium, because it is the most accessible both theoretically (1S states are relatively simple to treat) and experimentally (the higher excited states are predicted to cascade decay into lower states quite rapidly). In (1.1), the 3S_1 state, $l = 0$, appears separately because of the so-called annihilation graph. The hyperfine splitting is computed from the expectation values of the spin-spin and annihilation potentials between 3S_1 and 1S_0 states



(the other hyperfine operators contribute equally to both S states, and are included in the exchange graph above). The corresponding contributions to the splitting are [26]

	Para	Ortho
Fine Struct. (Spin-Spin)	$-21/64 m\alpha^4$	$1/192 m\alpha^4$
Annihilation	0	$1/4 m\alpha^4$
Hyperfine Splitting	$\frac{7}{12}m\alpha^4$	

(1.2)

Karplus and Klein (1952) [67], through their now standard computation, obtained the first radiative correction to the hyperfine splitting:

$$\Delta\nu_{hf} = m\alpha^4 \left(\frac{7}{12} - \frac{\alpha}{\pi} \left(\frac{8}{9} + \frac{\ln 2}{2} \right) \right) \approx 203.381 \text{ GHz}$$

Many additional graphs contribute to that order, and we shall not detail their techniques here.

Annihilation Rates

The positronium is a short-lived system. It decays into photons. The number of which can be deduced from selection rules (Yang, 1950 [202] and Wolfenstein and Ravenhall, 1952 [66], see also [9]).

A positronium state is an eigenstate of the parity P , charge conjugation C and of the combination CP^3 . The eigenvalues of those operators can be obtained in terms of those of L, S as

$$\begin{aligned} P &= (-1)^{l+1} \\ C &= (-1)^{l+s} \\ CP &= (-1)^{s+1} \end{aligned}$$

These expressions are obtained from the intrinsic parities of the constituents and the antisymmetry requirement on the exchange of the constituents. Parapositronium (orthopositronium) is a CP eigenstate with eigenvalue $-1 (+1)$. Since a system of n photons has a charge conjugation eigenvalue of

$$C(n\gamma) = (-1)^n$$

we obtain the selection rule

$$(-1)^{l+s} = (-1)^n$$

We therefore write, up to $J = 2$ (the principal quantum number can take any value)

$2S+1L_J$	J^{PC}	Number of γ	Dominant Annihilation mode
1S_0	0^{-+}	even	$Ps(^1S_0) \rightarrow \gamma\gamma$
3S_1	1^{--}	odd	$Ps(^3S_1) \rightarrow \gamma\gamma\gamma$
1P_1	1^{+-}	odd	$Ps(^1P_1) \rightarrow \gamma\gamma\gamma$
3P_0	0^{++}	even	$Ps(^3P_0) \rightarrow \gamma\gamma$
3P_1	1^{++}	even	$Ps(^3P_1) \rightarrow \gamma\gamma\gamma\gamma$
3P_2	2^{++}	even	$Ps(^3P_2) \rightarrow \gamma\gamma$
1D_2	2^{-+}	even	$Ps(^3D_1) \rightarrow \gamma\gamma$
3D_1	1^{--}	odd	$Ps(^3D_1) \rightarrow \gamma\gamma\gamma$
3D_2	2^{--}	odd	$Ps(^3D_2) \rightarrow \gamma\gamma\gamma$

³ This property, due to the special nature of positronium as a bound state made of an electron with a positron, has raised some interest in positronium as a test of the discrete symmetries.

The only mode that needs comment is $P_s (^3P_1) \rightarrow \gamma\gamma\gamma$. The two-photon mode is forbidden by the (Landau-Pomeranchuk-)Yang theorem (1950) [202]: a vector particle ($J = 1$) cannot decay into two photons, because of gauge invariance and special relativity. Most positronium state annihilation modes will be suppressed compared to their electric dipole transitions to lower states. Only the ground states 1S_0 and 3S_1 are dominantly decaying into photons, because the magnetic dipole transition $^3S_1 \rightarrow ^1S_0$ is highly suppressed.

In 1946, Pirenne [61] and Wheeler [60] separately developed a theoretical model to compute the decay rates of positronium. Their model is

$$\Gamma(P_s \rightarrow n\gamma) = \frac{1}{2J+1} |\phi(0)|^2 (4v_{rel}\sigma(e^-e^+ \rightarrow n\gamma))_{v_{rel} \rightarrow 0}$$

with v_{rel} the relative velocity of the e^+e^- pair in their center-of-mass frame, and $\phi(0)$ the positronium Schrödinger wavefunction, in configuration space, at zero separation. One can understand this model as a replacement of the scattering cross section initial flux factor by the probability of contact in the bound state. Obviously, this model applies to S -state annihilations only, since $\phi(0)$ is zero for $l \neq 0$.

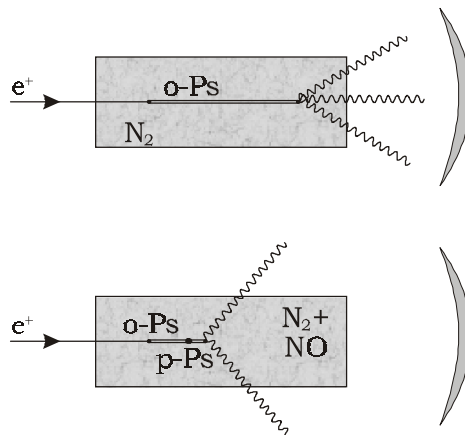
Pirenne and Wheeler were able to apply their formula to parapositronium (1S_0), while, in 1949, Ore and Powell [63] used the same model to compute the orthopositronium (3S_1) decay rate. The results were

$$\begin{aligned} \Gamma(p\text{-}Ps \rightarrow \gamma\gamma) &= \frac{\alpha^5 m}{2} \approx 8.0325 \times 10^9 \text{ sec}^{-1} \\ \Gamma(o\text{-}Ps \rightarrow \gamma\gamma\gamma) &= \alpha^6 m \frac{2(\pi^2 - 9)}{9\pi} \approx 7.2112 \mu\text{sec}^{-1} \end{aligned}$$

The orthopositronium lifetime is roughly 1000 times longer than the parapositronium one. At first sight, one would have expected a relative factor of $1/\alpha \approx 137$. Phase-space is responsible for an additional factor of 10.

1.1.2 Discovery and First Measurements (1951)

The discovery came in 1951. Martin Deutsch found evidence of orthopositronium formation in gases [34]. His technique is based on (1) the very different lifetime between both positronium species, and (2) the paramagnetic properties of the NO gas. This molecule has an isolated electron, hence is a catalyst for $o\text{-}Ps + NO \rightarrow p\text{-}Ps + NO$ by electron exchange. When positrons are slowed in a gas, both orthopositronium and parapositronium are produced. The lifetime of the parapositronium is too short for its decay photons to be observed. Adjunction of a small amount NO gas therefore changes the observed gamma ray spectrum. This is an evidence for orthopositronium formation.



By varying the gas pressures, the lifetime of orthopositronium at zero pressure can be extrapolated. The result was

$$\Gamma^{\text{exp}}(o\text{-}Ps) = (6.8 \pm 0.7) \mu\text{sec}^{-1}$$

This agrees with the result of Ore-Powell⁴.

The hyperfine splitting was measured in 1952, still by M. Deutsch and his colleagues [34]. By using magnetic fields (Zeeman effects) and radio frequencies (rf quenching techniques), they found

$$\Delta\nu_{hf}^{\text{exp}} = (203.2 \pm 0.3) \text{ GHz}$$

In good agreement with the theoretical expectation. Note that the precision is sufficient to test the presence of the annihilation potential contribution to the hyperfine splitting.

The first measurement of the parapositronium lifetime was performed in 1967 by Hughes [36], with the result

$$\Gamma^{\text{exp}}(p\text{-}Ps) = (7.99 \pm 1.00) \times 10^9 \text{ sec}^{-1}$$

in agreement with the Pirenne-Wheeler result.

Later, many transitions were observed, in good agreement with the theory. For example, in 1975 [40], the Lamb shift was measured at

$$\begin{aligned} \Delta\nu_{Lamb}^{\text{exp}} &= (8.628 \pm 0.006) \text{ GHz} \\ \Delta\nu_{Lamb}^{\text{th}} &= 8.625 \text{ GHz} \end{aligned}$$

where the first order radiative corrections account for 231 MHz to $\Delta\nu_{Lamb}^{\text{th}}$.

The agreement between experiment and theory is excellent. Even if the accuracy is not formidable, in view of the theoretical complexity, and of the many different types of effects already included, this was a great success for QED.

1.2 Current Situation (2002)

A peculiarity of positronium physics is the recurrent occurrence of "puzzles": at different stages, discrepancies occurred between theory and experiment. Ultimately, those disappeared through corrections to the computations, or more careful measurements. The recollection of the historical developments can be found in many places and we do not intend to present it here [85], [87]. Instead, we directly state the most recent achievements, but it should be clear that many groups were involved, especially on the theoretical side, for the computation and recomputation of the many loop diagrams necessary for high order radiative corrections.

1.2.1 Experimental Achievements

The latest experimental results for the decay rate of the parapositronium are

$$\Gamma_{p\text{-}Ps}^{\text{exp}} = \begin{cases} 7.99(11) \times 10^9 \text{ sec}^{-1} & \text{Yale (Gas), 1967 [38]} \\ 7.994(11) \times 10^9 \text{ sec}^{-1} & \text{Ann Arbor (Gas), 1982 [42]} \\ 7.9909(17) \times 10^9 \text{ sec}^{-1} & \text{Ann Arbor (Gas), 1994 [56]} \end{cases} \quad (1.3)$$

⁴ By that time, the Ore-Powell prediction was not the only one on the market. The 10% accuracy of the Deutsch measurement was sufficient to discriminate among the various theoretical computations.

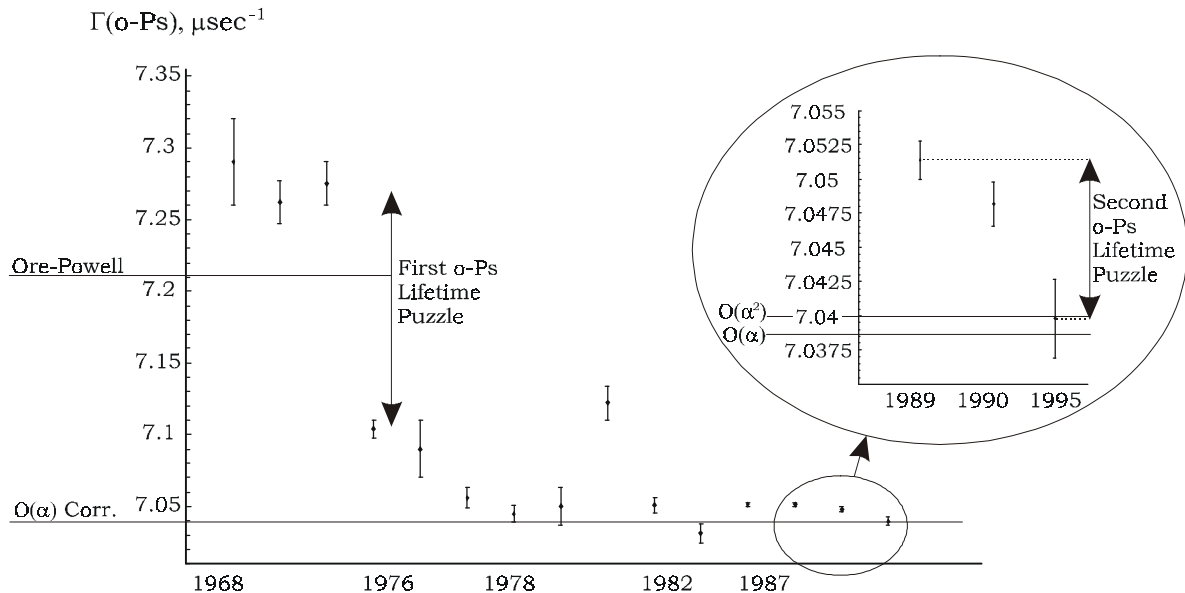
The orthopositronium lifetime is experimentally simpler to measure, being 1000 times larger than the parapositronium one. Results of various groups are

$$\Gamma_{o-Ps}^{\text{exp}} = \begin{cases} 7.0450 (60) \mu\text{sec}^{-1} & \text{London (Gas), 1978 [41]} \\ 7.0310 (70) \mu\text{sec}^{-1} & \text{Mainz (Vacuum), 1987 [46]} \\ 7.0398 (29) \mu\text{sec}^{-1} & \text{Tokyo (SiO}_2 \text{ Powder), 1995 [57]} \\ 7.0514 (14) \mu\text{sec}^{-1} & \text{Ann Arbor (Gas), 1989 [49]} \\ 7.0482 (16) \mu\text{sec}^{-1} & \text{Ann Arbor (Vacuum), 1990 [50]} \end{cases} \quad (1.4)$$

The most recent Ann Arbor and Tokyo results are mutually exclusive. This is known as the orthopositronium lifetime puzzle⁵. Note also that the medium used varies. It is instructive to represent the evolution of the experimental measurements over the last three decades. References to the original experimental works can be found in [101].

Year	$\Gamma_{o-Ps}^{\text{exp}}$	Technique	Year	$\Gamma_{o-Ps}^{\text{exp}}$	Technique
1951	6.8(7)	gas	1978	7.050(13)	vacuum
1968	7.29(3)	gas	1978	7.122(12)	vacuum
1973	7.262(15)	gas	1982	7.051(5)	gas
1973	7.275(15)	gas	1987	7.031(7)	vacuum
1976	7.104(6)	SiO ₂	1987	7.0516(13)	gas
1976	7.09(2)	vacuum	1989	7.0514(14)	gas
1978	7.056(7)	gas	1990	7.0482(16)	vacuum
1978	7.045(6)	gas	1995	7.0398(29)	SiO ₂

Graphically, the decrease in the measured rate is obvious (theoretical predictions are discussed in the next section)



Gas experiments are performed at various pressures, and then the result is extrapolated to vacuum, assuming a linear dependence. In principle, the closer to zero pressure one can get, the more precise is the result. In practice, a compromise has to be found because the efficiency of positronium formation quickly decreases with the pressure. Typically, at 1 atmosphere, as many as 25-50% of the incoming positrons bind into a positronium.

⁵ In fact, it should be called the second orthopositronium lifetime puzzle. In the mid- and late seventies, a similar situation occurred. It was later resolved in favor of the smallest lifetime measurement.

The Tokyo experiment uses SiO_2 powder. For grained materials, the same strategy as for gases could in principle be used; namely the measurement at various densities, and then extrapolation to vacuum. However, there is concern that the extrapolation to zero density may not be linear for powder, because positronium is formed inside the powder grains. Varying the density only accounts for the effects of the atomic collisions once the positronium has escaped the grain. Therefore, different data analysis techniques have to be designed. The Tokyo method does not rely on any sort of zero density extrapolation.

In conclusion, there seem to be arguments for the Tokyo result, while the consistency of both the gas and vacuum measurements of Ann Arbor is in their favor. The situation is unclear and further measurements are necessary.

Concerning hyperfine splitting measurements, the most precise date back to the late seventies- early eighties. It was found, including the other measured transitions,

Name	Splitting	Experiment [GHz]	Reference
$\Delta\nu_{hf}^{exp}$	$1^3S_1 - 1^1S_0$	203.3875 (16) 203.38910 (74)	Brandeis, 1974 [39] Yale, 1984 [43]
$\Delta\nu_{Lyman}^{exp}$	$2^3S_1 - 1^3S_1$	1233607.2189 (107) 1233607.2164 (32)	Stanford, 1989 [48] Stanford&Bell, 1993 [52]
$\Delta\nu_{Lamb0}^{exp}$	$2^3S_1 - 2^3P_0$	18.5041 (100) (17) 18.49965 (120) (400)	Ann Arbor, 1987 [45] Mainz, 1993 [53]
$\Delta\nu_{Lamb1}^{exp}$	$2^3S_1 - 2^3P_1$	13.0013 (39) (9) 13.01242 (67) (154)	Ann Arbor, 1987 [45] Mainz, 1993 [53]
$\Delta\nu_{Lamb}^{exp}$	$2^3S_1 - 2^3P_2$	8.6196 (27) (9) 8.6284 (28)	Ann Arbor, 1987 [45] Brandeis, 1975 [40]
$\Delta\nu_{Lamb3}^{exp}$	$2^3S_1 - 2^1P_1$	8.62438 (54) (140) 11.181 (13) 11.180 (5) (4)	Mainz, 1993 [53] 1993 [54] 1994 [55]

Other experimental results include the study of the Zeeman and Stark effects, tests of discrete symmetries C, P, T and CP, CPT (by setting upper bounds on $1^1S_0 \rightarrow \gamma\gamma$ or $3^1S_1 \rightarrow \gamma\gamma, \gamma\gamma\gamma\gamma$, by the analysis of angular correlations in $3^1S_1 \rightarrow \gamma\gamma, \dots$) [44], [51], search for new light particles (axions, SUSY,...), search for the mirror universe, search for positronium molecules, etc. Those studies lie somewhat out of our main concerns, and will not be discussed here.

1.2.2 Theoretical Achievements

The parapositronium and orthopositronium decay widths are

$$\begin{aligned}\Gamma_{p-Ps}^{th} &= \frac{\alpha^5 m}{2} \left(1 - A_p \frac{\alpha}{\pi} + 2\alpha^2 \ln \frac{1}{\alpha} + B_p \frac{\alpha^2}{\pi^2} - \frac{3\alpha^3}{2\pi} \ln^2 \frac{1}{\alpha} + C_p \frac{\alpha^3}{\pi} \ln \frac{1}{\alpha} + \delta_{4\gamma} \frac{\alpha^2}{\pi^2} + \mathcal{O}(\alpha^3) \right) \\ &= 7.989620(13) \times 10^9 \text{ sec}^{-1} \\ \Gamma_{o-Ps}^{th} &= \alpha^6 m \frac{2(\pi^2 - 9)}{9\pi} \left(1 - A_o \frac{\alpha}{\pi} - \frac{\alpha^2}{3} \ln \frac{1}{\alpha} + B_o \frac{\alpha^2}{\pi^2} - \frac{3\alpha^3}{2\pi} \ln^2 \frac{1}{\alpha} + C_o \frac{\alpha^3}{\pi} \ln \frac{1}{\alpha} + \delta_{5\gamma} \frac{\alpha^2}{\pi^2} + \mathcal{O}(\alpha^3) \right) \\ &= 7.039965(10) \mu\text{sec}^{-1}\end{aligned}$$

with coefficients

$$\begin{aligned}A_p &= 5 - \pi^2/4 & A_o &= 10.286606(10) \\ B_p &= 5.14(30) & B_o &= 44.52(26) \\ C_p &= -7.919(1) & C_o &= 5.517(1) \\ \delta_{4\gamma} &= 0.274(1) & \delta_{5\gamma} &= 0.19(1)\end{aligned}$$

The $\delta_{4\gamma}$ and $\delta_{5\gamma}$ are the contributions from the four photon and five photon final states, respectively. The parapositronium result agrees with the experiment, but the precision is not sufficient to test $\mathcal{O}(\alpha^2)$ radiative corrections. For orthopositronium, the theoretical value tends to favor the Tokyo group result, but again, experimental precision is not sufficient to test the $\mathcal{O}(\alpha^2)$ radiative corrections (see picture in the previous section).

The hyperfine splitting is computed to the same order, but with an analytic result

$$\begin{aligned}\Delta\nu_{hf} &= m\alpha^4 \left\{ \frac{7}{12} - \frac{\alpha}{\pi} \left(\frac{8}{9} + \frac{\ln 2}{2} \right) \right. \\ &\quad + \frac{\alpha^2}{\pi^2} \left(-\frac{5}{24}\pi^2 \ln \alpha + \frac{1367}{648} - \frac{5197}{3456}\pi^2 + \left(\frac{221}{144}\pi^2 + \frac{1}{2} \right) \ln 2 - \frac{53}{32}\zeta(3) \right) \\ &\quad \left. + \frac{\alpha^3}{\pi^3} \left(-\frac{7}{8}\pi^2 \ln^2 \alpha + \left(\frac{17}{3} \ln 2 - \frac{217}{90} \right) \pi^3 \ln \alpha \right) + \mathcal{O}(\alpha^3) \right\} \\ &\approx m\alpha^4 [0.5833 - 0.3933\alpha - 0.2083\alpha^2 \ln \alpha - 0.3928\alpha^2 - \dots] \\ &\approx 203.39169(41) \text{ GHz}\end{aligned}$$

This result exceeds the experimental values of [43] and [39] by 2.6 and 3.5 experimental standard deviations, respectively. The discrepancy is not too serious, but new measurements would really be welcomed.

Concerning references, most papers cited in the "Positronium Theory" section of the bibliography concern the computation of a part of the decay rate or hyperfine result. The latest results are presented in [124], [130] and [131].

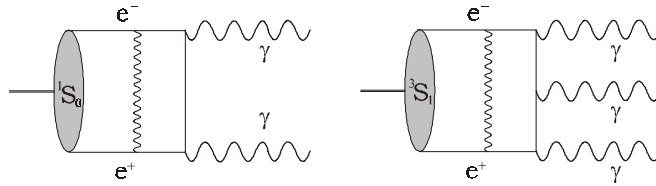
Other theoretical predictions have been obtained. In summary (see [132] and references cited there)

Name	Quantity	Theory
$\Delta\nu_{hf}$	$1^3S_1 - 1^1S_0$	203.39169 (41) GHz
$\Delta\nu_{hf;2}$	$2^3S_1 - 2^1S_0$	25.42469 (6) GHz
$\Delta\nu_{Lyman}$	$2^3S_1 - 1^3S_1$	1233607.2222 (6) GHz
$\Delta\nu$	$2^3S_1 - 2^3P_0$	18.49825 (9) GHz
$\Delta\nu$	$2^3S_1 - 2^3P_1$	13.01241 (9) GHz
$\Delta\nu_{Lamb}$	$2^3S_1 - 2^3P_2$	8.62570 (9) GHz
$\Delta\nu$	$2^3S_1 - 2^1P_1$	11.18537 (9) GHz
Γ_{p-Ps}	$1^1S_0 \rightarrow 2\gamma, 4\gamma$	$7.989620(13) \times 10^9 \text{ sec}^{-1}$
Γ_{o-Ps}	$1^3S_1 \rightarrow 3\gamma, 5\gamma$	$7.039965(10) \mu\text{sec}^{-1}$

Some Peculiarities

The positronium perturbative series have two peculiarities: corrections in $\ln \alpha$ appear, and the overall convergence is rather slow. In this subsection, we intend to explain qualitatively why, leaving more refined quantitative arguments to the next section.

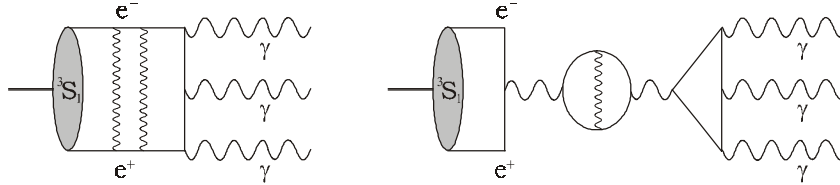
The slow convergence feature is traced to the contribution of so-called binding graphs



which account for roughly 80% of A_p [69] and roughly 90% of A_o [75], respectively. These diagrams have many interesting features, and we will discuss about them later. For now, one can understand that such diagrams are important because the exchanged photon is a binding photon, i.e. it is responsible for the binding of the electron

and positron. For such photons, the naive counting in powers of α fails. More precisely, the dynamics of the above process is such that, for e^+e^- near the mass shell, there is a huge enhancement factor, compensating the additional coupling constant.

Logarithmic corrections arise typically from "would-be" infrared singularities, i.e. singularities occurring if the electron and positron are on-shell. For example, the following diagrams introduce logarithmic corrections [74]



In the first case, one can see that logarithmic IR divergences will be introduced if the constituents are on-shell because of the intermediate electron and photon propagators. At low momentum, however, such divergences are cut-off by the binding energy $E_B = M - 2m = -m\alpha^2/4$. Hence, symbolically, one can understand that $\ln \alpha$ corrections can arise from integrations like

$$\int_{\sim -E_B}^{\sim m} \frac{dk}{k} = -\ln \frac{E_B}{m} \rightarrow \ln \alpha$$

That logarithmic correction is a soft-scale effect, i.e. arising from very soft momentum integration.

Similarly, the two-loop photon vacuum polarization insertion in the second graph introduces a $\alpha^2 \ln \alpha$ correction [70]. To see it, one just has to know that the fourth-order vacuum polarization has threshold singularities behaving like

$$\alpha^2 \ln \left| 1 - \frac{4m^2}{q^2} \right|$$

where q^2 is the momentum transfer flowing through the diagram. In the case depicted on the figure, that momentum is $q^2 = M^2 = 4m^2 - m^2\alpha^2$ hence

$$\alpha^2 \ln \left| 1 - \frac{4m^2}{q^2} \right|_{q^2 \rightarrow M^2} \alpha^2 \ln \frac{\alpha^2}{4}$$

It is important to note that such logarithmic corrections are really specific to bound state observables; for all of them, logarithmic corrections like $\ln \alpha$ or $\ln Z\alpha$ occur. They are intimately linked to the binding energy (mass defect). The current approach to these corrections is however quite different in that it uses the language of anomalous dimensions and renormalization group flow [128].

1.3 Theoretical Description of Positronium Decay

Now we turn to the theoretical description of bound state decays. It is not immediately obvious how to extend the quantum mechanical formalisms or the Bethe-Salpeter one; those were suited to the computation of energy levels or wavefunctions. To describe a decay process, some kind of model has to be constructed. Usually, such model will involve the bound state wavefunction in an essential way, so that all the previously cited formalisms will still be important.

A good model (or scheme) is a model allowing for a perturbative expansion. The lowest order approximation should be well-defined, while corrections should be obtained in a systematic way. These two points are not so easy to meet. Indeed, as we will see, issues of double counting plague decay computations. Further, there are

many difficulties associated with gauge invariance and infrared divergences. Finally, the relevance of the lowest order approximation is often problematic, as will be exposed at length in the next chapter.

1.3.1 Pirene-Wheeler Formula

The simplest of all decay formula has already been encountered; it is the Pirene-Wheeler formula ([60], [61])

$$\Gamma(Ps \rightarrow n\gamma) = \frac{1}{2J+1} |\phi(0)|^2 (4v_{rel}\sigma(e^-e^+ \rightarrow n\gamma))_{v_{rel} \rightarrow 0} \quad (1.5)$$

with $|\phi(0)|^2$ the Schrödinger wavefunction. This formula relates the decay rate to the scattering of the constituents at rest. The limit $v_{rel} \rightarrow 0$ enforces the correct selection rule, i.e. p - $Ps \rightarrow (2n)\gamma$ and o - $Ps \rightarrow (2n+1)\gamma$, because an e^+e^- pair at rest can decay into two (three) photons only if in a total spin 0 (1) state. The results for the parapositronium and orthopositronium decay rates have already been discussed, so we will be very brief and concentrate on p - $Ps \rightarrow \gamma\gamma$.

The lowest order result is obtained from ($\beta = E/m$ with E the center-of-mass energy)

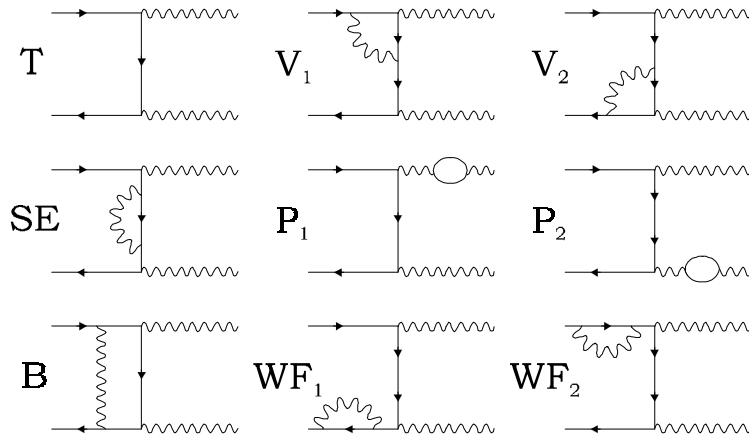
$$\sigma(e^+e^- \rightarrow \gamma\gamma)_{c.m.} = \frac{2\pi\alpha^2}{4m^2} \left[\frac{2(3\beta^4 - (\beta^2 - 1)^2) \log[\beta + \sqrt{\beta^2 - 1}]}{\beta^4(\beta^2 - 1)} - \frac{\beta^2 + 1}{\beta^3 \sqrt{\beta^2 - 1}} \right]$$

With $v_{rel} = 2\beta\sqrt{\beta^2 - 1}$, we find

$$\Gamma(p\text{-}Ps \rightarrow \gamma\gamma) = |\phi(0)|^2 \frac{4\pi\alpha^2}{m^2} = \frac{m\alpha^5}{2}$$

Radiative Corrections

The computation of the radiative corrections to p - $Ps \rightarrow \gamma\gamma$ was achieved by Harris and Brown [65], [69], [99], using the above formalism. The diagrams contributing, up to one-loop, to the scattering cross section are



with in addition the crossed processes. The first one (T) is the tree-level. Details of the calculations are in the appendix A.1.3, and we quote

$$\Gamma(p-Ps \rightarrow \gamma\gamma) = |\phi(0)|^2 \frac{4\pi\alpha^2}{m^2} \left[1 - \frac{\alpha}{\pi} \left(5 - \frac{\pi^2}{4} \right) + \frac{\pi\alpha}{v_{rel}} \right] \quad (1.6)$$

The mass m and coupling constant α are renormalized by the SE and $P_{1,2}$ diagram, respectively.

Note that some IR divergences proportional to v_{rel} have been cancelled by the limit $v_{rel} \rightarrow 0$ [99]. This cancellation is a selection rule cancellation: the IR divergences in $\sigma^{(1)}(e^+e^- \rightarrow \gamma\gamma)$ (first order) cancel against the IR bremsstrahlung divergences of $\sigma^{(0)}(e^+e^- \rightarrow \gamma\gamma\gamma)$. Since this last decay cannot contribute for an initial 1S_0 state, the corresponding IR divergences of $\sigma^{(1)}(e^+e^- \rightarrow \gamma\gamma)$ disappear when the initial e^+e^- pair is in a 1S_0 state.

The singularity for zero relative velocity is also an IR divergence, coming from the diagram B , the binding graph. The treatment of this divergence is special. In fact, it has to be dropped because it is already included in the wavefunction. Indeed, the wavefunction accounts for all the Coulomb photon exchanges between the e^+e^- . The $1/v_{rel}$ comes from the Coulomb part of the photon in B .

In a somewhat different reasoning, following Harris and Brown [69] (see also Schwinger [7], vol.III, pp99 and Merzbacher [3], pp249), one can remember from non-relativistic quantum mechanics that the long range Coulomb interaction between the e^+e^- modifies wavefunctions as

$$|\psi(0)|^2 \rightarrow |\psi(0)|^2 \frac{2\pi\alpha/v_{rel}}{1 - e^{-2\pi\alpha/v_{rel}}} \approx |\psi(0)|^2 \left(1 + \frac{\pi\alpha}{v_{rel}} \right)$$

where ψ is the initial e^+e^- wavefunction entering the *scattering process* (not to be confused with the bound state wavefunction). This correction factor is called the Sommerfeld factor. As a result, the Pirenne formula should be written

$$\Gamma(Ps \rightarrow n\gamma) = \frac{1}{2J+1} |\phi(0)|^2 (4v_{rel}\sigma^{Coul}(e^-e^+ \rightarrow n\gamma))_{v_{rel} \rightarrow 0}$$

where, to order α ,

$$\sigma^{Coul}(e^-e^+ \rightarrow n\gamma) \left(1 + \frac{\pi\alpha}{v_{rel}} \right) = \sigma(e^-e^+ \rightarrow n\gamma)$$

The final form for the correction is now simply

$$\Gamma(p-Ps \rightarrow \gamma\gamma) = \frac{m\alpha^5}{2} \left[1 - \frac{\alpha}{\pi} \left(5 - \frac{\pi^2}{4} \right) \right] \quad (1.7)$$

1.3.2 Convolution Formula

To avoid the kind of pathological velocity singularity encountered above, a more sophisticated model has to be built. To express the amplitude for the bound state decaying into a given final state, in terms of the amplitude for its e^-e^+ constituents to scatter into that final state, the first step is to relate the positronium state vector to the constituent state vectors. This is done through a convolution integral (see for example [17], [24]):

$$|Ps(J)\rangle = \sqrt{2M} \int \frac{d^3\mathbf{k}}{(2\pi)^3} \psi(\mathbf{k}) \frac{1}{\sqrt{2E_{\mathbf{k}}}} \frac{1}{\sqrt{2E_{\mathbf{k}}}} (|e^-(\mathbf{k}, \xi)\rangle \otimes |e^+(-\mathbf{k}, \xi')\rangle)_{\xi, \xi' \rightarrow J} \quad (1.8)$$

The state vector of the bound state is the sum of the combined state vectors of the constituents weighted by the momentum space Schrödinger wavefunction for the bound state. For the positronium ground state,

$$\psi(\mathbf{k}) = \phi(0) \frac{8\pi\gamma}{(\mathbf{k}^2 + \gamma^2)^2}$$

with $\phi(0)$ the configuration space wavefunction at zero separation and $\gamma^2 = m^2 - M^2/4$ (m the electron mass and M the positronium mass). The $\sqrt{2E_{\mathbf{k}}}$ and $\sqrt{2M}$ are just normalization factors for free states

$$|p\rangle = \sqrt{2E_p} a_p^\dagger |0\rangle$$

and ξ, ξ' stand for polarization states, which combine to give a total spin J to the bound state.

This formula exhibits two important features : first, the *constituents are always on-shell*. We are just averaging over residual velocity, with weights given by their respective probability to occur inside the positronium, i.e. by $\psi(\mathbf{k})$. On-shellness of the e^\pm is also obvious from their state normalization. Second, *non-perturbative effects are introduced non-relativistically*, through the function $\psi(\mathbf{k})$.

From the expression of the state vector of the bound state, one defines the amplitude for its decay as

$$\mathcal{M}(Ps(J) \rightarrow n\gamma) = \sqrt{2M} \int \frac{d^3\mathbf{k}}{(2\pi)^3} \psi(\mathbf{k}) \frac{1}{\sqrt{2E_{\mathbf{k}}}} \frac{1}{\sqrt{2E_{\mathbf{k}}}} \mathcal{M}(e^-(\mathbf{k}, \xi), e^+(-\mathbf{k}, \xi') \rightarrow n\gamma)_{\xi, \xi' \rightarrow J} \quad (1.9)$$

Now the amplitude inside the convolution integral is a scattering amplitude. It can be treated using quantum field perturbation theory. Finally, the width is calculated as

$$\Gamma(Ps(J) \rightarrow n\gamma) = \frac{1}{n!} \frac{1}{2J+1} \frac{1}{2M} \int d\Phi_{n\gamma} |\mathcal{M}(Ps(J) \rightarrow n\gamma)|^2 \quad (1.10)$$

with $1/n!$ the symmetry factor for the final state of n identical photons.

In the static limit, i.e. when $\mathbf{k} = 0$, the convolution formula is equivalent to the Pirenne formula (1.5). Indeed, if the velocity-dependent part of the scattering amplitude is neglected, we can approximate

$$\begin{aligned} \mathcal{M}(Ps(J) \rightarrow n\gamma) &\approx \left(\int \frac{d^3\mathbf{k}}{(2\pi)^3} \psi(\mathbf{k}) \right) \frac{\sqrt{2M}}{2m} \mathcal{M}(e^-(\mathbf{0}, \xi), e^+(\mathbf{0}, \xi') \rightarrow n\gamma)_{\xi, \xi' \rightarrow J} \\ &\approx \phi(0) \left(\frac{\sqrt{2M}}{2m} \mathcal{M}(e^-(\mathbf{0}, \xi), e^+(\mathbf{0}, \xi') \rightarrow n\gamma)_{\xi, \xi' \rightarrow J} \right) \end{aligned}$$

When integrated over phase-space, the factor in brackets is proportional to $[v_{rel}\sigma(e^-e^+ \rightarrow n\gamma)]_{v_{rel} \rightarrow 0}$.

Radiative Corrections

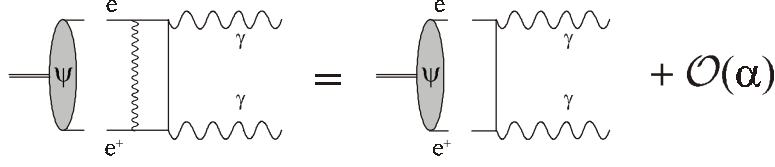
If the static limit is not taken, one can expect that the smearing introduced by the convolution will kill the velocity divergence encountered before. This is indeed the case, and it is interesting to see in some detail how it happens (see [84], [87]). All follows from the recursive property of the Schrödinger wavefunction

$$\psi(\mathbf{p}) = \frac{4\pi\alpha m}{\mathbf{p}^2 + \gamma^2} \int \frac{d^3\mathbf{q}}{(2\pi)^3} \frac{1}{(\mathbf{q} - \mathbf{p})^2} \psi(\mathbf{q})$$

which is the Bethe-Salpeter equation with a Coulomb ladder photon as kernel. Graphically,

$$\text{Diagrammatic representation of the Bethe-Salpeter equation: } \psi \text{ blob} = \psi \text{ blob} \text{ connected to } K_C \text{ box} = K_C \text{ box} = K_C \text{ box connected to Coulomb wavy line} \quad (1.11)$$

Now, looking back at the binding graph, one can see that when introduced in the convolution integral, its Coulomb piece will reproduce the lowest order result



Mathematically, the Coulomb part of the diagram B , when the constituents have momentum \mathbf{k} , has a piece like

$$B \sim \frac{2\gamma}{|\mathbf{k}|} \arctan \frac{|\mathbf{k}|}{\gamma} + \dots \quad (1.12)$$

This is of order α since $\gamma = m\alpha/2$. Now, when convoluted with the wavefunction, the integral is

$$\int d^3\mathbf{k} \psi(\mathbf{k}) \left[\frac{2\gamma}{|\mathbf{k}|} \arctan \frac{|\mathbf{k}|}{\gamma} + \dots \right] = 1 + \mathcal{O}(\alpha)$$

This explains how the lowest order is recovered. Therefore, by considering *only* one-loop graphs, one finds (1.7).

There is also a straightforward relation with the Sommerfeld factor. If the term (1.12) is expanded around $\gamma = 0$, one gets

$$\frac{2\gamma}{|\mathbf{k}|} \arctan \frac{|\mathbf{k}|}{\gamma} \approx \frac{\pi\gamma}{|\mathbf{k}|} \approx \frac{\pi\alpha}{2v_{rel}}$$

This is a contribution to the amplitude. When squared, the result (1.6) is found. Obviously, this singularity originates in the improper ordering of the limits $\gamma \rightarrow 0, v_{rel} \rightarrow 0$.

1.3.3 Bethe-Salpeter Loop

Using Bethe-Salpeter (BS) analyses, one starts with a four-dimensional integral [87]

$$\mathcal{M}(Ps \rightarrow n\gamma) = \int \frac{d^4k}{(2\pi)^4} Tr \left\{ \Psi(k) \Gamma_{scatt} (e^- (P/2 + k) e^+ (P/2 - k) \rightarrow n\gamma) \right\} \quad (1.13)$$

with Γ_{scatt} the off-shell scattering amplitude and P the positronium momentum. For example, in the case of $p-Ps \rightarrow \gamma\gamma$, it is

$$\Gamma_{scatt} = \varepsilon_{1\mu}^* \varepsilon_{2\nu}^* \left\{ i e \gamma^\mu \frac{i}{\not{k} - \frac{1}{2} \not{P} + \not{\not{1}} - m} i e \gamma^\nu + i e \gamma^\nu \frac{i}{\not{k} + \frac{1}{2} \not{P} - \not{\not{1}} - m} i e \gamma^\mu \right\}$$

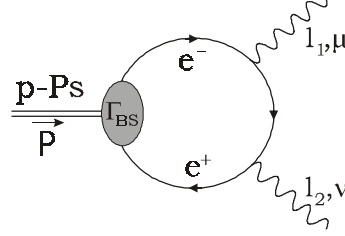
The BS amplitude (1.13) has a loop-like structure. This becomes apparent after identification of the BS vertex [19]

$$\Psi(k) = \frac{i}{\not{k} + \frac{1}{2} \not{P} - m} \Gamma_{BS} \left(\frac{P}{2} + k, \frac{P}{2} - k, P \right) \frac{i}{\not{k} - \frac{1}{2} \not{P} - m}$$

Hence

$$\mathcal{M}(Ps \rightarrow n\gamma) = \int \frac{d^4k}{(2\pi)^4} Tr \left\{ \Gamma_{BS}(\dots) \frac{i}{\not{k} - \frac{1}{2} \not{P} - m} \Gamma_{scatt} (e^- e^+ \rightarrow n\gamma) \frac{i}{\not{k} + \frac{1}{2} \not{P} - m} \right\} \quad (1.14)$$

In this representation, the BS vertex is an effective form factor for the bound state. Graphically, for the case of $p\text{-Ps} \rightarrow \gamma\gamma$



Barbieri-Remiddi Reduction

As is well-known, the BS equation cannot be solved exactly, and one has to rely on some approximations for the vertex (or wavefunction). The most popular one for positronium is that of Barbieri-Remiddi [73], which can be viewed as a four-dimensional generalization of the usual Schrödinger wavefunction. In general, the wavefunction is approximated as $\Psi(k) \sim \delta(k_0) \psi(\mathbf{k})$ in (1.13), so that the decay amplitude is given by a three-dimensional integral representation (see for example [87], [113]).

Specifically, the Barbieri-Remiddi wavefunction (BRW) is

$$\Psi_{0,sm}(p) = 2iD(W_0, p)(E_p - W_0)[\Lambda_+(\mathbf{p})\Gamma_{sm}\Lambda_-(\mathbf{p})(-\gamma_0)]\frac{2E_p}{E_p + m}\sqrt{\omega_p + W_0}\psi(\mathbf{p})$$

where $0, sm$ denotes the ground state, spin s, m . The definitions are

$$\begin{aligned} E_p &= \sqrt{\mathbf{p}^2 + m^2}, \quad W_0 = M/2 \\ D(W_0, p) &= \frac{1}{p_0^2 - (E_p - W_0 - i\varepsilon)^2} \\ \Lambda_{\pm}(\mathbf{p}) &= \frac{1}{2E_p}[E_p \pm (m - \boldsymbol{\gamma} \cdot \mathbf{p})\gamma_0] \end{aligned}$$

For the wavefunction spin part

$$\Gamma_{00} = \begin{pmatrix} 0 & 1 \\ 0 & 0 \end{pmatrix}, \quad \Gamma_{1m} = \begin{pmatrix} 0 & \boldsymbol{\sigma} \cdot \mathbf{e}_m \\ 0 & 0 \end{pmatrix}$$

where \mathbf{e}_m is the polarization vector of the orthopositronium state. Finally, the Schrödinger wavefunction at the heart of the BRW is as usual

$$\psi(\mathbf{p}) = \varphi_0 \frac{8\pi\gamma}{(\mathbf{p}^2 + \gamma^2)^2}$$

To recover the three-dimensional convolution integral, it suffices to note that the energy-dependent part of the BRW is a delta-function representation

$$\lim_{\omega_p \rightarrow W_0} iD(W_0, p)(E_p - W_0) = \lim_{\omega_p \rightarrow W_0} \frac{i(E_p - W_0)}{p_0^2 - (E_p - W_0 - i\varepsilon)^2} = \pi\delta(p_0)$$

which amounts to neglecting the binding energy in that part of the wavefunction. In that limit, up to normalization factors, the decay rate is

$$\mathcal{M}(Ps \rightarrow n\gamma) \sim \int \frac{d^3\mathbf{k}}{(2\pi)^4} \psi(\mathbf{k}) \frac{1}{2E_k} \text{Tr} \left\{ (1 + \gamma_0) \mathbf{P} (m - \not{k}') \Gamma_{scatt}(e^-(\mathbf{k}), e^+(-\mathbf{k}) \rightarrow n\gamma)(m + \not{k}) \right\} \quad (1.15)$$

with $k = (E_k, \mathbf{k})$, $k' = (E_k, -\mathbf{k})$ and $\mathbf{P} = \gamma^5$ for parapositronium, $\mathbf{P} = \not{\epsilon}$ for orthopositronium with polarization vector e^μ . The $(1 + \gamma_0) \mathbf{P}$ factor is the spin part of the wavefunction. Note well that compared to (1.13), the scattering amplitude Γ_{scatt} is now evaluated for an on-shell electron and positron.

The Starting Point

In general, there is great latitude in the treatment of the projectors. Usually, those are simplified to [121]

$$\mathcal{M}(Ps \rightarrow n\gamma) = \sqrt{2M} \int \frac{d^3\mathbf{k}}{(2\pi)^3} \psi(\mathbf{k}) \frac{m}{2E_{\mathbf{k}}} \text{Tr} \left\{ \frac{1 + \gamma^0}{\sqrt{2}} \mathbf{P} \Gamma_{scatt}(e^-(\mathbf{k}), e^+(-\mathbf{k}) \rightarrow n\gamma) \right\} \quad (1.16)$$

The difference between both formulas being treated as perturbations. Such a simplification of the projectors is very delicate, because of gauge invariance issues ((1.15) is gauge invariant thanks to the $m-$ \not{k}' and $m+$ \not{k} projectors on both sides of Γ_{scatt}). However, the formula (1.16) is the starting point of most modern applications. This is probably because (1.16) can be obtained simply from (1.9) by working out the constraint $\xi, \xi' \rightarrow J$.

Note well that this formula is sufficient to obtain the leading order approximation for the decay rate. Hence, it appears as a good perturbation basis. Further, it is rather simple since $\psi(\mathbf{k})$ is the Schrödinger wavefunction. In other words, summing only the effect of the Coulomb instantaneous interaction into the wavefunction is sufficient. A similar situation occurs for energy levels, since the Balmer formula is a rather good approximation. Wavefunction energy dependences, or departure from the simple Coulomb Schrödinger form, or corrections to the spin and projector parts are treated as (relativistic) perturbations. They are typically of the order of m/M , i.e. α^2 . To the relativistic corrections, one must add radiative corrections to the scattering amplitude Γ_{scatt} . For instance, order α corrections are simply computed using (1.16) as we have seen in the previous sections. At the end of the day, a consistent perturbation basis is built.

This closes the review of basic formulas used to compute decay rates in the standard approach. We have reached a very general form (1.13). So general, in fact, that approximation methods are compulsory. Practically, simpler expressions are used, and a consistent perturbation theory is built. Further, the non-relativistic QED (NRQED) effective theory gives a systematic to this perturbation theory (see for example [16], [93], [105], [109], [110], [112], [123]). This is the tool used in all recent advances in positronium physics, and more generally in QED bound state theory.

Chapter 2

A New Basis for QED Bound States

The present chapter is the core of the thesis. It consists of three main parts: (1) the contradiction of standard approaches with analyticity, (2) the resolution of the problem and (3) application to various processes. The results of this chapter were presented in our papers [29], [30], [31] and [32].

In the first part, problems with the standard approach perturbation theory are exposed. It is shown that the standard basis chosen is inappropriate, because it is in contradiction with a fundamental theorem of Quantum Field Theory (QFT), namely Low's theorem. The predictions of the standard basis for the energy spectra of the photons produced in the annihilation of positronium are wrong. This first result is very straightforward in the context of dispersion relations. To be more precise, we will clarify the approximation done in reducing the Bethe-Salpeter loop into the three-dimensional convolution formula used as a perturbation basis. In this way, the effects expanded perturbatively will be characterized.

In the second part, an alternative scheme of computation is presented. It amounts basically to a change of lowest order amplitude. Compared to the perturbative expansion in the standard approach, this new lowest order amplitude is a non-perturbative resummation of an infinite class of corrections. This resummation will be shown to be essential in order to deal with soft photons. Indeed, **in the standard non-relativistic QED (NRQED) approach, there is an inconsistency in the treatment of final state photons when their energies are of the order of the binding energy, because the NRQED momentum scaling rules are violated.**

To be able to use our new basis in practical applications, a simple computation method will be proposed. We will show that our non-perturbative bound state decay amplitudes are simply related to basic QED processes, easily dealt with using QFT perturbative techniques. At the end of the day, a consistent, well-defined lowest order basis for QED bound state decay computations is obtained.

The final sections contain the application of the method to various processes. The analytical properties of the amplitudes are analyzed and agree with Low's theorem. Further, the behavior of the series expansion is better than in NRQED approaches. Finally, extensions to other bound state problems (positronium formation, radiative transitions, hyperfine splitting,...) are briefly discussed.

2.1 Critical Analysis of Standard Approach Decay Formula

The purpose of this section is to analyze the reduction of the four-dimensional Bethe-Salpeter loop (1.13)

$$\mathcal{M}(Ps \rightarrow n\gamma) = \int \frac{d^4 k}{(2\pi)^4} Tr \{ \Psi(k) \Gamma_{scatt}(e^-(P/2+k), e^+(P/2-k) \rightarrow n\gamma) \} \quad (2.1)$$

to the three-dimensional convolution formula (1.16)

$$\mathcal{M}(Ps \rightarrow n\gamma) = \sqrt{2M} \int \frac{d^3 \mathbf{k}}{(2\pi)^3} \psi(\mathbf{k}) \frac{m}{2E_{\mathbf{k}}} Tr \left\{ \frac{1 + \gamma^0}{\sqrt{2}} \mathbf{P} \Gamma_{scatt}(e^-(\mathbf{k}), e^+(-\mathbf{k}) \rightarrow n\gamma) \right\} \quad (2.2)$$

where $\Psi(k)$ is the Barbieri-Remiddi wavefunction and $\psi(\mathbf{k})$ the Schrödinger one. Let us recall that the reduction usually proceeds by approximating the energy part of $\Psi(k)$ as $\Psi(k) \sim \delta(k_0) \psi(\mathbf{k})$ and neglecting some k dependences in the projectors. Then, the standard approach is to treat the difference between both formulas

as higher order perturbations. In other words, (2.2) is the basis of standard perturbation theory for decay rate computations.

Our goal is to use dispersion relation techniques to see whether the above choice for the lowest order is appropriate. Also, concerning the many effects expanded perturbatively, we want to address the behavior of the series expansion. The information gathered in the present section will motivate the form of the new basis we propose in the next section.

2.1.1 Problematic Properties of the Convolution Formula

We would like to answer the following questions, which we divide into three classes.

Factorization

The basic factorization of the bound state dynamics from the annihilation process. As we have seen, the four-dimensional loop (2.1) is essentially a loop model with a form factor for the bound state (see (1.14)). Under that form, both the bound state and decay dynamics are intimately linked. On the other hand, the convolution formula exhibits a higher degree of factorization of both processes, since the integration is only carried over three dimensions.

Another way to look at this reduction is to remark that in the loop (2.1), the constituents are off-shell, while in the convolution formula, the constituents are on-shell. It is crucial to analyze how the off-shellness of the constituents can be reintroduced perturbatively starting from (2.2). This is especially important in view of the present theoretical consideration, at order $\mathcal{O}(\alpha^2)$. Indeed, the non-perturbative phenomena responsible for the off-shellness of the electron and positron inside the positronium are of $\mathcal{O}(\alpha^2)$ (since positronium mass minus twice the electron mass is of that order).

Violation of energy conservation ? Positronium being a bound state, $M < 2m$ (M the positronium mass and m the electron mass). In (2.2), the total energy of the on-shell electron-positron pair entering the scattering process is $2\sqrt{\mathbf{k}^2 + m^2}$, clearly greater than M , and getting worse as \mathbf{k} increases in the integration. The same observation can be made about all the convolution-type formulas. An interpretation for this fact would be welcomed.

Projectors and Gauge Invariance

The enforcement of *gauge invariance* may be problematic. This is more technical. In general, one has to project the electron-positron pair into a spin state compatible with the total spin of the bound state. This bound state spin state is usually treated non-relativistically, introducing some potential threats to the gauge invariance of the decay amplitude. More precisely, Ward identities are satisfied if there are projectors on both sides of the scattering amplitudes, like for example as

$$Tr \{ \mathbf{P} (m - \not{k}') \Gamma_{scatt} (e^- (k'), e^+ (k) \rightarrow n\gamma) (m + \not{k}) \}$$

In the static limit $k = k' = (m, 0, 0, 0)$, this collapses to

$$Tr \{ 2m^2 (1 + \gamma^0) \mathbf{P} \Gamma_{scatt} (e^- (m, \mathbf{0}), e^+ (m, \mathbf{0}) \rightarrow n\gamma) \}$$

and one recognize the projector of (2.2). As a result, it appears that (2.2) is gauge invariant only in the static limit. If one is interested in the lowest order static result, (2.2) is just fine. If one wants to go beyond it, care is needed in the treatment of the projectors.

Another source of gauge invariance problems arises from the form of the Bethe-Salpeter loop itself (2.1). This is in fact more problematic. To understand it, it suffices to remember that to enforce the Ward identities, one needs cancellation among the various amplitudes contributing to a given process (for example, there is six diagrams contributing to $o\text{-}Ps \rightarrow \gamma\gamma\gamma$). Because of the momentum dependences of the form factor (i.e. of the wavefunction), this cancellation is spoiled, and the Ward identities are violated.

Analyticity

The last, and more important point, is *the analytical behavior in the soft photon limit*. The consequences of gauge invariance are well-known: one gets very tough constraints on the structure of amplitudes in the form of Ward-Takahashi Identities. For instance, any amplitude involving an external photon, $\mathcal{M} = \varepsilon_\mu \mathcal{M}^\mu$, must verify the Ward Identity $k_\mu \mathcal{M}^\mu = 0$, with k_μ the photon momentum and ε_μ its polarization vector. In addition to gauge invariance, since any probability amplitude is an analytical function, $\mathcal{M}^\mu(k, \dots)$ admits a Laurent expansion in each of its variables. It was F.E. Low who, in the fifties [204], first realized that the Ward identity restricts the form of the first two terms of the Laurent expansion in the external photon energy.

Low's theorem is a model-independent result, valid to all orders: for a complete amplitude, the soft-photon limit only depends on the quantum numbers of the external particles, and not on the details of the intermediate subprocesses. At the level of observables, the low-energy end of the photon spectrum is obtained by combining the amplitude behavior with that of the phase-space. The most characteristic spectra are

- *Charged particles and photons in external states.* The well-known bremsstrahlung emissions lead to an amplitude in $1/k$ for $k \rightarrow 0$ (k is the energy of one of the emitted photons). At the decay rate or cross section level, the IR divergent amplitude generates characteristic IR divergent spectra.
- *Only neutral self-conjugate bosons, including photons in external states.* The amplitude is in k for $k \rightarrow 0$ (k is again the energy of one of the photon). This statement is much stronger than what is sometimes thought of for a non-bremsstrahlung process. *On general ground, it shows that feeling confident with an IR safe computation is theoretically incorrect.* IR safety at the cross section or decay rate level is definitely not sufficient. When one constructs a model designed to describe some processes among neutral bosons and photons, one must ensure that the amplitude **vanishes** in the soft-photon limit.

It will be shown in the following that the standard approach amplitudes are in contradiction with Low's theorem, at each order. The origin of the problem can already be explained from the occurrence of on-shell charged particles in the intermediate stage. Indeed, models derived from Bethe-Salpeter analyses, or from QED non-relativistic effective theory (NRQED), always connect the process of annihilation of bound charged particles to that of scattering of real, asymptotic charged particles. The difficulty with such approaches is thereby apparent: asymptotic and bound charged particles have drastically different radiation properties: the former exhibit bremsstrahlung-type radiations, while the later do not radiate zero energy photons (for very low-energy photons, a positronium state is just a neutral, self-conjugate boson, hence it does not radiate in that limit). In the literature, it is assumed that the intermediate charged particle bremsstrahlung radiations are disposed off simply by projecting onto the required positronium spin state. This is indeed the case for the singular part of the bremsstrahlung radiation, but not for the constant part. In other words, Bremsstrahlung radiations typically lead to a Laurent expansion for the amplitude as

$$\mathcal{M}^\mu(k, \dots) = \mathcal{O}(1/k) + \mathcal{O}(1) + \mathcal{O}(k)$$

Low's theorem states that both the terms of $\mathcal{O}(1/k)$ and $\mathcal{O}(1)$ must disappear [204]. While the cancellation of $\mathcal{O}(1/k)$ terms is automatic from selection rules, that of $\mathcal{O}(1)$ terms is much more delicate. At the end of the day, the amplitudes fail to vanish in the soft-photon limit.

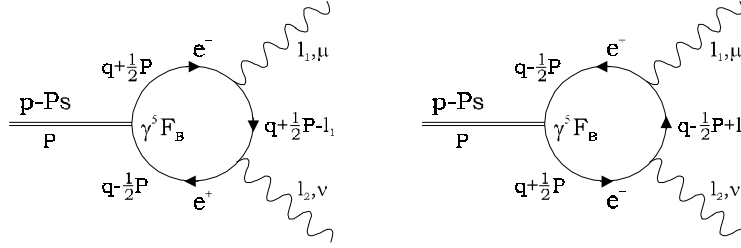
2.1.2 Dispersion Analysis of the BS Loop

Most of the previous questions can be answered simply in the context of dispersion relations. To begin with, let us take a four-dimensional loop model with a general form factor.

A Generalized Loop Model

Basically, we assume a loop structure for the decay amplitudes, similar to the Bethe-Salpeter loop. Positronium decays into a virtual electron-positron pair which subsequently annihilates into real or virtual photons (an odd number for ortho-states, an even number for para-states). The coupling of the positronium to its constituents is described by a form factor F_B , times a Dirac matrix structure consistent with the bound state quantum numbers. Remark that a constant form factor would amount to consider positronium as a point-like bound state. As we will see, F_B is in fact related to the bound state wavefunction.

For parapositronium decay into two photons, our model is represented



The corresponding amplitude is

$$\mathcal{M}(p\text{-Ps} \rightarrow \gamma\gamma) = \int \frac{d^4 q}{(2\pi)^4} F_B \text{Tr} \left\{ \gamma_5 \frac{i}{\not{q} - \frac{1}{2} \not{P} - m} \Gamma_{scatt}^{\mu\nu} \frac{i}{\not{q} + \frac{1}{2} \not{P} - m} \right\} \varepsilon_{1\mu}^* \varepsilon_{2\nu}^* \quad (2.3)$$

with P the positronium four-momentum and $F_B \equiv F_B(q^2, P \cdot q)$ the form factor. The tensor $\Gamma_{scatt}^{\mu\nu}$ is the scattering amplitude for off-shell e^+e^- , with incoming momenta $\frac{1}{2}P - q$ and $\frac{1}{2}P + q$, into two photons :

$$\begin{aligned} \Gamma_{scatt}^{\mu\nu} &= \Gamma_{scatt}^{\mu\nu} (e^+ (\frac{1}{2}P - q) e^- (\frac{1}{2}P + q) \rightarrow \gamma(l_1) \gamma(l_2)) \\ &= ie\gamma^\mu \frac{i}{\not{q} - \frac{1}{2} \not{P} + \not{l}_1 - m} ie\gamma^\nu + ie\gamma^\nu \frac{i}{\not{q} + \frac{1}{2} \not{P} - \not{l}_1 - m} ie\gamma^\mu \end{aligned} \quad (2.4)$$

Remarks :

- 1) The model is extended to orthopositronium decays through the replacement of γ_5 by \not{q} .
- 2) The electron and positron in the loop are never on-shell, because $M < 2m$.
- 3) F_B contains all the information about the bound state. Let us postulate a form for this coupling as (in the positronium center-of-mass frame)

$$F_B \equiv C \phi_0 \mathcal{F}(q_0, \mathbf{q}^2) (\mathbf{q}^2 + \gamma^2) \quad (2.5)$$

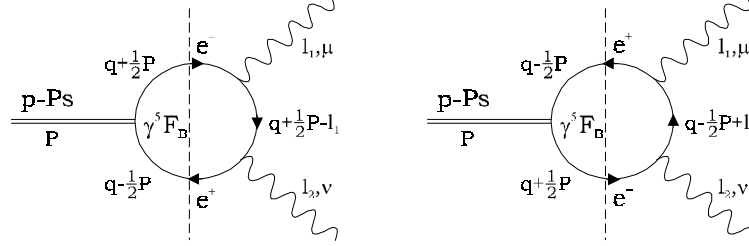
with C a constant, and $\gamma^2 = m^2 - M^2/4$ related to the binding energy $E_B = M - 2m$. In QED, E_B and γ^2 are related to the fine structure constant as $E_B \approx -m\alpha^2/4$ and $\gamma^2 \approx m^2\alpha^2/4$.

The Loop Model Reproduces Standard Decay Amplitudes

We can state our result in three steps (details are found in the appendix A.1.1). First, we define

$$\text{Im } \mathcal{T}(P^2) \equiv \text{Im } \mathcal{M}(p\text{-}Ps(P^2) \rightarrow \gamma\gamma) \quad (2.6)$$

with the absorptive part given by the two vertical cuts



Then, using an unsubtracted dispersion relation (see [6], [219]) with $s = P^2$:

$$\mathcal{T}(M^2) = \text{Re } \mathcal{T}(M^2) = \frac{1}{\pi} \int_{4m^2}^{\infty} \frac{ds}{s - M^2} \text{Im } \mathcal{T}(s) \quad (2.7)$$

($\mathcal{T}(M^2) = \text{Re } \mathcal{T}(M^2)$ since $M < 2m$), and changing variables, one recovers a factorized form (i.e. a convolution type amplitude):

$$\mathcal{M}(p\text{-}Ps \rightarrow \gamma\gamma) = \frac{C}{2} \int \frac{d^3\mathbf{k}}{(2\pi)^3} \frac{\phi_0 \mathcal{F}(0, \mathbf{k}^2)}{2E_{\mathbf{k}}} \text{Tr} \{ \gamma_5 (m - \not{k}') \Gamma_{scatt}(m + \not{k}) \} \quad (2.8)$$

with Γ given by $\Gamma_{scatt}^{\mu\nu}(e^-(k), e^+(k') \rightarrow \gamma\gamma) \varepsilon_{1\mu}^* \varepsilon_{2\nu}^*$ and $k = (E_{\mathbf{k}}, \mathbf{k})$, $k' = (E_{\mathbf{k}}, -\mathbf{k})$, i.e. the same Γ_{scatt} as in (2.2). Finally, if one further identifies

$$\begin{aligned} C &= \sqrt{M}/m \\ \psi(\mathbf{k}) &= \phi_0 \mathcal{F}(0, \mathbf{k}^2) \end{aligned}$$

by neglecting the \mathbf{k} dependence in the projectors $(m - \not{k}')$ and $(m + \not{k})$, (2.8) reduces to (2.2).

As a corollary, the energy-dependence of the form factor is demonstrated to be irrelevant. Indeed, the dispersion relation fixes $q_0 = 0$. From now on, we will simplify the notation and identify $\mathcal{F}(0, \mathbf{k}^2) = \mathcal{F}(\mathbf{k}^2)$.

Discussion

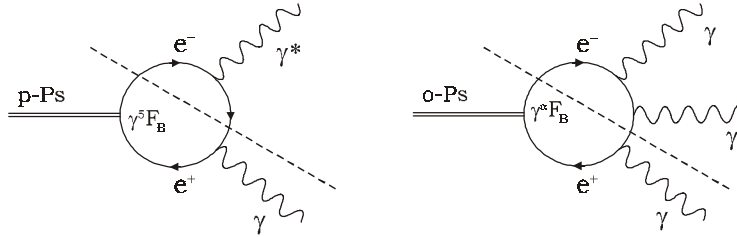
First, factorization appears simply as a manifestation of the optical theorem: the appearance of on-shell intermediate states is expected in the imaginary part. The dispersive integral "shifts" them off-shell: the amplitude at the physical point $s = M^2$ is purely real, i.e. only off-shell e^+e^- circulate inside the loop. Also, the apparent non-conservation of energy is explained, since the dispersive integral is done along the loop model imaginary part cut, where the initial energy is indeed sufficient to get on-shell constituents. In other words, the standard approach convolution amplitudes are constructed like in "old-fashioned perturbation theory". In the context of quantum field theory, their natural framework is dispersion theory.

Second, the spin projections are treated covariantly, since we took the BS vertex Γ_{BS} with its spin structure replaced by γ_5 or $\not{\epsilon}$ ($F_B(q_0, \mathbf{q})$ is a scalar), a replacement dictated by the bound state properties under parity and charge conjugation. This allows us to identify the correct covariant spin projectors for the e^+e^- pair, and to preserve manifest gauge invariance. This is more adequate since it is the moving electron-positron pair annihilating into photons that must be constrained to the required spin state.

Using dispersion relations to reduce the BS loop has the great advantage over approximate methods of being *exact*. Starting with a four-dimensional BS form factor or vertex function $\Gamma_{BS} \sim F_B(q_0, \mathbf{q})$, the dispersion

relations alone enforce $q_0 = 0$, i.e. the energy-dependence is set to zero, and no approximation for the energy part of the wavefunction are needed. This allows us to work in a formally relativistic environment; standard Quantum Field Theory techniques are thereby applicable.

Finally, when there is a virtual photon, or for three or more photon decay channels, the standard approach formula appears hopelessly wrong, since it neglects all the oblique cuts



Indeed, it is important to realize that only the vertical cuts need to be considered to reproduce (2.2). Since Cutkoski rule implies that all the cuts must be taken into account in order to produce analytical decay amplitudes, there is no way, using the standard formalism, to get analytical results. In other words, a perturbation theory starting with (2.2) as the lowest order basis will predict incorrect photon spectra.

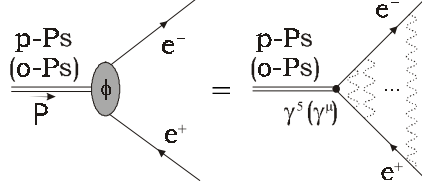
2.2 Lowest Order Decay Amplitudes

We have just seen that positronium amplitudes are built as loop amplitudes: the positronium couples to a virtual e^+e^- loop, to which a given number of photons are attached. This loop structure is essential, because oblique cuts have to be included. The coupling of positronium to its constituents is essentially determined by the positronium quantum numbers and wavefunction. Since the Schrödinger wavefunction contains the effects of the exchange of infinitely many Coulomb photons among the constituents (in the ladder approximation) [73], these effects are included also in the form factor. This choice of lowest order basis solves all the problems mentioned in the previous section.

A very simple method can be used to effectively compute such loop amplitudes: *any lowest order loop amplitude with a Coulomb form factor is the derivative with respect to the positronium mass of the corresponding point-like amplitude.* By point-like amplitude is meant the loop amplitude obtained by replacing the complicated Coulomb form factor for the bound state by a constant form factor. Symbolically, for parapositronium (orthopositronium) decay to an even (odd) number of real or virtual photons, the amplitude is

$$\begin{array}{c} \text{p-Ps} \\ \text{(o-Ps)} \\ \overrightarrow{P} \end{array} \left[\begin{array}{c} \text{e}^- \\ \text{e}^+ \end{array} \right] \phi \sim \frac{\partial}{\partial P^2} \left[\begin{array}{c} \text{p-Ps} \\ \text{(o-Ps)} \\ \overrightarrow{P} \end{array} \left[\begin{array}{c} \text{e}^- \\ \text{e}^+ \end{array} \right] \gamma^s (\gamma^s) \right]$$

where ϕ represents the Schrödinger wavefunction form factor, i.e.



and dashed photon lines stand for Coulomb photons.

The loop amplitude will constitute our new lowest order basis for perturbation theory. Its properties will be discussed later on. Extension to higher orders will be briefly commented at the end of the chapter.

2.2.1 A Simple Formula

Let us express mathematically the previous qualitative assertion, using the language of dispersion relations. The point-like loop amplitude (subscript p) can be computed from its imaginary part

$$\text{Im } \mathcal{T}_p (P^2) \equiv \text{Im } \mathcal{M}_p (Ps (P^2) \rightarrow n\gamma)$$

using an unsubtracted dispersion relation with $s = P^2$:

$$\mathcal{T}_p (M^2) = \text{Re } \mathcal{T}_p (M^2) = \frac{1}{\pi} \int_{4m^2}^{\infty} \frac{ds}{s - M^2} \text{Im } \mathcal{T}_p (s) \quad (2.9)$$

($\mathcal{T}_p (M^2) = \text{Re } \mathcal{T}_p (M^2)$ since $M < 2m$). The Schrödinger form factor which accounts for the non-trivial coupling of the bound state to its constituent is of the form

$$F_B (0, \mathbf{q}) = C \phi_o \mathcal{F} (\mathbf{q}^2) (\mathbf{q}^2 + \gamma^2) \quad \text{with } \mathcal{F} (\mathbf{q}^2) = \frac{8\pi\gamma}{(\mathbf{q}^2 + \gamma^2)^2} \quad (2.10)$$

where one can recognize $\phi (\mathbf{q}^2) \equiv \phi_o \mathcal{F} (\mathbf{q}^2)$ as the fundamental ($n = 1$) S -wave Schrödinger momentum space wavefunction. When expressed in terms of the dispersion relation variable, this form factor is only a function of the initial energy s (see appendix A.1.1):

$$F_B (s) = C \phi_o \frac{32\pi\gamma}{s - M^2}$$

The core of the derivative approach emerges from the observation that inserting F_B in (2.9) is equivalent to taking the derivative with respect to M^2

$$\begin{aligned} \mathcal{T}_{Coul} (M^2) &= \frac{1}{\pi} \int_{4m^2}^{+\infty} \frac{ds}{s - M^2} F_B (s) \text{Im } \mathcal{T}_p \\ &= (32\pi C \phi_o \gamma) \frac{1}{\pi} \int_{4m^2}^{+\infty} \frac{ds}{(s - M^2)^2} \text{Im } \mathcal{T}_p \end{aligned}$$

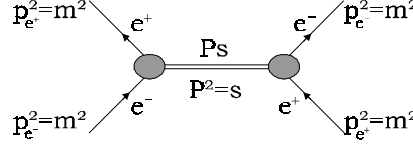
hence

$$\boxed{\mathcal{T}_{Coul} (M^2) = (32\pi C \phi_o \gamma) \frac{\partial}{\partial M^2} \mathcal{T}_p (M^2)} \quad (2.11)$$

which is the desired result. The case of other parapositronium decay channels, or orthopositronium decay modes is similarly treated (simply replace γ^5 by $\not{\epsilon}$ with ϵ^μ the orthopositronium polarization vector).

Remark that the form factor is inserted directly into the dispersion integral, and not in Feynman amplitudes (like in (2.1) or (2.3)). These two approaches are equivalent only in the punctual case (consider the momentum

flow through the form factor in each case). Working at the level of dispersion relations is much more in the spirit of the Bethe-Salpeter equation. Indeed, the wavefunction is extracted from the four-point Green's function, i.e. in configurations with an off-shell bound state (above threshold), and on-shell constituents:

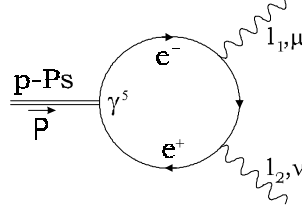


The picture shows that both the Bethe-Salpeter vertex and the dispersion integral (2.9) make use of the form factor F_B with the same kinematical configuration (diagrams with bremsstrahlung radiation off the electron lines are treated similarly). Further, we have seen that because of the momentum dependence of the form factor, neither (2.1) nor (2.3) is gauge invariant. Now, since the imaginary part of the point-like amplitude is gauge invariant, the decay amplitudes are constructed in a manifestly gauge invariant way.

The properties of our approach will be discussed at the end of the present section. Before, we will give two illustrative examples.

2.2.2 First Example: Parapositronium to Two Photons

The point-like amplitude for the decay $p\text{-}Ps \rightarrow \gamma\gamma$ is obtained by replacing the positronium and its Coulomb form factor by an elementary, point particle with a pseudoscalar γ_5 coupling to the electron current (with unit coupling constant)



plus the crossed process. The point bound state amplitude is fully relativistic, and standard loop integration techniques can be used. Explicitly, the point-like amplitude is (the subscript p is a reminder for point-like):

$$\begin{aligned} \mathcal{M}_p(p\text{-}Ps \rightarrow \gamma\gamma) &= ie^2 \int \frac{d^4q}{(2\pi)^4} \text{Tr} \{ \Gamma^{\mu\nu} \} \varepsilon_\mu(l_1) \varepsilon_\nu(l_2) \\ \Gamma^{\mu\nu} &= \gamma_5 \frac{1}{\not{q} + \not{l}_1 - m} \gamma^\mu \frac{1}{\not{q} - m} \gamma^\nu \frac{1}{\not{q} - \not{l}_2 - m} \\ &\quad + \gamma_5 \frac{1}{\not{q} + \not{l}_2 - m} \gamma^\nu \frac{1}{\not{q} - m} \gamma^\mu \frac{1}{\not{q} - \not{l}_1 - m} \end{aligned}$$

Carrying the trace, we readily obtain

$$\mathcal{M}_p(p\text{-}Ps \rightarrow \gamma\gamma) = -8m e^2 \varepsilon^{\mu\nu\rho\sigma} l_{1,\rho} l_{2,\sigma} \varepsilon_\mu(l_1) \varepsilon_\nu(l_2) \frac{\mathcal{I}_p(M^2)}{M^2}$$

where the dimensionless⁶ loop integral form factor is

$$\mathcal{I}_p(P^2) = \frac{-i}{(4\pi)^2} F \left[\frac{4m^2}{P^2} \right] \quad \text{with } F[a] = 2 \arctan^2(a-1)^{-1/2} \quad (2.12)$$

⁶ This criterion comes in because the dispersion relations (2.9) is built on the whole amplitude, and not just the loop form factor.

(the form factor function $F[a]$ for $a < 1$ can be defined from the above by analytic continuation). From the amplitude, the decay width is

$$\Gamma_p(p\text{-}Ps \rightarrow \gamma\gamma) = 16\pi\alpha^2 \frac{m^2}{M} |\mathcal{I}_p(M^2)|^2 = \frac{\pi M\alpha^2}{256} \left(1 + \frac{4\gamma^2}{M^2}\right) \left(\frac{4}{\pi^2} \arctan^2 \frac{M}{2\gamma}\right)^2 \quad (2.13)$$

where $\gamma^2 = m^2 - M^2/4$ is related to the binding energy $E_B = M - 2m$.

Coulomb Form Factor

To get the physical positronium decay amplitude and rate, simply replace in (2.13) the loop form factor $\mathcal{I}_p(M^2)$ by its derivative

$$\mathcal{I}_{Coul}(M^2) = (32\pi C\phi_o\gamma) \frac{\partial}{\partial M^2} \mathcal{I}_p(M^2) \quad (2.14)$$

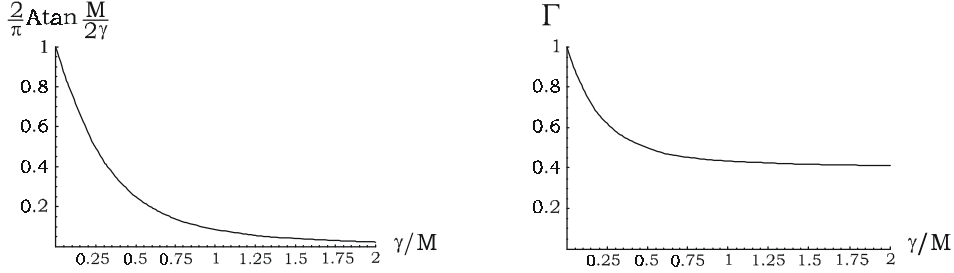
where ϕ_o is the S -wave fundamental state Schrödinger wavefunction at zero separation, and $C = \sqrt{M}/m$ is obtained by matching the static limit (i.e. $\gamma \rightarrow 0$) with the well-known lowest order result $\Gamma_{p\text{-}Ps} = m\alpha^5/2$ (See Appendix A.1.2). This gives

$$\mathcal{I}_{Coul}(M^2) = -i \frac{C\phi_o}{M} \left[\frac{2}{\pi} \arctan \frac{M}{2\gamma} \right]$$

The factor in square brackets is equal to 1 in the limit $\gamma \rightarrow 0$. Using $|\phi_o|^2 = \alpha^3 m^3/8\pi$, the decay rate into two photons is

$$\Gamma(p\text{-}Ps \rightarrow \gamma\gamma) = \frac{\alpha^5 m}{2} \left(1 + \frac{4\gamma^2}{M^2}\right) \left| \frac{2}{\pi} \arctan \frac{M}{2\gamma} \right|^2 \quad (2.15)$$

The decay rate is a decreasing function of the binding energy:



Enhanced Convergence

The result (2.15) contains some effects of the Coulomb interactions among the constituents, at all orders in α . Indeed, using $\gamma^2 = m^2 - M^2/4 \approx m^2\alpha^2/4$, the form factor can be expanded as (see the discussion in the appendix A.1.2)

$$\begin{aligned} \Gamma(p\text{-}Ps \rightarrow \gamma\gamma) &= \frac{\alpha^5 m}{2} \left(1 + \frac{4\gamma^2}{M^2}\right) \left(1 - \frac{4}{\pi} \frac{\gamma}{M} + \frac{16}{3\pi} \frac{\gamma^3}{M^3} - \mathcal{O}\left(\frac{\gamma^5}{M^5}\right)\right)^2 \\ &= \frac{\alpha^5 m}{2} \left(1 - 2\frac{\alpha}{\pi} + \mathcal{O}(\alpha^2)\right) \\ &\approx \frac{\alpha^5 m}{2} (1 - 0.637\alpha + \mathcal{O}(\alpha^2)) \end{aligned}$$

In other words, the binding energy effects included in our lowest order computation already account for a great deal of the relativistic and radiative corrections as presented in the literature (see chapter 1), namely,

$$\Gamma_{p-Ps} = \frac{\alpha^5 m}{2} (1 - \delta\Gamma_{p-Ps}) \quad (2.16)$$

where

$$\begin{aligned} \delta\Gamma_{p-Ps} &= A_p \frac{\alpha}{\pi} + 2\alpha^2 \ln \frac{1}{\alpha} + B_p \frac{\alpha^2}{\pi^2} - \frac{3\alpha^3}{2\pi} \ln^2 \frac{1}{\alpha} + C_p \frac{\alpha^3}{\pi} \ln \frac{1}{\alpha} + \delta_{4\gamma} \frac{\alpha^2}{\pi^2} \\ &\text{with } \begin{aligned} A_p &= 2.5326 & C_p &= -7.919 \quad (1) \\ B_p &= 5.14 \quad (30) & \delta_{4\gamma} &= 0.274 \quad (1) \end{aligned} \end{aligned} \quad (2.17)$$

Numerically, we can write

$$\Gamma_{p-Ps} = \frac{\alpha^5 m}{2} \frac{4m^2}{M^2} \left(\frac{2}{\pi} \arctan \frac{M}{2\gamma} \right)^2 (1 - \delta\Gamma'_{p-Ps})$$

with the same series (2.17), but with the reduced coefficients

$$\begin{aligned} A'_p &\approx 0.5326 \\ B'_p &\approx 0.607 \\ C'_p &\approx -3.919 \end{aligned}$$

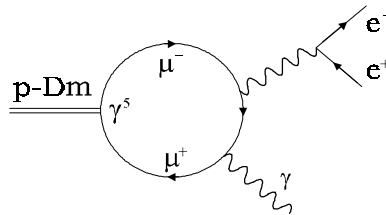
This last form is very interesting because binding energy corrections (i.e. γ dependent) are singled out, while the resulting purely perturbative (radiative and relativistic) corrections are much reduced. This means that one could, at least in principle, express the decay rate as a lowest order result, non-perturbative in the binding energy, times a rapidly converging perturbation series of radiative corrections. This is exactly what we have achieved.

Note finally that the corrections obtained here do not originate from oblique cuts, since there are no such cuts for the two real photon decay. Rather, they originate in the many relativistic effects we are summing by considering a four-dimensional loop model, and from the infinite sum of Coulomb photon contained inside the form factor. In the appendix A.1.2, the relation between the above correction and the spreading of the wavefunction (and to the Sommerfeld factor), are exposed.

2.2.3 Second Example: Paradimuonium and Low's Theorem

The paradimuonium decay $p-Dm \rightarrow \gamma e^+ e^-$ is the simplest QED bound state decay process where Low's theorem implications can be illustrated. The paradimuonium is the 1S_0 , $\mu^+ \mu^-$ electromagnetic bound state [95], [111]. In appendix A.1.4, the decay $K_S \rightarrow e^+ e^- \gamma$ is presented. This elementary particle decay process shares many interesting similarities with the present QED bound state case, especially regarding the enforcement of analyticity.

Following the same steps as for $p-Ps \rightarrow \gamma\gamma$, we first consider the point-like amplitude



(plus the crossed diagram) with the result

$$\Gamma_p(p-Dm \rightarrow e^+ e^- \gamma) = \frac{16\alpha^3 m^2}{3M} \int_0^{1-a_e} dx_\gamma |\mathcal{I}_p(M^2, x_\gamma)|^2 \rho(x_\gamma, a_e) \quad (2.18)$$

$$\text{with } \rho(x_\gamma, a_e) = \sqrt{1 - \frac{a_e}{1-x_\gamma}} [2(1-x_\gamma) + a_e] \frac{x_\gamma^3}{(1-x_\gamma)^2}$$

$$\mathcal{I}_p[P^2, x_\gamma] = \frac{-i}{(4\pi)^2} \frac{1}{x_\gamma} \left(F \left[\frac{4m^2}{M^2} \right] - F \left[\frac{4m^2}{M^2} \frac{1}{1-x_\gamma} \right] \right)$$

where m is the muon mass, M the dimuonium mass, x_γ the reduced photon energy $2E_\gamma/M$, $a_e = 4m_e^2/M^2$, m_e the electron mass, and with the function F defined in (2.12). In the limit $x_\gamma \rightarrow 0$, the spectrum $d\Gamma_p/dx_\gamma$ goes to zero as x_γ^3 as predicted by Low's theorem (the amplitude behaves as x_γ , and an additional factor x_γ comes from phase-space).

Taking the derivative of \mathcal{I}_p to get the corresponding Coulomb form factor, we find

$$\begin{aligned} \mathcal{I}_{Coul}(M^2, x_\gamma) &= (32\pi C\phi_o\gamma) \frac{\partial}{\partial M^2} \mathcal{I}_p(M^2, x_\gamma) \\ &= -i \frac{C\phi_o}{M} \frac{1}{x_\gamma} \left(\frac{2}{\pi} \arctan \frac{M}{2\gamma} - \frac{4\gamma y_\gamma}{\pi M} \arctan y_\gamma \right) \end{aligned} \quad (2.19)$$

$$\text{where } y_\gamma \equiv \left(\frac{4m^2}{M^2(1-x_\gamma)} - 1 \right)^{-1/2}$$

The decay rate is then obtained by replacing \mathcal{I}_p by \mathcal{I}_{Coul} in (2.18)

$$\Gamma(p-Dm \rightarrow e^+ e^- \gamma) = \frac{\alpha^6 m}{6\pi} \frac{4m^2}{M^2} \int_0^{1-a_e} dx_\gamma \left| \frac{2}{\pi} \arctan \frac{M}{2\gamma} - \frac{4\gamma y_\gamma}{\pi M} \arctan y_\gamma \right|^2 \frac{\rho(x_\gamma, a_e)}{x_\gamma^2}$$

Binding Energy Expansion and Analyticity

It is very instructive to analyze in some details this result. Consider the static limit $\gamma \rightarrow 0$ for the form factor:

$$\lim_{\gamma \rightarrow 0} \mathcal{I}_{Coul}(M^2, x_\gamma) = -i \frac{C\phi_o}{M x_\gamma} \quad (2.20)$$

In that limit, the standard lowest order result for the decay rate is recovered

$$\Gamma(p-Dm \rightarrow e^+ e^- \gamma) \stackrel{\gamma \rightarrow 0}{=} \frac{\alpha^6 m}{6\pi} \int_0^{1-a_e} dx_\gamma \frac{\rho(x_\gamma, a_e)}{x_\gamma^2}$$

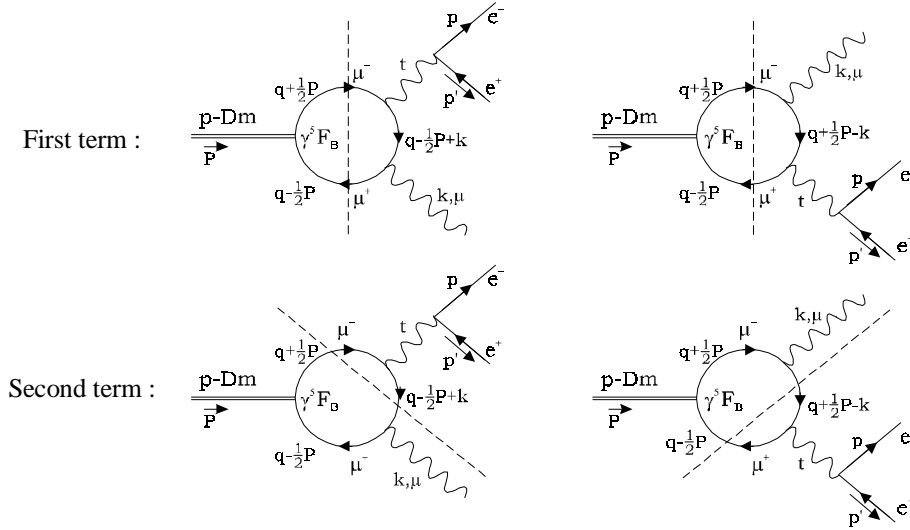
However, the differential rate $d\Gamma/dx_\gamma$ has a wrong behavior when $x_\gamma \rightarrow 0$. The spectrum is linear (in x_γ) in the limit $\gamma \rightarrow 0$, in contradiction with Low's theorem. Therefore, it appears that, contrary to the two real photon case, the limit $\gamma \rightarrow 0$ is far from smooth. It is inconsistent to consider both the soft-photon limit and the on-shell limit simultaneously. Explicitly, the incompatibility of the two limits is obvious if $x_\gamma \rightarrow 0$ is taken first

$$\begin{aligned} \lim_{x_\gamma \rightarrow 0} \mathcal{I}_{Coul}(M^2, x_\gamma) &= -i \frac{C\phi_o}{M\pi} \left(\frac{M}{2\gamma} + \left(1 + \frac{M^2}{4\gamma^2} \right) \arctan \frac{M}{2\gamma} \right) \\ &= -i \frac{C\phi_o}{M} \left(\frac{M^2}{8\gamma^2} + \frac{1}{2} - \frac{4\gamma}{3M\pi} + \dots \right) \end{aligned} \quad (2.21)$$

Mathematically, what these considerations show is that the limit $\gamma \rightarrow 0$ does not exist at $x_\gamma = 0$. It should be clear that one of the main virtues of our approach is its non-perturbative treatment of γ , leading to correct photon spectra.

The contradiction between analyticity and the static limit, i.e. the basis around which the NRQED perturbation theory is built, can be traced back to two different sources.

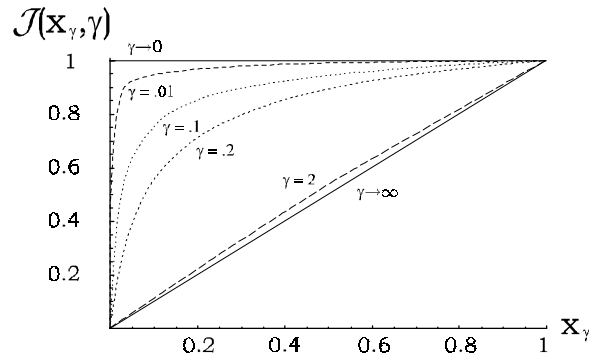
First, the second term of $\mathcal{I}_{Coul}(M^2, x_\gamma)$ (2.19) comes from the oblique cuts in the imaginary part (i.e. processes like $p-Dm \rightarrow \mu^+ \mu^- \gamma$ times $\mu^+ \mu^- (\gamma) \rightarrow e^+ e^- (\gamma)$)



Those are the processes neglected in standard approaches, because they are formally of order γ relative to vertical cuts processes (see (2.19)). This is an inconsistent approximation since it is the sum of the two terms of $\mathcal{I}_{Coul}(M^2, x_\gamma)$ that enforces Low's theorem. This can be seen by plotting

$$\mathcal{J}(x_\gamma, \gamma/M) = 1 - \frac{\frac{2\gamma}{M} y_\gamma \arctan y_\gamma}{\arctan \frac{M}{2\gamma}}$$

for $M = 1$ and various values of γ



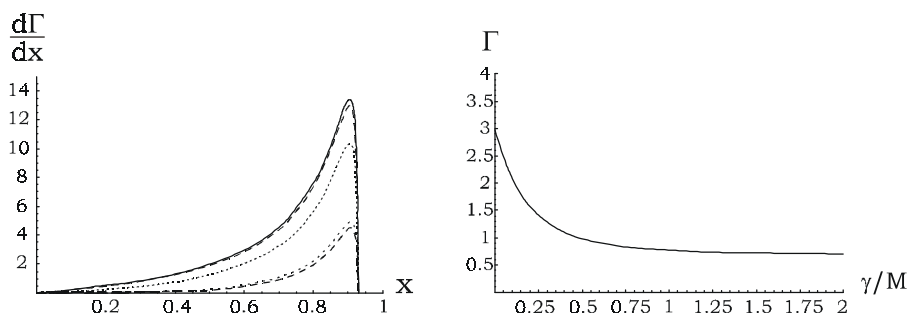
Therefore, two terms that would be treated as different orders in the NRQED perturbation series are needed simultaneously to enforce Low's theorem.

The second source of the NRQED problems is apparent on the picture and in (2.21). The form factor is not analytical on the whole phase-space when $\gamma = 0$. As the picture shows, even if $\gamma/M \ll 1$ for QED bound states, the limit $\gamma \rightarrow 0$ is not to be taken because it is singular. A breakdown occurs when the energy of the photon, x_γ , is of the order of γ/M . Furthermore, as a matter of principle, since the non-perturbative result is

not analytic, it cannot be expanded as a series in γ , and the NRQED perturbation series is not to be expected to converge. Needless to say, this is a serious drawback.

Total and Differential Rates

The binding energy effects on the spectrum and differential rate amount to overall suppression. As function of the binding energy, we have, for $a_e = .07$



The various curves in the first graph correspond to $\gamma = 0, .01, .1, 1, \infty$ (top to bottom). The distortions generated by the form factor on the low-energy end of the spectrum are not apparent, because of the spectrum function $\rho(x_\gamma, a_e)$, which is highly peaked near $x = 1 - a_e$. In particular, the singular transition from a x_γ^3 to a linear x_γ behavior near $x_\gamma = 0$ when $\gamma \rightarrow 0$ does not appear. Note that, as is the case for the two-photon decay mode, it is the factor $4m^2/M^2$ which is responsible for the non-vanishing of the rate as $\gamma \rightarrow \infty$.

More importantly, it can be shown by a numerical integration that the contribution of the oblique cuts to the total rate is of relative order γ and higher (their interference with vertical cut is of order γ , while alone, they stand at the order γ^2). In other words, while their presence is essential to get a correct spectrum, they can be omitted if one is interested in the total rate to lowest accuracy. The singular behavior of the spectrum is smeared out by the phase-space integration.

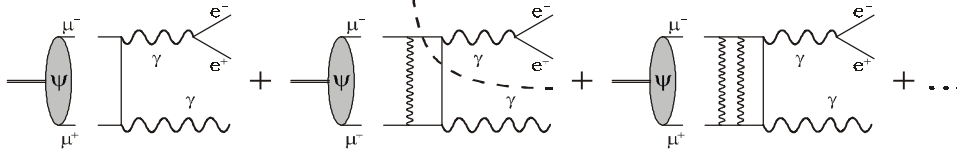
2.2.4 Conclusion

A new lowest order basis is proposed, along with a simple computation scheme. This new basis is manifestly gauge invariant, and formally relativistic. We want now to spend some time to analyze the enhanced convergence property, and then the analytical properties.

To understand why the binding energy correction we obtained can be interpreted as part of the relativistic and radiative corrections computed in the literature, it suffices to notice that the first order radiative corrections do contain a Coulomb photon exchange. Further, some relativistic corrections are simply generated in our approach because the propagators of the loop are treated exactly (no approximation for the spinors), and because the spin part of the wavefunction is taken as covariant. What is interesting is that our approach offers a simple computation scheme accounting for many non-trivial corrections. The remaining perturbation series converges much more rapidly. The special feature of bound state perturbation series, i.e. their slow convergence, is clearly identified as a binding energy effect, and we are now able to factorize it from the start. Further, it is especially clean in separating the effects of the binding energy from the purely radiative corrections. This is of interest, especially regarding QCD bound states, since there, the binding energy is not simply related to α_S .

The most interesting part of our result is of course its analytical properties. That is where it is really superior to the NRQED approach. The reason is simple to understand: when a soft photon is emitted, the scaling rules of NRQED are violated. The emitted photon energy is of the same order as the binding energy. One can therefore expect that a resummation of NRQED amplitudes will be necessary. Let us see how this arises.

In the context of NRQED, one would consider the oblique cuts as arising from higher order corrections,



In the second graph, we have illustrated a possible higher order reconstruction of the oblique cut. However, each of these graphs is separately badly behaved analytically, because at all stages one is selecting an initial state made of free e^+e^- . In other words, for a given vertical cut, the corresponding oblique cuts are always introduced at higher orders. Obviously, it is only by summing the whole series that the emitted photon will truly feel the binding of the charged particles. Our method of integrating the loop with its Coulomb form factor sums a minimal class of contributions so that the amplitude is well-behaved analytically. In other words, the infinite Coulomb photon summation contained in the form factor (or wavefunction) is not factorized from the decay process. This is a radical difference between NRQED and our approach.

The fact that an infinite summation is necessary is especially obvious from the behavior of the non-perturbative result we found. The energy spectrum of the photon in $p\text{-}Dm \rightarrow e^+e^-\gamma$ cannot be expressed perturbatively as a series in γ . Its low-energy point requires an exact treatment of γ .

In conclusion, NRQED is unable to describe the end-points of energy spectra, because of a violation of the momentum scaling rules at those phase-space points. Our method is a consistent resummation scheme, and, being sufficiently non-perturbative in the binding energy, the photon spectrum becomes well-behaved over the whole phase-space. We therefore obtain an analytical basis for perturbation theory. The perturbative treatment of higher orders will be discussed later. For total rates, our method offers a possibility to factorize binding energy corrections from purely radiative corrections.

2.3 Orthopositronium Decay

We now apply our method to the orthopositronium decay to three photons. This is a very interesting decay process.

In the first subsection, we shortly recall what is the lowest order basis chosen in standard computations, namely the Ore-Powell amplitude [63], and emphasize its analytical defects.

In the second subsection, the lowest order result we will obtain by integrating the loop with the Coulomb form factor inserted will be seen to be well-defined analytically. Further, our result will again show that a perturbation around $\gamma = 0$ is ill-defined. Also, we will again find that the bulk of the radiative corrections is accounted for already at our lowest order.

In the appendix A.2, one can find a detailed analysis of the three-photon phase-space, including tools to integrate over that three-body phase-space numerically. Also, the derivation of the Euler-Heisenberg Lagrangian, as well as the explicit expressions for the two-point photon function to one and two loops and for the four-point photon function to one loop are given.

2.3.1 Ore-Powell Spectrum

From the requirement of gauge invariance, and because of the quantum numbers of the initial and final particles involved (neutral self-conjugate bosons), Low's theorem predicts that *the decay amplitude must vanish linearly*

when the energy of one of the photons is going to zero

$$\mathcal{M}(o\text{-Ps} \rightarrow \gamma\gamma\gamma) \stackrel{\omega \rightarrow 0}{\sim} \mathcal{O}(\omega)$$

with ω the energy of one of the photons. The squared modulus of the amplitude therefore behaves as $\mathcal{O}(\omega^2)$ for small photon energy. Aside from that, the three-photon phase-space alone (i.e. with a constant decay amplitude) gives a differential rate as

$$\left. \frac{d\Gamma(o\text{-Ps} \rightarrow \gamma\gamma\gamma)}{dx} \right|_{\text{Phase-Space}} \sim x \quad (2.22)$$

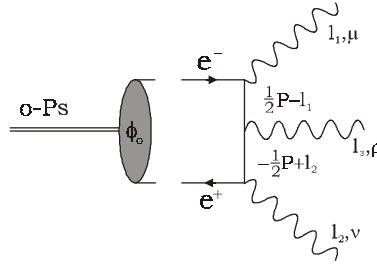
with $x = 2\omega/M$ the reduced photon energy, M the orthopositronium mass. Combining the amplitude with the phase-space, one finds that the low-energy end of the photon spectrum **must** behave as

$$\frac{d\Gamma(o\text{-Ps} \rightarrow \gamma\gamma\gamma)}{dx} \stackrel{x \rightarrow 0}{\sim} x^3$$

The standard approach at lowest order states that the orthopositronium decay rate is to be computed with the formula

$$\Gamma(o\text{-Ps} \rightarrow \gamma\gamma\gamma) = \frac{1}{3} |\phi(0)|^2 (4v_{rel}\sigma(e^-e^+ \rightarrow \gamma\gamma\gamma))_{v_{rel} \rightarrow 0}$$

with v_{rel} the relative velocity of the e^+e^- in their center-of-mass frame, and $\psi(0)$ the positronium Schrödinger wavefunction at zero separation (m is the electron mass).



As the picture shows (crossed processes are not drawn), this formula states that in first approximation, the positronium decay rate can be computed from the static limit of the scattering cross section $e^+e^- \rightarrow \gamma\gamma\gamma$ (initial particles at rest). Equivalently, it is found from the squared modulus amplitude for an e^+e^- pair at rest into $\gamma\gamma\gamma$. Summed over photon polarizations, this is easily shown to be [63]

$$\sum_{\text{polarizations}} \left| \mathcal{M}((e^+e^-)_{v_{rel}=0} \rightarrow \gamma\gamma\gamma) \right|^2 = \frac{(1-x_1)^2}{x_2^2 x_3^2} + \frac{(1-x_2)^2}{x_1^2 x_3^2} + \frac{(1-x_3)^2}{x_1^2 x_2^2}$$

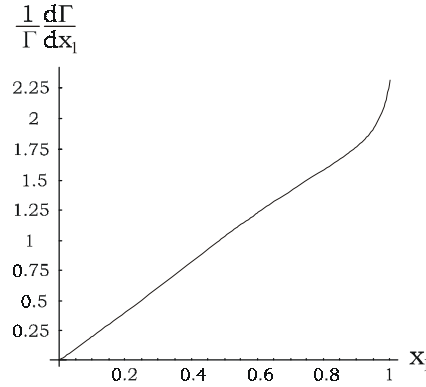
This modulus squared behaves as a constant when one of the x_i is vanishing (as can be seen by using energy-momentum conservation $x_1 + x_2 + x_3 = 2$, see appendix A.2 for details on the three-photon phase-space kinematics), while it should vanish as x_i^2 from Low's theorem. In turn, the well-known differential rate inherits an incorrect analytical behavior

$$\frac{d\Gamma(o\text{-Ps} \rightarrow \gamma\gamma\gamma)}{dx_1} = \frac{2\alpha^6 m}{9\pi} \Omega(x_1)$$

where the spectrum function is

$$\begin{aligned}
 \Omega(x_1) &= \int_{1-x_1}^1 dx_2 \left| \mathcal{M} \left((e^+ e^-)_{v_{r\epsilon l}=0} \rightarrow \gamma\gamma\gamma \right) \right|_{x_3=2-x_1-x_2}^2 \\
 &= \frac{2(2-x_1)}{x_1} + \frac{2(1-x_1)x_1}{(2-x_1)^2} + 4 \left[\frac{(1-x_1)}{x_1^2} - \frac{(1-x_1)^2}{(2-x_1)^3} \right] \ln(1-x_1) \\
 &= \frac{5}{3}x_1 + \mathcal{O}(x_1^2) \text{ near } x_1 = 0
 \end{aligned} \tag{2.23}$$

The (normalized) differential rate can be plotted



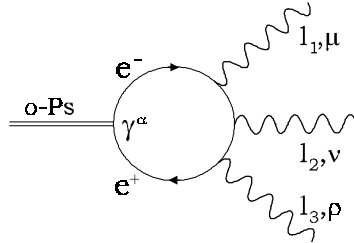
In the Ore-Powell model, the photon energy spectrum vanishes only linearly near zero, instead of the required $\Omega(x_1) = \mathcal{O}(x_1^3)$. In other words, this decay spectrum does violate the basic requirement of analyticity.

For completeness, recall that it is this differential rate that gives the total width

$$\Gamma(o\text{-Ps} \rightarrow \gamma\gamma\gamma) = \frac{2(\pi^2 - 9)}{9\pi} \alpha^6 m \quad \text{since} \quad \int_0^1 dx_1 \Omega(x_1) = \pi^2 - 9$$

2.3.2 Point-like Amplitude

The point-like amplitude is the standard light-by-light box diagram



plus five other ordering of the photon insertions. The amplitude can be found in many places [113], [205], see appendix A.2. The tensor $G_\alpha^{\lambda_1 \lambda_2 \lambda_3}$ describing the transition from an off-shell photon to three on-shell photons of helicity states $\lambda_1 \lambda_2 \lambda_3$ is such that

$$\sum_{\lambda_1 \lambda_2 \lambda_3} (G_\alpha^{\lambda_1 \lambda_2 \lambda_3} G^{*\lambda_1 \lambda_2 \lambda_3, \alpha}) = \frac{2^4 \alpha^3}{\pi} [R(123) + R(213) + R(312)]$$

where $R(123) \equiv R(x_1, x_2, x_3, a)$ (x_i is the reduced energy of the photon i and $a = 4m^2/M^2$). The $R(ijk)$ are given in terms of individual dimensionless helicity amplitudes as

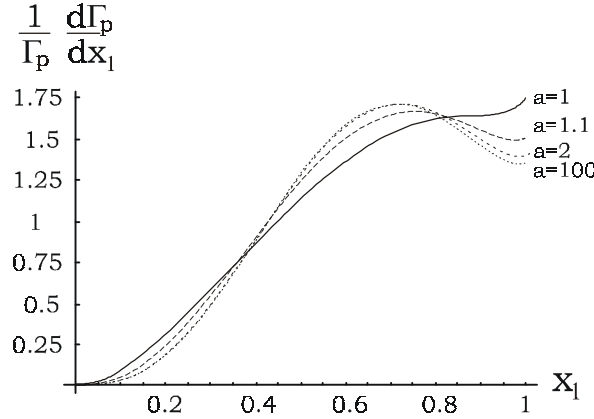
$$\begin{aligned}
 R(123) = & \frac{1}{3} \left| E_{-++}^{(2)}(123) \right|^2 + \left| E_{+++}^{(2)}(123) \right|^2 \\
 & + \frac{x_1}{x_2 x_3 (1-x_1)} \left| E_{-++}^{(1)}(213) \right|^2 + \frac{1}{x_1^2} \left| E_{+++}^{(1)}(123) + E_{+++}^{(1)}(132) \right|^2 \\
 & + \frac{(1-x_2)(1-x_3)}{x_1^2(1-x_1)} \left| \frac{1}{1-x_2} E_{+++}^{(1)}(123) - \frac{1}{1-x_3} E_{+++}^{(1)}(132) \right|^2
 \end{aligned} \tag{2.24}$$

The helicity amplitudes $E_{\pm\pm\pm}^{(n)}$ are complicated functions of x_i and a given in appendix A.2. The decay rate of a point-like vector positronium to three photons is then

$$\Gamma_p(o\text{-}Ps \rightarrow \gamma\gamma\gamma) = \frac{1}{9} \frac{\alpha^3}{2^5 \pi^4} M \int dx_1 dx_2 [R(123) + R(213) + R(312)]$$

with the three-body phase space written in terms of reduced photon energies as $\int d\Phi_3 = M^2 \int dx_1 dx_2 / 2^7 \pi^3$ (see [113], [23], appendix C.3).

Of special interest is the behavior of the low-energy end of the differential rate. For various values of the ratio $a = 4m^2/M^2$ (i.e. of the binding energy $E_B = M - 2m$), the photon spectrum, normalized to the total rate is



Sufficiently close to zero, the behavior is always like x_1^3 , as required by Low's theorem. As a increases, the x^3 behavior is getting more and more pronounced. In the limit $a \rightarrow \infty$, the normalized spectrum is

$$\frac{1}{\Gamma_p} \frac{d\Gamma_p}{dx_1} \stackrel{a \rightarrow \infty}{\approx} \frac{5}{17} x_1^3 \left(\frac{343}{3} - 207x_1 + \frac{973}{10} x_1^2 \right)$$

which is, as expected, the spectrum obtained from the Euler-Heisenberg effective theory [201]

$$\mathcal{L}_{E-H} = \frac{\alpha^2}{90m^4} \left[(F_{\mu\nu} F^{\mu\nu})^2 + \frac{7}{4} (F_{\mu\nu} \tilde{F}^{\mu\nu})^2 \right]$$

2.3.3 Coulomb Form factor and Ore-Powell Spectrum

To insert the Schrödinger wavefunction form factor, we define modified helicity amplitudes according to (2.11)

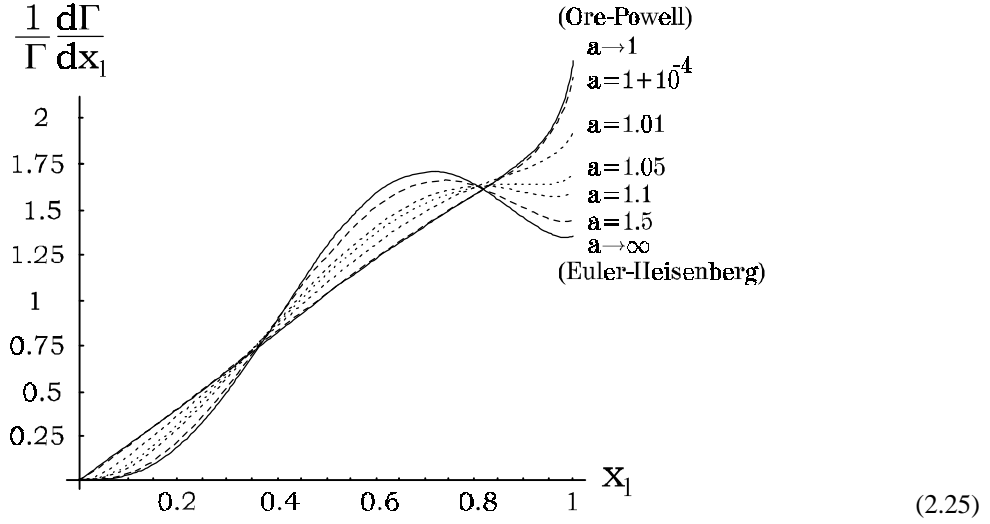
$$E_{\pm\pm\pm, Coul}^{(n)}(ijk, M^2) = (32\pi C \phi_o \gamma) \frac{\partial}{\partial M^2} E_{\pm\pm\pm}^{(n)}(ijk, M^2)$$

The resulting decay amplitude, and decay rate are constructed as in the punctual case, and we reach

$$\Gamma(o-Ps \rightarrow \gamma\gamma\gamma) = \alpha^6 m \frac{2}{9\pi} \left(\frac{4m^2}{M^2} \right)^2 \left(\frac{\mathcal{R}}{2\pi^2} \right)$$

$$\text{with } \mathcal{R} \equiv \int dx_1 dx_2 (R_{Coul}(123) + R_{Coul}(213) + R_{Coul}(312))$$

R_{Coul} is given by (2.24) with $E_{\pm++}^{(i)}$ in place of $E_{\pm++}^{(i)}$. Integrating over x_2 , we get the photon spectrum for various values of a



As long as $a \neq 1$, the spectrum behavior is in x_1^3 close to zero, i.e. roughly in the range $x_1 \in [0, a - 1]$. The properties of this spectrum as a varies are completely similar to that of $p-Dm \rightarrow \gamma e^+ e^-$, and one can show that the limits $\gamma \rightarrow 0$ and $x_1 \rightarrow 0$ are again incompatible. Contrary to that case, however, it is interesting to see that because of the highly correlated three-photon phase-space, the behavior of the spectrum at high energy is strongly dependent of its behavior at low energy. Therefore, the small effect of the binding energy on the emission of soft photons completely alters the shape of the spectrum.

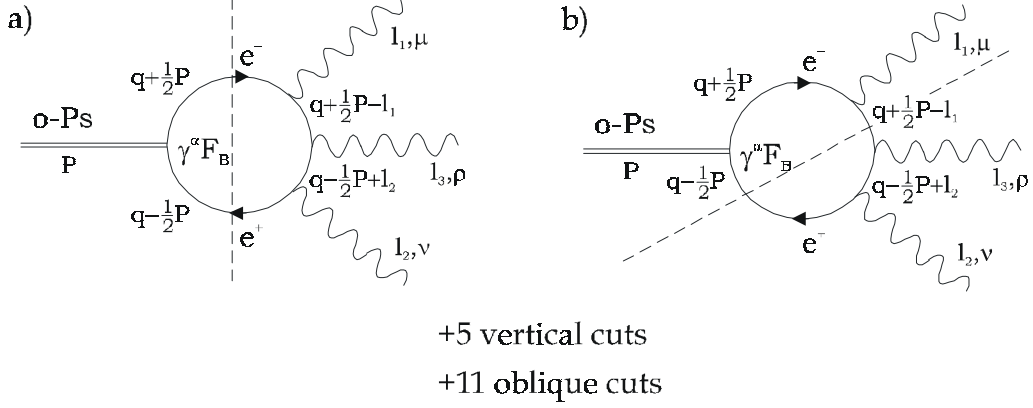
Looking at the wavefunction, it also appears that the behavior of the spectrum can be understood as

$$\mathcal{F}(\mathbf{q}^2) = \frac{8\pi\gamma}{(\mathbf{q}^2 + \gamma^2)^2} \rightarrow \begin{cases} \gamma \rightarrow 0 : \mathcal{F}(\mathbf{q}^2) \sim \delta^{(3)}(\mathbf{q}) & \rightarrow \text{Ore-Powell} \\ \gamma \rightarrow \infty : \mathcal{F}(\mathbf{q}^2) \sim 8\pi/\gamma^3 \sim \text{Constant} & \rightarrow \text{Euler-Heisenberg} \end{cases}$$

So that the whole range of possible wavefunctions, from the free constituents to the point-like bound state case is spanned as γ varies from 0 to ∞ . Correspondingly, one gets the spectrum evolution from the Ore-Powell to the Euler-Heisenberg one (i.e., the point-like spectrum in the limit $a \rightarrow \infty$).

In the context of dispersion relations, the contributions originating in the oblique cuts (processes like $o-Ps \rightarrow e^+ e^- \gamma$ times $e^+ e^- (\gamma) \rightarrow \gamma\gamma(\gamma)$ in the imaginary part, figure b) below) are essential to maintain a physical spectrum (i.e. in agreement with Low's theorem). Again, those oblique cuts are neglected in standard

approaches. Here, they are automatically accounted for since they are included in the point-like result.

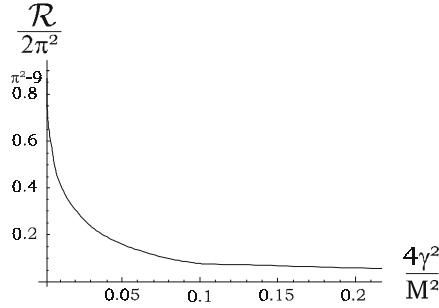


Note also that the spectrum for a point-like bound state at threshold corresponds to the spectrum for $a \sim 1.05$ in the Coulomb form factor case. The bound state decay spectra for $a < 1.05$ are unattainable in the point-like bound state case.

Concerning the total integrated rate, we recover the Ore-Powell result at threshold (oblique cuts are proportional to γ and $a = 1 \Leftrightarrow \gamma = 0$)

$$\Gamma(o-Ps \rightarrow \gamma\gamma\gamma) = \alpha^6 m \frac{2}{9\pi} \left(\frac{17.16}{2\pi^2} \right) = 4.75 \times 10^{-15} \text{ MeV} = \alpha^6 m \frac{2}{9\pi} (\pi^2 - 9)$$

As a increases, the total rate quickly decreases (remember $a = 4\gamma^2/M^2 + 1$)



By a numerical analysis, we found

$$\frac{\mathcal{R}}{2\pi^2} = (\pi^2 - 9) \left(1 - 15.412 \frac{\gamma}{M} + 122 \frac{\gamma^2}{M^2} - 889 \frac{\gamma^3}{M^3} + 1.92 \cdot 10^4 \frac{\gamma^4}{M^4} - \dots \right)$$

For orthopositronium, we can express γ in terms of α , and we find the binding energy corrections to the total rate

$$\Gamma(o-Ps \rightarrow \gamma\gamma\gamma) = \alpha^6 m \frac{2(\pi^2 - 9)}{9\pi} \left(1 - 12.1 \frac{\alpha}{\pi} + 80.2 \frac{\alpha^2}{\pi^2} - 502 \frac{\alpha^3}{\pi^3} + \dots \right) \quad (2.26)$$

This series is to be compared to the one presented in the literature (chapter 1), which is

$$\Gamma_{o-Ps} = \alpha^6 m \frac{2(\pi^2 - 9)}{9\pi} \left(1 - A_o \frac{\alpha}{\pi} - \frac{\alpha^2}{3} \ln \frac{1}{\alpha} + B_o \frac{\alpha^2}{\pi^2} - \frac{3\alpha^3}{2\pi} \ln^2 \frac{1}{\alpha} + C_o \frac{\alpha^3}{\pi} \ln \frac{1}{\alpha} + \delta_{5\gamma} \frac{\alpha^2}{\pi^2} \right)$$

with coefficients

$$\begin{aligned} A_o &= 10.286606 \quad (10) & C_o &= 5.517 \quad (1) \\ B_o &= 44.52 \quad (26) & \delta_{5\gamma} &= 0.19 \quad (1) \end{aligned}$$

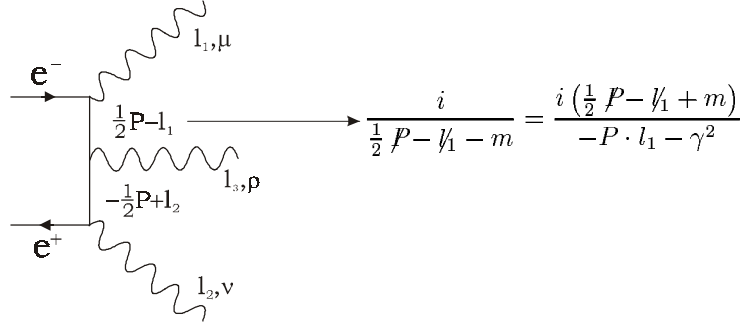
Again, the binding energy effects appear as responsible for the bulk of the radiative corrections at order α . Note that the origin of the slowness of the convergence of the corrections to Γ_{o-P_s} is clearly identified as coming from the perturbative expansion of binding energy effects (see (2.26)). In other words, the four-point fermionic loop with a Coulomb form factor is not well-behaved for $\gamma = 0$, and that limit appears as an inappropriate basis for perturbation theory.

2.3.4 A Simple Ansatz

To describe the distortion of the spectrum as the binding energy varies, a simple ansatz can be used. Let us modify the Ore-Powell amplitude modulus squared as

$$\sum_{\text{polarizations}} \left| \mathcal{M} \left((e^+ e^-)_{v_{rei}=0} \rightarrow \gamma \gamma \gamma \right) \right|^2 = \left(\frac{(1-x_1)^2}{x_2^2 x_3^2} + \frac{(1-x_2)^2}{x_1^2 x_3^2} + \frac{(1-x_3)^2}{x_1^2 x_2^2} \right) \prod_{i=1}^3 \left(\frac{x_i}{x_i + 2\gamma^2/M^2} \right)^2 \quad (2.28)$$

The reason for this form is the following. When only the vertical cut is taken into account, analytical problems are generated by the virtual fermion propagators, which can blow up when the energy of one of the photons is vanishing. A prescription to avoid this explosion is to consider that the external electrons have a mass of $M/2 < m$. Then, in the static limit, we have ($P^2 = M^2$)



and similarly for the other propagator. As long as $\gamma^2 \neq 0$, the propagators cannot generate poles. The Ore-Powell result is obtained with $M = 2m$, hence the virtual electron propagator is, in that limit

$$\frac{i \left(\frac{1}{2} P - l_1 + m \right)}{-P \cdot l_1 - \gamma^2} \xrightarrow{M=2m} \frac{i \left(\frac{1}{2} P - l_1 + m \right)}{-M^2 x_1 / 2}$$

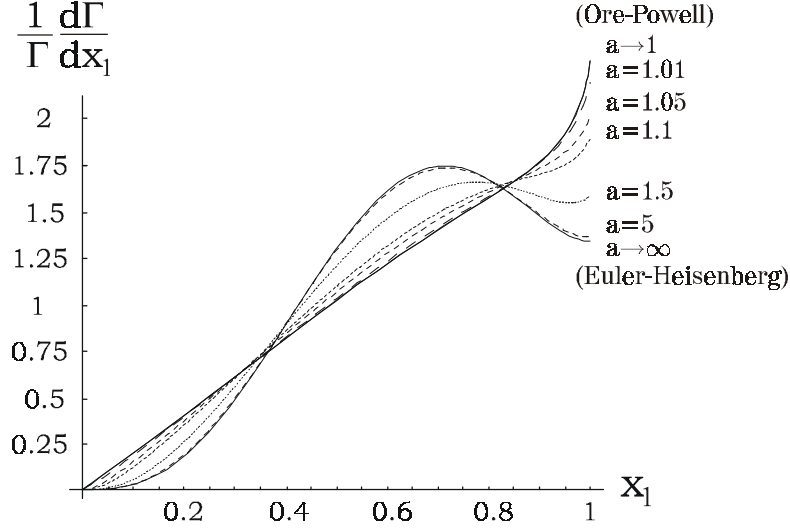
To replace those propagators by well-behaved ones, we multiply the Ore-Powell amplitude by the factor

$$\frac{-P \cdot l_1}{-P \cdot l_1 - \gamma^2} = \frac{x_1}{x_1 + 2\gamma^2/M^2}$$

leading to the prescription (2.28).

The obvious question: what is the point in considering this ansatz, built on the vertical cuts only, since we know that analyticity is restored by the oblique cuts? In other words, the vertical cut propagators do explode in the true fermion loop, but any non-analytical term is cancelled by similar divergences in the oblique cuts. The answer is that the ansatz can be simply integrated, and the final form for the differential rate can be useful for experimental fits. Another reason is that the analytical properties of the ansatz, as a function of γ and x_i , are very similar to the true fermion loop. Hence, the ansatz provides a valuable toy model, with which to study the various pathological kinematical limits.

The differential rate obtained from (2.28) for various binding energies is (the analytical expression is given in the appendix A.2)



The limit $\gamma \rightarrow 0$, reproduces the Ore-Powell spectrum exactly, by construction. On the other hand, the limit $\gamma \rightarrow \infty$ does not exactly reproduce the Euler-Heisenberg spectrum. Instead, we get

$$\frac{1}{\Gamma_{ansatz}} \frac{d\Gamma_{ansatz}}{dx_1} \stackrel{\gamma \rightarrow \infty}{=} x_1^3 \left(\frac{100}{3} - 60x_1 + 28x_1^2 \right)$$

to be compared to

$$\frac{1}{\Gamma_{E-H}} \frac{d\Gamma_{E-H}}{dx_1} = \frac{5}{17} x_1^3 \left(\frac{343}{3} - 207x_1 + \frac{973}{10} x_1^2 \right) \approx x_1^3 (33.63 - 60.88x_1 + 28.62x_1^2) \quad (2.29)$$

More precisely, the ansatz corresponds to the spectrum obtained from an Euler-Heisenberg Lagrangian with the scalar and pseudoscalar couplings of equal strengths

$$\mathcal{L}_{E-H,ansatz} \approx (F_{\mu\nu} F^{\mu\nu})^2 + (F_{\mu\nu} \tilde{F}^{\mu\nu})^2$$

We do not have an explanation for this peculiar fact.

Between the two limits, it is very important to note that the ansatz spectrum is moving away from the Ore-Powell spectrum at a much slower rate when a increases than the true Coulomb spectrum. Consequently, the ansatz cannot be used as it stands for fits. Further, the evolution of the total rate in terms of γ is smoother here, leading to smaller binding energy corrections (of order γ^2 instead of γ , see below).

Incompatible Limits and NRQED Expansion

For any value of $a > 1$, the spectrum behaves as x_1^3 close to $x_1 = 0$. Explicitly, with the definition $A = 2\gamma^2/M^2$,

$$\begin{aligned} \frac{d\Gamma_{ansatz}}{dx_1} = & \left(\frac{2}{9\pi} \alpha^6 m \right) \left[x_1^3 \left(\frac{5}{3A^2(A+1)^4} \right) - x_1^4 \left(\frac{9A^2 + 9A + 10}{3A^3(A+1)^5} \right) \right. \\ & \left. + x_1^5 \left(\frac{21A^4 + 42A^3 + 153A^2 + 140A + 75}{15A^4(A+1)^6} \right) + \mathcal{O}(x_1^6) \right] \end{aligned}$$

Obviously, this series is highly singular for $A = 0$, i.e. $\gamma = 0$. In the same way as for the decay $p\text{-}Dm \rightarrow e^+e^-\gamma$, it appears that the limits $\gamma \rightarrow 0$ and $x_1 \rightarrow 0$ are incompatible.

It is instructive to expand the differential rate around $\gamma = 0$, as is done in NRQED, and to analyze the various terms. The lowest order is of course the Ore-Powell result (2.23), while higher orders are more and more singular at $x_1 = 0$

$$\begin{aligned}\frac{d\Gamma_{ansatz}^{(0)}}{dx_1} &= \left(\frac{2}{9\pi}\alpha^6 m\right) \Omega(x_1) \\ &= \left(\frac{2}{9\pi}\alpha^6 m\right) \left(\frac{5}{3}x_1 + \mathcal{O}(x_1^2)\right) \\ \frac{d\Gamma_{ansatz}^{(1)}}{dx_1} &= \left(\frac{2}{9\pi}\alpha^6 m\right) \left(\frac{2\gamma^2}{M^2}\right) \left(-\frac{10}{3} - \frac{22}{3}x_1 + \mathcal{O}(x_1^2)\right) \\ \frac{d\Gamma_{ansatz}^{(2)}}{dx_1} &= \left(\frac{2}{9\pi}\alpha^6 m\right) \left(\frac{2\gamma^2}{M^2}\right)^2 \left(\frac{5}{x_1} + \frac{43}{3} + \frac{128}{5}x_1 + \mathcal{O}(x_1^2)\right) \\ &\quad \text{etc...}\end{aligned}$$

The integration over x_1 gives the result

$$\begin{aligned}\Gamma_{ansatz}^{(0)} &= \left(\frac{2}{9\pi}\alpha^6 m\right) (\pi^2 - 9) \\ \Gamma_{ansatz}^{(1)} &= \left(\frac{2}{9\pi}\alpha^6 m\right) \left(-\frac{3}{4}(4 + \pi^2)\right) \frac{2\gamma^2}{M^2} \\ \Gamma_{ansatz}^{(2)} &= \infty ??\end{aligned}$$

In the terminology of NRQED, the Ore-Powell result $\Gamma_{ansatz}^{(0)}$ is the lowest order, while the $\Gamma_{ansatz}^{(1)}$ is the first "relativistic correction". Even if the behavior of this first relativistic correction is highly unphysical near $x_1 = 0$, a IR finite answer can nevertheless be generated. This kind of correction is obtained, for example, in [99], [107]. A finite result cannot be obtained beyond that order, and special techniques have to be designed to deal with the divergences. Obviously, all these difficulties simply originate in the badly chosen basis for perturbation theory.

To close this section, if the exact total rate is expanded around $A = 0$, one finds

$$\Gamma_{ansatz} = \left(\frac{2}{9\pi}\alpha^6 m\right) \left[(\pi^2 - 9) - \frac{3}{4}(\pi^2 + 4) \frac{2\gamma^2}{M^2} + \left(\frac{57}{4} + \frac{27}{16}\pi^2 - 15 \log \frac{2\gamma^2}{M^2}\right) \frac{4\gamma^4}{M^4} + \dots \right]$$

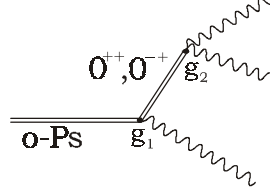
Finite corrections at each order are obtained, the divergence encountered above is replaced by $\log 2\gamma^2/M^2$, which could be called, again in analogy with standard bound state terminology, a non-analytic term. Indeed, if the binding energy is expressed in terms of the fine structure constant, we get corrections of the type

$$\frac{4\gamma^4}{M^4} \log \frac{2\gamma^2}{M^2} \sim \alpha^4 \left(\frac{1}{32} \ln \alpha - \frac{3}{64} \log 2 \right)$$

This illustrates some techniques used in NRQED, which amounts to extract such logarithmic corrections, with the hope that the remaining corrections can be computed perturbatively (note well, however, that we do not claim that all logarithmic corrections are of that type). All these complexities can be circumvented with the use of our method .

2.3.5 A Scalar and Pseudoscalar Resonance Model

We continue our study of analyticity in three-photon decay by taking a model where the initial vector particle first decays into a (pseudo)scalar plus a photon, with then the (pseudo)scalar decaying to two photons. Graphically



The couplings of the scalar and pseudoscalar to two photons are

$$\begin{aligned} \begin{array}{c} \text{O}^{++} \\ \text{P}=\mathbf{p}+\mathbf{q} \end{array} & \begin{array}{c} \text{p},\mu \\ \text{q},\nu \end{array} & g_2 (g^{\mu\nu} p \cdot q - p^\nu q^\mu) \\ \begin{array}{c} \text{O}^{-+} \\ \text{P}=\mathbf{p}+\mathbf{q} \end{array} & \begin{array}{c} \text{p},\mu \\ \text{q},\nu \end{array} & g_2 (\varepsilon^{\mu\nu\rho\sigma} p_\rho q_\sigma) \end{aligned}$$

The couplings with a photon replaced by the orthopositronium are the same (with $g_2 \rightarrow g_1$). The scalar or pseudoscalar propagator is

$$\Delta(p) = \frac{i}{p^2 - M_R^2 + i\varepsilon}$$

with M_R the pseudoscalar and the scalar mass (we take them as equal here). Note that the constants g_1, g_2 have dimension of 1/mass.

The Photon Spectrum and Phase-Space Singularity

We will study the photon spectrum as the mass of the virtual resonance varies. The modulus squared of the amplitude (there are three non-equivalent ordering of the photons) is the same for the scalar and pseudoscalar. After integration, one gets the differential and total rates (the expressions are rather lengthy, and since the computation is straightforward, will not be reproduced here). Of special interest is the low energy behavior of the photon spectrum

$$\frac{d\Gamma}{dx} \sim \frac{a_R(7a_R - 6) + 2}{12a_R^2(a_R - 1)^2} x^3 + \mathcal{O}(x^4)$$

with $a_R = M_R^2/M_{P_s}^2$. As expected, the spectrum is in x^3 near zero. The two singularities at $a_R = 0$ and 1 are interesting. Explicitly, the differential rate at those points is

$$\begin{aligned} a_R = 0 & : \quad \frac{1}{\Gamma} \frac{d\Gamma}{dx} = \frac{16}{7}x - \frac{8}{7}x^2 + \frac{20}{21}x^3 \\ a_R = 1 & : \quad \frac{1}{\Gamma} \frac{d\Gamma}{dx} = \frac{1}{\pi^2 - \frac{37}{4}} \left(\frac{5}{3}x^3 - 2x^2 + 6x - 4 - \frac{8(1-x)^2}{(2-x)x} \log(1-x) \right) = \frac{1}{\pi^2 - \frac{37}{4}} (2x + \mathcal{O}(x^2)) \end{aligned}$$

These behaviors are in contradiction with Low's theorem. This problem is due to our computation, which is wrong when the scalar propagator singularity is inside the phase-space, i.e. for a_R between 0 and 1. In fact, the spectrum, and rate, can only be defined for $a_R = 0, a_R = 1$, where there is an analytical problem, and for $a_R > 1$, where the spectrum is well-behaved.

Before turning to the resolution of the analytical problem, note that when $a_R \rightarrow \infty$, the normalized spectrum becomes

$$a_R \rightarrow \infty : \quad \frac{1}{\Gamma} \frac{d\Gamma}{dx} = 35x^3 - 65x^4 + \frac{63}{2}x^5 \quad (2.30)$$

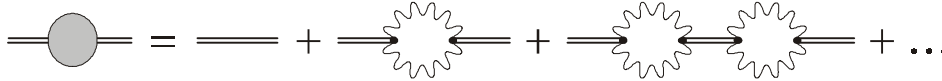
which is nearly the Euler-Heisenberg one. In fact, this is the spectrum obtained from $\mathfrak{L} \approx (F_{\mu\nu}F^{\mu\nu})^2$ or $\mathfrak{L} \approx (F_{\mu\nu}\tilde{F}^{\mu\nu})^2$. The small difference between (2.30) and (2.29) is due to the contribution coming from the interference between both terms of the Euler-Heisenberg Lagrangian.

Resummation and Finite Width Effects

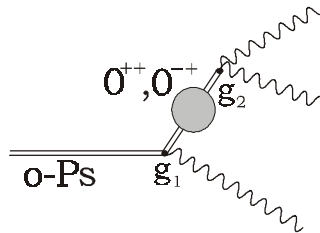
To correctly describe the process when the scalar (or pseudoscalar) mass is smaller than the positronium one, we will need to sum an infinite class of diagrams. Again, we find that analyticity requires some kind of resummation for some values of the parameters of the theory. This is strictly similar to the Coulomb resummation (or binding energy resummation) we advocate to cure NRQED in three-body decays. Here, the resummation is even simpler to understand: if the (pseudo)scalar can decay into two photons, it has a finite width. Hence, its propagator, after renormalization, should be of the form

$$\Delta(p) = \frac{i}{p^2 - M_R^2 + iM_R\Gamma_R - i\varepsilon}$$

Graphically, the summation is



Repeating the same computation as above with this new propagator

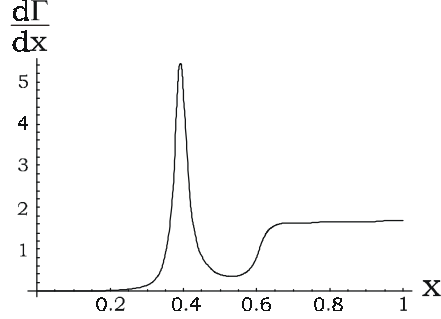


the differential rate behaves near zero as

$$\frac{d\Gamma}{dx} \sim \frac{a_R(7a_R - 6) + 2 + 7G_R^2}{12[a_R^2 + G_R^2][(a_R - 1)^2 + G_R^2]} x^3 + \mathcal{O}(x^4)$$

with $G_R = M_R\Gamma_R/M_{Ps}^2$. For all values of a_R , the spectrum is now in agreement with Low's theorem. Further, the differential rate can now be defined for all a_R , and exhibit a standard Breit-Wigner shape, like for example

for $a_R = 0.6$ and $G_R = 0.02$:



The resonance appears at $x = 1 - a_R$, while a sharp increase appears for $x = a_R$. For low energy, the spectrum vanishes as x^3 . If G_R increases, the Breit-Wigner peak will decrease and spread, and in the limit $G_R \rightarrow \infty$, the spectrum is again (2.30).

In the physical case of the positronium, the above treatment could apply to the computation of the parapositronium contribution to the orthopositronium lifetime. Indeed, the mass of the parapositronium is less than that of the orthopositronium. The parapositronium width has to be taken into account. Another application could be the quantitative estimation of the scale anomaly contribution to the orthopositronium width. Indeed, this anomaly should show up in the scalar channel. This analysis has not yet been done, but is an interesting perspective because it is obvious that the standard factorized approach will miss such contributions. We will encounter again the scale anomaly in the next section.

Finally, let us emphasize that the present model is not designed to represent the physics of the analytical problem of standard positronium computation. That problem has to do with the definition of the initial state, and needs a loop model with a Coulomb wavefunction form factor (i.e., containing a Coulomb photon resummation). The possible recombination of the electron and positron into a parapositronium, after having emitted a soft photon is a different problem, which should be treated using the technique of the present section. In other words, if the Pirenne-Wheeler formula is used to compute the amplitude of the present resonance process, an incorrect spectrum would be found for all values of a_R and G_R , since it is its treatment of the initial on-shell electron-positron pair which is incorrect.

2.4 Application to Other Processes

In this final section, we present several extensions of the method.

First, we present the application of the method involving the photon vacuum polarization. This includes the one-photon virtual decay $o-Dm \rightarrow e^+e^-$ and the weak decay $o-Ps \rightarrow \nu\bar{\nu}$. Also, a connection to the scale anomaly is briefly discussed.

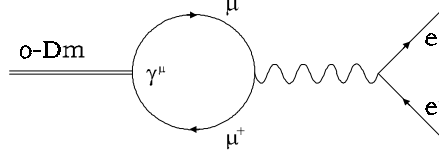
Then, we accommodate the derivative formula (2.11) for radial excitations, by considering the pion decay $\pi^0 \rightarrow \gamma o-Ps$. This is also the first example of a production process.

The next application is a bit different, in that it concerns the spectroscopic observables. We compute the hyperfine splitting by taking double derivative of vacuum polarization graphs, and using the language of mass renormalization.

The section ends with qualitative descriptions of other possible extensions, namely positronium, dimuonium high-energy formations and radiative transitions among positronium states. Finally, the extension of the method to higher orders of perturbation theory is briefly discussed.

2.4.1 Orthodimuonium and Photon Vacuum Polarization

We now consider the decay $o\text{-D}m \rightarrow \gamma^* \rightarrow e^+e^-$



The point-like amplitude is easily obtained in terms of the (divergent) photon vacuum polarization function

$$\mathcal{M}_p(o\text{-D}m \rightarrow e^+e^-) = \varepsilon_\mu(P) (P^2 g^{\mu\nu} - P^\mu P^\nu) \Pi_p(P^2) \frac{1}{P^2} \{\bar{u}(p) \gamma_\nu v(p')\}$$

where

$$\Pi_p(P^2) = -\frac{e}{4\pi^2} \left[\frac{D}{3} + \frac{5}{9} + \frac{4}{3\zeta} + \frac{2}{3} \left(1 - \frac{4}{\zeta}\right) \left(1 + \frac{2}{\zeta}\right) \frac{\arctan \frac{1}{\sqrt{4/\zeta-1}}}{\sqrt{4/\zeta-1}} \right] \quad (2.31)$$

with $\zeta = P^2/m^2$, m the muon mass and $D = 2/\varepsilon - \gamma_{Euler} + \log 4\pi\mu^2/m^2$ in dimensional regularization.

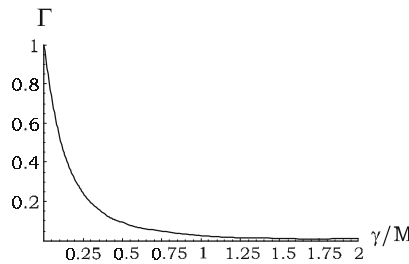
The Coulomb form factor will be obtained from the derivative of the vacuum polarization, with respect to $P^2 = M^2$:

$$\begin{aligned} \Pi_{Coul}(M^2) &= (32\pi C\phi_o\gamma) \frac{\partial}{\partial M^2} \Pi_p(M^2) \\ &= \frac{eC\phi_o}{M} \left[\frac{8}{\pi} \left(\gamma \frac{6m^2 + M^2}{3M^3} - \frac{4m^4}{M^4} \arctan \frac{M}{2\gamma} \right) \right] \\ &= \frac{eC\phi_o}{M} \left[1 - \frac{32}{3\pi} \frac{\gamma}{M} + 8 \frac{\gamma^2}{M^2} - \frac{128}{3\pi} \frac{\gamma^3}{M^3} + \dots \right] \end{aligned} \quad (2.32)$$

This has the effect of removing the divergence, as it should. The decay rate is

$$\begin{aligned} \Gamma(o\text{-D}m \rightarrow e^+e^-) &= \frac{\alpha}{3} \frac{M^2 + 2m_e^2}{M} \sqrt{1 - a_e} |\Pi_{Coul}(M^2)|^2 \\ &= \frac{\alpha^5 m}{6} \left(1 + \frac{a_e}{2}\right) \sqrt{1 - a_e} \left| 1 - \frac{32}{3\pi} \frac{\gamma}{M} + 8 \frac{\gamma^2}{M^2} - \dots \right|^2 \end{aligned}$$

To leading order in γ , we recover the standard result $\Gamma(o\text{-D}m \rightarrow e^+e^-) \approx \alpha^5 m/6$ when $a_e \ll 1$. As a function of the binding energy γ/M , the decay rate is a rapidly decreasing function (the plot is normalized to one at $\gamma = 0$)



For electromagnetic bound states, the binding energy is related to the fine structure constant, hence the corrections can be cast into

$$\begin{aligned}\Gamma(o-Dm \rightarrow e^+e^-) &= \frac{\alpha^5 m}{6} \left(1 + \frac{a_e}{2}\right) \sqrt{1-a_e} \left(1 - \frac{16}{3} \frac{\alpha}{\pi} + \left(\pi^2 + \frac{64}{9}\right) \frac{\alpha^2}{\pi^2} + \dots\right) \\ &\approx \frac{\alpha^5 m}{6} \left(1 + \frac{a_e}{2}\right) \sqrt{1-a_e} (1 - 1.70\alpha + 1.72\alpha^2 + \dots)\end{aligned}$$

Compared to the binding energy corrections to the parapositronium two-photon decay rate, the present corrections are much bigger. This is due to the high sensitivity of the form factor function near $\gamma = 0$ (see picture above). Note finally that the binding energy corrections obtained here, at order α , again account for a great deal of the total corrections (computed using the standard factorized formalism), which are

$$\Gamma^{LO+NLO}(o-Dm \rightarrow e^+e^-) = \frac{\alpha^5 m}{6} \left(1 + \frac{a_e}{2}\right) \sqrt{1-a_e} \left(1 - 4\frac{\alpha}{\pi} + \dots\right) \left(1 + C\frac{\alpha}{\pi}\right)$$

The last factor contains the radiative corrections to the intermediate photon propagator and to the final e^+e^- vertex, and is of no interest for our discussion.

Scale Anomaly

The decay rate is related to the derivative of the photon vacuum polarization function. In turn, this derivative is related to the scale anomaly [207], [220]. This means that in principle, the decay rate receives a contribution coming from the scale anomaly. As we will see, this contribution is subleading.

The anomalous Ward identity of interest to us is

$$p^2 \frac{\partial}{\partial p^2} \Pi_p(p^2, m^2) = -\frac{1}{2} \Delta(p^2, m^2) - \frac{e^2}{12\pi^2}$$

where

$$\Delta(p^2, m^2) (p^\mu p^\nu - g^{\mu\nu} p^2) = \int dx dy e^{ipy} \langle 0 | T \{ \theta_\alpha^\alpha(x) J_\mu(y) J_\nu(0) \} | 0 \rangle$$

and θ_α^α is the trace of the improved energy-momentum tensor. The additional term $e^2/12\pi^2$ on the right-hand side is the scale anomaly; it does not appear classically. Taking only that contribution into account, we get the scale anomaly contribution to the Coulomb form factor

$$\Pi_{Coul}^{Anom}(M^2) = (32\pi C\phi_o\gamma) \frac{1}{M^2} \left[-\frac{e}{12\pi^2}\right] = \frac{eC\phi_o}{M} \left(-\frac{8}{3\pi} \frac{\gamma}{M}\right)$$

At the level of the decay rate, let us keep the dominant contribution coming from $\Delta(p^2, m^2)$, and the anomaly contribution as the only correction

$$\begin{aligned}\Gamma^{Anom}(o-Dm \rightarrow e^+e^-) &= \frac{\alpha}{3} \frac{M^2 + 2m_e^2}{M} \sqrt{1-a_e} \left| \frac{eC\phi_o}{M} + \Pi_{Coul}^{Anom}(M^2) \right|^2 \\ &= \frac{\alpha^5 m}{6} \left(1 + \frac{a_e}{2}\right) \sqrt{1-a_e} \left| 1 - \frac{8}{3\pi} \frac{\gamma}{M} \right|^2 \\ &= \frac{\alpha^5 m}{6} \left(1 + \frac{a_e}{2}\right) \sqrt{1-a_e} \left| 1 - \frac{16}{3\pi} \frac{\gamma}{M} \right|\end{aligned}$$

Therefore, the scale anomaly accounts for 25% of the complete binding energy correction.

Note that if, for some reason, the anomalous contribution was to be omitted from binding energy corrections, we would write

$$\begin{aligned}\Gamma^{Anom}(o-Dm \rightarrow e^+e^-) &= \frac{\alpha}{3} \frac{M^2 + 2m_e^2}{M} \sqrt{1-a_e} |\Pi_{Coul}(M^2) - \Pi_{Coul}^{Anom}(M^2)|^2 \\ &= \frac{\alpha^5 m}{6} \left(1 + \frac{a_e}{2}\right) \sqrt{1-a_e} \left|1 - \frac{8}{\pi} \frac{\gamma}{M} + \dots\right|^2 \\ &= \frac{\alpha^5 m}{6} \left(1 + \frac{a_e}{2}\right) \sqrt{1-a_e} \left|1 - 4 \frac{\alpha}{\pi} + \dots\right|\end{aligned}$$

And this is exactly the result of the standard computation! The reason for this is rather obscure, probably accidental.

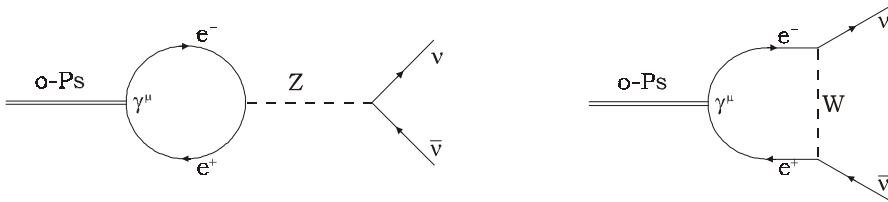
Nevertheless, an interesting question arises: is the scale anomaly a true physical contribution to the decay rate? In the derivative approach, the scale anomaly automatically shows up, while it is not clear how it could arise in the NRQED standard approach. We take the point of view that the scale anomaly is not included in the standard approaches. Furthermore, higher orders will never introduce it, so it is a truly new contribution. The reason for this point of view is the following. The anomaly never shows up in the imaginary part of amplitudes. The standard approach in the static limit amounts to consider the imaginary part at threshold (i.e. the process is factorized), hence the anomaly will be missed at lowest order. Similarly, higher orders are computed by introducing corrections to the wavefunction or scattering amplitudes, but the factorization is still used, i.e. one is again working at the level of the imaginary parts. Since, at no stage in the NRQED process, the loop with its Coulomb form factor is explicitly integrated, the scale anomaly will be missed.

This does not answer the question, but just shows that our result is definitely not attainable by NRQED analyses. At present, even if we do not see any compelling reason not to include the scale anomaly, none of the two approaches is fully justified.

To conclude this section, note well that such scale anomaly contributions, if missed by current theoretical computations, could introduce sizeable corrections in QCD. This is especially important since leptonic decays like $J/\psi \rightarrow e^+e^-$ are very well measured, and have a close connection to the so-called $\rho - \pi$ puzzle (see chapter 3 and 4 for additional details).

Orthopositronium Decay to Neutrinos

To explain the discrepancy between the experimental measurement and the theoretical value of the orthopositronium lifetime, one could invoke an invisible contribution to the width. Such undetected decay particles could be neutrinos, or new, beyond the standard model particles. Here we present the computation of the decay width into an electron neutrino-antineutrino pair $o-Ps \rightarrow \nu_e \bar{\nu}_e$, through a Z boson in the s channel and a W in the t channel



We will replace gauge boson propagators by $1/M_Z^2$ and $1/M_W^2$. Then, both point like amplitudes can be expressed as

$$\mathcal{M}_p(o-Ps \rightarrow \nu_e \bar{\nu}_e) = \varepsilon_\mu(P) \left(\Pi_{Zp}(P^2) + \Pi_{Wp}(P^2) \right) M^2 \{ \bar{u}(p) \gamma_\nu (1 - \gamma_5) v(p') \}$$

For the Z boson exchange, this form emerges because the axial part of the Z coupling does not contribute. One essentially recovers the photon vacuum polarization as form factor, up to coupling constants

$$\Pi_{Zp}(P^2) = \frac{G_F}{\sqrt{2}} \frac{(-1 + 4 \sin^2 \theta_W)}{2} \left(\frac{\Pi_p(P^2)}{e} \right)$$

with $\Pi_p(P^2)$ given by (2.31), $G_F/\sqrt{2} = g^2/8M_W^2$ and $M_W = M_Z \cos \theta_W$. For the W exchange, the loop integration has to be done explicitly, using dimensional regularization (this is compulsory, in order to deal with the quadratic divergences). After the loop integration, the Dirac structure $\gamma^\mu (1 - \gamma_5)$ emerges and one can factor out the form factor, again expressed in terms of the photon vacuum polarization

$$\Pi_{Wp}(P^2) = \frac{G_F}{\sqrt{2}} \left(\frac{\Pi_p(P^2)}{e} \right)$$

The Coulomb form factor is of course the same as before (see (2.32))

$$\Pi_{Coul}(M^2) = (32\pi C\phi_o\gamma) \frac{\partial}{\partial M^2} \left(\frac{\Pi_p(M^2)}{e} \right) = \frac{C\phi_o}{M} \left[\frac{8}{\pi} \left(\gamma \frac{6m^2 + M^2}{3M^3} - \frac{4m^4}{M^4} \arctan \frac{M}{2\gamma} \right) \right]$$

Replacing Π_p/e by Π_{Coul} in Π_{Zp} , Π_{Wp} , summing both contributions, one get the lowest order positronium decay amplitude $\mathcal{M}(o-Ps \rightarrow \nu_e \bar{\nu}_e)$. From it, the decay rate is simply computed

$$\begin{aligned} \Gamma(o-Ps \rightarrow \nu_e \bar{\nu}_e) &= \frac{G_F^2}{384\pi M} (1 + 4 \sin^2 \theta_W)^2 |\Pi_{Coul}(M^2)|^2 \\ &= \frac{G_F^2 \alpha^3 m^5}{24\pi^2} (1 + 4 \sin^2 \theta_W)^2 \left(\frac{M^2}{4m^2} \right)^2 \left[1 - \frac{32}{3\pi} \frac{\gamma}{M} + 8 \frac{\gamma^2}{M^2} - \frac{128}{3\pi} \frac{\gamma^3}{M^3} + \dots \right]^2 \end{aligned}$$

At threshold, $M = 2m$, we recover the result presented in the literature [108]. Obviously, this decay rate is very small, of the order of

$$\frac{\Gamma(o-Ps \rightarrow \nu_e \bar{\nu}_e)}{\Gamma(o-Ps \rightarrow \gamma\gamma\gamma)} \approx 6.1 \times 10^{-18}$$

This is much too small to be of any interest.

For other neutrino flavors, only the Z exchange graph contributes, with the same result except for a minus sign:

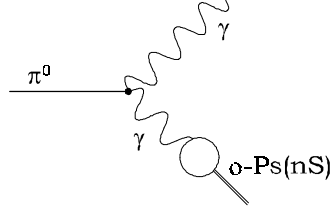
$$\Gamma(o-Ps \rightarrow \nu_{\mu,\tau} \bar{\nu}_{\mu,\tau}) = \frac{G_F^2 \alpha^3 m^5}{24\pi^2} (1 - 4 \sin^2 \theta_W)^2 \left(\frac{M^2}{4m^2} \right)^2 \left[1 - \frac{32}{3\pi} \frac{\gamma}{M} + 8 \frac{\gamma^2}{M^2} - \frac{128}{3\pi} \frac{\gamma^3}{M^3} + \dots \right]^2$$

This amounts to a suppression of a factor of about 250 relative to the electron neutrino case.

As a final remark, we note that if the Fermi coupling had not been used, there is a delicate issue concerning gauge invariance. Indeed, the general formalism states that to get the orthopositronium decay amplitude, one can first construct the equivalent process with a photon in place of the orthopositronium. For the W exchange graph, this is not the case since the orthopositronium cannot couple directly to the W . Moreover, for the corresponding photon graph, that coupling is important to preserve gauge invariance. Further studies should clarify the use of the derivative method in weak interaction processes.

2.4.2 Pion Decay to Orthopositronium and Radial Excitations

The technique of taking the derivative of point-like amplitudes can be extended to other spherically symmetric wavefunctions. The decay $\pi^0 \rightarrow \gamma o\text{-}Ps$ is a good example [82]



To get a sensible theoretical prediction, one must sum the decay rates over the infinite tower of radial excitations $o\text{-}Ps(nS)$ in the final state ($o\text{-}Ps(nS)$ means n th radial excitation of the S -wave $J = 1$ positronium state). From the standard Schrödinger wavefunction for hydrogen states (see appendix C.1), we can write a general expression for the form factor for nS radial excitations as

$$\mathcal{I}_{Coul,n}(M_n^2) = (32\pi C\phi_{noo}) \left[{}_1F_1 \left(1 - n, 2, 16\gamma_n^2 \frac{\partial}{\partial M_n^2} \right) \right] \left[\gamma_n(M_n^2) \frac{\partial}{\partial M_n^2} \mathcal{I}_p(M_n^2) \right] \quad (2.34)$$

with

$$|\phi_{noo}| = \sqrt{\frac{m^3 \alpha^3}{8\pi n^3}} \quad \gamma_n = \sqrt{m^2 - M_n^2/4}$$

Where we have denoted M_n the mass of the $o\text{-}Ps(nS)$ state. The hypergeometric functions are essentially the well-known Laguerre polynomials ((2.34) is equally valid for parapositronium).

For the case at hand, \mathcal{I}_p is the photon vacuum polarization (2.31), where m refers now to the electron mass. The pion decay rate into orthopositronium states can be written as

$$R_{oPs(nS)} = \frac{\Gamma(\pi^0 \rightarrow \gamma o\text{-}Ps(nS))}{\Gamma(\pi^0 \rightarrow \gamma\gamma)} = 2e^2 |\Pi_{Coul,n}(M_n^2)|^2 \left(1 - \frac{M_n^2}{m_\pi^2} \right)^3 \left[1 + \mathcal{O}\left(\frac{M_n^2}{m_{\rho,\omega}^2}\right) \right]$$

The $M_n^2/m_{\rho,\omega}^2 \approx 10^{-6}$ corrections arise from the form factor for pion to two photons. The mass ratio $M_n^2/m_\pi^2 \approx 10^{-4}$ is also negligible compared to binding energy corrections, to which we now turn. Up to corrections of order γ_n^2 , we can write using $\gamma_n \approx m\alpha/2n$

$$R_{oPs(nS)} = \frac{\alpha^4}{2} \frac{1}{n^3} \left(1 - 2A_n \frac{\gamma_n}{M_n} + \dots \right) = \frac{\alpha^4}{2} \frac{1}{n^3} \left(1 - \frac{1}{2n} A_n \alpha + \dots \right)$$

(the A_n are the numerical coefficients found by expanding $\Pi_{Coul,n}(M_n^2)$). Summing over n , we find

$$\sum_n R_{oPs(nS)} = \frac{\alpha^4}{2} \zeta(3) (1 - 1.66\alpha) \approx 1.684 \times 10^{-9}$$

where $\alpha^4/2 \approx (1.418 \times 10^{-9})$ is obtained from the contribution of the $o\text{-}Ps(1S)$ only. For comparison, [82] found the radiative correction to be $(1 - 0.92\alpha)$. The experimentally quoted branching fraction is [98]

$$\left. \frac{\Gamma(\pi^0 \rightarrow \gamma Ps)}{\Gamma(\pi^0 \rightarrow \gamma\gamma)} \right|_{\text{exp}} = (1.9 \pm 0.3) \times 10^{-9}$$

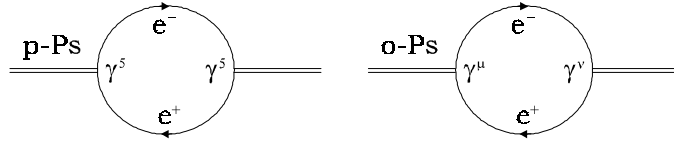
so the agreement is good.

What this little exercise shows is the power of our method as a mean to partially compute higher order corrections. More importantly, it is by now apparent that other, more complicated wavefunctions can easily be accommodated for. Any wavefunction that can be expressed, even approximately, from derivatives of the

Coulomb one can fit in our scheme. This may open the way to many applications in QCD, as we will see in chapter 4.

2.4.3 Hyperfine Splitting and Mass Renormalization

We implement here the renormalization of the positronium state. The idea is to consider the bare positronium mass M as equal to twice the electron mass m , and then to carry a (finite) mass renormalization. The diagrams contributing, at lowest order, to this mass shift will be obtained as the second derivatives of the vacuum polarization loops:



Let us first obtain the mass renormalization equations, and then discuss the results numerically.

Mass Renormalization

For a pseudoscalar parapositronium state, the resummation of the Dyson series is trivial. The parapositronium propagator is then

$$G(q^2) = \frac{i}{q^2 - M_o^2 - \Pi_{para}(q^2)}$$

Of interest to us is the mass shift, defined from the pole of $G(q^2)$

$$M_{R,para}^2 - M_o^2 = \Pi_{para}(M_R^2) \rightarrow M_{R,para} - M_o = \frac{\Pi_{para}(M_{R,para}^2)}{2M_o} \quad (2.35)$$

For the orthopositronium, the transverse part of the bare propagator is

$$G_0^{\mu\nu}(q^2) = \frac{-i \left(g^{\mu\nu} - \frac{q^\mu q^\nu}{q^2} \right)}{q^2 - M_o^2 + i\varepsilon}$$

The self-energy of the vector positronium will be of the form

$$\Pi^{\mu\nu}(q^2) = (q^2 g^{\mu\nu} - q^\mu q^\nu) \Pi_{ortho}(q^2)$$

Proceeding with the resummation of the Dyson series, we end up with

$$G^{\mu\nu}(q^2) = \frac{-i \left(g^{\mu\nu} - \frac{q^\mu q^\nu}{q^2} \right)}{q^2 (1 - \Pi_{ortho}(q^2)) - M_o^2}$$

Again, the propagator pole is at $q^2 = M_R^2$, hence

$$M_{R,ortho}^2 - M_o^2 = M_R^2 \Pi_{ortho}(M_R^2) \rightarrow M_{R,ortho} - M_o = \frac{M_{R,ortho}}{2} \Pi_{ortho}(M_{R,ortho}^2) \quad (2.36)$$

The two equations (2.35) and (2.36) are self-consistent equations. By identifying $M_o = 2m$ and $M_{R,para(ortho)} = M_{para(ortho)}$, they are of the form

$$\begin{cases} E_B^{para} \equiv M_{para} - 2m = \frac{\Pi_{para}(M_{para}^2)}{4m} \equiv f^{para}(E_B^{para}) \\ E_B^{ortho} \equiv M_{ortho} - 2m = \frac{M_{ortho}}{2} \Pi_{ortho}(M_{ortho}^2) \equiv f^{ortho}(E_B^{ortho}) \end{cases}$$

Our approach will be to generate corrections to $E_B^{para(ortho)}$ by plugging the non-relativistic result $E_B = -m\alpha^2/4$ into $f^{para(ortho)}$.

Second Derivatives and Hyperfine Splitting

The double derivatives of the vacuum polarization loops are

$$\Pi_{para(ortho)}(M^2) = \frac{1}{2} (32\pi C \phi_o \gamma)^2 \frac{1}{2} \left(\frac{\partial}{\partial M^2} \right)^2 \Pi_{p; para(ortho)}(M^2)$$

where a factor of 1/2 corrects for the factor 2 appearing in the derivative of $1/(s - M^2)^2$, while the other accounts for the double counting of Coulomb photon exchanges.

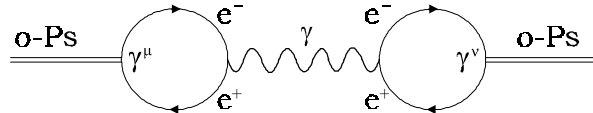
The computations are straightforward. For parapositronium, the point-like quadratic divergence disappears and we find

$$\begin{aligned} E_B^{para} &\equiv M_{para} - 2m = \frac{\Pi_{para}(M_{para}^2)}{4m} \\ &= -\frac{4|\phi_o|^2}{Mm} \left[\left(\frac{4\gamma^2}{M^2} + 1 \right) \frac{\arctan \frac{M}{2\gamma}}{2\gamma/M} - \frac{\frac{4\gamma^2}{M^2} - 1}{\frac{4\gamma^2}{M^2} + 1} \right]_{M=M_{para}} \\ &= -\frac{m\alpha^2}{4} - \frac{9m\alpha^4}{128} + \frac{m\alpha^5}{6\pi} - \frac{115m\alpha^6}{8192} + \dots \end{aligned}$$

Where we have used $|\phi_o|^2 = m^3\alpha^3/8\pi$, $\gamma^2 = m^2 - M_{para}^2/4$ and $M_{para} = 2m - m\alpha^2/4$ in the right hand side. Proceeding similarly with the orthopositronium renormalization, we consider the second derivative of the photon vacuum polarization function:

$$\begin{aligned} E_{B(1)}^{ortho} &\equiv M_{ortho} - 2m = \frac{M_{ortho}}{2} \Pi_{ortho}(M_{ortho}^2) \\ &= \frac{4|\phi_o|^2}{M^2} \left[\left(\frac{4\gamma^2}{M^2} + 1 \right) \left(\frac{20\gamma^2}{M^2} - 1 \right) \frac{\arctan \frac{M}{2\gamma}}{\gamma/M} - \frac{2 + \frac{176}{3} \frac{\gamma^2}{M^2} + 160 \frac{\gamma^4}{M^4}}{\frac{4\gamma^2}{M^2} + 1} \right]_{M=M_{ortho}} \\ &= -\frac{m\alpha^2}{4} + \frac{27m\alpha^4}{128} - \frac{2m\alpha^5}{3\pi} + \frac{1301m\alpha^6}{8192} + \dots \end{aligned} \quad (2.37)$$

At the order α^4 , there is also the annihilation diagram



whose contribution is $\Pi_{ortho}^{Ann, \mu\nu}(M^2) = -i(P^2 g^{\mu\nu} - P^\mu P^\nu) (\Pi_{Coul}(P^2))^2$. Using $\Pi_{Coul}(P^2)$ as given by (2.32), the dominant contribution in the limit $\gamma \rightarrow 0$ is

$$\Pi_{ortho}^{Ann}(P^2) = \frac{\alpha^4}{4} + \dots \rightarrow E_{B(2)}^{ortho, Ann} = \frac{M_{ortho}}{2} \Pi_{ortho}^{Ann}(M_{ortho}^2) = \frac{m\alpha^4}{4} + \dots$$

Hence the lowest loop contributions to the hyperfine splitting are, to order α^4 :

$$\Delta E_{hf} = \left(E_{B(1)}^{ortho} + E_{B(2)}^{ortho,Ann} \right) - E_B^{para} = m\alpha^4 \left[\frac{17}{32} + \dots \right] = m\alpha^4 [0.5313 + \dots]$$

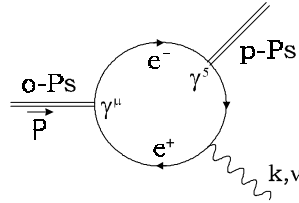
This is to be compared to the result (see chapter 1)

$$\begin{aligned} \Delta E_{hf} &= m\alpha^4 \left\{ \frac{7}{12} - \frac{\alpha}{\pi} \left(\frac{8}{9} + \frac{\ln 2}{2} \right) \right. \\ &\quad + \frac{\alpha^2}{\pi^2} \left(-\frac{5}{24} \pi^2 \ln \alpha + \frac{1367}{648} - \frac{5197}{3456} \pi^2 + \left(\frac{221}{144} \pi^2 + \frac{1}{2} \right) \ln 2 - \frac{53}{32} \zeta(3) \right) \\ &\quad \left. + \frac{\alpha^3}{\pi^3} \left(-\frac{7}{8} \pi^2 \ln^2 \alpha + \left(\frac{17}{3} \ln 2 - \frac{217}{90} \right) \pi^3 \ln \alpha \right) + \mathcal{O}(\alpha^3) \right\} \\ &\approx m\alpha^4 [0.5833 - 0.3933\alpha - 0.2083\alpha^2 \ln \alpha - 0.3928\alpha^2 - \dots] \end{aligned}$$

It is not surprising that our method does not reproduce exactly the above result, because we have neglected many diagrams (like electron self-energy insertions for example), and because we used the lowest order non-relativistic binding energy $E_B = -m\alpha^2/4$ and wavefunction $|\phi_o|^2 = m^3\alpha^3/8\pi$ as a basis. Taken individually, the corrections of $\mathcal{O}(\alpha^4)$ to the para- and orthopositronium masses are off by more than 50%. On the other hand, the difference between both corrections, giving the hyperfine splitting, is surprisingly good. Again, it seems that all the effects contained in the lowest order loop (with all the ladder Coulomb photon exchanges in the form factor) suffice to account for most of the radiative corrections. In conclusion, further studies of the application of our method to hyperfine splitting appear as necessary.

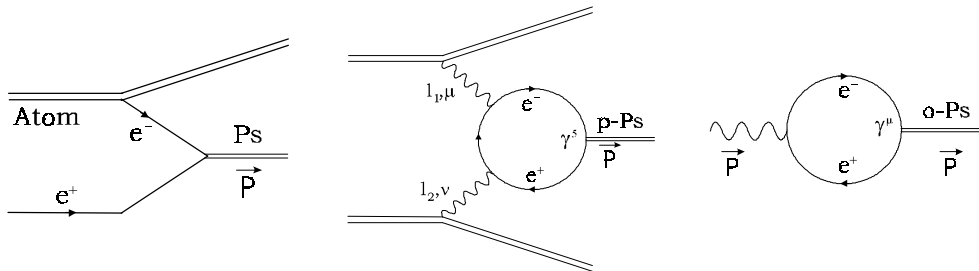
2.4.4 Possible Extensions

We have seen that the parapositronium and orthopositronium are easily dealt with using the derivative formula (2.11). It should not be difficult to extend the formalism to transitions among positronium states



Usually, such transitions are computed using the quantum mechanical formalism for magnetic dipole transitions. Here, we just have to compute a Feynman diagram, in a formally relativistic framework. In any case, the transition $o\text{-Ps} \rightarrow p\text{-Ps} + \gamma$ is very small compared to the decay $o\text{-Ps} \rightarrow \gamma\gamma\gamma$.

Another simple extension is the description of positronium (or dimuonium) production processes, like for example



The last graph is to be understood as a sub-process (see the $\pi^0 \rightarrow \gamma P_s$ production mechanism discussed in the previous section). Those processes are interesting because they constitute a theoretical laboratory for the quarkonium production case.

Still in connection with the corresponding QCD case, the description of higher excited states should be made possible using our formalism. Naively, we can expect that their decay amplitude will be computed from point-like amplitude with a well-chosen Dirac structure

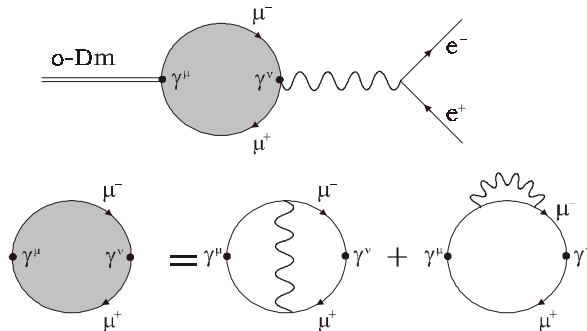
$$\begin{aligned}
 {}^1S_0 &: \gamma_5 \\
 {}^3S_1 &: \gamma_\mu \\
 {}^1P_1 &: q_\mu \gamma_5 \\
 {}^3P_0 &: 1 \\
 {}^3P_1 &: \gamma_\mu \gamma_5 \\
 {}^3P_2 &: q_\mu \gamma_\nu + q_\nu \gamma_\mu + \frac{2}{3} \not{q} \left(-g_{\mu\nu} + \frac{q_\mu q_\nu}{q^2} \right) \\
 &\dots
 \end{aligned}$$

These identifications suffice to enforce the correct selection rules (like for example ${}^1P_1, {}^3P_1 \not\rightarrow \gamma\gamma$). To be able to extend the derivative formalism, we also need to know the wavefunctions. Those are given in appendix C.1, but not in a very convenient form. In particular, it is not clear at present how to deal with the angular part of those wavefunction (the S -state was especially simple, since spherically symmetric).

The final extension we want to mention is the hydrogen atom and the muonium. In other words, the case of unequal constituent masses. The wavefunctions are the same as that of the positronium (except for the reduced mass). Anyway, for unequal masses, the bound state does not usually annihilate. The only exception is $(\mu^+ e^-) \rightarrow \bar{\nu}_\mu \nu_e$. Description of this process using the present formalism will be undertaken in the near future.

2.4.5 Higher Orders

At first sight, the extension to higher orders is straightforward. It suffices to take derivative of two-loop point-like QED amplitudes. This will regenerate the tree-level result, introduce all the corrections of order α , along with corrections of higher orders. Logarithmic corrections will also be automatically generated from the threshold singularities of the two-loop (or higher) graphs. For example, the following graphs are sufficient to get the complete decay rate up to order α



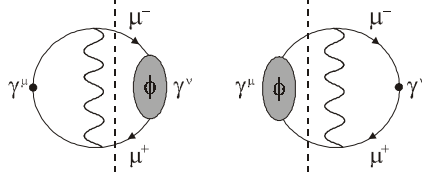
The tree level result is regenerated because of the Coulomb part of the binding graph (photon exchange between the $e^+ e^-$). This is due to the iterative nature of the Bethe-Salpeter equation (see (1.11)). Note that the Coulomb part of the binding graph also generates order α corrections, as exposed in [87].

Unfortunately, things are less simple because precisely of the binding graph. To see what happens, let us apply our derivative formula on the two-loop photon vacuum polarization graph (see appendix A.2), evaluated

at the positronium mass. We find the Coulomb form factor

$$\Pi_{Coul}^{2Loop}(M^2) = \frac{eC\phi_o}{M} \left[2 - \frac{4\alpha}{\pi} - \frac{2}{3}\alpha^2 \log \alpha + \mathcal{O}(\alpha^2) \right]$$

The first term, 2, is the signal that something has gone wrong. We would have expected a 1 instead. The problem is simple to understand. When one simply takes a derivative, the form factor is introduced inside the cut, hence we generate



This is not correct; it is a double counting. Those diagrams are responsible for regenerating twice the lowest order. Instead, we should consider only one of them, or proceed first by inserting the Coulomb form factor inside the imaginary part. Note that, if naively divided by two, the two-loop corrections become

$$\begin{aligned} \Pi_{Coul}^{2Loop}(M^2) &= \frac{eC\phi_o}{M} \left[1 - \frac{2\alpha}{\pi} - \frac{1}{3}\alpha^2 \log \alpha + \mathcal{O}(\alpha^2) \right] \\ \rightarrow \Gamma(o-Dm \rightarrow e^+e^-) &= \frac{\alpha^5 m}{6} \left(1 + \frac{a_e}{2} \right) \sqrt{1 - a_e} \left(1 - \frac{4\alpha}{\pi} - \frac{2}{3}\alpha^2 \log \alpha + \mathcal{O}(\alpha^2) \right) \left(1 + C\frac{\alpha}{\pi} \right) \end{aligned}$$

which agrees to order α with the standard result. Future work should clarify the use of the method at higher orders.

In any case, it should be obvious that the extension to higher order is possible in principle. The present difficulty is only technical. Of course, we are still a long way from an exact order α^2 computation, necessary to compete with other computation schemes. This was not our objective. Instead, we think that we have successfully constructed a well-defined perturbation theory for QED bound state computations.

2.5 Conclusion

In summary, we have analyzed the QED bound state decay formalism, using dispersion relations. The two principal results were

- 1- The approximation done in standard approach to reduce the four-dimensional Bethe-Salpeter loop is essentially a neglect of all but the vertical cut of the loop.
- 2- The four-dimensional loop amplitude, with the Coulomb form factor inserted at the level of the dispersive integral, and with a covariant description of the bound state spin, is obtained as the derivative of the corresponding point-like bound state QED amplitude.

Since all the cuts are needed to preserve analyticity, and since a simple computational scheme is available, we therefore conclude that QED bound state computations must be developed from a new perturbative basis. Lowest order amplitudes constructed in this way have many properties

- 1- They are simple to compute, in a formally relativistic framework.
- 2- They are automatically gauge invariant.
- 3- They sum an infinite class of correction already at the lowest order.
- 4- They factorize the binding energy effects from the radiative corrections in the perturbative series, leading to enhanced convergence.
- 5- They predict correct photon spectra, i.e. spectra in agreement with Low's theorem. This is impossible using a perturbative NRQED approach.

While the main motivation for constructing a new basis was the conflict between NRQED and analyticity in three-body decays, the method can be applied (or will be extended) to a variety of other processes (higher excited states, hyperfine splitting, radiative transitions,...).

Also, our method apply to lowest order amplitudes, while present theoretical considerations in positronium physics are at two loops and beyond. As said, our goal was to implement analyticity in bound state computations, so it is natural to start with the lowest order. Anyway, to be competitive, our method should have to be applied at two loops now. As we have seen in the previous section, there is no obstruction to this extension, at least in principle.

The simplicity of the method may be accidental, but could also be the signal of some more fundamental physics involving Coulomb bound states. For example, the fact that the derivative of the photon vacuum polarization contains all the necessary information about the positronium binding is very interesting. Further, the appearance of the scale anomaly as a binding energy effect needs further study.

Chapter 3

Overview of Quarkonium Theory

This chapter presents the observables of quarkonium physics, as well as the theoretical description of quarkonium decays. It begins with a brief summary of the spectroscopy of heavy quark-antiquark bound states, and of the annihilation modes of the quarkonium ground states. Then, the standard theoretical framework for the description of quarkonium annihilation is developed from the positronium annihilation one. Finally, the theoretical predictions are compared to the experimental data, and the strong coupling extraction is performed. All the material of this chapter is standard, and just serves to set the stage for the next chapter, where binding energy effects will be introduced as a cure for the standard approach analytical defects.

This chapter is not intended to present the history of quarkonium physics. Only the notions of interest to us are introduced. Also, the modern framework of quarkonium theory, i.e. non-relativistic QCD (NRQCD), will not be discussed. This omission has no consequence, the simple computation scheme presented in this chapter is a good illustration of more advanced techniques. In particular, the basic factorization hypothesis is central to all models. Further, the formulas we will derive are still used in many practical applications. For reviews on NRQCD, we refer to [93], [171], [176], [178], [179], [188], [189], [190], [192] and references cited there.

3.1 Quarkonium Physics Observables

3.1.1 Heavy Quarkonium Spectroscopy

In the quark model, a meson is made of a quark with an antiquark. Since the quarks are spin $1/2$ fermions, their association into a meson can take only specific quantum numbers. The following table summarizes the naming scheme for unflavored mesons [223]

J^{PC}	0^{-+}	1^{+-}	1^{--}	0^{++}
	2^{-+}	3^{+-}	2^{--}	1^{++}
	\vdots	\vdots	\vdots	\vdots
$^{2S+1}L_J$	$^1(L\text{ even})_J$	$^1(L\text{ odd})_J$	$^3(L\text{ even})_J$	$^3(L\text{ odd})_J$
$u\bar{d}, u\bar{u} - d\bar{d}, d\bar{u}$	π	b	ρ	a
$a(u\bar{u} + d\bar{d}) + b(s\bar{s})$	η, η'	h, h'	ω, ϕ	f, f'
$c\bar{c}$	η_c	h_c	$J/\psi, \psi$	χ_c
$b\bar{b}$	η_b	h_b	Υ	χ_b

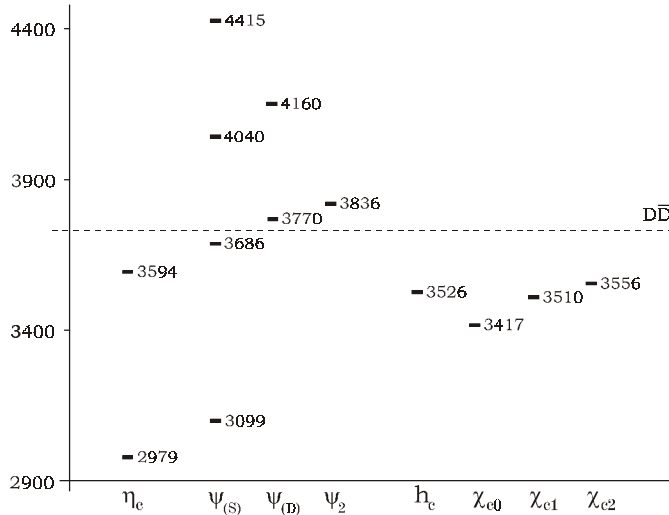
Links between quantum numbers are

$$\begin{aligned}
 P &= (-1)^{L+1} \\
 C &= (-1)^{L+S} \\
 G &= (-1)^{L+S+1}
 \end{aligned}$$

with C only relevant for neutral mesons. The $c\bar{c}$ ($b\bar{b}$) mesons are collectively called charmonium (bottomonium or, less often, beautyonium).

Each $^{2S+1}L_J$ state appears with all its radial excitations, as an infinite tower of states. The particles' names receive an extension (nL) with n the analog of the principal quantum number. For charmonium, the experimentally observed states are [223]

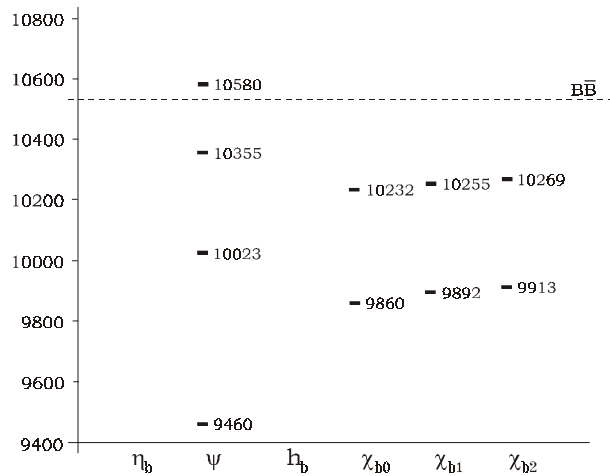
$^{2S+1}L_J$	L	S	J^{PC}	$n = 1$	$n = 2$	$n = 3, 4, \dots$
1S_0	0	0	0^{-+}	$\eta_c(1S)$ [2979]	$\eta_c(2S)$ [3594]	
3S_1	1	1	1^{--}	$J/\psi(1S)$ [3099]	$\psi(2S)$ [3686]	ψ [4040], ψ [4415]
1P_1	1	0	1^{+-}	$h_c(1P)$ [3526]		
3P_0	1	1	0^{++}	$\chi_{c0}(1P)$ [3417]		
3P_1			1^{++}	$\chi_{c1}(1P)$ [3510]		
3P_2			2^{++}	$\chi_{c2}(1P)$ [3556]		
1D_2	2	0	2^{-+}			
3D_1		1	1^{--}	ψ [3770]	ψ [4160]	
3D_2			2^{--}	ψ_2 [3836]		
3D_3			3^{--}			



The identification of higher 1^{--} states as 3S_1 radial excitations or 3D_1 states is not well-established. The occurrence of D -states around 3800 MeV is supported by the indications for the 3D_2 state $\psi_2(1D)$, 2^{--} , at 3836 MeV, so that ψ [3770] is probably the 3D_1 . Another possibility is that the 1^3D_1 and 2^3S_1 states are mixed into the mass eigenstates ψ [3686] and ψ [3770]. For the tower of 3S_1 radial excitations, a remarkable feature is the equal spacing between n -levels (compare with the Balmer series, in $1/n^2$). Also apparent on the figure, the fine and hyperfine splitting are sizeable compared to the spacing between principal levels. Anyway, all energy spacings are small compared to the bound state mass.

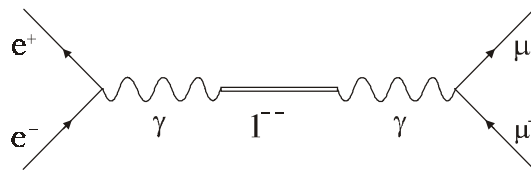
For bottomonium, fewer states have already been observed [223]

$2S+1L_J$	L	S	J^{PC}	$n = 1$	$n = 2$	$n = 3, 4, \dots$
1S_0	0	0	0^{-+}	$\Upsilon(1S)$ [9460]	$\Upsilon(2S)$ [10023]	$\Upsilon(3S)$ [10355], $\Upsilon(4S)$ [10580], ...
3S_1		1	1^{--}			
1P_1	1	0	1^{+-}			
3P_0		1	0^{++}	$\chi_{b0}(1P)$ [9860]	$\chi_{b0}(2P)$ [10232]	
3P_1			1^{++}	$\chi_{b1}(1P)$ [9892]	$\chi_{b1}(2P)$ [10255]	
3P_2			2^{++}	$\chi_{b2}(1P)$ [9913]	$\chi_{b2}(2P)$ [10269]	



Some higher 1^{--} states have also been observed at 10860 and 11020 MeV. As for charmonium, the identification of those states as 3S_1 or 3D_1 is not straightforward.

For both charmonium and bottomonium, the states with quantum number 1^{--} are the most well-established. This is simple to understand from the experimental setting used to detect such resonances, i.e. e^+e^- colliders. A resonance with the quantum number of the photon is easily found in the s -channel



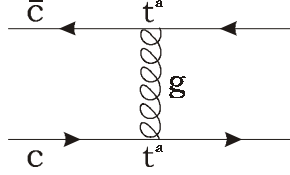
The discovery of the ψ and Υ family was made while studying such channels. The establishment of χ states is relatively easy because of the $E1$ transition from 3S_1 states. On the other hand, the singlet states are rather difficult to observe, because the $M1$ transition $^3S_1 \rightarrow ^1S_0 + \gamma$ is very weak.

Potential Models

For QED bound states, a non-relativistic approach based on the Schrödinger equation with the Coulomb potential gave rather good results for the spectrum. For quarkonium, we do not know the potential. One could think of the analog of the QED Coulomb potential $-\alpha/r$, which is for QCD

$$V(r) = -C_F \frac{\alpha_S}{r} = -\frac{4}{3} \frac{\alpha_S}{r}$$

with $C_F = (N^2 - 1) / 2N$. This effective potential arises from the graph



Unfortunately, such a potential does not support confinement since there is a continuum of states (and, as we have said, the Balmer series does not fit well the observed spectrum).

To account for the confinement, various phenomenological potentials have been proposed, whose parameters are fitted to reproduce the observed spectrum⁷ (see [150], [154], [162], [170], [199]). The most popular one is the Cornell potential

$$V_{Cornell}(r) = -\frac{a}{r} + \sigma r \quad \text{Fit Parameters: } \begin{cases} m_c = 1.84 \text{ GeV}, m_b = 5.18 \text{ GeV} \\ a = 0.52 \\ \sigma = 0.18 \text{ GeV}^2 \end{cases} \quad (3.1)$$

At short distance, the interaction is described by a Coulomb potential, while the linear rise is felt at larger distances, and is responsible for confinement (note that if the Coulomb part is matched to the QCD Coulomb interaction, one finds $\alpha_S \approx 0.4$, but the scale is not clear). The parameter σ is called the string tension. More advanced forms have also been proposed, in which the Coulomb part is taken as $-C_F \alpha_S(r) / r$, with $\alpha_S(r)$ the running coupling.

Other forms have been proposed, with no connection to the perturbative QCD potential. Among them, let us quote

$$V_{Power\ Law}(r) = C + b (r/r_0)^\nu \quad \text{Fit Parameters: } \begin{cases} m_c = 1.8 \text{ GeV}, m_b = 5.174 \text{ GeV} \\ C = -8.064 \text{ GeV} \\ b = 6.898 \text{ GeV} \\ \nu = 0.1 \end{cases}$$

$$V_{Logarithm}(r) = C + b \log(r/r_0) \quad \text{Fit Parameters: } \begin{cases} m_c = 1.5 \text{ GeV}, m_b = 4.906 \text{ GeV} \\ C = -0.6635 \text{ GeV} \\ b = 0.733 \text{ GeV} \end{cases}$$

where $r_0 = 1 \text{ GeV}^{-1}$ is introduced for dimensional reasons.

The above potentials are quite successful in describing the spin-independent part of the spectrum. To describe the fine and hyperfine structure, QCD inspired potentials have been constructed (accounting for tensor forces, spin-orbit couplings,...). In general, the technique amounts to the non-relativistic reduction of amplitudes to effective potentials. Various complicated theoretical issues are involved in those studies, and therefore lie out of our main concerns (see for example [11], [18], [159], [187], [195], [196]).

3.1.2 Heavy Quarkonium Decay

Similarly to positronium, quarkonium decays either through the annihilation of its constituents or through transitions to lower states. In this section, the coarse pattern of experimental branching ratios is presented. Unfortunately, this is only possible for charmonium, because there is not enough experimental information concerning bottomonium. The coarse pattern should however be quite similar for both (the only new feature is the opening of the $\tau^+\tau^-$ channel in bottomonium decay).

⁷ In some cases, the observed decay rates, especially the leptonic modes, also serve as input for the fits.

In the following, only S -states will be analyzed

	Mass (MeV)	Width (MeV)
η_c	2979.8 ± 1.8	13.2 ± 3.5
J/ψ	3096.87 ± 0.04	0.087 ± 0.005
$\psi(2S)$	3685.96 ± 0.09	0.277 ± 0.031

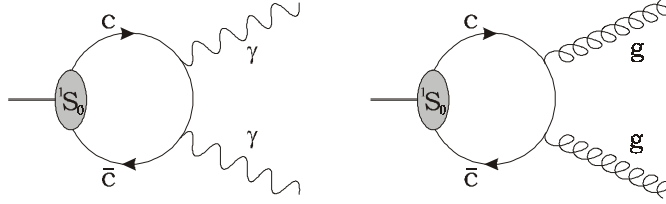
The very small width of the J/ψ or $\psi(2S)$ is due to the Zweig rule, as will be discussed below. Note that the η_c width is not well-established, since recent reported measurements range from $11.0 \pm 8.0 \pm 4.1$ MeV [141] to $27.0 \pm 5.8 \pm 1.4$ MeV [138].

The η_c Decay

The decay modes of interest to us are [223]

$$\begin{aligned} B(\eta_c \rightarrow \gamma\gamma) &= (3.0 \pm 1.2) \times 10^{-4} \\ B(\eta_c \rightarrow had.) &\approx 1 \end{aligned}$$

The η_c is a pseudoscalar, like the parapositronium, and therefore can decay only into an even number of photons, or into at least two gluons. The branchings can then be understood simply in terms of the processes



The emitted gluons, being colored, hadronize to form the final state hadrons. The relative strength of both processes is in agreement with the rough theoretical expectation

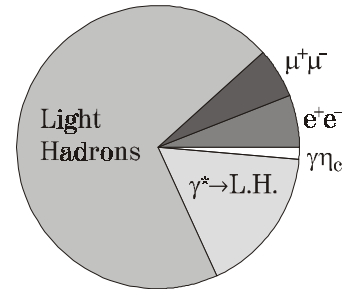
$$\frac{B(\eta_c \rightarrow \gamma\gamma)}{B(\eta_c \rightarrow gg)} \sim \frac{\alpha^2}{\alpha_S^2} \sim 6 \times 10^{-4}$$

with $\alpha_S \sim 0.3$.

The ψ Decay

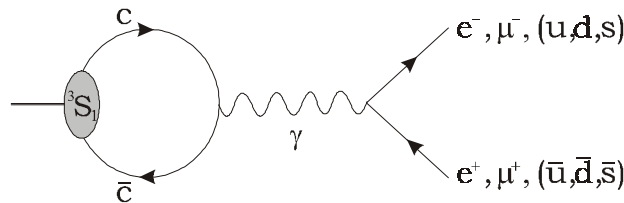
For J/ψ , the main branchings are [223]

$B(J/\psi \rightarrow X)$	X	%
Leptonic	e^+e^-	5.93 ± 0.10
	$\mu^+\mu^-$	5.88 ± 0.10
Hadronic	$hadrons(+\gamma)$	87.7 ± 0.5
	$\gamma^* \rightarrow L.H. (+\gamma)$	17.0 ± 2.0
Transitions	$\gamma\eta_c$	1.3 ± 0.4



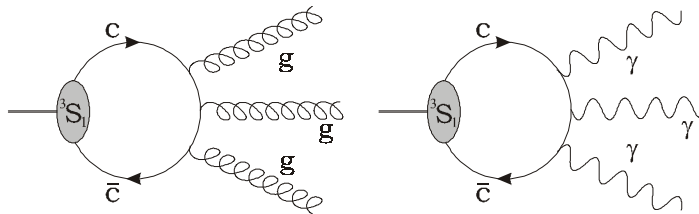
Note that the virtual photon transition to light hadrons (L.H.), as well as the transition to η_c are included into the total hadronic width.

As for the orthopositronium, the J/ψ can decay into an odd number of photons. The simplest decay mode is therefore the one virtual photon mode (both the photon and the J/ψ have quantum numbers 1^{--})



The leptonic modes, as well as roughly 20% of the hadronic mode are of that type.

Since gluons are colored objects, the corresponding one-gluon process is forbidden (the J/ψ is colorless). This is the origin of the small width of the J/ψ , and is called the Zweig rule. Indeed, if the one-gluon mode were allowed, it would have a width of more than a thousand times ($\sim \alpha_s^2/\alpha^2$) the one-photon one. Instead, the dominant strong decay mode proceeds through three gluons

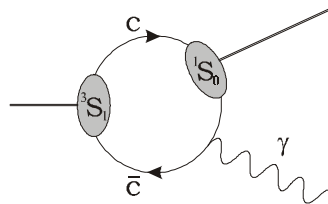


We have also indicated the not yet observed three photon mode, to emphasize the similarity to the orthopositronium decay. A rough estimate shows that the three-gluon decay branching is of the same order of magnitude as the one-photon one

$$\frac{B(J/\psi \rightarrow ggg)}{B(J/\psi \rightarrow \gamma^* \rightarrow e^+e^-)} \sim \frac{1}{10} \frac{\alpha_s^6}{\alpha^2} \sim 1.4$$

where we have included a factor 1/10 to account for the three-body phase-space suppression factor, like for orthopositronium decay.

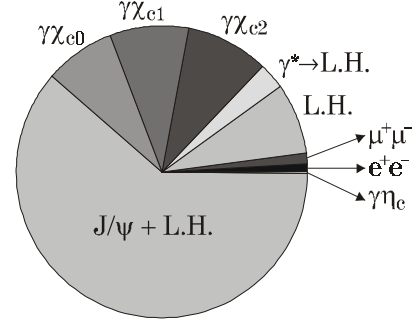
Finally, the radiative transition can be depicted



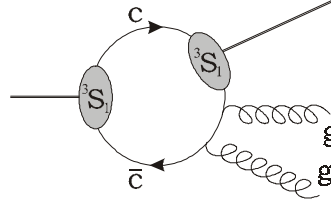
It is the analog of the magnetic transition $o-Ps \rightarrow p-Ps + \gamma$, and is therefore quite small.

Finally, for the radial excitation $\psi(2S)$ [223]

$B(\psi(2S) \rightarrow X)$	X	%
Leptonic	e^+e^-	0.79 ± 0.05
	$\mu^+\mu^-$	1.2 ± 0.4
Hadronic	$hadrons(+\gamma)$	98.1 ± 0.3
	$\gamma^* \rightarrow had. (+\gamma)$	2.9 ± 0.4
Transitions	$\gamma\eta_c$	0.28 ± 0.06
	$J/\psi + had.$	61 ± 4
	$\gamma\chi_{c0}$	9.3 ± 0.9
	$\gamma\chi_{c1}$	8.7 ± 0.8
	$\gamma\chi_{c2}$	7.9 ± 0.8



Again, the virtual photon mode and all the transitions are included into the hadronic mode. The transition $2S \rightarrow 1S$ cannot proceed by emission of one photon (Furry's theorem). Instead, the bulk of it involves a two-pion emission $\psi(2S) \rightarrow J/\psi \pi\pi$. Those transitions proceed through two-gluon emission



Note also that the allowed transitions to P -states are roughly 30 times stronger than the forbidden one to $\gamma\eta_c$.

3.1.3 Other Quarkonium Physics Observables

Exclusive Rates into Hadrons

Many exclusive decay modes of the η_c , J/ψ and $\psi(2S)$ into hadrons have been measured [223]. We do not intend to give an account of them, because they are of no direct interest to us in the present work. Indeed, it is not possible to relate exclusive decay modes to the decay modes into gluons described above, since a quantitative description of the hadronization process does not exist at present. Note however that using the flavor $SU(2)$ or $SU(3)$ group, one can extract interesting information, such as for example the relative strength (as well as the relative phase) of the one-photon electromagnetic and three-gluon strong decay modes contributing to a given multiplet of decay channels (like $J/\psi \rightarrow vector + pseudoscalar$ for example), see [169], [184]. Again, there is no clear quantitative way to relate such information to the perturbative picture of the heavy quark annihilation channels, and we will not detail these analyses.

Quarkonium Production

In proton-proton colliders, or heavy ion colliders, one can search for the formation of charmonium states. There are many different mechanisms that can lead to the formation of a charm-anticharm pair (Drell-Yan, Gluon fusion,...). The interest of charmonium production has been revived by data from HERA and the TEVATRON on charmonium production in high energy ep and $p\bar{p}$ collisions. Also, observation of J/ψ suppression by NA38

in nucleus-nucleus collisions raises the possibility to explore the phase structure of QCD. In particular, the suppression of J/ψ production in $Pb - Pb$ collision is sometimes interpreted as a signal of deconfinement. In a different context, the charmonium decay channels of the B mesons have many interesting properties for the study of CP violation ($B \rightarrow J/\psi K_S$ permits the extraction of the unitary triangle angle β in an especially clean way (no FSI) [18]).

It is in describing quarkonium formation that NRQCD has found one of its greatest successes. Indeed, the simple color singlet model (CSM) is in strong disagreement with experimental data (the predictions of the CSM underestimate the production rates). Let us recall that the CSM model simply assumes that the process of quarkonium formation factorizes as the creation of a free colorless $Q\bar{Q}$ pair (thus in a color singlet state) followed by its binding into a quarkonium state. NRQCD, on the other hand, led to the so-called color octet mechanism. The production mechanism receives a significant contribution from processes where the $Q\bar{Q}$ pair is created in an octet state (typically, by a single gluon). In other words, one introduces dynamical gluons into the quarkonium wavefunction. A further success of NRQCD is that, by invoking color octet contribution, one is able to get rid of IR singularities in P -wave charmonium production, for which the CSM is rather non-predictive.

For further information on the quarkonium production models, we refer to the abundant recent literature (see for example [167], [171], [198] and references cited there).

3.2 Quarkonium Annihilation Rates

In this section, we collect all the annihilation rates of heavy quarkonia $Q\bar{Q}$ into photons and gluons calculated in the appendix B.2, and include the radiative corrections as obtained in the literature. The framework is that of perturbative QCD. There are many references. Some early works are [144], [145], [146]. For more modern approaches, see for example [11], [147], [149], [151], [153], [164], [167], [191]. Others are listed in the bibliography, or can be found in the bibliography of the cited papers.

The central hypothesis used to compute annihilation rates is essentially the static limit, i.e. the bound state mass is taken to equal twice the constituent mass. The basic formula is then the old Pirenne-Wheeler positronium one

$$\Gamma(Ps \rightarrow n\gamma) = \frac{1}{2J+1} |\phi(0)|^2 (4v_{rel}\sigma(e^-e^+ \rightarrow n\gamma))_{v_{rel} \rightarrow 0}$$

adapted to the quarkonium case. One therefore assumes that the quarkonium wavefunction, in momentum space, satisfies

$$\psi(\mathbf{k}) \xrightarrow{M \rightarrow 2m} \delta(\mathbf{k})$$

up to a constant. We have discussed at length the limitation of that formula in the QED case. For instance, oblique cuts are completely missed, and predicted spectra will be in contradiction with analyticity.

The raison d'être of this section is its status in current quarkonium physics (see for example the introductory review in [223]). Our goal is to exhibit various problems occurring in the comparison to experimental data.

3.2.1 Decay Rate Formula and Selection Rules

The first thing to do is to translate the basic formula for decay rates to the case of quarkonium. Indeed, color factors will appear. The difference with the pure QED case is the non-abelian nature of QCD, which introduces multi-gluon vertices. Also, the basic selection rules are no longer valid. A pseudoscalar quarkonium can decay into three gluons, even without any multi-gluon vertex. The fact that such a decay is not identically zero for gluons is due to color degrees of freedom: there are eight different QCD gauge bosons. Indeed, the three-

photon decay is impossible due to the compulsory symmetrization of the six possible permutations of photon insertions in the quark current. For gluons, one can antisymmetrize such insertions, provided the color degrees of freedom are also antisymmetrized. With these remarks in mind, we can proceed and write down the general decay amplitude for a quarkonium.

For a quark-antiquark bound state, the state vector is expressed as

$$|^{2S+1}S_J\rangle \sim \frac{1}{\sqrt{N}} \sum_{\text{colors}} |Q_i \bar{Q}_i\rangle$$

with N the number of colors. The amplitude is then calculated as

$$\mathcal{M}(^{2S+1}S_J \rightarrow X) = \frac{1}{\sqrt{N}} \text{Tr} [P_J \Gamma(Q(k) \bar{Q}(k) \rightarrow X)]$$

with

$$P_{J=0} = \frac{k + m_Q}{\sqrt{2}} \gamma_5; \quad P_{J=1} = \frac{k + m_Q}{\sqrt{2}} \not{\epsilon}$$

and the static limit $k = (m, 0, 0, 0)$. The trace is carried over both the Dirac space and the color degrees of freedom. The mass m_Q is the mass of the constituents, i.e. the heavy quark mass. As we have said, the present formalism assumes that the binding energy is negligible, i.e. $M = 2m_Q$. For electromagnetic bound states this was a good approximation (the difference being of order α^2), but for quarkonia, the experimental spectrum shows that binding energy can be a sizeable fraction of the mass M . The philosophy we will follow is, whenever possible, to express our results in terms of M rather than m_Q , especially for the phase-space boundaries.

In conclusion, the master formulas for quarkonium annihilation rates are

$$\begin{aligned} \Gamma(^J S(Q\bar{Q}) \rightarrow ng) &= \frac{1}{2J+1} \frac{1}{N} \frac{1}{M^2} |\phi_0|^2 \int d\Phi_n \sum_{\text{pol, Col}} |\text{Tr} [P_J \Gamma(Q\bar{Q} \rightarrow ng)]|^2 \\ \Gamma(^J S(Q\bar{Q}) \rightarrow n\gamma) &= \frac{1}{2J+1} \frac{1}{n!} \frac{N}{M^2} |\phi_0|^2 \int d\Phi_n \sum_{\text{pol}} |\text{Tr} [P_J \Gamma(Q\bar{Q} \rightarrow n\gamma)]|^2 \end{aligned}$$

with $\int d\Phi_n$ the phase-space integration.

Remarks

1) Remember to include a charge factor for each quark coupling to the photon.

2) Note that in each case, the final polarization of a gluon or photon can be replaced with more complicated expressions. For example, the decay amplitude into $gq\bar{q}$ is obtained with the substitution

$$\varepsilon_{\mu, \alpha}^*(l_1) \rightarrow \frac{-g_{\mu\alpha}}{l_1^2} \delta_{ab} \left\{ \bar{v}_i(p) \gamma^\alpha (t^b)_{ij} u_j(p') \right\}$$

and so on. Of course, the trace in the expression of $\mathcal{M}(^1S(Q\bar{Q}) \rightarrow X)$ does not apply to those factors. They are summed over when squaring the amplitude. Remember that if it is a three-gluon vertex which replaces an external gluon polarization, the corresponding processes with ghost states must be included. Such states need not be considered when external gluons are attached to the Q quark current since ghosts do not couple to matter fields.

3) Decay rates into photons will always be expressible in terms of the corresponding positronium decay rates by a very simple substitution $\alpha \rightarrow e_Q^2 \alpha$ and a factor N . For decays into gluons, some amplitudes will collapse to the corresponding photon ones, but with more complicated color factors:

$$\text{Tr} [P_J \Gamma(Q\bar{Q} \rightarrow ng)] \rightarrow (\text{Color Factor}) \times \text{Tr} [P_J \Gamma(Q\bar{Q} \rightarrow n\gamma)]$$

Anyway, there is a lot of possible gluonic channels which do not exist for photons, since selection rules

are different and since QCD is not abelian. As a result, specific decay amplitudes are very different in general.

Inclusive Rate and Duality

The basic decay rate into gluons has somehow to be translated into observables. Gluons never appear as asymptotic states, but hadrons are observed instead. One usually relies on duality concepts to relate the gluonic decay rate to the inclusive hadronic rate. Such a procedure is only an approximation. One way to view such a change of basis is as follows. One can view the hadronization as a final state interaction, so our presentation is inspired from Watson's theorem. Let us analyze the decay η_c into hadrons. The gluonic and hadronic basis are related as

$$\begin{pmatrix} gg \\ ggg \\ gq\bar{q} \\ \vdots \end{pmatrix} = S_{Duality} \begin{pmatrix} had_1 \\ had_2 \\ had_3 \\ \vdots \end{pmatrix} \equiv \begin{pmatrix} gg \rightarrow had_1 & gg \rightarrow had_2 & gg \rightarrow had_3 & \cdots \\ ggg \rightarrow had_1 & ggg \rightarrow had_2 & ggg \rightarrow had_3 & \cdots \\ gq\bar{q} \rightarrow had_1 & gq\bar{q} \rightarrow had_2 & gq\bar{q} \rightarrow had_3 & \cdots \\ \vdots & \vdots & \vdots & \ddots \end{pmatrix} \begin{pmatrix} had_1 \\ had_2 \\ had_3 \\ \vdots \end{pmatrix} \quad (3.2)$$

which leads to

$$\begin{pmatrix} \eta_c \rightarrow gg \\ \eta_c \rightarrow ggg \\ \eta_c \rightarrow gq\bar{q} \\ \vdots \end{pmatrix} = S_{Duality} \begin{pmatrix} \eta_c \rightarrow had_1 \\ \eta_c \rightarrow had_2 \\ \eta_c \rightarrow had_3 \\ \vdots \end{pmatrix} \quad (3.3)$$

It is important to remark that in these formulas, the gluonic states are viewed as asymptotic. As soon as one is considering asymptotic gluons, one can introduce real gluonic states in intermediate states (this is due to the optical theorem). Therefore, we will make the additional assumption that an exclusive decay into hadrons is factorized into a gluonic decay followed by a hadronization transition from gluons into hadrons. This means that one is neglecting non-absorptive effects in a specific exclusive decay channel.

The change of basis in (3.2) is made through $S_{Duality}$, the transition S -matrix from gluons to hadrons. Such a matrix is taken as unitary, in first approximation. In the context of final state interactions, this hypothesis was called *elasticity*, while in the present context, we will speak of *duality*. This denomination is justified since from (3.3), we directly obtain

$$|\eta_c \rightarrow gg|^2 + |\eta_c \rightarrow ggg|^2 + |\eta_c \rightarrow gq\bar{q}|^2 + \cdots = |\eta_c \rightarrow had_1|^2 + |\eta_c \rightarrow had_2|^2 + |\eta_c \rightarrow had_3|^2 + \cdots$$

Note that to leading order in α_S , only the first term $\eta_c \rightarrow gg$ contributes.

3.2.2 Pseudoscalar Quarkonium Decay

For pseudoscalar quarkonium decay, rates are [155]

	Lowest Order Decay Widths	Radiative Corrections
$^1S_0 \rightarrow \gamma\gamma$	$48\pi\alpha^2 e_Q^4 \frac{ \phi_0 ^2}{M^2}$	$\frac{\alpha_S}{\pi} \left(\frac{\pi^2}{3} - \frac{20}{3} \right) \approx -3.4 \frac{\alpha_S}{\pi}$
$^1S_0 \rightarrow gg$	$\frac{32}{3}\pi\alpha_S^2 \frac{ \phi_0 ^2}{M^2}$	$\frac{\alpha_S}{\pi} B_Q$
$^1S_0 \rightarrow \gamma l^+ l^-$	$16e_Q^4 \alpha^3 \frac{ \phi_0 ^2}{M^2} F(m_l)$	not known
$^1S_0 \rightarrow gq\bar{q}$	$\frac{64}{9}\alpha_S^3 \frac{ \phi_0 ^2}{M^2} F(m_q)$	is a correction to $^1S_0 \rightarrow gg$

where e_Q is the heavy quark charge, in units of e , M is the quarkonium mass and

$$F(m) = \frac{4}{3} \sqrt{1 - \frac{m^2}{m_Q^2}} \left(\frac{m^2}{m_Q^2} - 4 \right) + 2 \ln \left(\frac{1 + \sqrt{1 - m^2/m_Q^2}}{1 - \sqrt{1 - m^2/m_Q^2}} \right)$$

with m_Q the heavy quark mass ($= M/2$ here) and B_Q is given below. Note that these rates are often given in terms of the radial wavefunction, which is related to the wavefunction by the spherical harmonic normalization

$$|\phi_0|^2 = \frac{|R_0|^2}{4\pi}$$

Radiative Corrections to $^1S_0 \rightarrow \gamma\gamma$ and Velocity Singularity

For all the decay modes, the quoted radiative corrections omit singular terms in $1/v_{rel}$ with v_{rel} the relative velocity of the quarks in the bound states. Such singularities cancel in ratio of decay modes. To be a bit more explicit, let us consider the two-photon width. Including the radiative corrections, the rate is

$$\Gamma(^1S_0 \rightarrow \gamma\gamma) = \Gamma_0 \left(1 - \frac{4\alpha_S}{3\pi} \left(5 - \frac{\pi^2}{4} \right) \right)$$

In fact, this result is obtained from the Harris and Brown QED computation of the correction to the scattering $e^+e^- \rightarrow \gamma\gamma$ with incoming e^+e^- at rest (see chapter 1)

$$\sigma(e^+e^- \rightarrow \gamma\gamma) = \sigma_0(e^+e^- \rightarrow \gamma\gamma) \left(\left(1 + \frac{\pi\alpha}{v_{rel}} \right) - \frac{\alpha}{\pi} \left(5 - \frac{\pi^2}{4} \right) \right)$$

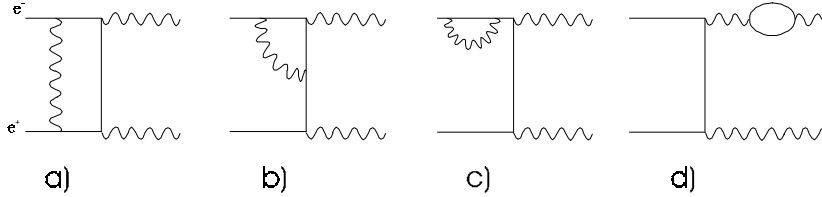
This exhibits the well-known Coulomb singularity in $1/v_{rel}$ of the binding graph. The Sommerfeld factor prescription is to absorb such a divergence into the wavefunction. In QED, this is simple to understand since the Schrödinger wavefunction is the infinite sum of ladder Coulomb exchange graphs. In QCD, we assume that the same mechanism is at work, and absorb such singularities into the wavefunction [151]. Then, the QCD correction is obtained with the substitution $\alpha \rightarrow \frac{4}{3}\alpha_S$, since for each gluon loop insertion there is a factor

$$\sum_{l,a} t_{jl}^a t_{li}^a = C_F \delta_{ij} = \frac{4}{3} \delta_{ij}$$

For example, the quark self-energy is in term of the electron self-energy

$$\Sigma_{quark}(\not{p}) = \frac{g^2}{e^2} \left(\sum_{l,a} t_{ji}^a t_{li}^a \right) \Sigma_{electron}(\not{p}) = \frac{4}{3} \frac{\alpha_S}{\alpha} \Sigma_{electron}(\not{p})$$

The same can be said for all the other diagrams (except *d*, which is discussed below):



and the crossed ones. By the way, remember that it is the first diagram that generates the $1/v_{rel}$ singularity.

Radiative Corrections to $^1S_0 \rightarrow gg$ and Renormalization Scheme

It is interesting to discuss the radiative corrections to the strong decay. Since we work at the inclusive level, these corrections include many different final states [151]

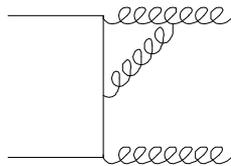
$$\begin{aligned} \Gamma(^1S_0 \rightarrow \text{light hadrons}) &= \Gamma(^1S_0 \rightarrow gg) + \Gamma(^1S_0 \rightarrow ggg) + \sum_q \Gamma(^1S_0 \rightarrow qq\bar{q}) \\ &= \Gamma(^1S_0 \rightarrow gg) \left(1 + B_Q \frac{\alpha_s}{\pi} \right) \end{aligned}$$

The coefficient B_Q is given by (in the \overline{MS} scheme)

$$\begin{aligned} B_Q(\mu) &= \beta_0 \ln \frac{\mu}{m_Q} + \frac{71}{6} - \frac{31}{24} \pi^2 + \beta_0 \left(\frac{4}{3} - \ln 2 \right) \\ &= \beta_0 \ln \frac{\mu}{m_Q} + 6.127 - 0.427 n_f \end{aligned}$$

where $\beta_0 = 11 - 2/3 n_f$. This coefficient depends on the renormalization scale μ . To be able to compare the expressions used in various papers, it is necessary to discuss the scale and scheme dependence of the coefficient $B_Q(\mu)$. This is the goal of the next few paragraphs.

Such a logarithmic scale dependence in the coefficient $B_Q(\mu)$ comes from the scale dependence of the strong coupling constant, hence there is no scale dependence for the electromagnetic decay radiative correction coefficients. This can be simply understood from the diagram *d* above. In QED, it is simply taken into account by a renormalization of the fine structure constant $\alpha_{bare} \rightarrow \alpha_{phys}$. If all internal photons are replaced by gluons, the internal UV divergences and scheme dependences take care of themselves. On the other hand, if the external photons are also replaced by gluons, the picture changes since external gluon vacuum polarization graphs generate scheme dependences. In fact, the situation is a bit more complicated because of three-gluon vertices like



but the main idea remains correct: most internal corrections combine into a finite correction, while the remaining infinite corrections linked with the external lines are absorbed into α_S by a renormalization at a scale μ , giving

to both the correction $B_Q(\mu)$ and the strong coupling $\alpha_S(\mu)$ a scale (and scheme) dependence. The momentum dependence of $\alpha_S(\mu)$ is described in the appendix B.1, along with the relevant equations for the running.

Writing this scale dependence explicitly, the corrected decay rate is

$$\Gamma(^1S_0 \rightarrow \text{light hadrons}) = \frac{32}{3} \pi \frac{|\phi_0|^2}{M^2} \alpha_S^2(\mu) \left\{ 1 + B_Q(\mu) \frac{\alpha_S(\mu)}{\pi} \right\}$$

This scale dependence is removed by redefining both B_Q and α_S at the common physical scale of the process, here $\mu = m_Q$

$$\Gamma(^1S_0 \rightarrow \text{light hadrons}) = \frac{32}{3} \pi \frac{|\phi_0|^2}{M^2} \alpha_S^2(m_Q) \left\{ 1 + B_Q(m_Q) \frac{\alpha_S(m_Q)}{\pi} \right\}$$

Retaining terms up to order α_S^2 , equating the above two results (and generalizing to an arbitrary power of α_S for future use; here, $p = 2$) leads to

$$\begin{aligned} \delta\Gamma &= \alpha_S^p(\mu) \left\{ 1 + B_Q(\mu) \frac{\alpha_S(\mu)}{\pi} \right\} = \alpha_S^p(m_Q) \left\{ 1 + B_Q(m_Q) \frac{\alpha_S(m_Q)}{\pi} \right\} \\ &= \alpha_S^p(\mu) \left(1 - p \alpha_S(\mu) \frac{\beta_0}{2\pi} \ln \left[\frac{m_Q}{\mu} \right] \right) \left\{ 1 + B_Q(m_Q) \frac{\alpha_S(\mu)}{\pi} \left(1 - \alpha_S(\mu) \frac{\beta_0}{2\pi} \ln \left[\frac{m_Q}{\mu} \right] \right) \right\} \\ &= \alpha_S^p(\mu) \left(1 + \left(B_Q(m_Q) - p \frac{\beta_0}{2} \ln \left[\frac{m_Q}{\mu} \right] \right) \frac{\alpha_S(\mu)}{\pi} + O(\alpha_S^2(\mu)) \right) \end{aligned}$$

where we have used the one-loop running equation. Equating the first and last lines, the scale dependence of B_Q is

$$B_Q(m_Q) = B_Q(\mu) + \frac{p\beta_0}{2} \ln \frac{\mu}{m_Q}$$

In other words, the scale dependence of the correction is entirely determined by the scale dependence of $\alpha_S(\mu)$, as expected. The resulting picture is

$$B_Q(\mu) = \frac{p\beta_0^{(n_1)}}{2} \ln \frac{\mu}{m_Q} + X(\beta_0^{(n_2)})$$

where X is scale independent. The numbers n_1 and n_2 are flavor numbers, and as the notation suggests, n_1 is not necessarily equal to n_2 . Indeed, their origins are different. The origin of n_1 is in the number of flavors used to run α_S , while n_2 depends on the specific radiative corrections to the process under consideration. From these remarks, one can see that to give B_Q , there is a number of conventions to fix: scheme, flavor numbers n_1 and n_2 and scale. Unfortunately, there is no universal agreement. Let us review some conventions used in the literature.

1) **The Grunberg scale:** The more natural choice is $\mu = m_Q$

$$B_Q^{\mu=m_Q} = 6.13 - 0.43n_f$$

since each gluon carries an energy roughly equal to m_Q . In this scheme, the coefficient B_Q depends on n_f . Its value for charmonium is obtained with $n_f = 3$ as $B_c = 4.85$ while for bottomonium, with $n_f = 4$, $B_b = 4.42$. This is the scheme we will choose in the present work⁸.

2) **The Barbieri scale:** Another scale is used by *Barbieri et al.* [151] who take $\mu = 2m_Q$ to get

$$B_Q^{\mu=2m_Q} = 13.8 - 0.89n_f$$

Note that in their original paper, the \overline{MS} scheme was employed. Furthermore, they used four flavours in

⁸ The Grunberg scale is usually defined so that the strong correction to some specific ratio of decay modes vanishes [157]. In doing so, μ is found to be very close to the natural scale m_Q .

the running of α_S while only 3 for the n_f dependent part of B_Q . They obtained

$$B_Q^{\text{Barbieri}} = \beta_0^{(4)} \left(\frac{1}{2} \ln 4\pi - \frac{1}{2} \gamma + \ln \frac{\mu}{m_Q} \right) + \frac{71}{6} - \frac{31}{24} \pi^2 + \beta_0^{(3)} \left(\frac{4}{3} - \ln 2 \right) \stackrel{\mu=2m_Q}{=} 18.76$$

which translated into the \overline{MS} scheme (simply drop the γ and $\ln 4\pi$)

$$B_Q^{\text{Barbieri}} = \beta_0^{(4)} \ln \frac{\mu}{m_Q} + \frac{71}{6} - \frac{31}{24} \pi^2 + \beta_0^{(3)} \left(\frac{4}{3} - \ln 2 \right) \stackrel{\mu=2m_Q}{=} 10.62$$

For comparison, if $n_f = 3$ everywhere, the correction is

$$B_Q = \beta_0^{(3)} \ln \frac{\mu}{m_Q} + \frac{71}{6} - \frac{31}{24} \pi^2 + \beta_0^{(3)} \left(\frac{4}{3} - \ln 2 \right) \stackrel{\mu=2m_Q}{=} 11.13$$

3) **The Brodsky-Lepage-Mackenzie Scale:** The BLM scheme [211] redefines B_Q at a scale such that all n_f dependence in B_Q are moved into the strong coupling. This leads to

$$B_Q^{\text{BLM}} = -0.965$$

with $\mu = 0.52466m_Q = 0.26233M$. Note, however, that it may be a problem to run the coupling down to such a low scale (for $Q = c$, $\mu \approx 700MeV$).

There is a certain relevance in discussing such schemes. It is indeed necessary to have an unambiguous value of the first order coefficient to estimate the convergence of the perturbation series. In view of the above, the coefficient varies as ($n_f = 3$) 4.83, 11.1, -0.97 respectively. With an α_S of around 0.3, the Barbieri prescription leads to $B_Q^{\mu=2m_Q} \frac{\alpha_S}{\pi} > 1$, which is not very convenient for a series expansion parameter. The BLM scheme is sometimes advocated as an unambiguous scheme with which to check the perturbation series [211]. Its drawback is that it is not applicable when three-gluon vertex loop diagrams are present.

Photon Spectrum in $^1S_0 \rightarrow \gamma l^+ l^-$

This is the first occurrence of analytical problems in quarkonium physics. Since we are using the simple model of Pirenne and Wheeler, the photon spectrum is in contradiction with Low's theorem. This is equally true for the gluon energy spectrum in $^1S_0 \rightarrow gq\bar{q}$, but let us take the electromagnetic mode for illustration, so that confinement does not enter the discussion.

In the present theory, the normalized differential rate is

$$\frac{1}{\Gamma(^1S_0(Q\bar{Q}) \rightarrow \gamma\gamma)} \frac{d\Gamma(^1S_0(Q\bar{Q}) \rightarrow \gamma l^+ l^-)}{dx} = \frac{\alpha}{3\pi} \frac{\rho(x, m_l^2/m_Q^2)}{x^2}$$

where the phase-space spectrum is

$$\rho(x, a) = \sqrt{1 - \frac{a}{1-x}} [a + 2(1-x)] \frac{x^3}{(1-x)^2}$$

with x the reduced photon energy $x = 2E_\gamma/M$.

Close to $x = 0$, the spectrum is linear in x , while Low's theorem requires a cubic spectrum. Exactly the same phenomenon was encountered in the discussion of $p\text{-}Dm \rightarrow \gamma e^+ e^-$, to which we refer for additional information.

3.2.3 Vector Quarkonium Decays

For vector quarkonia, the results are [155], [18]

	Lowest Order Decay Widths	Radiative Corrections
${}^3S_1 \rightarrow \gamma^* \rightarrow l^+l^-$	$16\pi (e_Q^2 \alpha^2) \frac{ \phi_0 ^2}{M^2} G(m_l)$	$-\frac{16}{3} \frac{\alpha_S}{\pi}$
${}^3S_1 \rightarrow \gamma^* \rightarrow q\bar{q}$	$48\pi (e_Q^2 e_q^2 \alpha^2) \frac{ \phi_0 ^2}{M^2} G(m_q)$	$-\frac{13}{3} \frac{\alpha_S}{\pi}$
${}^3S_1 \rightarrow \gamma\gamma\gamma$	$\frac{64(\pi^2 - 9)}{3} (e_Q^6 \alpha^3) \frac{ \phi_0 ^2}{M^2}$	$-12.6 \frac{\alpha_S}{\pi}$
${}^3S_1 \rightarrow ggg$	$\frac{160(\pi^2 - 9)}{81} \alpha_S^3 \frac{ \phi_0 ^2}{M^2}$	$\frac{\alpha_S}{\pi} B_Q^{ggg}$
${}^3S_1 \rightarrow \gamma gg$	$\frac{128(\pi^2 - 9)}{9} e_Q^2 \alpha \alpha_S^2 \frac{ \phi_0 ^2}{M^2}$	$\frac{\alpha_S}{\pi} B_Q^{\gamma gg}$

with

$$G(m) = \left(1 + \frac{m^2}{2m_Q^2}\right) \sqrt{1 - \frac{4m^2}{M^2}} \approx 1 \text{ for } m \ll m_Q$$

The strong radiative correction coefficients $B_Q^{\gamma gg}$ and B_Q^{ggg} are scale dependent, as for the pseudoscalar quarkonium two-gluon decays. The decays into three gluons and two-gluons plus a photon are corrected as

$$\begin{aligned} B_Q^{ggg} &= \frac{3}{2} \beta_0 \ln \frac{\mu}{m_Q} - 0.26 - 1.16n_f \\ B_Q^{\gamma gg} &= \beta_0 \ln \frac{\mu}{m_Q} - 4.37 - 0.77n_f \end{aligned}$$

which give, at the Grunberg scale ($\mu = m_Q$)

	B_Q^{ggg}	$B_Q^{\gamma gg}$
$Q = c \Rightarrow n_f = 3$	-3.7	-6.7
$Q = b \Rightarrow n_f = 4$	-4.9	-7.4

As for the two-gluon mode of the 1S_0 , those corrections do contain different processes. For example, B_Q^{ggg} accounts for ${}^3S_1 \rightarrow 3g, 4g, ggq\bar{q}$, [156].

Let us also note that the correction to the three-photon decay as quoted without justifications in [155], [18] is suspicious. Instead, we would expect it to be simply 4/3 times the QED orthopositronium $\mathcal{O}(\alpha)$ correction, i.e.

$$-\frac{4}{3} (10.3) \frac{\alpha_S}{\pi} = -13.7 \frac{\alpha_S}{\pi}$$

Differential Rates

For the three vector particle decay modes, the present formalism is essentially the Ore-Powell one (see [149], [156]). Therefore, the differential rates are

$$\begin{aligned}\frac{d\Gamma(^3S_1 \rightarrow \gamma\gamma\gamma)}{dx_1} &= \frac{64}{3} \frac{e_Q^6 \alpha^3}{M^2} |\phi_0|^2 \Omega(x_1) \\ \frac{d\Gamma(^3S_1 \rightarrow ggg)}{dx_1} &= \frac{160}{81} \alpha_S^3 \frac{|\phi_0|^2}{M^2} \Omega(x_1) \\ \frac{d\Gamma(^3S_1 \rightarrow gg\gamma)}{dx_1} &= \frac{128}{9} e_Q^2 \alpha \alpha_S^2 \frac{|\phi_0|^2}{M^2} \Omega(x_1)\end{aligned}$$

with again

$$\begin{aligned}\Omega(x_1) &= \frac{2(2-x_1)}{x_1} + \frac{2(1-x_1)x_1}{(2-x_1)^2} + 4 \left[\frac{(1-x_1)}{x_1^2} - \frac{(1-x_1)^2}{(2-x_1)^3} \right] \ln(1-x_1) \\ &= \frac{5}{3}x_1 + \mathcal{O}(x_1^2) \text{ near } x_1 = 0\end{aligned}$$

This spectrum is in contradiction with Low's theorem, hence cannot be correct. For further information, we refer to the discussion on the orthopositronium decay.

The interest of the contradiction with Low's theorem is greatly enhanced in quarkonium physics. Contrary to the orthopositronium case, both the spectrum for $J/\psi \rightarrow \gamma + \text{hadrons}$ or $\Upsilon \rightarrow \gamma + \text{hadrons}$ have been observed, and disagree with the Ore-Powell prediction. We will analyze that fact in the next chapter.

3.3 Analysis of Inclusive Charmonium Decay

In this section we use the theoretical decay rates reviewed in the previous section to extract information from the experimental data for the charmonium, and, when applicable, for the bottomonium. The kind of information that can be retrieved are the strong coupling α_S , ratios of wavefunctions, and predictions for yet unobserved modes. The approach followed is inspired from [155], [167].

3.3.1 Pseudoscalar Charmonium Decay

The ratio of the two-gluon rate to the two-photon rate is, including radiative corrections taken at the scale $\mu \approx m_Q \approx M/2$,

$$\frac{\Gamma(^1S_0(Q\bar{Q}) \rightarrow \text{Light hadrons})}{\Gamma(^1S_0(Q\bar{Q}) \rightarrow \gamma\gamma)} = \frac{9}{8} \frac{\alpha_S^2}{\alpha^2} \left\{ 1 + 8.2 \frac{\alpha_S}{\pi} \right\}$$

Using the η_c experimental values, we can obtain the strong coupling and the η_c wavefunction as:

$$\begin{aligned}\alpha_S(m_c) &= 0.30 \pm 0.04 \\ |R_0|^2 &= 4\pi |\phi_0|^2 = (0.33 \pm 0.11) \text{ GeV}^3\end{aligned}$$

The error quoted is purely experimental. The neglected terms of order $\alpha_S^2 \sim 0.1$ give an idea of the theoretical errors.

If one uses the scale of *Barbieri et al.* (but in \overline{MS}), the correction to the ratio is

$$\frac{\Gamma(^1S_0(Q\bar{Q}) \rightarrow \text{Light hadrons})}{\Gamma(^1S_0(Q\bar{Q}) \rightarrow \gamma\gamma)} = \frac{9}{8} \frac{\alpha_S^2(2m_Q)}{\alpha^2} \left\{ 1 + 14.46 \frac{\alpha_S}{\pi} \right\}$$

which is a huge correction (in MS , the coefficient is 22.3). Solving for $\alpha_S(2m_c)$ gives $\alpha_S(2m_c) = 0.266$. When run down to m_c , we get $\alpha_S(m_c) = 0.34$. At the scale of the charm, the scale ambiguity generates a huge ambiguity of order $\alpha_S^2 \sim 0.1$, which is the theoretical error quoted above.

Finally, a more recent experimental determination is [138]

$$\begin{aligned} B(\eta_c \rightarrow \gamma\gamma) &= (2.8 \pm 1.1) \times 10^{-4} \\ \Gamma(\eta_c \rightarrow \text{hadrons}) &= 27 \pm 7 \text{ MeV} \end{aligned}$$

giving the same value of α_S

$$\begin{aligned} \alpha_S(m_c) &\sim 0.31 \\ |R_0|^2 &= 4\pi |\phi_0|^2 \sim (0.65) \text{ GeV}^3 \end{aligned}$$

3.3.2 Vector Charmonium Decay

Vector Charmonium Radiative Decay into Hadrons

The rate for vector quarkonium decay into electron-positron can be used to estimate the rate for hadronic decay via a photon. Including radiative corrections,

$$\frac{\sum_q \Gamma(^3S_1(Q\bar{Q}) \rightarrow \gamma \rightarrow q\bar{q})}{\Gamma(^3S_1(Q\bar{Q}) \rightarrow e^+e^-)} = 3(e_u^2 + e_d^2 + e_s^2) \left\{ 1 + \frac{\alpha_S}{\pi} \right\} \approx 2.1$$

A more precise determination of this ratio uses the experimental electron-positron annihilation cross section

$$R(q^2) \Big|_{q^2=M_{Q\bar{Q}}^2} = \frac{\sigma(e^+e^- \rightarrow \gamma(q^2) \rightarrow \text{hadrons})}{\sigma(e^+e^- \rightarrow \gamma(q^2) \rightarrow e^+e^-)} \Big|_{q^2=M_{Q\bar{Q}}^2} \approx \frac{\Gamma(^3S_1(Q\bar{Q}) \rightarrow \gamma \rightarrow \text{hadrons})}{\Gamma(^3S_1(Q\bar{Q}) \rightarrow e^+e^-)}$$

For the case of J/ψ , $R(M_{J/\psi}^2) = 2.5 \pm 0.3$ and

$$B(J/\psi \rightarrow \gamma \rightarrow \text{hadrons}) = 2.5 \times B(J/\psi \rightarrow e^+e^-) = (15 \pm 2) \%$$

as quoted in [223].

Vector Charmonium Hadronic Width

The ratios we analyze are, for $n_f = 3$ and the scale $\mu = m_c$

$$\frac{\Gamma(J/\psi \rightarrow ggg)}{\Gamma(J/\psi \rightarrow e^+e^-)} = \frac{10(\pi^2 - 9)}{81\pi} \frac{\alpha_S^3(m_c)}{e_Q^2 \alpha^2} \left\{ 1 + 1.6 \frac{\alpha_S(m_c)}{\pi} \right\} \quad (3.4)$$

$$\frac{\Gamma(J/\psi \rightarrow \gamma gg)}{\Gamma(J/\psi \rightarrow ggg)} = \frac{36}{5} \frac{e_Q^2 \alpha}{\alpha_S(m_c)} \left\{ 1 - 2.9 \frac{\alpha_S(m_c)}{\pi} \right\} \quad (3.5)$$

where the radiative corrections to ggg include $4g$, $ggq\bar{q}$, and those to γgg include γggg and $\gamma gq\bar{q}$.

To compare with experimental data, we would need the measured values of $\Gamma(J/\psi \rightarrow ggg)$ and $\Gamma(J/\psi \rightarrow \gamma gg)$. Since these are unavailable, we will proceed differently. First, we write the total J/ψ width as

$$\Gamma_{tot} = \Gamma(J/\psi \rightarrow ggg) + \Gamma(J/\psi \rightarrow \gamma gg) + \sum_{l=e,\mu} \Gamma(J/\psi \rightarrow l^+l^-) + \sum_{q=u,d,s} \Gamma(J/\psi \rightarrow \gamma \rightarrow q\bar{q}) + \Gamma(J/\psi \rightarrow \eta_c \gamma)$$

from which we extract the combination

$$\frac{\Gamma(J/\psi \rightarrow ggg) + \Gamma(J/\psi \rightarrow \gamma gg)}{\Gamma_{tot}} \approx 70\% \quad (3.6)$$

Solving equation (3.4), (3.5) and (3.6), we find

$$\begin{cases} B(J/\psi \rightarrow ggg) = 63\% \\ B(J/\psi \rightarrow \gamma gg) = 6.5\% \\ \alpha_S(m_c) = 0.19 \end{cases} \quad (3.7)$$

i.e. a quite small α_S value. Note that the γgg branching is roughly a tenth of the ggg branching.

One can also work at the Brodsky-Lepage-Mackenzie (BLM) scale $\mu = 0.157M \equiv \xi M$. Remember that this scale is defined such that B_c^{ggg} is independent of n_f (for $\eta_c \rightarrow gg$, the BLM scale was $\mu = 0.26M$). The ratios become

$$\frac{\Gamma(J/\psi \rightarrow ggg)}{\Gamma(J/\psi \rightarrow e^+e^-)} \stackrel{BLM}{=} \frac{10(\pi^2 - 9)}{81\pi} \frac{\alpha_S^3(\xi M)}{e_Q^2 \alpha^2} \left\{ 1 - 14.0 \frac{\alpha_S(\xi M)}{\pi} \right\} \quad (3.8)$$

$$\frac{\Gamma(J/\psi \rightarrow \gamma gg)}{\Gamma(J/\psi \rightarrow ggg)} \stackrel{BLM}{=} \frac{36}{5} \frac{e_Q^2 \alpha}{\alpha_S(\xi M)} \left\{ 1 + 2.27 \frac{\alpha_S(\xi M)}{\pi} \right\} \quad (3.9)$$

since the same scale renders $B_c^{\gamma gg}$ independent of n_f . The interest of the BLM scheme is its supposed unambiguous check of the perturbation expansion. The coefficient -14 in the above formula shows that perturbative QCD may be completely wrong when applied to quarkonium decays. Finally, remark that since those coefficients are now independent of n_f , the above formulas are equally valid for bottomonium.

We have chosen not to work in this scheme because the running down to $\mu = 0.157M$ using perturbative QCD is questionable. As a manifestation of this breakdown, the system of (3.8), (3.9) and (3.6) does not admit real solutions. The reason why below a certain scale the system becomes impossible is quite clear: $B_c^{ggg} \alpha_S / \pi$ become less than -1 . For $\alpha_S \sim 0.3$, the ratio (3.8) of branching fractions is negative!

Finally, let us also quote the Grunberg scale, i.e. the scale such that the correction to the ratio (3.4) vanishes

$$\begin{aligned} n_f = 3 : \quad \mu &= 0.89m_c \\ n_f = 4 : \quad \mu &= 0.97m_c \end{aligned}$$

What is remarkable with this scale is that it is so close to the natural scale m_c .

The branching fraction $B(J/\psi \rightarrow \gamma gg)$ can be compared with experiment:

$$B^{\text{exp}}(J/\psi \rightarrow \gamma(x > 0.6) + X) = (4.1 \pm 0.8)\% \quad (3.10)$$

where x stands for $2E_\gamma/M_{J/\psi}$. On the theoretical side, from the prediction (3.7), we can obtain an estimate of $J/\psi \rightarrow \gamma(x > 0.6) + X$ by integrating the Ore-Powell spectrum between $x = 0.6$ and $x = 1$

$$B(J/\psi \rightarrow \gamma(x > 0.6)gg) = B(J/\psi \rightarrow \gamma gg) \times \frac{\int_{0.6}^1 \Omega(x_1) dx_1}{\int_0^1 \Omega(x_1) dx_1} = B(J/\psi \rightarrow \gamma gg) \times 0.637$$

This gives with (3.7), i.e. $B(J/\psi \rightarrow \gamma gg) = 6.5\%$:

$$B^{th}(J/\psi \rightarrow \gamma(x > 0.6)gg) = 4.1\%$$

in agreement with experiment (3.10). The reason for this rather good estimate can be found in the cancellation of corrections (relativistic, binding energy,...) in the ratio $\gamma gg/ggg$, since both involve the same kinematics. The main problem is that the observed photon spectrum is much softer than the QCD predicted photon spectrum, even if the integrated rate is in good agreement. This will be discussed in the next chapter.

The same type of analyzes can be carried out for $\psi(2S)$ decay channels. The main difference is the huge branching fraction $B(\psi(2S) \rightarrow J/\psi + X) = (61 \pm 4)\%$. The total width thus gives

$$\begin{aligned} \Gamma_{tot} = & \Gamma(\psi(2S) \rightarrow ggg) + \Gamma(\psi(2S) \rightarrow \gamma gg) + \sum_{l=e,\mu,\tau} \Gamma(\psi(2S) \rightarrow l^+l^-) + \sum_{q=u,d,s} \Gamma(\psi(2S) \rightarrow \gamma \rightarrow q\bar{q}) \\ & + \sum_{n=1,2} \Gamma(\psi(2S) \rightarrow \eta_c(nS) + \gamma) + \sum_{J=0,1,2} \Gamma(\psi(2S) \rightarrow \chi_{cJ}(1P) + \gamma) + \Gamma(\psi(2S) \rightarrow J/\psi + X) \end{aligned}$$

i.e.

$$\frac{\Gamma(\psi(2S) \rightarrow ggg) + \Gamma(\psi(2S) \rightarrow \gamma gg)}{\Gamma_{tot}} \approx 7.3\%$$

which leads to

$$\begin{cases} B(\psi(2S) \rightarrow ggg) = 7.2\% \\ B(\psi(2S) \rightarrow \gamma gg) = 0.78\% \\ \alpha_S(m_c) = 0.18 \end{cases}$$

which is consistent with the J/ψ results; it gives again a small value for $\alpha_S(m_c)$ compared to the value extracted from η_c decays.

Three-Photon Decay

Finally, we can predict the width ${}^3S_1(Q\bar{Q}) \rightarrow \gamma\gamma\gamma$ relative to the ggg one as

$$\frac{\Gamma({}^3S_1(Q\bar{Q}) \rightarrow ggg)}{\Gamma({}^3S_1(Q\bar{Q}) \rightarrow \gamma\gamma\gamma)} = \frac{5}{54} \frac{\alpha_S^3}{e_Q^6 \alpha^3} = \frac{135}{128} \frac{\alpha_S^3}{\alpha^3}$$

which implies

$$\frac{\Gamma(J/\psi \rightarrow \gamma\gamma\gamma)}{\Gamma(J/\psi \rightarrow ggg)} \sim 10^{-5}$$

so that experimental sensitivity is nearing the theoretical prediction. Note that we have dropped the radiative correction

$$\Gamma(J/\psi \rightarrow \gamma\gamma\gamma) = \Gamma_0 \left(1 - 12.6 \frac{\alpha_S}{\pi}\right)$$

The huge coefficient renders the perturbation series problematic. For instance, for $\alpha_S > 0.25$ the rate becomes negative.

3.3.3 Ratios of Wavefunctions

Comparison of Vector and Scalar Wavefunctions

We can use the ratio

$$\frac{\Gamma(^1S_0(Q\bar{Q}) \rightarrow \gamma\gamma)}{\Gamma(^3S_1(Q\bar{Q}) \rightarrow e^+e^-)} = 3e_Q^2 \frac{|\phi_0(^1S_0)|^2 M_{3S}^2}{|\phi_0(^3S_1)|^2 M_{1S}^2} \left\{ 1 + \frac{\pi^2 - 4\alpha_S}{3\pi} \right\}$$

where we have included radiative corrections. Non-relativistically, the wavefunctions are the same. Furthermore, the mass difference is negligible at this level, hence

$$\frac{\Gamma(^1S_0(Q\bar{Q}) \rightarrow \gamma\gamma)}{\Gamma(^3S_1(Q\bar{Q}) \rightarrow e^+e^-)} \approx 3e_Q^2 \left\{ 1 + \frac{\pi^2 - 4\alpha_S}{3\pi} \right\}$$

For charmonium, we get with $\alpha_S = 0.3 \pm 0.1$

$$\frac{\Gamma(\eta_c \rightarrow \gamma\gamma)}{\Gamma(J/\psi \rightarrow e^+e^-)} = \frac{4}{3} \left\{ 1 + \frac{\pi^2 - 4\alpha_S}{3\pi} \right\} \approx 1.6 \pm 0.1$$

while the experimental values give

$$\frac{B(\eta_c \rightarrow \gamma\gamma) \cdot \Gamma_{\eta_c}}{B(J/\psi \rightarrow e^+e^-) \cdot \Gamma_{J/\psi}} = \frac{(3.0 \pm 1.2) \times 10^{-4}}{(5.93 \pm 0.10) \times 10^{-2}} \times \frac{13.2 \pm 3.5}{(87 \pm 5) \times 10^{-3}} \approx 0.8^{+0.8}_{-0.5}$$

The central value is too low by about a factor 2. This could be due to relativistic corrections (especially in the difference of the wavefunctions, due for example to spin-spin forces), to binding energy effects.... Note however that errors are quite big: the theoretical prediction is still in the experimental range, so that it is difficult to draw any conclusions about the equality of 1S_0 and 3S_1 wavefunctions.

Radial Excitation Wavefunction

With the experimental measurements of $J/\psi \rightarrow e^+e^-$ and $\psi(2S) \rightarrow e^+e^-$, we can estimate the ratio of wavefunctions of both states as

$$\frac{|\phi_0(\psi(2S))|^2}{|\phi_0(J/\psi)|^2} = \frac{M_{\psi(2S)}^2}{M_{J/\psi}^2} \frac{\Gamma(\psi(2S) \rightarrow e^+e^-)}{\Gamma(J/\psi \rightarrow e^+e^-)} = \left(\frac{3686}{3097} \right)^2 \frac{(8.5 \pm 0.7) \times 10^{-3}}{(6.02 \pm 0.19) \times 10^{-2}} \frac{(277 \pm 31)}{(87 \pm 5)} = 0.6 \pm 0.2 \quad (3.11)$$

As expected, the wavefunction at zero separation decreases as n increases. The three-gluon branchings extracted before also give the ratio of wavefunctions

$$\frac{|\phi_0(\psi(2S))|^2}{|\phi_0(J/\psi)|^2} = \frac{M_{\psi(2S)}^2}{M_{J/\psi}^2} \frac{B(\psi(2S) \rightarrow ggg) \cdot \Gamma_{\psi(2S)}}{B(J/\psi \rightarrow ggg) \cdot \Gamma_{J/\psi}} \approx \left(\frac{3686}{3097} \right)^2 \frac{(0.072)}{(0.64)} \times \frac{(277)}{(87)} \approx 0.5$$

Obviously, the errors are still much too large to get a clear coherence test among determinations.

3.3.4 Conclusion: Fit to the Charmonium Data

To close this analysis, it is interesting to proceed in the opposite way, i.e. to infer values for the various decay modes from specific values of $\alpha_S(m_c)$

$$\begin{array}{c|cccc} m_c [GeV] & 1.3 & 1.5 & 1.7 & 2 \\ \hline \alpha_S(m_c) & 0.378 & 0.347 & 0.325 & 0.300 \end{array}$$

obtained by running down the world average of $\alpha_S(M_Z) \approx 0.118$, with the three-loop beta function (see appendix B.1). To estimate the wavefunctions, we use the electromagnetic decay rates

$$\begin{cases} \Gamma^{\text{exp}}(\eta_c \rightarrow \gamma\gamma) = (7.6 \pm 1.2) \text{ keV} \\ \Gamma^{\text{th}}(\eta_c \rightarrow \gamma\gamma) = 48\pi\alpha^2 e_Q^4 \xi_1 \left(1 - 3.4 \frac{\alpha_S}{\pi}\right) \\ \Gamma^{\text{exp}}(J/\psi \rightarrow e^+e^-) = (5.26 \pm 0.37) \text{ keV} \\ \Gamma^{\text{th}}(J/\psi \rightarrow e^+e^-) = 16\pi e_Q^2 \alpha^2 \xi_3 \left(1 - \frac{16}{3} \frac{\alpha_S}{\pi}\right) \end{cases}$$

where we have denoted

$$\xi_{2J+1} = \frac{|\phi_0(2J+1S)|^2}{M^2}$$

This gives

$$\begin{array}{c|cccc} \alpha_S(m_c) & 0.378 & 0.347 & 0.325 & 0.300 \\ \hline \xi_1 [MeV] & 8.1 \pm 1.2 & 7.6 \pm 1.2 & 7.36 \pm 1.1 & 7.06 \pm 1.1 \\ \xi_3 [MeV] & 12.3 \pm 0.9 & 10.8 \pm 0.8 & 9.85 \pm 0.70 & 9.01 \pm 0.63 \end{array}$$

Taking those values, we get

	$m_c = 1.3$	$m_c = 1.5$	$m_c = 1.7$	$m_c = 2$	
$\eta_c \rightarrow \gamma\gamma$	7.6*	7.6*	7.6*	7.6*	keV
$\eta_c \rightarrow \gamma e^+ e^-$	0.13	0.13	0.12	0.12	keV
$\eta_c \rightarrow X$	61	47	39	31	MeV
$J/\psi \rightarrow l^+ l^-$	5.26*	5.26*	5.26*	5.26*	keV
$J/\psi \rightarrow \gamma\gamma\gamma$	7.8	6.8	6.2	5.7	eV
$J/\psi \rightarrow X$	0.63	0.46	0.36	0.27	MeV
$J/\psi \rightarrow \gamma + X$	14	14	13	12	keV

*Input

where X stands for the totality of hadron states.

A recent measurement [138] of the η_c width was twice the older one, at

$$\Gamma(\eta_c \rightarrow had) = 27 \pm 5.8 \pm 1.4 \text{ MeV}$$

which is in quite good agreement with the theory. On the J/ψ side, the theoretical predictions do not fit the experimental values. The width for ggg is greater than the total measured width of J/ψ , $\Gamma_{tot} = 87 \pm 5 \text{ keV}$, by 5 – 10 times !

This same fact was apparent before, in the extracted value of the strong coupling

$$\begin{aligned} \eta_c &\rightarrow \alpha_S = 0.3 \\ J/\psi &\rightarrow \alpha_S = 0.2 \end{aligned}$$

The η_c value is consistent with the world average, but not the J/ψ one.

As a first trivial explanation, it could be that the c quark mass may be too low for QCD perturbation theory. If, however, we insist in taking seriously this first order $pQCD$ analysis, we need a powerful suppression effect. Usually, people invoke relativistic corrections like [167]

$$\Gamma = \Gamma_0 \left(1 + C \frac{v^2}{c^2}\right)$$

with v the relative $c\bar{c}$ velocity and $C < 0$. In charmonium, these relativistic corrections can be sizeable because

$$v^2/c^2 \approx 0.24$$

In the next chapter, the observed suppression of vector quarkonium decays will be explained by binding energy effects.

3.3.5 Vector Bottomonium Decay

For the $b\bar{b}$ bottomonium states, experimental data are quite reduced, 1S_0 states have not been observed yet and branching fractions for vector states (the Υ family) are rather scarce. We will thus only present a limited analysis, with emphasis on the strong coupling extraction at the b quark mass. Indeed, it is interesting to see whether the extracted values of $\alpha_S(m_b)$ are in better agreement than $\alpha_S(m_c)$ with the world average value.

Leptonic Width

The leptonic widths for bottomonium are

$$\begin{cases} \Gamma(\Upsilon \rightarrow e^+e^-) = (2.52 \pm 0.17) \% \\ \Gamma(\Upsilon \rightarrow \mu^+\mu^-) = (2.48 \pm 0.07) \% \\ \Gamma(\Upsilon \rightarrow \tau^+\tau^-) = (2.67 \pm 0.15) \% \end{cases}$$

From these, we can estimate the width $\Gamma(\Upsilon \rightarrow \gamma \rightarrow \text{hadrons})$ using

$$\frac{\Gamma(\Upsilon \rightarrow \gamma \rightarrow \text{hadrons})}{\Gamma(\Upsilon \rightarrow e^+e^-)} \approx R(q^2)|_{q^2=M_{b\bar{b}}^2} \approx 3.5$$

Then

$$B(\Upsilon \rightarrow \gamma \rightarrow \text{hadrons}) = 3.5 \times B(\Upsilon \rightarrow e^+e^-) = (8.6 \pm 0.4) \%$$

Vector Bottomonium Hadronic Width

We proceed as for the charmonium. The ratios we analyze are (in the Grunberg scale)

$$\frac{\Gamma(\Upsilon \rightarrow ggg)}{\Gamma(\Upsilon \rightarrow e^+e^-)} = \frac{10(\pi^2 - 9)}{81\pi} \frac{\alpha_S^3}{e_Q^2 \alpha^2} \left\{ 1 + 0.43 \frac{\alpha_S}{\pi} \right\} \quad (3.12)$$

$$\frac{\Gamma(\Upsilon \rightarrow \gamma gg)}{\Gamma(\Upsilon \rightarrow ggg)} = \frac{36 e_Q^2 \alpha}{5 \alpha_S} \left\{ 1 - 2.5 \frac{\alpha_S}{\pi} \right\} \quad (3.13)$$

To further compare with experimental data, we extract the combination $\Gamma(\Upsilon \rightarrow ggg) + \Gamma(\Upsilon \rightarrow \gamma gg)$ from the total rate as

$$\begin{aligned} \Gamma_{tot} &= \Gamma(\Upsilon \rightarrow ggg) + \Gamma(\Upsilon \rightarrow \gamma gg) + \sum_{l=e,\mu,\tau} \Gamma(\Upsilon \rightarrow l^+l^-) + \sum_{q=u,d,s,c} \Gamma(\Upsilon \rightarrow \gamma \rightarrow q\bar{q}) + \Gamma(\Upsilon \rightarrow \eta_b \gamma) \\ &= \Gamma(\Upsilon \rightarrow ggg) + \Gamma(\Upsilon \rightarrow \gamma gg) + (3 + R) \Gamma(\Upsilon \rightarrow e^+e^-) \\ &\rightarrow \frac{\Gamma(\Upsilon \rightarrow ggg) + \Gamma(\Upsilon \rightarrow \gamma gg)}{\Gamma_{tot}} \approx 1 - (3 + R) B(\Upsilon \rightarrow e^+e^-) \approx 83.8\% \end{aligned} \quad (3.14)$$

where we have neglected $\Upsilon \rightarrow \eta_b \gamma$. Solving the equations (3.12), (3.13) and (3.14), we find

$$\begin{cases} B(\Upsilon \rightarrow ggg) = 82\% \\ B(\Upsilon \rightarrow \gamma gg) = 2.3\% \\ \alpha_S(m_b) = 0.177 \end{cases}$$

Extrapolated to the Z^0 mass, this gives a strong coupling of

$$\alpha_S(m_b) = 0.177 \rightarrow \alpha_S(M_Z) = 0.104$$

i.e. a quite small value. Note that usually, people use the BLM scheme, i.e. $\mu = 0.157M_\Upsilon$. This does not change the conclusion: one obtains at the BLM scale a strong coupling of $\alpha_S(0.157M_\Upsilon) = 0.25$, i.e. when run up to m_b , $\alpha_S(m_b) = 0.18$.

This closes our basic review of quarkonium annihilation modes as described in the standard factorized approaches. In the next chapter, the binding energy effects will be introduced, as a cure for the analytical defects of factorized models.

Chapter 4

Binding Energy Effects on Quarkonium Annihilation Rates

In the standard schemes, quarkonium annihilation amplitudes are constructed assuming a factorization of the bound state dynamics from the perturbative decay process. As discussed in the previous chapter, the basic model is simply the extension to quarkonium of the Pirenne-Wheeler model

$$\Gamma(P_s \rightarrow n\gamma) = \frac{1}{2J+1} |\phi(0)|^2 (4v_{rel}\sigma(e^-e^+ \rightarrow n\gamma))_{v_{rel} \rightarrow 0}$$

As we have extensively discussed in the case of positronium, a modification of the quarkonium annihilation description is unavoidable, since the predictions of any approach based on factorization are in contradiction with analyticity. One has to introduce binding energy effects. Compared to positronium however, the introduction of such effects is not just a matter of principle; it can change the whole picture of quarkonium physics since the typical quarkonium binding energies are huge

$$\frac{4m_e^2}{M_{P_s}^2} \equiv 1 + \frac{4\gamma_{P_s}^2}{M_{P_s}^2} = 1 + \mathcal{O}(\alpha^2)$$

$$\frac{4m_D^2}{M_{J/\psi}^2} \equiv 1 + \frac{4\gamma_{J/\psi}^2}{M_{J/\psi}^2} \approx 1.45 \quad (4.1)$$

$$\frac{4m_B^2}{M_{\Upsilon}^2} \equiv 1 + \frac{4\gamma_{\Upsilon}^2}{M_{\Upsilon}^2} \approx 1.25 \quad (4.2)$$

For these rough estimates, the constituent mass of the heavy quark is taken as the mass of the corresponding lowest heavy flavored meson. We are forced to proceed in this way since twice the running mass of the heavy quark is less than the bound state mass (the origin of this fact is confinement). Another approach would be to use the quark masses found in spectroscopic studies (see (3.1)). This leads to very similar estimates for the binding energies.

We will review in this chapter the implications of binding energy effects for a number of problems in quarkonium physics: the α_S extraction, the $\rho\pi$ puzzle, the photon spectrum in inclusive radiative decays, and the radiative transitions between quarkonium states. The discussion will remain at a qualitative level in most cases. The purpose is only to show that binding energy effects indeed lead to significant modifications, and that those modifications go in the right direction, i.e. that binding energy effects can be invoked to explain the various quarkonium puzzles. We are unable at present to do a quantitative analysis because a number of complicated issues have to be resolved first, like for example the precise form of the quarkonium wavefunctions.

4.1 Binding Energy Effects on Quarkonium Physics

The section begins with a discussion of the quarkonium wavefunction. Then, the various problems cited above are systematically reviewed.

4.1.1 QCD Quarkonium Wavefunctions

To apply our method to the quarkonium, we need its wavefunction. No matter its form, it will always be possible to express it as a combination of functions for which the derivative method applies. For example, the set of functions built on the Coulomb wavefunction (see appendix C.1)

$$\mathcal{F}_n(\mathbf{p}^2) = \frac{\sqrt{\pi}\Gamma(n)}{\Gamma(n-3/2)} \frac{8\pi\gamma^{2n-3}}{(\mathbf{p}^2 + \gamma^2)^n}$$

can serve as a basis in which the quarkonium wavefunction can be expanded. All these functions are accommodated in the derivative method through the operator

$$\begin{aligned} F_n(s) &= C\phi_0 \mathcal{F}_n(\mathbf{p}^2) (\mathbf{p}^2 + \gamma^2) \Big|_{s=4(\mathbf{p}^2+m^2)} \\ &= C\phi_0 \frac{\Gamma(n)}{\Gamma(n-3/2)} 2^{2n+1} \pi^{3/2} \gamma^{2n-3} \frac{1}{(s-M^2)^{n-1}} \\ &\rightarrow C\phi_0 \frac{2^{2n+1} \pi^{3/2} \gamma^{2n-3}}{\Gamma(n-3/2)} \left(\frac{\partial}{\partial M^2} \right)^{n-1} \end{aligned}$$

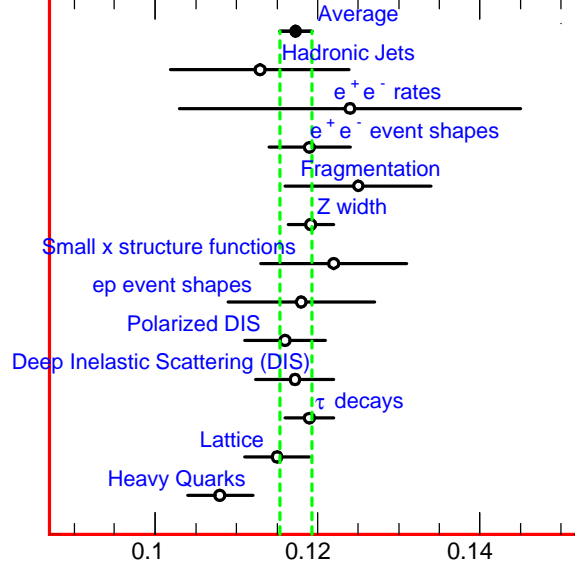
It remains to find an expression for the quarkonium wavefunction. This is not an easy task. The form of the QCD potential is not well-established (there are many alternatives). Further, in QCD, the parameter γ cannot be defined straightforwardly. For all these reasons, in the present section, we will simply take for quarkonium the form factor of positronium, with the binding energy defined by the $D\bar{D}$ threshold. This will illustrate what can be expected from binding energy effects on total and differential rates.

Further, because of confinement, the configuration space quarkonium wavefunctions should be less spread than the Coulomb one. In turn, the momentum space wavefunctions are more spread out around $\mathbf{p} = 0$ for quarkonium than for positronium. But we know that the binding energy corrections are always proportional to the spreading, in momentum space, of the wavefunction. Therefore, the binding energy corrections computed with a Coulomb form factor will be lower estimates, the true corrections being more important.

Another approach would be to take each of the charmonium potentials and compute the wavefunctions by solving the Schrödinger equation. Then, these solutions would be expressed in the basis of the Coulomb wavefunctions. Such studies are in project, and have not been completed yet. The present section is a first step in that direction.

4.1.2 Strong Coupling Extraction

The value of α_S as extracted from quarkonium physics does not fit well with the values obtained from other QCD observable measurements [223]



We have seen in the previous chapter that the value of α_S extracted from charmonium and bottomonium inclusive decay rates are

	$\alpha_S(m_Q)$	$\alpha_S(M_Z)$
η_c	0.31	0.117
J/ψ	0.19	0.096
Υ	0.18	0.107

where we have run the values up to M_Z using three-loop running, and $n_f = 4$ between m_c and m_b , $n_f = 5$ between m_b and M_Z (see appendix B.1). The value of α_S extracted from $\eta_c \rightarrow \gamma\gamma/\eta_c \rightarrow gg$ is in the world average range, but falls short of it when extracted from $J/\psi \rightarrow ggg, gg\gamma/J/\psi \rightarrow e^+e^-$ or $\Upsilon \rightarrow ggg, gg\gamma/\Upsilon \rightarrow e^+e^-$.

From the computation done in the positronium case, we know that binding energy effects will suppress the decay rates. As a result, one will need a greater α_S to fit to the observed rates. This is the general mechanism we invoke to explain the discrepancy between the quarkonium α_S determinations and the world average. In other words, the smallness of the extracted α_S in standard approaches is, in our view, the signal that the factorization hypothesis is inappropriate, and that a loop model has to be considered.

Electromagnetic Decays

We begin our study with the electromagnetic processes (see chapter 3)

$$\begin{aligned}\Gamma(\eta_c \rightarrow \gamma\gamma) &= 48\pi\alpha^2 e_Q^4 \frac{|\phi_0|^2}{M^2} \left(1 - 3.4 \frac{\alpha_S}{\pi}\right) \\ \Gamma(J/\psi \rightarrow l^+l^-) &= 16\pi (e_Q^2 \alpha^2) \frac{|\phi_0|^2}{M^2} G(m_l) \left(1 - \frac{16}{3} \frac{\alpha_S}{\pi}\right) \\ \Gamma(J/\psi \rightarrow \gamma\gamma) &= \frac{64(\pi^2 - 9)}{3} (e_Q^6 \alpha^3) \frac{|\phi_0|^2}{M^2} \left(1 - 12.6 \frac{\alpha_S}{\pi}\right)\end{aligned}$$

and the corresponding Υ decays.

In the case of positronium, we saw that the bulk of the first order radiative corrections is accounted for by binding energy effects. The same mechanism will be invoked for quarkonium, so that the strong corrections will be replaced by a function of the binding energy. Of course, it will not be possible to directly test this hypothesis since the quarkonium binding energy relation to the strong coupling is not known.

Let us start with the pseudoscalar charmonium electromagnetic decay

$$\Gamma(\eta_c \rightarrow \gamma\gamma) = 48\pi\alpha^2 e_Q^4 \frac{|\phi_0|^2}{M^2} B_{\gamma\gamma} \left(\frac{4\gamma^2}{M^2} \right)$$

with

$$B_{\gamma\gamma}(x) = (1+x) \left| \frac{2}{\pi} \arctan \frac{1}{\sqrt{x}} \right|^2$$

By taking the value of γ/M given in (4.1) and (4.2), we get the suppression factor. It is interesting to match this suppression to the perturbative correction $1 - 3.4\alpha_S/\pi$, to extract a value of α_S :

	$B_{\gamma\gamma}$	$\alpha_S = \frac{\pi}{3.4} (1 - B_{\gamma\gamma})$	$\alpha_S(M_Z)$
η_c	0.64	$\alpha_S(m_c) = 0.41$	0.12
η_b	0.76	$\alpha_S(m_b) = 0.35$	0.14

Note again that, at present, the matching with the perturbative QCD result has no grounding. Moreover, the corresponding scale is not clear (it could be that this is α_S at some low scale, between γ and m_c). Finally, α_S^2/π^2 corrections are probably quite sizeable. In view of all these rough approximations involved (especially in the definition of the binding energy values (4.1) and (4.2)), the consistency of the values is surprisingly good; the binding energy suppressions are of the order of the perturbative QCD corrections.

Let us proceed similarly with the leptonic decay of the vector quarkonium

$$\Gamma(J/\psi \rightarrow l^+ l^-) = 16\pi (e_Q^2 \alpha^2) \frac{|\phi_0|^2}{M^2} G(m_l) B_{l+l-} \left(\frac{4\gamma^2}{M^2} \right)$$

with

$$B_{l+l-}(x) = \left[\frac{2}{3\pi} \left(\sqrt{x}(5+3x) - 3(1+x)^2 \arctan \frac{1}{\sqrt{x}} \right) \right]^2$$

Then, for J/ψ and Υ , we get

	B_{l+l-}	$\alpha_S = \frac{3\pi}{16} (1 - B_{l+l-})$	$\alpha_S(M_Z)$
J/ψ	0.17	$\alpha_S(m_c) = 0.5$	0.12
Υ	0.24	$\alpha_S(m_b) = 0.4$	0.15

Again, the matching gives surprisingly good results.

The final decay

$$\Gamma(J/\psi \rightarrow \gamma\gamma\gamma) = \frac{64(\pi^2 - 9)}{3} (e_Q^6 \alpha^3) \frac{|\phi_0|^2}{M^2} B_{\gamma\gamma\gamma} \left(\frac{4\gamma^2}{M^2} \right)$$

is more complicated to handle since we do not have an analytical expression for $B_{\gamma\gamma\gamma}$. Numerically, we found

	$B_{\gamma\gamma\gamma}$
J/ψ	0.01
Υ	0.03

In this case, the matching gives $\alpha_S(m_c) \approx \alpha_S(m_b) \approx 0.25$, since it is around that value that perturbative QCD corrections force the total rate to vanish. Obviously, this later fact is now well interpreted as a strong suppression due to binding energy effects.

It is important to remark that, in all the previous cases, the factorization of the binding energy effects out of the perturbation series will enhance their convergence. The same phenomenon was observed in positronium physics. Here, it becomes vital to proceed along our approach, to avoid inconsistencies (such as corrections greater than unity).

Strong Decays

Introducing binding energy corrections for strong decays is more complicated because of the issue of double counting. In the electromagnetic modes, the final state particles do not experience the strong interaction, hence the whole α_S correction comes from initial state radiative corrections. This is the same situation as in the positronium case. Here, the situation is much more complicated because, first, there are strong corrections to the final state also, and second, because we are considering inclusive rates, so that decays to many gluons, quark pairs,... also contribute.

Instead of searching for a definite prescription to deal with all those decays, let us simply consider the two-gluon mode of the η_c , and the three gluon mode of the J/ψ , to illustrate what can happen. The binding energy corrections to the two-photon and two-gluon modes of the η_c are the same. Hence, the ratio of the two modes is not corrected, and this explains why a value of α_S consistent with the World average can be extracted from them. For the three-gluon mode, we write

$$\frac{\Gamma(J/\psi \rightarrow ggg)}{\Gamma(J/\psi \rightarrow e^+e^-)} = \frac{10(\pi^2 - 9)}{81\pi} \frac{\alpha_S^3(m_Q)}{e_Q^2 \alpha^2} \frac{B_{\gamma\gamma\gamma}\left(\frac{4\gamma^2}{M^2}\right)}{B_{e^+e^-}\left(\frac{4\gamma^2}{M^2}\right)}$$

We have found previously that $\alpha_S(m_Q) \approx 0.19$. Now, the binding energy correction factor corrects this value as

$$\alpha_S(m_Q) \approx 0.19 \sqrt[3]{\frac{B_{e^+e^-}\left(\frac{4\gamma^2}{M^2}\right)}{B_{\gamma\gamma\gamma}\left(\frac{4\gamma^2}{M^2}\right)}} \approx 0.45$$

When run to M_Z , we get $\alpha_S(M_Z) \approx 0.12$, in rough agreement with the world average.

We expect that the same mechanism will work for the other decay processes, i.e. that the necessary compensation of the binding energy suppression by the strong coupling will lead to an overall enhancement of α_S .

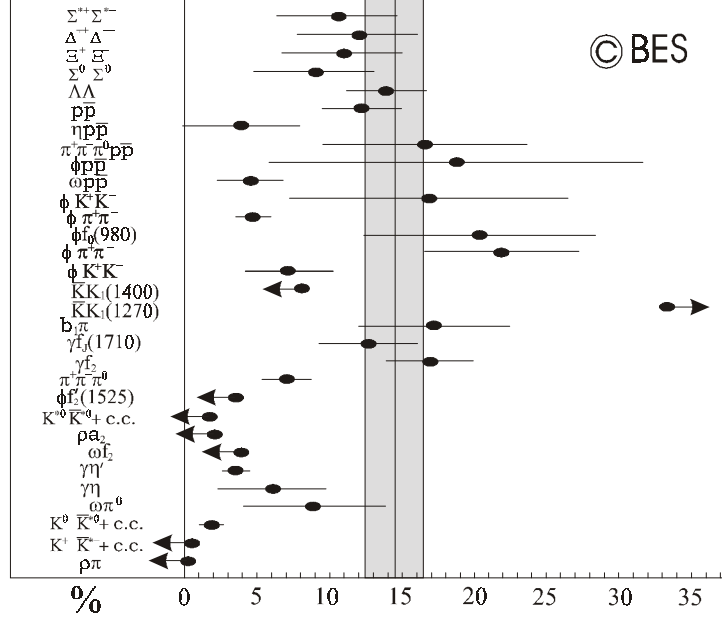
4.1.3 Rho-pi Puzzle

The rho-pi puzzle is the apparent violation of the 14% rule in exclusive hadronic decay channels of the J/ψ and $\psi(2S)$, especially $J/\psi, \psi(2S) \rightarrow \rho\pi$ ([165], [175], [177], [181], [183], [186], [193], [194], [200]). The 14% rule follows simply from the identity

$$\begin{aligned} \frac{B(\psi(2S) \rightarrow ggg)}{B(J/\psi \rightarrow ggg)} &= \frac{\alpha_S^3(\psi(2S))}{\alpha_S^3(J/\psi)} \frac{\Gamma_{tot}(J/\psi)}{\Gamma_{tot}(\psi(2S))} \frac{|\phi_0(\psi(2S))|^2/M_{\psi(2S)}^2}{|\phi_0(J/\psi)|^2/M_{J/\psi}^2} \\ &= \frac{\alpha_S^3(\psi(2S))}{\alpha_S^3(J/\psi)} \frac{B(\psi(2S) \rightarrow e^+e^-)}{B(J/\psi \rightarrow e^+e^-)} \\ &= \frac{\alpha_S^3(\psi(2S))}{\alpha_S^3(J/\psi)} (14 \pm 1)\% = (12 \pm 1)\% \end{aligned}$$

and then from the additional assumption that the exclusive decay branchings follow the same rule (i.e., that the hadronization has no effect).

Many exclusive hadronic decay modes of the $\psi(2S)$ and J/ψ that have been measured. Their ratios are [137], [139]



The 14% rule is more or less valid, except for a few channels like $J/\psi, \psi(2S) \rightarrow \rho\pi, KK^*$, which fall short of the 14% rule by as much as a factor of 60. No convincing explanation of this fact has been proposed yet (the most popular explanation is the presence of a glueball [160], [163], [173]).

Here, what we just want to point out, is that the 14% rule will not survive binding energy effects. For gluonic modes, a prefactor appears

$$\frac{B(\psi(2S) \rightarrow ggg)}{B(J/\psi \rightarrow ggg)} = \frac{B_{\gamma\gamma\gamma}(\psi(2S)) B_{e^+e^-}(J/\psi)}{B_{\gamma\gamma\gamma}(J/\psi) B_{e^+e^-}(\psi(2S))} (12 \pm 1) \% \quad (4.3)$$

But the electromagnetic part is unaffected by such effects:

$$\frac{B(\psi(2S) \rightarrow \gamma \rightarrow hadrons)}{B(J/\psi \rightarrow \gamma \rightarrow hadrons)} = \frac{B(\psi(2S) \rightarrow e^+e^-)}{B(J/\psi \rightarrow e^+e^-)} = (14.1 \pm 1.2) \%$$

This could explain why the $\rho\pi$ decay exhibits the violation of the 14% rule, while not the purely electromagnetic $\omega\pi$ decay (which is isospin violating).

Unfortunately, with our parametrization of the binding energy in terms of the D meson mass, the prefactor in (4.3) enhances the $\psi(2S)$ three gluon mode compared to the J/ψ , because the ggg mode is enhanced close to the threshold for $D\bar{D}$ creation. In our view, this is the signal that the constituent mass chosen is inappropriate to correctly describe the dynamics. For instance, if one takes the Lagrangian c quark mass of $1.2 - 1.5 GeV$, it is clear that the J/ψ is very close to the threshold, while now it is the $\psi(2S) \rightarrow ggg$ which is strongly suppressed. The treatment of bound states above the constituent mass is clearly complicated because such a phenomenon is a manifestation of confinement. Further studies are necessary, but in any case, it should be clear that binding energy effects introduce an important violation of the naive 14% rule.

Scale Anomaly

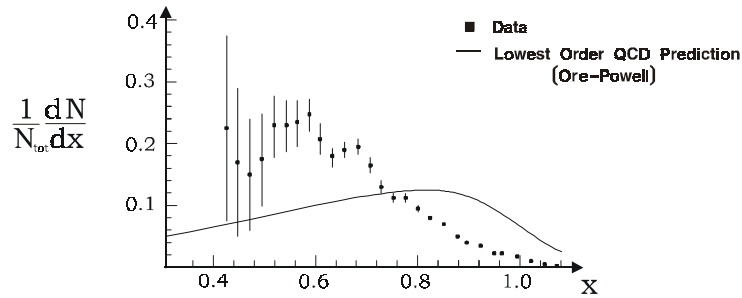
We have seen that the binding energy corrections to the decay $o-Dm \rightarrow e^-e^+$ receive a contribution from the QED scale anomaly, a contribution which is apparently missed by standard factorized computations. The same probably happens for the leptonic decay $J/\psi \rightarrow e^+e^-$. This would be far reaching: the leptonic mode has

always been considered as clean, and is used to extract the J/ψ wavefunction. This, in turn, will affect both the 14% rule, the extraction of α_S and so on.

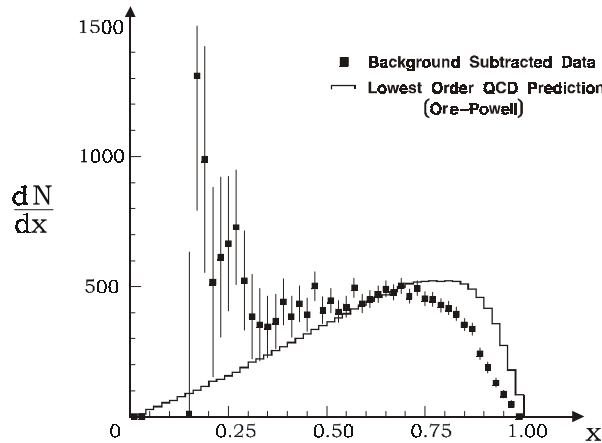
A complete study of all those effects has yet to be done, and is left for future work.

4.1.4 Photon Spectrum in Quarkonium Inclusive Radiative Decays

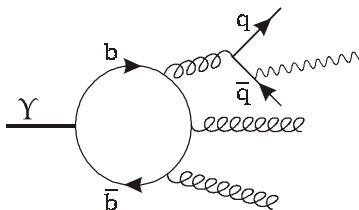
The next aspect of quarkonium physics to be discussed in some details is the photon spectrum in $J/\psi \rightarrow \gamma + hadrons$ and $\Upsilon \rightarrow \gamma + hadrons$, which is described in terms of the underlying processes $J/\psi, \Upsilon \rightarrow \gamma gg$. It is indeed in spectra that the modifications due to the binding energy may be directly observed. As we have seen when discussing the orthopositronium decay, the photon spectrum found using the Pirenne-Wheeler formula is in contradiction with Low's theorem. By introducing binding energy effects, the spectra should move from the wrong Ore-Powell prediction towards the Euler-Heisenberg one, i.e. softer at both the low energy and high energy end points. This behavior is what is observed for the $J/\psi \rightarrow \gamma + hadrons$ [134], [135]



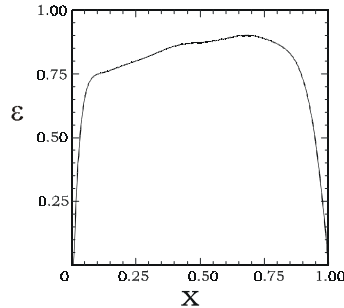
and for the $\Upsilon \rightarrow \gamma + hadrons$ [136], [140]



In both cases, the increase at low energy is due to bremsstrahlung processes ([168], [180], [185], [197])



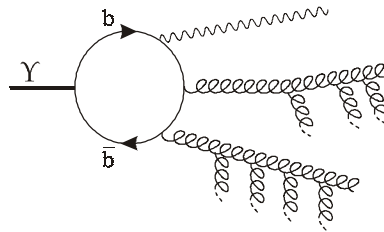
and the Ore-Powell prediction has been corrected for the efficiency. For example, in the Υ case, the efficiency varies as [140]



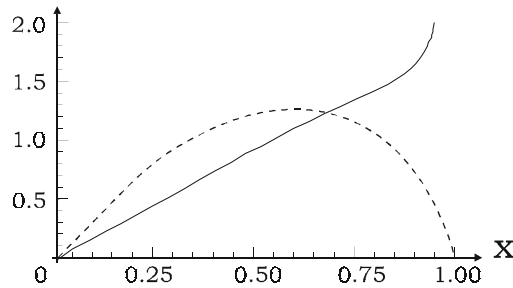
The suppression of the spectrum at its high end point is greater for the J/ψ than for the Υ , as expected since the binding energy is greater for J/ψ . To explain such a strong suppression purely in terms of binding energy effects is not possible though; even the Euler-Heisenberg spectrum is unable to fit the observed spectrum.

Field’s Model

The fact that even the Euler-Heisenberg point-like result seems to be insufficiently suppressed is rather surprising, but understandable from the point of view of Field’s model [161]. This model introduces some distortion of the photon energy spectrum because of gluon dynamics. It can be viewed as a tentative introduction of hadronization effects. Because gluons can radiate additional gluons, the ”prompt” gluons emitted from the quark line acquire an invariant mass



This means that the high end point of the photon spectrum must be modified, since in presence of such massive gluons, the maximum energy the photon can take away is reduced. The result of Field’s Monte Carlo simulation is



where the plain line is the Ore-Powell spectrum, and the dotted line is the Field’s model spectrum.

Obviously, Field’s model is in contradiction with analyticity (it is built on the Ore-Powell lowest order result). It should therefore be quite clear that it has to be modified somehow. In fact, it would be interesting to repeat Field’s computation, but taking the binding energy corrected spectrum as a lowest order basis. This analysis should lead to correct spectra (i.e. consistent with Low’s theorem), and in agreement with experiments. It is left for future studies.

4.1.5 Transitions among Quarkonium States

There are many possible transitions among quarkonium states, like for example

	%
$J/\psi \rightarrow \gamma\eta_c$	1.3 ± 0.4
$\psi(2S) \rightarrow \gamma\eta_c$	0.28 ± 0.06
$\psi(2S) \rightarrow J/\psi + had.$	61 ± 4
$\psi(2S) \rightarrow \gamma\chi_{c0}$	9.3 ± 0.9
$\psi(2S) \rightarrow \gamma\chi_{c1}$	8.7 ± 0.8
$\psi(2S) \rightarrow \gamma\chi_{c2}$	7.9 ± 0.8
$\chi_{c0} \rightarrow \gamma J/\psi$	0.66 ± 0.18
$\chi_{c1} \rightarrow \gamma J/\psi$	27.3 ± 1.6
$\chi_{c2} \rightarrow \gamma J/\psi$	13.5 ± 1.1

Most of these transitions involve the χ states, for which a treatment is still lacking in our model. The hadronic transition $\psi(2S) \rightarrow J/\psi + had.$ is generally dealt with using some low energy techniques like chiral perturbation theory, and will not be considered here. There remains the $M1$ (suppressed) transition $J/\psi \rightarrow \gamma\eta_c$. This decay, as a first approach, can be described assuming a point-like structure for the J/ψ and the η_c . In other words, we assume that binding energy is so important that the structure of the bound states is no longer relevant. Such processes are calculated using a loop model, with the coupling $J/\psi c\bar{c}$ and $\eta_c c\bar{c}$ given by $\gamma^\mu F_{J/\psi}$ and $\gamma_5 F_{\eta_c}$, respectively. Then, it is easy to find

$$\Gamma(\eta_c \rightarrow \gamma\gamma) = \frac{N e_Q^4 \alpha^2}{16\pi^3} \left(\frac{m_c}{F_{\eta_c}} \right)^2 \frac{\Lambda_{\gamma\gamma}^2 (4m_c^2/M_{\eta_c}^2)}{M_{\eta_c}}$$

$$\Gamma(J/\psi \rightarrow \eta_c \gamma) = \frac{N e_Q^2 \alpha}{96\pi^4} \left(\frac{m_c}{F_{\eta_c} F_{J/\psi}} \right)^2 \left(1 - \frac{M_{\eta_c}^2}{M_{J/\psi}^2} \right) \frac{\Lambda_{\eta_c \gamma}^2 (4m_c^2/M_{J/\psi}^2, 4m_c^2/M_{\eta_c}^2)}{M_{J/\psi}}$$

with

$$\Lambda_{\gamma\gamma}(B) = 2 \arctan^2 \frac{1}{\sqrt{B-1}}$$

$$\Lambda_{\eta_c \gamma}(B, C) = 2 \arctan^2 \frac{1}{\sqrt{B-1}} - 2 \arctan^2 \frac{1}{\sqrt{C-1}}$$

The second term appearing for $\Lambda_{\eta_c \gamma}$ comes from the contribution of oblique cuts (for $\Lambda_{\gamma\gamma}$, there is only vertical cuts).

We now take the J/ψ and η_c couplings identical (this is valid to leading order, in the non-relativistic approximation). Using the measured value for the branching $J/\psi \rightarrow \gamma\eta_c$, we find

$$F \equiv F_{\eta_c} = F_{J/\psi} = \begin{cases} 0.29 \pm 0.03 & m_c = 1.5 \text{ GeV} \\ 0.33 \pm 0.03 & m_c = 2.0 \text{ GeV} \end{cases}$$

Plugging these values into the two-photon width,

$$\Gamma^{th}(\eta_c \rightarrow \gamma\gamma) = \begin{cases} (3.0 \pm 0.6) \times 10^{-3} \text{ MeV} & m_c = 1.5 \text{ GeV} \\ (4.1 \pm 0.7) \times 10^{-3} \text{ MeV} & m_c = 2.0 \text{ GeV} \end{cases}$$

to be compared with the experimental value

$$\Gamma(\eta_c \rightarrow \gamma\gamma) = (4 \pm 2) \times 10^{-3} \text{ MeV}$$

In conclusion, the point-like approximation, with in addition the assumption of equal couplings, is consistent with the (not yet very precise) experimental data.

4.2 Conclusion

We have seen in this chapter that binding energy effects can play an important role in quarkonium physics. While their introduction was motivated by analyticity, and in particular photon spectra, they lead to important corrections in all aspects of quarkonium physics. They can explain, at least in part, the $\rho\pi$ puzzle, the smallness of α_S as extracted from vector quarkonia and the softness of the photon spectra in inclusive vector quarkonium radiative decays.

To close this chapter, we just want to point towards other applications, which are currently active research subjects in the literature.

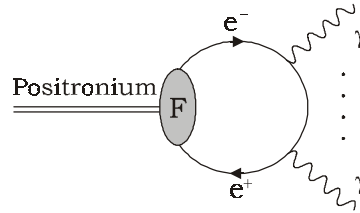
One obvious extension is the description of P -wave quarkonium states, the $\chi_{c,b}$, and in particular, the two-photon decay modes of the χ_{c0} and χ_{c2} which have been studied experimentally [142], [143]. Such a study, of course, will rely to some extent on the corresponding results for QED P -wave positronium states. Therefore, we are not yet in a position to say much.

Once the above extension is established, it can be interesting to push the formalism further down in energy, close to or less than 1 GeV, in order to describe particles such as the ϕ , or scalars f_0, σ , tensors f_2 , and so on. For instance, in the case of the ϕ , it is established that a description in terms of a $K\bar{K}$ loop is adequate ([216], [221]), with a point-like coupling of the ϕ to the $K\bar{K}$. The matching with the corresponding s quark loop, with a non-constant form factor, can lead to interesting information about QCD. Concerning scalar states, the prediction of their two-photon decay rates is important for instance in the identification of the quark model multiplets (see for example [166], [172]).

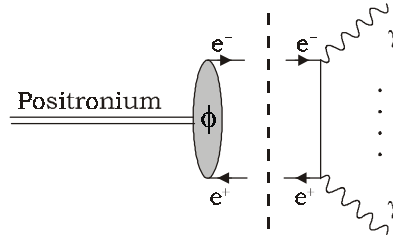
Another aspect that would need to be studied is quarkonium production (see for instance [167], [171], [198]). Examples of production mechanisms are the Drell-Yan process, gluon fusion, photon to vector quarkonia transitions,... In first approximation, it is always assumed that some kind of factorization holds, in order to separate the perturbative creation of a heavy quark pair from their non-perturbative hadronization into a quarkonium state. As mentioned before, in the NRQCD context, the quark pair is not necessarily in a color singlet state. This would have to be incorporated in the present loop model context. Anyway, it should be clear that binding energy effects are also important in production mechanisms.

Conclusions and Perspectives

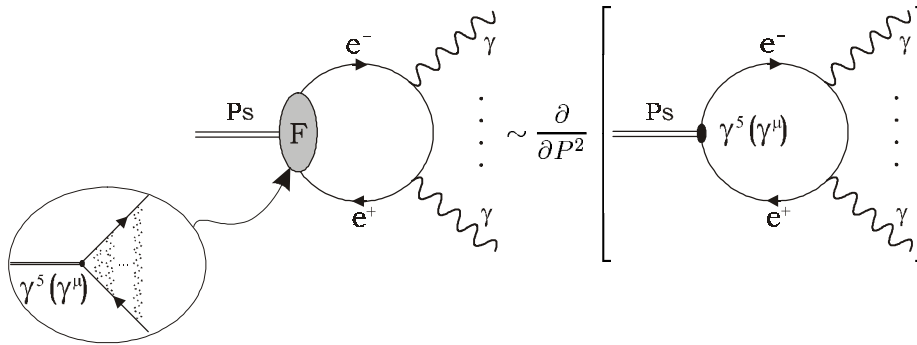
In this thesis, we have presented a method to deal with bound state annihilation through Lorentz invariant form factors. Typically, a decay amplitude is built as a loop amplitude, with a form factor inserted to account for the non-trivial structure of the bound state:



This is to be compared to the standard factorized method, symbolically:



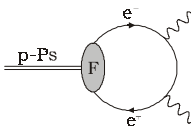
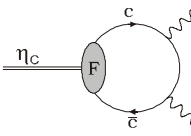
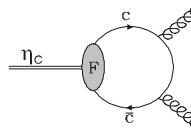
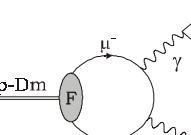
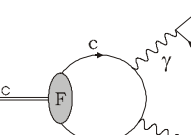
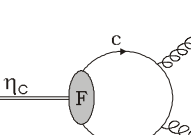
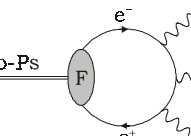
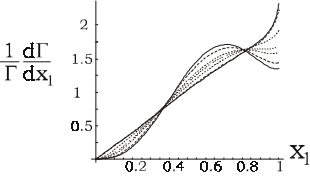
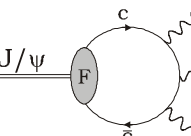
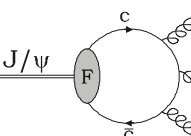
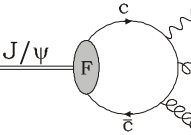
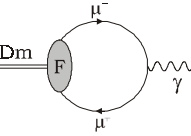
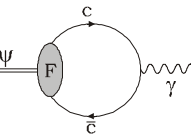
For QED bound states, we have shown how to relate that form factor to the bound state Schrödinger wavefunction, so that total decay rates agree with the ones computed using a factorized approach (at least at lowest order). From that analysis, it emerges that one can simply take the derivative of point-like QED amplitudes to account for the bound state structure



Concerning differential rates, our form factor method is definitely superior to factorized approaches like NRQED, since it does not contradict Low's theorem. This property of our method follows from its non-perturbative treatment of the binding energy, and from the four-dimensional loop structure of the amplitude (taking into account oblique cuts). For a review of the properties of the method, we refer to section 2.5.

For QCD bound states, the stage is set for more elaborate studies. Effective form factors can be retrieved from quarkonium phenomenological potentials. For simplicity, in the present work, we have used a phenomenological form factor obtained from the Coulomb wavefunction, with an ad-hoc parametrization of the binding energy (to be short, the c and b constituent masses have been taken as the masses of the lightest D and B mesons, respectively). The analysis was therefore qualitative, but already at that level, interesting conclusions have been obtained.

The following table reviews the main processes studied in the thesis. Also indicated are the main properties or consequences of the form factor approach obtained in each case:

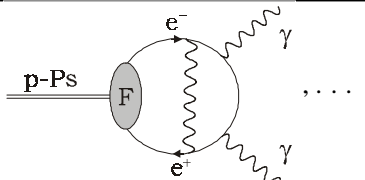
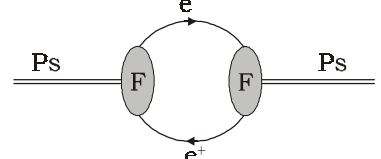
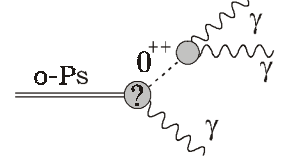
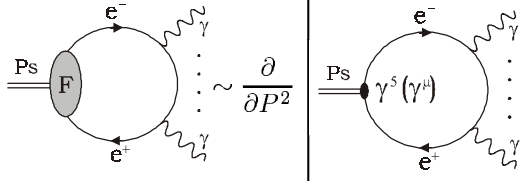
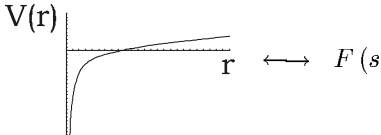
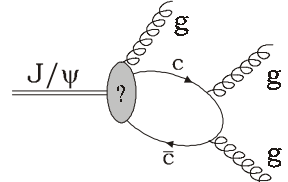
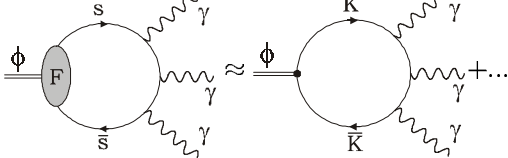
QED	QCD	
	Electromagnetic	Strong
 <p>→ Increased Convergence</p>	 <p>→ No BEE on the extraction of α_S</p>	
 <p>→ Low's Theorem</p>		
  <p>→ { Low's Theorem Increased Convergence</p>		  <p>→ BEE ⇒ Softening of the photon spectrum</p>
 <p>→ { Increased Convergence Scale Anomaly</p>		<p>→ BEE { Extraction of α_S $\rho\pi$ puzzle (no 14% rule)</p>

BEE = Binding Energy Effect

The method presented here may be extended to a great variety of processes. The following table summarizes some of them:

	QED	QCD
Higher excited state Decays (P,D,...-wave)		χ_c decays,...
Transitions between states		$\left\{ \begin{array}{l} J/\psi \rightarrow \eta_c \gamma \\ \chi_c \rightarrow J/\psi \gamma \\ \psi(2S) \rightarrow J/\psi gg \\ \dots \end{array} \right.$
Production rates		$\left\{ \begin{array}{l} J/\psi \text{ production} \\ B \rightarrow J/\psi K_S \\ \dots \end{array} \right.$
Fine and Hyperfine Splittings		Quarkonium Spectrum (mixing ?)
Unequal constituent masses		B_c mesons,...

Some questions which remain open in para- and orthopositronium physics, or concerning the application of the method to quarkonium physics are

Positronium	
1. How to deal with higher order corrections, compulsory to compete with other techniques ?	
2. What is the exact meaning of "renormalization" in the hyperfine splitting computation ? (i.e., is the bare Ps mass really $2m_e$?)	
3. Is the Scale Anomaly a missed contribution to $o\text{-Ps} \rightarrow \gamma\gamma\gamma$, thereby explaining the $o\text{-Ps}$ lifetime puzzle ?	
4. Why is the derivative technique so simple ? (i.e., is there a fundamental property of Coulomb bound states behind this ?)	
Quarkonium	
5. What are the quarkonium wavefunctions ? (or alternatively, which of the proposed charmonium potential is giving the best fit to the decay rates ?)	
6. Is it necessary to extend (and if yes, how) the form factor approach to account for all the color octet model contributions ?	
7. Can the method be extended to light mesons such as the ϕ (1020), and what can be learned about duality ?	
Positronium and Quarkonium	
8. Why is there a kind of duality between binding energy corrections and first order radiative corrections for lowest lying S states (what we called "increased convergence") ?	

The third question is probably the most interesting one. Indeed, the scale anomaly could provide a solution to the orthopositronium lifetime puzzle within the framework of QED. This is to be contrasted to recent attempts invoking the mirror world [129], extra dimensions [133] or new light particles [115]. It would also be a nice evidence of a non-trivial quantum field effect at the level of atomic physics.

Concerning quarkonium physics, the present method may provide the most promising discriminating test among phenomenological potentials, because decay rates get sensitive to the whole wavefunction, and not only its value at zero separation. This is however not as simple as it seems, because one should be sure to keep the sizeable strong radiative corrections under control (i.e., to avoid double counting). Also, NRQCD analyses have shown that a color octet contribution has to be introduced to fit the data. From our point of view, it is not clear whether this is an artefact of the NRQCD method, or a true physical contribution that needs to be introduced in the present form factor approach. In conclusion, the main limitation of the form factor approach in quarkonium physics is simply the lack of a reliable computation technique from first principle. Using a mixture of QCD and effective potential arguments is rather suspicious, and in any cases difficult to control.

Finally, the last question needs comments. We have repeatedly argued in the text that the increased convergence of the perturbation series, when binding energy corrections are factored out, comes from the fact that binding energy corrections already account for a great deal of radiative and relativistic corrections. This is certainly true, but is not the whole story. For instance, binding energy corrections and radiative corrections do not scale similarly with the principal quantum number n (as n increases, the binding energy corrections decrease while the radiative corrections stay the same). In other words, it appears that it is only for the lowest lying s -states that binding energy corrections and radiative corrections are roughly the same. More suprisingly, we have presented some indications that the same rough equality holds for the lowest lying s -states $\eta_c, J/\psi$ and η_b, Υ . This could be the signal of some kind of sum rule that needs to be discovered.

In conclusion, the form factor approach to bound system introduced in this thesis offers interesting perspectives for a number of theoretical problems. While bound states are the most common states of matter encountered in Nature, they are also very difficult to deal with theoretically. Any new information should therefore be seen as a great opportunity to reach a better understanding.

Appendix A

Resources for QED Bound states

A.1 Parapositronium

A.1.1 Details of the Dispersion Study

Let us prove the assertion that

Dispersion relations constructed on the vertical cut imaginary parts of the loop model reproduce standard convolution-type amplitudes.

We will particularize the discussion to the parapositronium decay into 2γ , for which there are vertical cut contributions only. Let us emphasize that the whole discussion of this section is readily extended to any para- or orthopositronium vertical cut contributions to the decay amplitude.

We first compute the imaginary part of (2.3) for an arbitrary initial squared mass P^2 . Considering the two possible vertical cuts, we obtain $\text{Im } \mathcal{T}$ by replacing the two propagators on each side of $\Gamma^{\mu\nu}$ by delta functions

$$\begin{aligned} \text{Im } \mathcal{T} (P^2) &\equiv \text{Im } \mathcal{M}^{\mu\nu} (p-P s \rightarrow 2\gamma) \varepsilon_{1\mu}^* \varepsilon_{2\nu}^* \\ &= \int \frac{d^4 q}{2(2\pi)^2} F_B \delta \left(\left(q - \frac{P}{2} \right)^2 - m^2 \right) \delta \left(\left(q + \frac{P}{2} \right)^2 - m^2 \right) \\ &\quad \times \text{Tr} \left\{ \gamma_5 \left(\not{q} - \frac{P}{2} + m \right) \Gamma^{\mu\nu} \left(\not{q} + \frac{P}{2} + m \right) \right\} \varepsilon_{1\mu}^* \varepsilon_{2\nu}^* \end{aligned}$$

After a straightforward integration over q^0 and $|\mathbf{q}|$, with $P = (\sqrt{P^2}, \mathbf{0})$, we reach

$$\text{Im } \mathcal{T} (P^2) = \frac{1}{16\pi} \sqrt{1 - \frac{4m^2}{P^2}} \theta (P^2 - 4m^2) \int \frac{d\Omega_{\mathbf{q}}}{4\pi} F_B \text{Tr} \left\{ \gamma_5 \left(\not{q} - \frac{P}{2} + m \right) \Gamma^{\mu\nu} \left(\not{q} + \frac{P}{2} + m \right) \right\} \varepsilon_{1\mu}^* \varepsilon_{2\nu}^*$$

In the course of the derivation, the delta functions forced $q^0 = 0$ and $|\mathbf{q}| = \sqrt{P^2/4 - m^2}$. In other words, the electron momenta are

$$\frac{1}{2}P \pm q = \left(\sqrt{\frac{P^2}{4}}, \pm \mathbf{q} \right) \text{ with } \left(\frac{1}{2}P \pm q \right)^2 = \frac{P^2}{4} - |\mathbf{q}|^2 = m^2 \quad (\text{A.1})$$

This kinematics is to be understood in the trace evaluation. The angular dependence arises from the relative orientations of \mathbf{q} and the photon momentum l_1 . Note also that the relation (A.1) cannot be satisfied for the physical value $P^2 = M^2 < 4m^2$. This is obvious since the loop cannot have an imaginary part for the physical bound states, its constituents being always off-shell. From the kinematics (A.1) one can prove that the factors on both sides of $\Gamma^{\mu\nu}$ are true projectors, which serve to enforce gauge invariance in the expression

$$\left(\not{q} - \frac{1}{2}\not{P} + m\right) \Gamma^{\mu\nu} \left(\not{q} + \frac{1}{2}\not{P} + m\right)$$

Indeed, those two projectors play exactly the same role as external spinors when establishing Ward identities.

The real part will now be calculated using an unsubtracted dispersion relation

$$\text{Re } T(M^2) = \frac{P}{\pi} \int_{4m^2}^{+\infty} \frac{ds}{s - M^2} \text{Im } T(s = P^2) \quad (\text{A.2})$$

where it is understood that P^2 should be replaced by s everywhere, i.e. scalar products that will appear when evaluating the trace should be expressed with the kinematics defined for an initial energy s . Since $M^2 < 4m^2$, the principal part can be omitted and $T(M^2) = \text{Re } T(M^2)$. Now let us write the form factor in the general form

$$F_B \equiv C\phi_o \mathcal{F}(\mathbf{q}^2) (\mathbf{q}^2 + \gamma^2) = C\phi_o \mathcal{F}(s/4 - m^2) \cdot (s - M^2) / 4 \quad (\text{A.3})$$

with $\gamma^2 \equiv m^2 - M^2/4$ and ϕ_o the bound state wavefunction at zero separation. Then (A.2) can be written as

$$\begin{aligned} T(M^2) &= C\phi_o \int_{4m^2}^{+\infty} ds \int \frac{d\Omega_{\mathbf{q}}}{4\pi} \mathcal{F}(s/4 - m^2) \frac{\sqrt{1 - 4m^2/s}}{64\pi^2} \\ &\quad \times \text{Tr} \left\{ \gamma_5 \left(\not{q} - \frac{P}{2} + m \right) \Gamma^{\mu\nu} \left(\not{q} + \frac{P}{2} + m \right) \right\} \varepsilon_{1\mu}^* \varepsilon_{2\nu}^* \end{aligned}$$

Let us transform the s integral back into a $|\mathbf{q}|$ integral, keeping in mind the constraints obtained when extracting the imaginary part. Using $\mathbf{q}^2 = s/4 - m^2$, $ds = 8|\mathbf{q}| d|\mathbf{q}|$, the decay amplitude dispersion integral is

$$T(M^2) = \frac{C}{2} \phi_o \int \frac{d^3\mathbf{q}}{(2\pi)^3} \frac{\mathcal{F}(\mathbf{q}^2)}{\sqrt{P^2(\mathbf{q})}} \text{Tr} \left\{ \gamma_5 \left(\not{q} - \frac{P(\mathbf{q})}{2} + m \right) \Gamma^{\mu\nu} \left(\not{q} + \frac{P(\mathbf{q})}{2} + m \right) \right\} \varepsilon_{1\mu}^* \varepsilon_{2\nu}^*$$

where, as the notation suggests, it is understood that any P^2 appearing in the amplitude must be replaced by $4|\mathbf{q}|^2 + 4m^2$. In particular, $\sqrt{P^2(\mathbf{q})}$ can be replaced by $2E_{\mathbf{q}}$ with $E_{\mathbf{q}} = \sqrt{|\mathbf{q}|^2 + m^2}$. This amounts to consider the scattering amplitude with incoming on-shell electron-positron having momenta $(\frac{1}{2}P(\mathbf{q}) \pm q)^2 = m^2$ (since $q^0 = 0$). Note the fact that $E_{\mathbf{q}} > M/2$, namely that apparently the energy is not conserved. This is not surprising since the present formula is a dispersion integral, done along the cut where $P^2(\mathbf{q}) > 4m^2$. Finally, in view of the kinematics, we introduce $k = \frac{1}{2}P(\mathbf{q}) + q$ and $k' = \frac{1}{2}P(\mathbf{q}) - q$ (hence $E_k = E_{k'} = E_{\mathbf{q}}$ and $\mathbf{k} = -\mathbf{k}' = \mathbf{q}$) to write the amplitude simply as

$$T(M^2) = \frac{C}{2} \int \frac{d^3\mathbf{k}}{(2\pi)^3 2E_{\mathbf{k}}} [\phi_o \mathcal{F}(\mathbf{k}^2)] \text{Tr} \left\{ \gamma_5 (-\not{k}' + m) \Gamma^{\mu\nu}(k, k', l_1) (\not{k} + m) \right\} \varepsilon_{1\mu}^* \varepsilon_{2\nu}^* \quad (\text{A.4})$$

where $\Gamma^{\mu\nu}(k, k', l_1)$ is the amplitude for on-shell $e^-(k) e^+(k')$ scattering into 2γ . Gauge invariance is present due to the two projectors, well defined since $k^2 = k'^2 = m^2$. This ends our demonstration, and $T(M^2) = \mathcal{M}(p\text{-}Ps \rightarrow \gamma\gamma)$.

A.1.2 Sommerfeld Factor and Form Factors

To reach a better understanding of the parapositronium two-photon decay rate, we now repeat the derivation using the language of dispersion relations. This is necessary because we will want to try different forms of form factor F_B , and thereby get information on the physical content of the binding energy corrections.

The loop integral $\mathcal{I}_p(P^2)$ has an imaginary part obtained by cutting the propagators

$$\text{Im}\mathcal{I}_p(P^2) = \frac{1}{2} \int \frac{d^4q}{(2\pi)^4} P^2 \frac{2\pi i \delta\left((q - \frac{1}{2}P)^2 - m^2\right) 2\pi i \delta\left((q + \frac{1}{2}P)^2 - m^2\right)}{\left(q - \frac{1}{2}P + l_1\right)^2 - m^2}$$

Using an unsubtracted dispersion relation and inserting the Coulomb form factor, we reach the two equivalent forms for the loop form factor

$$\mathcal{I}_{Coul}(M^2) = \frac{C\phi_o}{2} \frac{1}{32\pi^2} \int_{4m^2}^{+\infty} ds \mathcal{F}(s/4 - m^2) \ln \left[\frac{1 + \sqrt{1 - \frac{4m^2}{s}}}{1 - \sqrt{1 - \frac{4m^2}{s}}} \right] \quad (\text{A.5a})$$

$$= \frac{C\phi_o}{2} \int \frac{d^3\mathbf{q}}{(2\pi)^3} \mathcal{F}(\mathbf{q}^2) \frac{1}{\sqrt{|\mathbf{q}|^2 + m^2 + |\mathbf{q}| \cos \theta_{\mathbf{q}}}} \quad (\text{A.5b})$$

where we have set $F_B \equiv C\phi_o \mathcal{F}(\mathbf{q}^2) (\mathbf{q}^2 + \gamma^2)$ (see 2.10). The first expression is obtained by integration of the second one over the angular variable $\theta_{\mathbf{q}}$, and by defining $s = 4(\mathbf{q}^2 + m^2)$.

Decay Rate in the Static Limit

Let us first analyze the static limit, i.e. $\gamma^2 \rightarrow 0$ for the form factor. To compute the decay rate in that limit, we do not need to specify F_B . We just need to know that the function $\mathcal{F}(\mathbf{q}^2)$ is normalized to unity and behaves as a delta function of the momentum in the limit of vanishing binding energy

$$\int \frac{d^3\mathbf{q}}{(2\pi)^3} \mathcal{F}(\mathbf{q}^2) = 1, \quad \lim_{\gamma \rightarrow 0} \mathcal{F}(\mathbf{q}^2) = (2\pi)^3 \delta^{(3)}(\mathbf{q}) \quad (\text{A.6})$$

By setting $\mathcal{F}(\mathbf{q}^2) = (2\pi)^3 \delta^{(3)}(\mathbf{q})$ in (A.5b), we must recover exactly the lowest order decay rate

$$\Gamma(p-Ps \rightarrow \gamma\gamma) = \frac{1}{2} \alpha^5 m \quad (\text{A.7})$$

In some sense, the static limit serves as a boundary condition for the behavior of \mathcal{F} . We get

$$\mathcal{I}_{Coul,Static}(M^2) = \frac{C\phi_o}{2} \int \frac{d^3\mathbf{q}}{(2\pi)^3} (2\pi)^3 \delta^{(3)}(\mathbf{q}) \frac{1}{\sqrt{|\mathbf{q}|^2 + m^2 + |\mathbf{q}| \cos \theta}} = \frac{C\phi_o}{2} \left[\frac{1}{m} \right]$$

Importantly, this result is independent of the binding energy : the loop does not introduce any corrections in the static limit. The decay rate in that limit is therefore:

$$\Gamma(p-Ps \rightarrow \gamma\gamma) = 16\pi\alpha^2 \frac{m^2}{M} |\mathcal{I}_{Coul,Static}(M^2)|^2 = \frac{1}{2} \alpha^5 m \left(\frac{m^2}{M} C^2 \right)$$

with $|\phi_0|^2 = \alpha^3 m^3 / 8\pi$. It remains to match C such that purely kinematical corrections vanish (M factors in the above formula arise from products like $(l_1 \cdot l_2) = M^2/2$ and from the $1/2M$ decay width factor, while m comes from electron propagators in the loop and from the wavefunction ϕ_0). With the definition $C = \sqrt{M}/m$,

the decay rate is exactly $\frac{1}{2}\alpha^5 m$ as it should. In other words, the value for C obtained by matching (2.8) and (2.2) is such that no correction arises from factors M/m in the static limit.

To conclude, let us repeat that we have not specified the form factor. This means that any form factor which has a three-dimensional delta function limit for $\gamma^2 \rightarrow 0$ gives the correct lowest order decay rate $\alpha^5 m/2$. In the following, we shall present three forms, all built on the Schrödinger momentum wavefunction.

Schrödinger Form Factors and Binding Energy Corrections

Using either the formula (A.5a) or the derivative approach (2.11), we will now go through different calculations of $\Gamma(p-Ps \rightarrow \gamma\gamma)$, obtained for specific choices of F_B (or equivalently, $\mathcal{F}(\mathbf{q}^2)$). Namely:

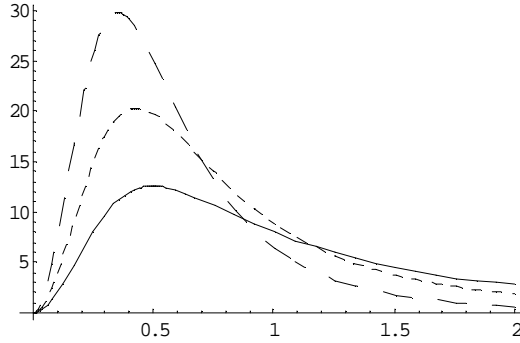
$$\mathcal{F}_I(\mathbf{q}^2) = \frac{8\pi\gamma}{(\mathbf{q}^2 + \gamma^2)^2} \quad (\text{A.8a})$$

$$\mathcal{F}_{II}(\mathbf{q}^2) = \frac{32\pi\gamma^3}{(\mathbf{q}^2 + \gamma^2)^3} \quad (\text{A.8b})$$

$$\mathcal{F}_{III}(\mathbf{q}^2) = \frac{2\gamma}{|\mathbf{q}|} \arctan \frac{|\mathbf{q}|}{\gamma} \times \mathcal{F}_I(\mathbf{q}^2) \quad (\text{A.8c})$$

where $\gamma^2 = m^2 - M^2/4 \approx m^2\alpha^2/4$. As discussed previously, \mathcal{F}_I is just the Schrödinger momentum wavefunction for the bound state. The \mathcal{F}_{II} form factor has no clear signification and only serves the purpose of illustration. Finally, we will show that \mathcal{F}_{III} can be viewed as a Coulomb binding corrected Schrödinger form factor, in the spirit of the Sommerfeld factor. Of course, we know that the form factor to be used must be related to the Bethe-Salpeter wavefunction, and that it is the first form factor \mathcal{F}_I that emerges from the reduction of the Barbieri-Remiddi wavefunction through dispersion relations (2.8). Anyway, from the analysis of \mathcal{F}_{III} , we will clearly identify the physical content of the binding energy corrections due to \mathcal{F}_I , and thereby avoid double counting.

All these form factors satisfy the delta limit property (A.6), but are differently peaked near $|\mathbf{q}| = 0$. Graphically, $\mathbf{q}^2 \mathcal{F}(\mathbf{q}^2)$, as function of \mathbf{q}^2 with $\gamma = .5$ (\mathcal{F}_I plain, \mathcal{F}_{II} dashed and \mathcal{F}_{III} small dashed lines) is



As a result, we expect that all of them will reproduce the lowest order decay rate (A.7), but will introduce some γ dependent corrections proportional to their spreading around $|\mathbf{q}| = 0$. Such corrections can then be expressed in terms of the fine-structure constant, yielding a corrected lowest order rate of

$$\Gamma(p-Ps \rightarrow \gamma\gamma) = \frac{1}{2}\alpha^5 m (1 + \delta_\Gamma(\mathcal{F}))$$

The physics of each form factor is discussed below. If we naively add the present corrections δ_Γ to the radiative corrections up to order $\alpha^2 \ln \alpha$

$$\Gamma_{p-Ps} = \frac{\alpha^5 m}{2} \left(1 - \left(5 - \frac{\pi^2}{4} \right) \frac{\alpha}{\pi} + 2\alpha^2 \ln \frac{1}{\alpha} + \delta_\Gamma(\mathcal{F}) \right)$$

the theoretical value is modified as

Lowest-order Form factor	Corrections δ_Γ	Decay Rate, with Radiative Corrections plus δ_Γ
<i>Static Limit</i>	0	$7.9895 \times 10^9 \text{ sec}^{-1}$
\mathcal{F}_I	-0.637α	$7.9527 \times 10^9 \text{ sec}^{-1}$
\mathcal{F}_{II}	$-0.25\alpha^2$	$7.9894 \times 10^9 \text{ sec}^{-1}$
\mathcal{F}_{III}	$-1.73\alpha^2$	$7.9887 \times 10^9 \text{ sec}^{-1}$
Experiments		$(7.9909 \pm 0.0017) \times 10^9 \text{ sec}^{-1}$

where the experimental measurement (1.3) is also included for comparison.

Discussion

If the $\delta_\Gamma (\mathcal{F}_I)$ is naively added to the order α radiative corrections, one ends up with excessive corrections, quite far from the experimental value. Our goal is to show that one should not add them, because it would amount to a double counting. Obviously, first order radiative corrections do contain a Coulomb photon exchange contribution. In the language of NRQED, one should consider the exact integration result (2.15) as a resummation of some higher order effects.

As stated in the text, the standard approach regarding $\delta_\Gamma (\mathcal{F}_I)$ is simply to discard it, hoping that it will be generated by radiative corrections. This is inappropriate, but let us nevertheless continue with the idea, and expose one of the technique used to get rid of the exact form factor integration corrections.

The basic idea is to absorb the Coulomb correction into the wavefunction. To this end, consider the third form factor. We view it as a representation of the modification of the intermediate e^+e^- state due to Coulomb photon exchange. When dispersion relations are used, one considers intermediate states as asymptotic states, and integrate over the corresponding phase-space. This is the application of the optical theorem for absorptive parts. Let us assume that, due to the modification of the asymptotic Hilbert space by the long-range Coulomb interactions, a correction factor must be introduced in

$$\mathcal{M}(p\text{-}Ps \rightarrow \gamma\gamma) \sim \int d^3\mathbf{q} \psi(\mathbf{q}^2) \times S(\mathbf{q}) \times \mathcal{M}(e_{\mathbf{q}}^- e_{-\mathbf{q}}^+ \rightarrow \gamma\gamma) \quad (\text{A.9})$$

and that this factor is

$$S(\mathbf{q}) = \frac{2\gamma}{|\mathbf{q}|} \arctan \frac{|\mathbf{q}|}{\gamma} \quad (\text{A.10})$$

In some sense, one could think of $S(\mathbf{q})$ as the Sommerfeld factor of Harris and Brown [69]. Due to long range Coulomb interactions, the wavefunction at contact ϕ_o is "renormalized" by

$$|\phi_o|^2 \rightarrow |\phi_o|^2 \frac{2\pi\alpha/v}{1 - e^{-2\pi\alpha/v}} \approx |\phi_o|^2 \left(1 + \frac{\pi\alpha}{v}\right) \quad (\text{A.11})$$

by using $v \gg \alpha$, i.e. $|\mathbf{q}| \gg \gamma$, with v the center-of-mass velocity. Correspondingly, $S(\mathbf{q})$ for small binding energy is

$$S(\mathbf{q}) \approx \frac{\pi\gamma}{|\mathbf{q}|} \approx \frac{\pi\alpha}{2v}$$

The factor of 2 arises because $S(\mathbf{q})$ is defined at the amplitude level, while the Sommerfeld factor is at the decay rate level.

The same arctangent factor arises in the work of [84], [87] on $\mathcal{O}(\alpha)$ radiative corrections, by a detailed analysis of the binding graph and its Coulombic part (which is, after all, an initial state Coulombic interaction).

In conclusion, if one is interested in the lowest approximation (i.e. the $m\alpha^5/2$) the static limit is just fine. If one wants the lowest approximation to $\mathcal{O}(\alpha)$ accuracy, one must consider it as arising from the $\mathcal{O}(\alpha)$ binding graph, as demonstrated by Adkins [87]. In other words, by taking *only* $\mathcal{O}(\alpha)$ diagrams for the scattering

amplitude $e^+e^- \rightarrow \gamma\gamma$, one finds

$$\Gamma(p\text{-}Ps \rightarrow \gamma\gamma) = \frac{1}{2}m\alpha^5 \left(1 - \frac{\alpha}{\pi} \left(5 - \frac{\pi^2}{4}\right)\right) + \mathcal{O}(\alpha^2)$$

The "1" in the above expression is the lowest approximation to $\mathcal{O}(\alpha)$ accuracy, arising from the $\mathcal{O}(\alpha)$ amplitude. To reproduce it using our effective form factor method, the Coulomb corrected Schrödinger form factor \mathcal{F}_{III} is to be used, as in [87].

What we gained using our method is a better understanding of its relation to the Sommerfeld factor, i.e. asymptotic Coulomb interactions. \mathcal{F}_{III} being more peaked than \mathcal{F}_I , the suppression of the intermediate phase-space is interpreted as a manifestation of the iterative structure of Bethe-Salpeter construction of the wavefunction. Therefore, the method of [87] is nothing but the rephrasing of that of Harris and Brown [69]. However, the method of [87] or the present integration of \mathcal{F}_{III} is surely more appropriate, because one does not rely on static limits, hence avoids the well-known static divergence $1/v_{rel}$ of radiative corrections to $e^-e^+ \rightarrow \gamma\gamma$.

A.1.3 Radiative Corrections to Parapositronium Decay

In this section, the computation of the radiative correction to the two-photon decay rate is presented. We will use the standard technique throughout, i.e. compute the corrections in the static limit, and then use a Sommerfeld factor to extract the final IR divergence. This is a bit different from the Harris and Brown computation [69], since their work was simply to reduce the one-loop computation of $\sigma(e^+e^- \rightarrow \gamma\gamma)$ of Brown and Feynman [65]. Here, we will do the complete computation.

The tree-level width is

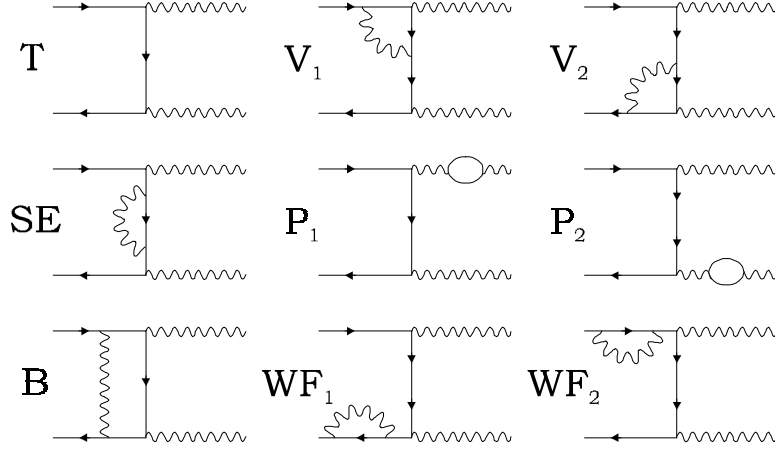
$$\Gamma(p\text{-}Ps \rightarrow \gamma\gamma) = \frac{4\pi\alpha^2}{m^2} |\phi_0|^2 = \frac{1}{2}\alpha^5 m$$

with ϕ_0 the configuration space Schrödinger wavefunction of the positronium at zero separation. We intend to compute the radiative correction to order α . To get a finite result, the associated bremsstrahlung processes parapositronium $\rightarrow \gamma\gamma\gamma$ also have to be calculated. Fortunately, thanks to selection rules (charge conjugation), this decay is not allowed. Therefore, even if it could appear as quite exotic, this decay channel is maybe the simplest realistic example of radiative correction calculation.

For the purpose of comparison, we present the computation using multiplicative renormalization and BPHZ renormalization. Details can be found at the end of this section.

i. Multiplicative Renormalization

The diagrams are



with in addition the crossed processes. The first one (T) is the tree-level. For the others, the calculations are at the end of this section, and we quote

$$\begin{array}{l}
\text{SE} \\
\text{V}_1+\text{V}_2 \\
\text{WF}_1+\text{WF}_2 \\
\text{B} \\
\text{P}_1+\text{P}_2
\end{array}
\left| \begin{array}{l}
\frac{\alpha}{2\pi} [-D - 2 + 8 \log 2 + \mathcal{O}(\varepsilon)] \\
\frac{\alpha}{2\pi} \left[2D + \frac{\pi^2}{2} - 8 \log 2 + \mathcal{O}(\varepsilon) \right] \\
\frac{\alpha}{2\pi} [-D - 4 - 2 \log \nu + \mathcal{O}(\nu, \varepsilon)] \\
\frac{\alpha}{2\pi} \left[-4 + 2 \log \nu + \frac{4\pi}{\sqrt{\nu}} + \mathcal{O}(\nu, \varepsilon) \right] \\
\frac{\alpha}{2\pi} \left[-\frac{4}{3}D + \mathcal{O}(\varepsilon) \right]
\end{array} \right.$$

where $\nu = m_\gamma^2/m^2$ is an IR cutoff (m the electron mass, m_γ the photon mass used as an IR regulator). Let us make some comments about the calculation. First, the self-energy insertion correction is computed from the full propagator

$$\Gamma_{SE}^{\mu\nu} = (-ie^2) \gamma^\nu \frac{Z_2}{\not{p} - \not{k} - m - Z_2 \sum_R(p-k)} \gamma^\mu + \text{Crossed}$$

But this is more than is needed at order α , so we truncate the full propagator

$$\begin{aligned}
\frac{1}{\not{p} - m_0 - \Sigma(p)} &= \frac{1}{\not{p} - m_0 - \delta_m + \delta_m - \Sigma(p)} \\
&= \frac{1}{\not{p} - m} + \frac{1}{\not{p} - m} (\Sigma(p) - \delta_m) \frac{1}{\not{p} - m} + \dots
\end{aligned}$$

The first term generates the already computed lowest order correction, and can be discarded. The result quoted in the table is then obtained with

$$\delta_m = \Sigma_2(m) = \frac{\alpha m}{4\pi} (3D + 4) + \mathcal{O}(\varepsilon) \tag{A.12}$$

The WF and P corrections are a bit special. They arise from the LSZ formula. Indeed, the decay amplitude is related to the S -matrix element through Z_i factors, introducing the corrections

$$\begin{aligned}\mathcal{M}_{(0+1)}(p-Ps \rightarrow \gamma\gamma) &= Z_2 Z_3 (\mathcal{M}_{(0)}(p-Ps \rightarrow \gamma\gamma) + \mathcal{M}_{(1)}(p-Ps \rightarrow \gamma\gamma)) \\ &= \mathcal{M}_{(0)} + ((Z_2 - 1) + (Z_3 - 1)) \mathcal{M}_{(0)} + \mathcal{M}_{(1)} + \dots\end{aligned}$$

where $\mathcal{M}_{(1)}$ contains B, SE, V corrections (strictly speaking, the figures are wrong because external lines are amputated; instead, they should be understood as reminder of the LSZ external line factors). Therefore, the decay rate is, to order α

$$\begin{aligned}\Gamma(p-Ps \rightarrow \gamma\gamma) &\sim \mathcal{M}_{(0+1)}^2 \sim \mathcal{M}_{(0)}^2 + 2((Z_2 - 1) + (Z_3 - 1)) \mathcal{M}_{(0)}^2 \\ &\quad + \mathcal{M}_{(1)}^* \mathcal{M}_{(0)} + \mathcal{M}_{(0)}^* \mathcal{M}_{(1)} + \mathcal{O}(\alpha^2)\end{aligned}$$

The first term is the lowest order (tree-level), while the rest constitutes the $\mathcal{O}(\alpha)$ corrections.

The WF corrections are then computed from

$$Z_2 - 1 = \Sigma'_2(m) = \frac{\alpha}{4\pi} [-D - 4 - 2 \log \nu] \quad (\text{A.13})$$

while P corrections are

$$Z_3 - 1 = \Pi(0) = -\frac{\alpha}{3\pi} D$$

The only effect of this last correction is to change the bare charges at the vertex of the annihilation $e^+e^- \rightarrow \gamma\gamma$ to the renormalized one $e = \sqrt{Z_3}e_0$. Specifically,

$$\Gamma^{(0)}(p-Ps \rightarrow \gamma\gamma) = |\phi_0|^2 \frac{4\pi\alpha_0^2}{m^2} = |\phi_0|^2 \frac{4\pi\alpha^2}{m^2} \left(1 + 2\frac{\alpha}{3\pi} D\right)$$

Hence

$$\Gamma_P^{(1)}(p-Ps \rightarrow \gamma\gamma) = |\phi_0|^2 \frac{4\pi\alpha^2}{m^2} \left(1 + 2\frac{\alpha}{3\pi} D + 2(Z_3 - 1)\right) = |\phi_0|^2 \frac{4\pi\alpha^2}{m^2}$$

Therefore, as soon as the charge is taken as renormalized, we can forget about the Z_3 corrections. Combining all the other corrections, we get

$$\Gamma_{all}^{(1)}(p-Ps \rightarrow \gamma\gamma) = |\phi_0|^2 \frac{4\pi\alpha^2}{m^2} \left[-\frac{\alpha}{\pi} \left(5 - \frac{\pi^2}{4} - \frac{2\pi}{\sqrt{\nu}} + \mathcal{O}(\nu, \varepsilon) \right) \right]$$

with the renormalized coupling constant α^2 .

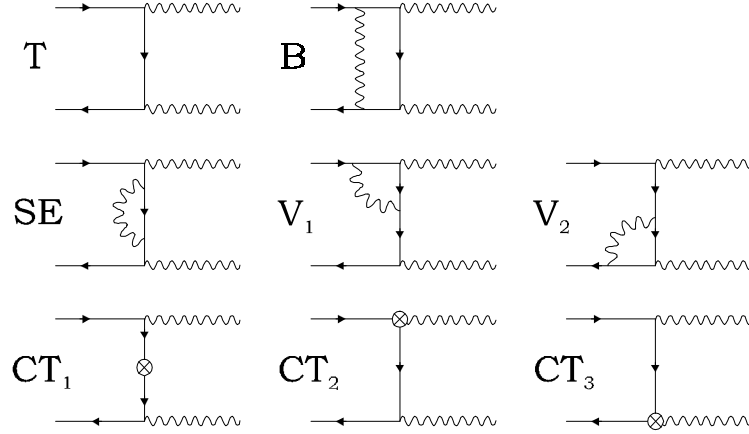
1– Note that the combination $V + P + SE$ is IR finite, because the intermediate electron is off-shell. On the other hand, the external lines introduce IR divergence trough WF and B . In fact, the result we found is the result of Harris and Brown, except that the velocity divergence is replaced by an IR divergence in $1/\sqrt{\nu}$. So this bad divergence is really a Coulombic divergence, due to the soft photon exchange between the initial state particles. Taking into account the Coulombic long range interaction among the initial state e^+e^- by introducing a Sommerfeld factor, the diverging term is seen to cancel exactly, leaving

$$\Gamma_{all}^{(1)}(p-Ps \rightarrow \gamma\gamma) = |\phi_0|^2 \frac{4\pi\alpha^2}{m^2} \left[-\frac{\alpha}{\pi} \left(5 - \frac{\pi^2}{4} \right) \right]$$

2– The Z_3 factors are seen to renormalize the electric charge at the vertex of the scattering $e^+e^- \rightarrow \gamma\gamma$. One could wonder how the α of $|\phi_0|^2 = \alpha^3 m^3 / 8\pi$ get renormalized. In fact, the standard view concerning this is Hydrogen-like. Recall that in hydrogen atom energy level computations, one is introducing vacuum polarization as a very small correction; the Lamb shift. Usually, it is argued that all such corrections are $\mathcal{O}(\alpha^2)$.

ii. BPHZ Renormalization

Now, the diagrams are



with again the corresponding crossed channels. First, note that there is no external line correction in the counterterm method, because the fields have been rescaled. The various results are

$$\begin{array}{l} V_1+V_2 \\ SE \\ B \\ CT_1 \\ CT_2+CT_3 \end{array} \left| \begin{array}{l} \frac{\alpha}{2\pi} \left[2D + \frac{\pi^2}{2} - 8 \log 2 + \mathcal{O}(\varepsilon) \right] \\ \frac{\alpha}{2\pi} [-4D + 2 - 8 + 8 \log 2] \\ \frac{\alpha}{2\pi} \left[-4 + 2 \log \nu + \frac{4\pi}{\sqrt{\nu}} + \mathcal{O}(\nu, \varepsilon) \right] \\ \frac{2\delta'_m}{m} \\ 4(Z_1 - 1) \end{array} \right.$$

Note that the $(Z_2 - 1) \not{p}$ part of the mass counterterm does not contribute (because an odd number of Dirac matrix insertions into the fermion current vanishes). Also, the vertex counterterms are trivial to write down. Then, since $Z_1 = Z_2$, the CT amplitudes are (using (A.12) and (A.13))

$$\begin{array}{l} CT_1 \\ CT_2+CT_3 \end{array} \left| \begin{array}{l} \frac{2\delta'_m}{m} = \left(2(1 - Z_2) + 2\frac{\delta_m}{m} \right) = \frac{\alpha}{2\pi} [4D + 8 + 2 \log \nu] \\ 4(Z_2 - 1) = \frac{\alpha}{2\pi} [-2D - 8 - 4 \log \nu] \end{array} \right.$$

When combined with their respective amplitudes, we get

$$\begin{array}{l} V_1+V_2+CT_2+CT_3 \\ SE+CT_1 \\ B \end{array} \left| \begin{array}{l} \frac{\alpha}{2\pi} \left[\frac{\pi^2}{2} - 8 - 8 \log 2 - 4 \log \nu \right] \\ \frac{\alpha}{2\pi} [2 + 8 \log 2 + 2 \log \nu] \\ \frac{\alpha}{2\pi} \left[-4 + 2 \log \nu + \frac{4\pi}{\sqrt{\nu}} + \mathcal{O}(\nu, \varepsilon) \right] \end{array} \right.$$

All UV divergences have disappeared. The combination gives the final expression for the corrected decay rate

$$\Gamma_{\text{alt}}^{(1)}(p\text{-}Ps \rightarrow \gamma\gamma) = |\phi_0|^2 \frac{4\pi\alpha^2}{m^2} \left[-\frac{\alpha}{\pi} \left(5 - \frac{\pi^2}{4} - \frac{2\pi}{\sqrt{\nu}} + \mathcal{O}(\nu, \varepsilon) \right) \right]$$

No electric charge renormalization was necessary, since the lowest order is immediately computed with the renormalized charge as coupling. Note that the Ward identity $Z_1 = Z_2$ used here was also present in multiplicative renormalization, in the form $e = \sqrt{Z_3}e_0$.

Both the mass and the vertex counterterms are IR divergent. In turn, all the UV finite corrections appear IR divergent: the external lines divergences spill along the whole fermion line. This is quite undesirable on physical grounds, since it is really the radiations from the initial e^+e^- state that create IR divergences. This was especially clear in the method of multiplicative renormalization. On the other hand, the present method is rather straightforward from a computational stand. The general philosophy regarding the BPHZ method is that of a very powerful book-keeping, ideally suited to the systematics of perturbative expansion. Indeed, the SE insertions in multiplicative renormalization required an expansion of the full propagator. Beyond one-loop, this kind of procedure quickly becomes too cumbersome.

The two methods are therefore complementary: multiplicative renormalization has a straightforward physical interpretation, especially concerning the origin of both IR and UV divergences, while the BPHZ renormalization is in most practical computations (beyond one-loop) the only manageable computation method.

Details for the Computation of Radiative Corrections

The parapositronium decay rate is computed from the formula

$$\Gamma(p\text{-}Ps \rightarrow \gamma\gamma) = \frac{1}{2} \frac{1}{M^2} |\phi_0|^2 \int d\Phi_A \sum_{pol} \left| Tr \left[\frac{1}{\sqrt{2}} (\not{p} + m) \gamma_5 \Gamma^{\mu\nu} (e^+ e^- \rightarrow \gamma\gamma) \right] \varepsilon_\mu(k) \varepsilon_\nu(k') \right|^2$$

where M is the positronium mass, m the electron mass, $d\Phi_A$ the two-photon phase-space (with the associated $1/2$ factor in front) and $|\phi_0|^2 = \alpha^3 m^3 / 8\pi$ the configuration-space Schrödinger wavefunction at zero separation. The amplitude $\Gamma^{\mu\nu} (e^+ e^- \rightarrow \gamma\gamma)$ is the scattering amplitude in the static limit, i.e. with both electron and positron having momenta $p = (m, 0, 0, 0)$. Finally, at the present level of precision, $M = 2m$.

The scattering amplitude is modified by radiative corrections. We intend to compute the first order corrections to the positronium decay rate from the one-loop or order α corrections to the scattering amplitude

$$\Gamma_{\mu\nu} = \Gamma_{\mu\nu}^{(0)} + \Gamma_{\mu\nu}^{(1)} + \dots$$

From this, the first order correction to the width is obtained as the interference between first order and leading order scattering amplitudes

$$\Gamma^{(1)}(p\text{-}Ps \rightarrow \gamma\gamma) = \frac{1}{2} \frac{1}{M^2} |\phi_0|^2 \int d\Phi_A Tr \left[\frac{1}{\sqrt{2}} (\not{p} + m) \gamma_5 \Gamma^{(1)\mu\nu} \right]^* Tr \left[\frac{1}{\sqrt{2}} (\not{p} + m) \gamma_5 \Gamma_{\mu\nu}^{(0)} \right] + h.c.$$

Therefore, we will calculate the contribution to $\Gamma^{(1)}$ of each correction in turn. We will proceed according to multiplicative renormalization (see the figures above).

iii. Tree-Level Decay Rate

To tree level, the scattering amplitude $\Gamma^{\mu\nu}$ is extracted from the scattering amplitude $e^+e^- \rightarrow \gamma\gamma$ in the static limit

$$Tr \left\{ \frac{1}{\sqrt{2}} (\not{p} + m) \gamma_5 \Gamma^{(0)\mu\nu} \right\} = ie^2 Tr \left\{ \frac{1}{\sqrt{2}} (\not{p} + m) \gamma_5 \frac{\gamma^\mu \not{k} \gamma^\nu - \gamma^\nu \not{k} \gamma^\mu}{2(k \cdot p)} \right\} = \frac{2\sqrt{2}\epsilon^2}{(k \cdot l)} \varepsilon^{\mu\nu\rho\sigma} p_\rho k_\sigma$$

Note that this amplitude is manifestly gauge invariant. Squaring and summing over polarization,

$$\sum_{pol} \left| Tr \left[\frac{1}{\sqrt{2}} (\not{p} + m) \gamma_5 \Gamma^{\mu\nu} (e^+ e^- \rightarrow \gamma\gamma) \right] \varepsilon_\mu(k) \varepsilon_\nu(k') \right|^2 = 256\pi^2 \alpha^2$$

The width is then simply

$$\Gamma(p\text{-}Ps \rightarrow \gamma\gamma) = \frac{1}{2} \frac{1}{M^2} \int d\Phi_A 256\pi^2 \alpha^2 |\phi_0|^2 = \frac{4\pi\alpha^2}{m^2} |\phi_0|^2 = \frac{\alpha^5 m}{2}$$

iv. One-Loop Corrections : Self Energy Insertion

There are two terms

$$\begin{aligned} \Gamma_{\Sigma}^{\mu\nu} &= (-ie^2) \gamma^\nu \frac{1}{\not{p} - \not{k} - m} \sum (p-k) \frac{1}{\not{p} - \not{k} - m} \gamma^\mu + \text{Crossed} \\ \Gamma_{\delta m}^{\mu\nu} &= -(-ie^2) \gamma^\nu \frac{1}{\not{p} - \not{k} - m} \delta_m \frac{1}{\not{p} - \not{k} - m} \gamma^\mu + \text{Crossed} \end{aligned}$$

with $2p = k + k'$. The self energy function is to one-loop

$$\begin{aligned} -i\Sigma_2(k) &= \frac{-ie^2}{(4\pi)^2} \int dx [-(2-\varepsilon)(1-x) \not{k} + (4-\varepsilon)m] A(k^2) \\ A(k) &= \left(\frac{4\pi\omega^2}{m^2}\right)^{\varepsilon/2} \Gamma(\varepsilon/2) \left(x - x(1-x) \frac{k^2}{m^2} + (1-x) \frac{\mu^2}{m^2}\right)^{-\varepsilon/2} \end{aligned} \quad (\text{A.14})$$

with μ is an IR cutoff, ω is the dimensional regularization dimension parameter. The renormalization constant $\delta_m = \Sigma_2(m)$ is calculated from (A.14) (an IR cutoff is not necessary, δ_m is IR finite)

$$\Sigma_2(m) = \frac{e^2}{(4\pi)^2} \left(\frac{4\pi\omega^2}{m^2}\right)^{\varepsilon/2} \Gamma(\varepsilon/2) \int dx [2x^{-\varepsilon} + (2-\varepsilon)x^{1-\varepsilon}] = \frac{\alpha m}{4\pi} (3D+4) + \mathcal{O}(\varepsilon)$$

Now, computing the traces we get

$$\begin{aligned} \text{Tr}[(\not{p} + m) \gamma_5 \Gamma_{\Sigma}^{\mu\nu}] &= 4 \frac{\alpha^2}{m^2} (\varepsilon - 4) (\varepsilon^{\mu\nu\rho\sigma} p_\rho k_\sigma) \int dx A(-m^2) \\ \text{Tr}[(\not{p} + m) \gamma_5 \Gamma_{\delta m}^{\mu\nu}] &= 4\delta_m \frac{e^2}{m^3} \varepsilon^{\mu\nu\rho\sigma} k_\rho l_\sigma \end{aligned}$$

using $p^2 = m^2$, $(p \cdot k) = m^2$, $(p-k)^2 = -m^2$ and $k^2 = 0$. Therefore, the correction to the decay width is obtained as

$$\begin{aligned} \Gamma_{\Sigma}^{(1)}(p\text{-}Ps \rightarrow \gamma\gamma) &= \frac{\alpha^5 m}{2} \left[\frac{\alpha}{2\pi} (\varepsilon - 4) \int dx A(-m^2) \right] \\ \Gamma_{\delta m}^{(1)}(p\text{-}Ps \rightarrow \gamma\gamma) &= \frac{\alpha^5 m}{2} \left(\frac{2\delta_m}{m} \right) \end{aligned}$$

Since the self-energy function $A(-m^2)$ is not evaluated on-shell, it is IR convergent and we can set $\mu^2 = 0$. It remains to work on the divergent integral. We have, expanding around $d = 4$

$$(\varepsilon - 4) \int dx A(-m^2) = (\varepsilon - 4) \left(\frac{4\pi\omega^2}{m^2}\right)^{\varepsilon/2} \Gamma(\varepsilon/2) \int dx (x(2-x))^{-\varepsilon/2} = -4 \left[D + \frac{3}{2} - 2 \log 2 \right] + \mathcal{O}(\varepsilon)$$

Therefore, the results are

$$\begin{aligned} \Gamma_{\Sigma}^{(1)}(p\text{-}Ps \rightarrow \gamma\gamma) &= \frac{\alpha^5 m}{2} \left[\frac{\alpha}{2\pi} (-4D + 2 - 4(2 - 2 \log 2)) \right] \\ \Gamma_{\delta m}^{(1)}(p\text{-}Ps \rightarrow \gamma\gamma) &= \frac{\alpha^5 m}{2} \left[\frac{\alpha}{2\pi} (3D + 4) \right] \end{aligned}$$

Combining both self energy corrections, we get the final result

$$\Gamma_{SE}^{(1)}(p-Ps \rightarrow \gamma\gamma) = \frac{\alpha^5 m}{2} \left[\frac{\alpha}{2\pi} (-D - 2 + 8 \log 2) \right]$$

Note that this result is free of any IR divergences. There remains a UV divergence in the result. This is expected. This divergence can be viewed as the $\sqrt{Z_2}$ factors that will combine with the vertex corrections, ensuring the finiteness of the combination.

v. One-Loop Corrections : Vertex Corrections

There are four diagrams : the two photon permutations with a correction to the first vertex, and the two corresponding to the second vertex. Let us consider the first two corrections:

$$\Gamma_{V_a}^{\mu\nu} = (-ie^2) \left[\gamma^\nu \frac{1}{\not{p} - \not{k} - m} \Gamma^\mu(p, p-k) + \gamma^\mu \frac{1}{\not{k} - \not{p} - m} \Gamma^\nu(p, k-p) \right]$$

with $2p = k + k'$. The vertex function $\Gamma^\mu(p, p-k)$ is a quite complicated function of the momenta. A general decomposition for it is

$$\Gamma^\mu(p, p') = \gamma^\mu A(p, p') + B(p, p') N$$

with $A(p, p')$ a divergent quantity and $B(p, p')$ the finite remainder, while N stand for a complicated tensor and Dirac structure. Let us write

$$\begin{aligned} A(p, p') &= \frac{\alpha}{4\pi} \int dx dy dz \delta(x+y+z-1) \frac{(2-d)^2}{2} \frac{\Gamma(2-d/2)}{(4\pi)^{d/2-2}} \left(\frac{1}{\Delta_\Gamma} \right)^{2-d/2} \\ B(p, p') &= -\frac{\alpha}{4\pi} \int dx dy dz \delta(x+y+z-1) \frac{1}{\Delta_\Gamma} \end{aligned}$$

One feature of this decomposition is that A and B are the same for both diagrams, since

$$\Delta_\Gamma(p, p-k) = \Delta_\Gamma(p, k-p) = m^2 [y(y-1) - x(x-1) + (1-z) + z\nu]$$

with $\nu = \mu^2/m^2$. Then

$$Tr[(\not{k} + m) \gamma_5 \Gamma_{V_a}^{\mu\nu}] = 4e^2 \left[\frac{A}{m^2} + 2(y^2 - 2y - x^2) B \right] \varepsilon^{\mu\nu\rho\sigma} k_\rho l_\sigma$$

The resulting contribution is

$$\Gamma_{V_a}^{(1)}(p-Ps \rightarrow \gamma\gamma) = \frac{\alpha^5 m}{2} 2 [2A + 4m^2 (y^2 - 2y - x^2) B] \equiv \frac{\alpha^5 m}{2} \frac{\alpha}{4\pi} [I_1 + I_2]$$

It remains to work on the Feynman parameter integrals. These can be written as

$$\begin{aligned} I_1 &= \left(\frac{4\pi\omega^2}{m^2} \right)^{\varepsilon/2} \Gamma(\varepsilon/2) \int_0^1 dx \int_0^{1-x} dy (2-d)^2 (y(y-1) - x(x-1) + (1-z) + z\nu)^{d/2-2} \\ &= 2D - 4 - 4 \int_0^1 dx \int_0^{1-x} dy \log [y(y-1) - x(x-1) + (1-z) + z\nu] + \mathcal{O}(\varepsilon) \\ &= 2D + 2 - \frac{\pi^2}{2} + \mathcal{O}(\varepsilon) \\ I_2 &= 4 \int_0^1 dx \int_0^{1-x} dy \frac{x^2 - y^2 + 2y}{y(y-1) - x(x-1) + (1-z) + z\nu} \\ &= -2 + \pi^2 - 8 \log 2 \end{aligned}$$

Note that again, there is no IR divergence in those integrals. Finally, the vertex correction is

$$\Gamma_V^{(1)}(p-Ps \rightarrow \gamma\gamma) = \frac{\alpha^5 m}{2} \left(\frac{\alpha}{2\pi} \left[2D + \frac{\pi^2}{2} - 8 \log 2 \right] \right)$$

where we have multiplied by two to account for the (identical) corrections to the second vertex.

vi. One-Loop Corrections : Wavefunction Renormalization

As explained in the main text, we only need to compute the electron wavefunction renormalization constant Z_2 . In the on-shell renormalization scheme that we are using, it is given by $Z_2 - 1 = \Sigma'_2(m)$. This is can be evaluated from (A.14)

$$\begin{aligned} \Sigma'_2(m) &= \frac{\alpha}{4\pi} \int dx \left[\left(\frac{4\pi\omega^2}{m^2} \right)^{\varepsilon/2} \frac{(\varepsilon-2)(1-x)\Gamma(\varepsilon/2)}{(x^2+(1-x)\nu)^{\varepsilon/2}} + \frac{4x(1-x)^2}{x^2+(1-x)\nu} \right] \\ &= \frac{\alpha}{4\pi} \int dx \left[-2(1-x)(D-1-\log x^2) + \frac{4x(1-x)^2}{x^2+(1-x)\nu} \right] + \mathcal{O}(\varepsilon) \\ &= \frac{\alpha}{4\pi} [-D-4-2\log\nu] \end{aligned}$$

To get the correction to the decay rate, we consider the four diagrams with external electron line renormalization. There is a factor $\sqrt{Z_2} \rightarrow 1 + \frac{1}{2}\Sigma'_2(m)$ on external lines, i.e.

$$\left(\sqrt{Z_2} \right)_{\text{direct}}^2 + \left(\sqrt{Z_2} \right)_{\text{crossed}}^2 = 2 \left(1 + \frac{1}{2}\Sigma'_2(m) \right)^2 = 2 + 2\Sigma'_2(m) + \dots$$

The leading order 2 reproduces the leading order amplitude for $e^+e^- \rightarrow \gamma\gamma$. The final correction induced by the wavefunction renormalization is

$$\Gamma_{WF}^{(1)}(p-Ps \rightarrow \gamma\gamma) = \frac{\alpha^5 m}{2} \frac{\alpha}{2\pi} [-D-4-2\log\nu]$$

vii. One-Loop Corrections : Binding Correction

We now turn to the most difficult part of the calculation: the binding graph. The amplitude is

$$\Gamma_B^{\mu\nu} = \int \frac{d^4q}{(2\pi)^4} \left\{ (-ie\gamma^\alpha) \frac{i}{\not{q}-\not{k}'-m} \Lambda^{\mu\nu} \frac{i}{\not{q}+\not{k}-m} (-ie\gamma^\beta) \right\} \frac{-ig_{\alpha\beta}}{q^2-\mu^2}$$

with $2p = k + k'$ and

$$\Lambda^{\mu\nu} = (-ie\gamma^\nu) \frac{i}{\not{q}+\not{p}-\not{k}-m} (-ie\gamma^\mu) + (-ie\gamma^\mu) \frac{i}{\not{q}-\not{p}+\not{k}-m} (-ie\gamma^\nu)$$

where the two terms stand for the direct and crossed diagrams. The decay amplitude is constructed as before. We can simplify the calculation by noting that the crossed diagram denominator is equal to the direct one if $q \rightarrow -q$. This motivates us to change the sign of q in the crossed diagram. The trace then gives

$$Tr[(\not{k}+m)\gamma_5\Gamma_B^{\mu\nu}] = -16ie^4 \int \frac{d^4q}{(2\pi)^4} \frac{1}{D} \left(\begin{aligned} &2q^\mu \varepsilon^{\nu\rho\sigma\tau} p_\rho k_\sigma q_\tau - 2q^\nu \varepsilon^{\mu\rho\sigma\tau} p_\rho k_\sigma q_\tau \\ &+ 2p \cdot q \varepsilon^{\mu\nu\rho\sigma} p_\rho q_\sigma - 2k \cdot q \varepsilon^{\mu\nu\rho\sigma} p_\rho q_\sigma \\ &+ q^2 \varepsilon^{\mu\nu\rho\sigma} p_\rho q_\sigma + \varepsilon^{\mu\nu\rho\sigma} p_\rho k_\sigma (2m^2 + q^2) \end{aligned} \right)$$

with the denominator

$$D = \left((q-p)^2 - m \right) \left((q+p-k)^2 - m^2 \right) \left((q+p)^2 - m^2 \right) (q^2 - \mu^2)$$

From here, the procedure is standard: introduction of Feynman parameters, loop momentum shift, and loop momentum integration in d -dimension. We get

$$\text{Tr}[(\not{k} + m) \gamma_5 \Gamma_B^{\mu\nu}] = \frac{8\alpha^2}{3m^2} \varepsilon^{\mu\nu\rho\sigma} k_\rho l_\sigma \int dx dy dz dw \, 6\delta(1-x-y-z-w) \times \left\{ \frac{2(y^2+1) + (y+1)(x-y-z)(x+y-z)}{\{(x-z)^2 - (y-2)y + w\nu\}^2} - \frac{3y-1}{(x-z)^2 - (y-2)y + w\nu} \right\}$$

After the (quite difficult) integration,

$$\text{Tr}[(\not{k} + m) \gamma_5 \Gamma_B^{\mu\nu}] = \frac{8\alpha^2}{m^2} \varepsilon^{\mu\nu\rho\sigma} k_\rho l_\sigma \left[-2 + \log \nu + \frac{2\pi}{\sqrt{\nu}} + \mathcal{O}(\nu) \right]$$

Finally, the contribution to the width is obtained as

$$\Gamma^{(1)}(p\text{-}Ps \rightarrow \gamma\gamma) = \frac{\alpha^5 m \alpha}{2 \pi} \left[-2 + \log \nu + \frac{2\pi}{\sqrt{\nu}} + \mathcal{O}(\nu) \right]$$

With this final correction, we can now combine all the results. This is done in the main text.

A.1.4 Dispersion Relations and Kaon Decay

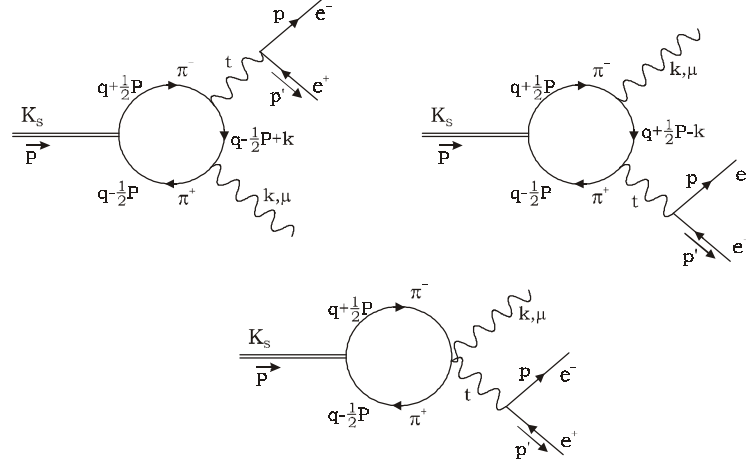
The amplitude for $K_S^0 \rightarrow \gamma e^+ e^-$ is computed at lowest order in a pion loop model. The pion is treated as a point-like charged particle, which allows simple scalar QED treatment. Special attention is paid to the low energy behavior of the amplitude.

Decay Amplitude and Loop Integration

The amplitude for kaon decay into $\gamma e^+ e^-$ is given by

$$\mathcal{M}(K_S^0 \rightarrow \gamma e^+ e^-) = -2ie^3 \mathcal{M}(K_S^0 \rightarrow \pi^+ \pi^-) \varepsilon_\mu^*(k) \frac{\{\bar{u}(p) \gamma_\nu v(p')\}}{t^2} \int \frac{d^d q}{(2\pi)^d} \mathcal{M}^{\mu\nu}(\pi^+ \pi^- \rightarrow \gamma\gamma)$$

with $t = p + p' = P - k$. The $\pi^+ \pi^- \rightarrow \gamma\gamma$ amplitude arises from the one-photon and two-photon (the so-called seagull graph) coupling



as

$$\mathcal{M}^{\mu\nu} (\pi^+ \pi^- \rightarrow \gamma\gamma) = \frac{(2q - k)^\mu (2q + t)^\nu - g^{\mu\nu} (q^2 - m^2)}{\left((q + t)^2 - m^2 \right) \left((q - k)^2 - m^2 \right) (q^2 - m^2)}$$

with m the pion mass. The amplitude $\mathcal{M} (K_S^0 \rightarrow \pi^+ \pi^-)$, taken as a constant, has been factored out. The integration is done using dimensional regularization to preserve gauge invariance and get a finite result. We obtain

$$\int \frac{d^d q}{(2\pi)^d} \mathcal{M}^{\mu\nu} (\pi^+ \pi^- \rightarrow \gamma\gamma) = \frac{-i}{(4\pi)^2} \int_0^1 dx \int_0^{1-x} dy \left[\frac{4xy}{\Delta} [g^{\mu\nu} (k \cdot t) - t^\mu k^\nu] + \frac{y(1-2y)}{\Delta} g^{\mu\nu} t^2 \right]$$

The denominator function is $\Delta = m^2 (1 - 4(a - b)xy + 4by(y - 1))$ with the definitions $a = M^2/4m^2$, $b = t^2/4m^2$ and M the kaon mass. In the kaon rest-frame, $b = M^2(1 - \omega)/4m^2$ with ω the reduced photon energy $2k^0/M$. When integrating over Feynman parameters, the last term vanishes. Therefore, the gauge invariance of the amplitude becomes manifest

$$\mathcal{M} (K_S^0 \rightarrow \gamma e^+ e^-) = \frac{-2e^3}{(4\pi)^2} \mathcal{M} (K_S^0 \pi^+ \pi^-) \frac{1}{m^2} F(a, b) \varepsilon_\mu^*(k) \{\bar{u}(p) \gamma_\nu v(p')\} \frac{g^{\mu\nu} (k \cdot t) - t^\mu k^\nu}{t^2} \quad (\text{A.15})$$

where the Feynman parameter integral is

$$F(a, b) = \int_0^1 dy \int_0^{1-y} dx \frac{4xy}{1 - 4(a - b)xy + 4by(y - 1) + i\varepsilon}$$

The prescription $i\varepsilon$ gives the sign of the imaginary part.

Feynman Parameter Integration via Dispersion Relations

To calculate $F(a, b)$, we shall use dispersion relations (see for example [6], [219]). A direct integration is possible, but we shall gain insight into the dynamics of the process by using dispersion techniques.

Further, one can see that in the soft photon limit $\omega \rightarrow 0$ (or $b \rightarrow a$), $\text{Im } F(a, b)$ behaves as a constant. Indeed, applying L'Hospital's rule twice, we get

$$\text{Im } F\left(\frac{M^2}{4m^2}, \frac{M^2(1-\omega)}{4m^2}\right) \stackrel{\omega \rightarrow 0}{\equiv} \pi \frac{2m^4}{M^4} \frac{1}{\sqrt{1-4m^2/M^2}} \quad (\text{A.19})$$

while individually the contribution of each cut is divergent as $1/(a-b)^2 \sim 1/\omega^2$. We will come back to this point later.

ix. Dispersive Part Integral

In order to write down the unsubtracted dispersion integral, let us express $\text{Im } F(a, b)$ as a function of the available energy through $a(s) = s/4m^2$ and $b(s) = s(1-\omega)/4m^2$. Then

$$\text{Re } F(a(s_o), b(s_o)) = \frac{P}{\pi} \int \frac{ds}{s-s_o} \text{Im } F(a(s), b(s)) \quad (\text{A.20})$$

with $s_o < 4m^2$, such that we can omit the principal part. For such a kinematics

$$F(a(s_o), b(s_o)) = \text{Re } F(a(s_o), b(s_o))$$

In the next subsection we shall analytically continue F to the physical value $s_o = M^2$. The result of (A.20) is easily obtained in terms of the integrals

$$\int_0^1 \frac{dy}{y_o - y} \ln \left[\frac{1+\sqrt{1-y}}{1-\sqrt{1-y}} \right] = 2 \arcsin^2 \sqrt{\frac{1}{y_o}}, \quad \int_0^1 \frac{dy}{y_o - y} \sqrt{1-y} = 2 - 2\sqrt{y_o-1} \arcsin \sqrt{\frac{1}{y_o}}$$

valid for $y_o > 1$ (see [6]). We can write $F(a, b)$ with $0 < a < 1$ and $0 < b < 1$ as

$$F(a, b) = -\frac{1}{2(a-b)} + \frac{1}{(a-b)^2} \left(\frac{1}{2} (f(a) - f(b)) + b(g(a) - g(b)) \right) \quad (\text{A.21})$$

in terms of $f(x) \equiv \arcsin^2 \sqrt{x}$ and $g(x) \equiv \sqrt{\frac{1-x}{x}} \arcsin \sqrt{x}$.

x. Analytic Continuation

The results for $a > 1$ and $b > 1$, are obtained by analytic continuation of (A.21). The analytic continuation of $f(a)$ and $g(a)$ are

$$\begin{aligned} f(x) &= \arcsin^2(\sqrt{x}) = -\left(\ln(\sqrt{x} + \sqrt{x-1}) - \frac{1}{2}i\pi \right)^2 \\ g(x) &= \sqrt{\frac{1-x}{x}} \arcsin \sqrt{x} = \sqrt{\frac{x-1}{x}} \left(\ln(\sqrt{x} + \sqrt{x-1}) - \frac{1}{2}i\pi \right) \end{aligned}$$

The equalities hold for $x \in C, \text{Im } x > 0$. The right hand sides define the analytical continuation for $x > 1$. Hence the result is conveniently expressed as (A.21) with

$$\begin{aligned} f(x) &= \begin{cases} \arcsin^2(\sqrt{x}) & 0 < x < 1 \\ -\left(\ln(\sqrt{x} + \sqrt{x-1}) - \frac{1}{2}i\pi \right)^2 & x > 1 \end{cases} \\ g(x) &= \begin{cases} \sqrt{\frac{1-x}{x}} \arcsin(\sqrt{x}) & 0 < x < 1 \\ \sqrt{\frac{x-1}{x}} \left(\ln(\sqrt{x} + \sqrt{x-1}) - \frac{1}{2}i\pi \right) & x > 1 \end{cases} \end{aligned} \quad (\text{A.22})$$

Had we chosen to analytically continue f and g in the lower half complex plane, their imaginary parts would have had the opposite sign. One can verify from (A.22) that the upper half complex plane analytic continuation reproduces $\text{Im } F(a, b)$ as given in (A.17). This result corresponds to [212] where a sign mistake has to be corrected, and to [218], [216].

Decay Width, Differential Width and Low's Theorem

The differential decay width is given by $d\Gamma(K_S^0 \rightarrow e^+e^-\gamma) = \frac{1}{2M} \sum_{spin} |\mathcal{M}|^2 d\Phi_3$. After a straightforward integration over the electron-positron phase-space, we get the differential rate in terms of the reduced photon energy ω :

$$\frac{d\Gamma(K_S^0 \rightarrow e^+e^-\gamma)/d\omega}{\Gamma(K_S^0 \rightarrow \pi^+\pi^-)} = \frac{\alpha^3}{3\pi^3} \frac{\left| F\left(\frac{1}{a_\pi}, \frac{1-\omega}{a_\pi}\right) \right|^2}{a_\pi^2 \sqrt{1-a_\pi}} \sqrt{1 - \frac{a_e}{1-\omega}} [a_e + 2(1-\omega)] \frac{\omega^3}{(1-\omega)^2}$$

with $a_e = 4m_e^2/M^2$ and $a_\pi = 4m^2/M^2 = 1/a$. The bounds on the ω integration are $\omega_{\min} = 0$ and $\omega_{\max} = 1 - a_e$. A numerical integration of the differential rate gives the prediction for the rate $K_S^0 \rightarrow e^+e^-\gamma$ relative to $K_S^0 \rightarrow \pi^+\pi^-$

$$R_{\pi^+\pi^-} = \frac{\Gamma(K_S^0 \rightarrow e^+e^-\gamma)}{\Gamma(K_S^0 \rightarrow \pi^+\pi^-)} \simeq 4.70 \times 10^{-8} \quad (\text{A.23})$$

where the real and imaginary part of $F\left(\frac{1}{a_\pi}, \frac{1-\omega}{a_\pi}\right)$ contribute for 1.26×10^{-8} and 3.43×10^{-8} , respectively.

Let us turn to the soft photon behavior of the differential width. We have to analyze the loop integral function $F\left(\frac{1}{a_\pi}, \frac{1-\omega}{a_\pi}\right)$. This function tends to a constant for very low ω :

$$F\left(\frac{1}{a_\pi}, \frac{1-\omega}{a_\pi}\right) \xrightarrow{\omega \rightarrow 0} -\frac{a_\pi}{4} + \frac{a_\pi^2}{4(a_\pi - 1)} g\left(\frac{1}{a_\pi}\right) \quad (\text{A.24})$$

(note that for $a_\pi < 1$, the imaginary part of (A.24) is the same as in (A.19)). Let us emphasize the strong cancellation between the two cuts in the soft photon limit. Individually, each cut diverges as ω^2 , but their combination is convergent. Since the remainder of the amplitude tends to zero like ω (due to the $[g^{\mu\nu}(k \cdot t) - t^\mu k^\nu]$ factor), *Low's theorem is verified: the amplitude behaves as ω close to $\omega = 0$* . The resulting spectrum is thus in ω^3 (ω^2 from the squared amplitude and a ω from phase space). In other words, had we forgotten one cut, the resulting spectrum behavior would have been divergent as $1/\omega$ instead of vanishing like ω^3 . In fact, this ω^3 spectrum is exactly the same as in the $\pi^0 \rightarrow e^+e^-\gamma$ differential decay rate.

xi. Comparison with the Two-Photon Decay Mode

From the amplitude (A.15), we readily obtain the amplitude for $K_S^0 \rightarrow \gamma\gamma$ by removing the electron current, the photon propagator and by taking the limit $\omega \rightarrow 1$:

$$\mathcal{M}(K_S^0 \rightarrow \gamma\gamma) = \frac{-2\alpha}{4\pi} \frac{\mathcal{M}(K_S^0 \rightarrow \pi^+\pi^-)}{m^2} \varepsilon_\mu^*(k) \varepsilon_\nu^*(k') [g^{\mu\nu}(k \cdot k') - k'^\mu k^\nu] F\left(\frac{M^2}{4m^2}, 0\right)$$

with $F\left(\frac{1}{a_\pi}, 0\right) = \frac{1}{2} a_\pi^2 \left\{ f\left(\frac{1}{a_\pi}\right) - \frac{1}{a_\pi} \right\}$ i.e.

$$F\left(\frac{M^2}{4m^2}, 0\right) = \frac{4m^4}{M^2} \left(\frac{i\pi}{M^2} \ln \left[\frac{1 + \sqrt{1 - \frac{4m^2}{M^2}}}{1 - \sqrt{1 - \frac{4m^2}{M^2}}} \right] - \frac{1}{2} \left(\frac{1}{m^2} - \frac{\pi^2}{M^2} + \frac{1}{M^2} \ln^2 \left[\frac{1 + \sqrt{1 - \frac{4m^2}{M^2}}}{1 - \sqrt{1 - \frac{4m^2}{M^2}}} \right] \right) \right) \quad (\text{A.25})$$

which corresponds to the result given in [6], [218], [214]. The relative decay rate is :

$$\frac{\Gamma(K_S^0 \rightarrow \gamma\gamma)}{\Gamma(K_S^0 \rightarrow \pi^+\pi^-)} = \frac{\alpha^2}{\pi^2} \frac{1}{a_\pi^2 \sqrt{1-a_\pi}} \left| F\left(\frac{1}{a_\pi}, 0\right) \right|^2 \simeq 2.94 \times 10^{-6}$$

while the experimental value for this ratio is $(3.5 \pm 1.3) \times 10^{-6}$ [223].

We can now compare the two electromagnetic modes :

$$R_{\gamma\gamma} = \frac{\Gamma(K_S^0 \rightarrow e^+e^-\gamma)}{\Gamma(K_S^0 \rightarrow \gamma\gamma)} \simeq 0.016$$

in accordance with [208]. This ratio $R_{\gamma\gamma}$ is similar to [223]

$$\frac{\Gamma(\pi^0 \rightarrow e^+e^-\gamma)}{\Gamma(\pi^0 \rightarrow \gamma\gamma)} \simeq 0.012$$

The small difference is due to the phase-space factor. The similarity between a constant coupling model like for $\pi^0 \rightarrow e^+e^-\gamma$ and the present loop model can be understood from the behavior of the photon energy spectrum. Indeed, the pure phase-space spectrum is very strongly peaked at high ω , and therefore the decay rate is quite insensitive to the details of the $F\left(\frac{1}{a_\pi}, \frac{1-\omega}{a_\pi}\right)$ function. Specifically, if we replace $F\left(\frac{1}{a_\pi}, \frac{1-\omega}{a_\pi}\right)$ by its value for $\omega = 1$ (A.25) we find the ratio $R_{\pi^+\pi^-} \simeq 4.671 \times 10^{-8}$, very close to (A.23).

The discussion of the more general case of non-constant form factor, i.e. if the amplitude $\mathcal{M}(K_S^0 \rightarrow \pi^+\pi^-)$ is not taken as a constant, can be found in [29], [30] and references cited there.

A.2 Orthopositronium

A.2.1 Phase-space Structure

The goal of this section is to set up the kinematics of three-photon decays, along with numerical methods for parametrizing the associated three-body phase-space. Suppose that we are considering a process $V \rightarrow \gamma\gamma\gamma$, V a vector particle, with coupling constant $e^3 g_V$. When there are no angular dependences in the amplitude, the only relevant variable are the energy of two of the photons (see C.3)

$$d\Phi_3 = (2\pi)^4 \delta^4(P - k_1 - k_2 - k_3) \frac{d^3k_1}{(2\pi)^3 2w_1} \frac{d^3k_2}{(2\pi)^3 2w_2} \frac{d^3k_3}{(2\pi)^3 2w_3} = \frac{dw_1 dw_2}{4(2\pi)^3}$$

The amplitude is cast into a function of only $P^2 = M^2$, w_1 and w_2 . This is achieved by first removing one of the photon momenta using the energy conservation $k_3 = P - k_1 - k_2$. Then, there remains only scalar products such as $P \cdot k_i = Mw_i$ since the V particle is at rest $P = (M, 0, 0, 0)$, and

$$k_1 \cdot k_2 = w_1 w_2 - |\mathbf{p}_1| |\mathbf{p}_2| \cos \theta_{12}$$

Momentum conservation can serve to fix this angle

$$\cos \theta_{12} = \frac{M^2 - 2Mw_1 - 2Mw_2 + 2w_1 w_2}{2 |\mathbf{p}_1| |\mathbf{p}_2|}$$

Hence

$$k_1 \cdot k_2 = M(w_1 + w_2) - M^2/2$$

Finally, if we define the reduced photon momenta as $x_i = 2w_i/M$, we get

$$\begin{aligned} d\Phi_3 &= M^2 \frac{dx_1 dx_2}{16(2\pi)^3} \\ P \cdot k_i &= \frac{1}{2} M^2 x_i \\ k_i \cdot k_j &= \frac{1}{2} M^2 (x_i + x_j - 1) = \frac{1}{2} M^2 (1 - |\varepsilon^{ijk} x_k|) \end{aligned}$$

The decay rate is then obtained by integration over x_2 $[1 - x_1, 1]$ and x_1 $[0, 1]$. The final variable we will use is the reduced mass of the particles running in the loop $a = 4m^2/M^2$. In terms of all these variables, the differential decay probability is $dP(x_1, x_2, x_3, a) = \sum_{pol} |\mathcal{M}|^2$. Then, the decay rate is expressed as

$$\begin{aligned} \Gamma_{tot}(V \rightarrow \gamma\gamma\gamma) &= \frac{1}{2M} \frac{1}{3!} e^6 g_V^2 \int d\Phi_3 \frac{1}{3} dP(x_1, x_2, x_3, a) \\ &= \frac{1}{72} \alpha^3 g_V^2 M \int_0^1 dx_1 \int_{1-x_1}^1 dx_2 dP(x_1, x_2, 2 - x_1 - x_2, a) \end{aligned}$$

Note how we factored the coupling constant from the amplitude.

Of utmost interest to us will be the differential rate (i.e. the photon energy spectrum)

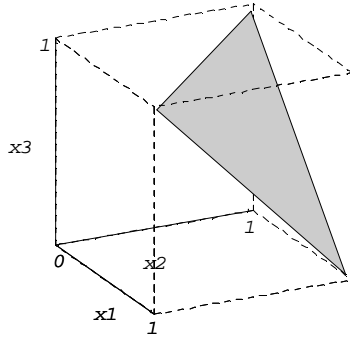
$$\frac{d\Gamma(V \rightarrow \gamma\gamma\gamma)}{dx_1} = \frac{1}{72} \alpha^3 g_V^2 M \left[\int_{1-x_1}^1 dx_2 dP(x_1, x_2, 2 - x_1 - x_2, a) \right]$$

and the normalized differential rate $\Gamma_{tot}^{-1} d\Gamma/dx_1$.

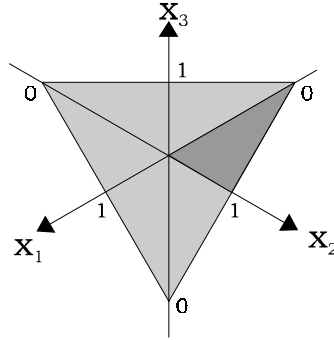
Numerical Approximation for the Phase-Space Integrations

The amplitudes we have to manipulate are very complicated, and, in general, numerical methods are the only alternative. Further, to save a substantial amount of computer time, it is a good idea to fully exploit the symmetry of phase-space. The method we present here is borrowed from Adkins [87], and will be used in all our computations (except for the simple Ore-Powell approximation, because it can be straightforwardly integrated analytically).

Energy-momentum conservation implies that the photon reduced energies lies within the plane $x_1 + x_2 + x_3 = 2$, and since $x_i \in [0, 1]$, phase-space is restricted to a triangular area



The differential probability $dP(x_1, x_2, x_3, a)$ is fully symmetric under permutations of x_1, x_2, x_3 . This means that only a sixth of phase-space needs to be computed

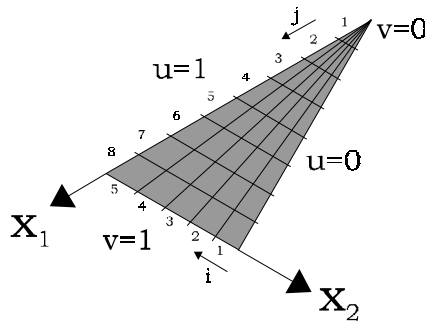


where the center-point corresponds to $(2/3, 2/3, 2/3)$. We choose the darker sixth of the triangle in which $x_2 \geq x_3 \geq x_1$.

Now, to get an estimate for the phase-space probability distribution, we have to evaluate $dP(x_1, x_2, x_3, a)$ at various points inside the dark triangle. To this end, we can introduce auxiliary variables as a coordinate system for the dark triangle:

$$\begin{cases} x_1 = \frac{v}{6}(3+u) \\ x_2 = 1 - \frac{uv}{3} \end{cases}$$

When u, v runs between 0 and 1, the x_1, x_2, x_3 span the dark area. Then, we divide the triangle into $I \times J$ cells, or bins (here with $I = 5$ and $J = 8$):



For $i = 1, \dots, I, j = 1, \dots, J$, the point at the center of each bin has coordinate:

$$\begin{cases} u_i = i\frac{1}{I} - \frac{1}{2I} \\ v_j = j\frac{1}{J} - \frac{1}{2J} \end{cases}$$

We can then construct a matrix out of the differential probability (for a given value of a)

$$dP\left(\frac{v_j}{6}(3+u_i), 1 - \frac{u_i v_j}{3}, 1 - \frac{v_j}{6}(3-u_i), a\right)$$

It is the computation of that matrix that takes so much computer time. Of course, the values of I and J to be used to get a reliable answer depend on the assumed smoothness of the differential probability. As we will see, in most cases, a coarse grained mesh $I \times J$ of 40 to 100 points is sufficient to get a total rate at the percent level of precision, because of the high redundancy of phase-space (i.e. 40 points in the dark triangle means 6×40 points for the whole phase-space). Note finally that the chosen parametrization has one technical advantage in

that evaluations of the differential probability on phase-space boundaries never occur. This is welcome since a numerical evaluation there is highly unstable (if not divergent), especially numerical integrations.

Once the matrix is found, we use some *Mathematica* tools to build interpolation functions. Namely, we construct an interpolation like

$$F_{int}[u, v] = \text{Interpolation} \left[\left(dP \left(\frac{v_j}{6} (3 + u_i), 1 - \frac{u_i v_j}{3}, 1 - \frac{v_j}{6} (3 - u_i), a \right) \right)_{i,j} \right]$$

Then, an interpolation to the whole phase-space is built by expressing back u, v in terms of reduced photon energies, as

$$dP_{int}(x_1, x_2, x_3; a) = \begin{cases} x_1 \leq x_3 \leq x_2 : F_{int} \left[2x_1 + x_2 - 1, \frac{3(1-x_2)}{2x_1 + x_2 - 1} \right] \\ x_1 \leq x_2 \leq x_3 : F_{int} \left[2x_1 + x_3 - 1, \frac{3(1-x_3)}{2x_1 + x_3 - 1} \right] \\ \dots \end{cases}$$

Note that at this step, we rely on *Mathematica* to extrapolate the interpolation beyond its range, since boundaries are now included (if one suspect that the differential probability is not smooth, sizeable loss of precision could occur. Increasing the number of bins is then compulsory). From this interpolation of phase-space, the differential rate, spectrum and total rate can be obtained simply by numerical integrations.

A.2.2 Euler-Heisenberg Lagrangian

The Euler-Heisenberg Lagrangian [201] is the one-loop QED effective action. It can be computed using the Schwinger Proper time technique [10], [18], [28], [203]. For a constant field strength, the result is expressed in closed form to all orders as

$$\mathcal{L}_{eff}^{(1)} = -\frac{1}{8\pi^2} \int_0^\infty \frac{d\tau}{\tau^3} e^{-m^2 \tau} \left[(e\tau)^2 ab \frac{\cosh(ea\tau) \cos(eb\tau)}{\sinh(ea\tau) \sin(eb\tau)} - 1 + C \right]$$

with a, b solutions of $a^2 - b^2 = \mathbf{E}^2 - \mathbf{B}^2$ and $ab = \mathbf{E} \cdot \mathbf{B}$. This expression was obtained in 1951 by Schwinger [203].

To get the various couplings, we expand the term in square brackets as a series in τ . Each order corresponds to a new term in the effective Lagrangian

$$\mathcal{L}_{eff}^{(1)} = \mathcal{L}_0^{(1)} + \mathcal{L}_2^{(1)} + \mathcal{L}_4^{(1)} + \mathcal{L}_6^{(1)} + \mathcal{L}_8^{(1)} + \mathcal{L}_{10}^{(1)} + \dots$$

with

$$\begin{aligned} \mathcal{L}_0^{(1)} &= -\frac{1}{8\pi^2} C \int_0^\infty \frac{d\tau}{\tau^3} e^{-m^2 \tau} \\ \mathcal{L}_2^{(1)} &= -\frac{\alpha}{6\pi} (a^2 - b^2) \int_0^\infty \frac{d\tau}{\tau} e^{-m^2 \tau} \\ \mathcal{L}_4^{(1)} &= \frac{4\alpha^2}{90m^4} (a^4 + 5b^2 a^2 + b^4) \\ \mathcal{L}_6^{(1)} &= -\frac{16\pi\alpha^3}{315m^8} (2a^6 + 7b^2 a^4 - 7b^4 a^2 - 2b^6) \\ \mathcal{L}_8^{(1)} &= \frac{256\pi^2\alpha^4}{945m^{12}} (3a^8 + 10b^2 a^6 - 7b^4 a^4 + 10b^6 a^2 + 3b^8) \\ \mathcal{L}_{10}^{(1)} &= -\frac{2048\pi^3\alpha^5}{1485m^{16}} (10a^{10} + 33b^2 a^8 - 22b^4 a^6 + 22b^6 a^4 - 33b^8 a^2 - 10b^{10}) \end{aligned}$$

Transcribed into $F_{\mu\nu}F^{\mu\nu} = 2(\mathbf{E}^2 - \mathbf{B}^2)$ and $F_{\mu\nu}\tilde{F}^{\mu\nu} = 4(\mathbf{E} \cdot \mathbf{B})$:

$$\begin{aligned}\mathcal{L}_0^{(1)} &= -\frac{1}{8\pi^2}C \int_0^\infty \frac{d\tau}{\tau^3} e^{-m^2\tau} \\ \mathcal{L}_2^{(1)} &= -\frac{\alpha}{12\pi}F_{\mu\nu}F^{\mu\nu} \int_0^\infty \frac{d\tau}{\tau} e^{-m^2\tau} \\ \mathcal{L}_4^{(1)} &= \frac{\alpha^2}{90m^4} \left((F_{\mu\nu}F^{\mu\nu})^2 + \frac{7}{4} (F_{\mu\nu}\tilde{F}^{\mu\nu})^2 \right) \\ \mathcal{L}_6^{(1)} &= -\frac{\pi\alpha^3}{315m^8} \left(4(F_{\mu\nu}F^{\mu\nu})^3 + \frac{13}{2} (F_{\mu\nu}F^{\mu\nu}) (F_{\mu\nu}\tilde{F}^{\mu\nu})^2 \right) \\ \mathcal{L}_8^{(1)} &= \frac{\pi^2\alpha^4}{945m^{12}} \left(48(F_{\mu\nu}F^{\mu\nu})^4 + 88(F_{\mu\nu}F^{\mu\nu})^2 (F_{\mu\nu}\tilde{F}^{\mu\nu})^2 + 19(F_{\mu\nu}\tilde{F}^{\mu\nu})^4 \right) \\ \mathcal{L}_{10}^{(1)} &= -\frac{4\pi^3\alpha^5}{1485m^{16}} \left(160(F_{\mu\nu}F^{\mu\nu})^5 + 332(F_{\mu\nu}F^{\mu\nu})^3 (F_{\mu\nu}\tilde{F}^{\mu\nu})^2 + 127(F_{\mu\nu}F^{\mu\nu}) (F_{\mu\nu}\tilde{F}^{\mu\nu})^4 \right)\end{aligned}$$

The first term is just an infinite energy shift, and can be set to zero $C = 0$. To compute the UV divergent $\mathcal{L}_2^{(1)}$ term, a regularization procedure must be introduced. Using a simple UV cutoff

$$\mathcal{L}_{Z_2}^{(1)} = \int_{1/\Lambda^2}^\infty \frac{d\tau}{\tau} e^{-m^2\tau} = \log \frac{\Lambda^2}{m^2} - \gamma$$

And one can recognize the photon wavefunction renormalization constant, up to irrelevant finite terms.

Feynman Rules for the Four-photon Vertex

Instead of directly give the Feynman rules associated with the Euler-Heisenberg Lagrangian, we consider the pieces

$$\begin{aligned}\mathfrak{L}_{(1)} &= \frac{\alpha^2}{90m^4} (F_{\mu\nu}F^{\mu\nu})^2 \\ \mathfrak{L}_{(2)} &= \frac{\alpha^2}{90m^4} (F_{\mu\nu}F^{\nu\rho}F_{\rho\sigma}F^{\sigma\mu}) \\ \mathfrak{L}_{(3)} &= \frac{\alpha^2}{90m^4} (F_{\mu\nu}\tilde{F}^{\mu\nu})^2 \equiv \frac{\alpha^2}{90m^4} \left[-2(F_{\mu\nu}F^{\mu\nu})^2 + 4(F_{\mu\nu}F^{\nu\rho}F_{\rho\sigma}F^{\sigma\mu}) \right]\end{aligned}$$

where

$$\tilde{F}^{\mu\nu} = \frac{1}{2}\varepsilon^{\mu\nu\rho\sigma}F_{\rho\sigma}$$

and the identity in the third line is easily established from contractions of Levi-Civita symbols.

For each term, the Feynman rules are (with the momentum flow $d = a + b + c$, i.e. d in-going, a, b, c out-going)

$$\begin{aligned}\Gamma_{(1)}^{\mu\nu\rho\sigma}(a, b, c; d) &= \frac{16i\alpha^2}{45m^4}V_0 \\ \Gamma_{(2)}^{\mu\nu\rho\sigma}(a, b, c; d) &= \frac{4i\alpha^2}{45m^4} \sum_{i=1}^8 V_i \\ \Gamma_{(3)}^{\mu\nu\rho\sigma}(a, b, c; d) &= -2\Gamma_{(1)}^{\mu\nu\rho\sigma}(a, b, c; d) + 4\Gamma_{(2)}^{\mu\nu\rho\sigma}(a, b, c; d)\end{aligned}$$

where

$$\begin{aligned}
V_0 &= ((d^\mu a^\sigma - g^{\mu\sigma} ad)(c^\nu b^\rho - g^{\nu\rho} bc) + (c^\mu a^\rho - g^{\mu\rho} ac)(d^\nu b^\sigma - g^{\nu\sigma} bd) + (b^\mu a^\nu - g^{\mu\nu} ab)(d^\rho c^\sigma - g^{\rho\sigma} cd)) \\
V_1 &= d^\mu c^\sigma b^\rho a^\nu + d^\nu c^\sigma b^\mu a^\rho + d^\rho c^\mu b^\sigma a^\nu + d^\mu c^\nu b^\sigma a^\rho + d^\rho c^\nu b^\mu a^\sigma + d^\nu c^\mu b^\rho a^\sigma \\
V_2 &= g^{\mu\nu} [(dc)b^\rho a^\sigma - (ad)c^\sigma b^\rho - (ac)d^\rho b^\sigma + (dc)b^\sigma a^\rho - (bd)c^\sigma a^\rho - (bc)d^\rho a^\sigma] \\
V_3 &= g^{\mu\rho} [(db)c^\nu a^\sigma - (ad)c^\nu b^\sigma - (ab)d^\nu c^\sigma + (db)a^\nu c^\sigma - (cd)a^\nu b^\sigma - (bc)d^\nu a^\sigma] \\
V_4 &= g^{\mu\sigma} [(bc)a^\rho d^\nu - (ab)c^\nu d^\rho - (ac)d^\nu b^\rho + (bc)a^\nu d^\rho - (bd)c^\nu a^\rho - (cd)b^\rho a^\nu] \\
V_5 &= g^{\nu\rho} [(ad)c^\sigma b^\mu - (ab)c^\sigma d^\mu - (ac)d^\mu b^\sigma + (ad)c^\mu b^\sigma - (db)c^\mu a^\sigma - (dc)b^\mu a^\sigma] \\
V_6 &= g^{\nu\sigma} [(ac)d^\rho b^\mu - (ab)c^\mu d^\rho - (bc)d^\mu a^\rho + (ac)b^\rho d^\mu - (ad)c^\mu b^\rho - (cd)b^\mu a^\rho] \\
V_7 &= g^{\rho\sigma} [(ab)c^\nu d^\mu - (ac)d^\nu b^\mu - (bc)a^\nu d^\mu + (ab)d^\nu c^\mu - (bd)a^\nu c^\mu - (ad)c^\nu b^\mu] \\
V_8 &= g^{\mu\sigma} g^{\nu\rho} [(ab)(cd) + (bd)(ac)] + g^{\mu\rho} g^{\nu\sigma} [(ad)(bc) + (ab)(cd)] + g^{\mu\nu} g^{\rho\sigma} [(bc)(ad) + (bd)(ac)]
\end{aligned}$$

The Euler-Heisenberg Feynman rules can then be reconstructed since

$$\begin{aligned}
\mathfrak{L}_{E-H} &= \frac{\alpha^2}{90m^4} \left[-\frac{5}{2} (F_{\mu\nu} F^{\mu\nu})^2 + 7 (F_{\mu\nu} F^{\nu\rho} F_{\rho\sigma} F^{\sigma\mu}) \right] \\
&\rightarrow \Gamma_{E-H}^{\mu\nu\rho\sigma}(a, b, c; d) = -\frac{5}{2} \Gamma_{(1)}^{\mu\nu\rho\sigma} + 7 \Gamma_{(2)}^{\mu\nu\rho\sigma}
\end{aligned}$$

In the text, we prefer to use the Lagrangian under the form

$$\begin{aligned}
\mathfrak{L}_{E-H} &= \frac{\alpha^2}{90m^4} \left[(F_{\mu\nu} F^{\mu\nu})^2 + \frac{7}{4} (F_{\mu\nu} \tilde{F}^{\mu\nu})^2 \right] \\
&\rightarrow \Gamma_{E-H}^{\mu\nu\rho\sigma}(a, b, c; d) = \Gamma_{(1)}^{\mu\nu\rho\sigma} + \frac{7}{4} \Gamma_{(3)}^{\mu\nu\rho\sigma}
\end{aligned}$$

to exhibit explicitly the scalar and pseudoscalar currents. The Feynman rules remain of course identical.

A.2.3 The Photon Two-point Function

The photon vacuum polarization reads

$$\Pi^{\mu\nu}(k^2) = ie^2 \int \frac{d^4 p}{(2\pi)^4} \text{Tr} \left[\gamma^\mu \frac{i}{\not{p} - m + i\varepsilon} \gamma^\nu \frac{i}{\not{p} + \not{k} - m + i\varepsilon} \right]$$

Using dimensional regularization techniques, which preserve gauge invariance, we find

$$\Pi^{\mu\nu}(k^2) = \frac{2\alpha}{\pi} (k^2 g^{\mu\nu} - k^\mu k^\nu) \int_0^1 dx x(x-1) \frac{\Gamma(2 - \frac{d}{2})}{(4\pi\omega^2)^{d/2-2}} \left(\frac{1}{m^2 - x(1-x)k^2} \right)^{2-\frac{d}{2}}$$

Expanding in terms of $\varepsilon = 4 - d$, with $\Pi^{\mu\nu}(k^2) = (k^2 g^{\mu\nu} - k^\mu k^\nu) \Pi(k^2)$

$$\begin{aligned}
\Pi(k^2) &= -\frac{\alpha}{3\pi} D - \frac{2\alpha}{\pi} \int_0^1 dx x(x-1) \log \left(\frac{m^2 - x(1-x)k^2}{m^2} \right) + O(\varepsilon) \\
D &= \frac{2}{\varepsilon} - \gamma + \log \left[\frac{4\pi\omega^2}{m^2} \right]
\end{aligned}$$

Note that we may also integrate over x the non-expanded expression, with the result expressed in terms of hypergeometric functions

$$\Pi(k^2) = -\frac{\alpha}{3\pi} \frac{\Gamma(2 - \frac{d}{2})}{(4\pi\omega^2/m^2)^{d/2-2}} F(2 - \frac{d}{2}, 2, \frac{5}{2}, \frac{k^2}{4m^2})$$

A completely integrated expression for the finite part can be obtained simply as

$$\Pi_R(k^2) = \frac{2\alpha}{\pi} \int_0^1 dx x(1-x) \log(1-x(1-x)\zeta) \quad (\text{A.26})$$

with $\zeta = k^2/m^2$. A direct integration gives (see for example [9])

$$\Pi_R(k^2) = -\frac{\alpha}{\pi} \left[\frac{5}{9} + \frac{4}{3\zeta} + \frac{2}{3} \left(1 - \frac{4}{\zeta}\right) \left(1 + \frac{2}{\zeta}\right) \mathcal{J}(\zeta) \right]$$

The function $\mathcal{J}(\zeta)$ is

$$\mathcal{J}(\zeta) = \begin{cases} \frac{1}{\sqrt{4/\zeta-1}} \arctan \frac{1}{\sqrt{4/\zeta-1}} & 0 < \zeta < 4 \\ -\frac{1}{\sqrt{1-4/\zeta}} \operatorname{arctanh} \frac{1}{\sqrt{1-4/\zeta}} & \zeta < 0 \\ \frac{1}{2\sqrt{1-4/\zeta}} \left(\log \frac{1-\sqrt{1-4/\zeta}}{1+\sqrt{1-4/\zeta}} + i\pi \right) & \zeta > 4 \end{cases}$$

where each term is obtain by analytic continuation. In fact, the first two lines are identical, due to the properties of arctangent functions. The last equality is valid in the upper complex plane

$$\frac{1}{\sqrt{4/\zeta-1}} \arctan \frac{1}{\sqrt{4/\zeta-1}} \stackrel{\xi \in \mathbb{C}^+}{=} \frac{1}{2\sqrt{1-4/\zeta}} \left(\log \frac{1-\sqrt{1-4/\zeta}}{1+\sqrt{1-4/\zeta}} + i\pi \right)$$

The real part of $\Pi_R(k^2)$, for all k^2 , is therefore

$$\Pi_R(k^2) = -\frac{\alpha}{\pi} \left[\frac{5}{9} + \frac{2}{3\zeta} - \frac{2}{3} \sqrt{4/\zeta-1} (1+2/\zeta) \operatorname{arccot} \sqrt{4/\zeta-1} - \frac{i\pi}{3} \theta(\zeta-4) \left(1 + \frac{2}{\zeta}\right) \sqrt{1-4/\zeta} \right]$$

Two-loop Vacuum Polarization

The photon two-loop vacuum polarization function is ([7], [217]):

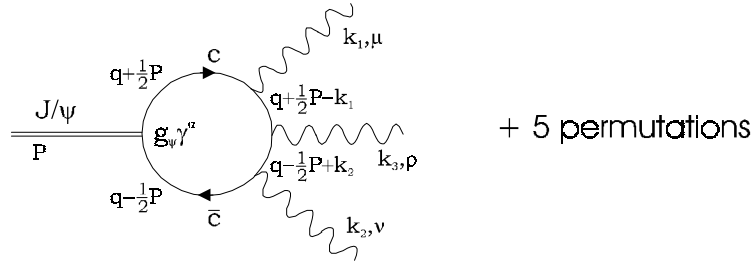
$$\begin{aligned} \Pi_R(\zeta) = & -\frac{\alpha^2}{16\pi^2} \left[\frac{10}{3} + \frac{26}{3\zeta} - \frac{4(1-\zeta)(3+2\zeta)}{3\zeta} G(\zeta) + \frac{2(1-\zeta)(1-16\zeta)}{3\zeta} G^2(\zeta) \right. \\ & \left. - \frac{2(1+2\zeta)}{3\zeta} \left[1 + 2\zeta(1-\zeta) \frac{d}{d\zeta} \right] \frac{I(\zeta)}{\zeta} \right] \end{aligned}$$

with

$$\begin{aligned}
G(\zeta) &= \frac{2y \ln y}{y^2 - 1} \\
I(\zeta) &= 6[\zeta(3) + 4Li_3(-y) + 2Li_3(y)] - 8[2Li_2(-y) + Li_2(y)] \ln y \\
&\quad - 2[2 \ln(1+y) + \ln(1-y)] \ln^2 y \\
y &= \frac{\sqrt{1 - 1/\zeta} - 1}{\sqrt{1 - 1/\zeta} + 1}
\end{aligned}$$

A.2.4 The Photon Four-point Function

We are interested in the four-point function only for a specific kinematics, i.e. that of the decay of a massive photon into three real photons. We can pictorially represent our process as



Where the g_ψ is an arbitrary coupling constant.

The corresponding amplitude is given in terms of the vector to three-photon current [113], [205]

$$G_\alpha^{\lambda_1 \lambda_2 \lambda_3} = \frac{i e^4}{4\sqrt{2}\Delta} \left\{ \begin{aligned} &\mathcal{E}_{\lambda_1 \lambda_2 \lambda_3}^{(1)}(123) \left(k_{2,\alpha} - \frac{x_2}{x_1} k_{1,\alpha} \right) - \mathcal{E}_{\lambda_1 \lambda_3 \lambda_2}^{(1)}(132) \left(k_{3,\alpha} - \frac{x_3}{x_1} k_{1,\alpha} \right) \\ &+ i \varepsilon_{\alpha\mu\nu\rho} k_1^\mu k_2^\nu k_3^\rho \mathcal{E}_{\lambda_1 \lambda_2 \lambda_3}^{(2)}(123) \end{aligned} \right\}$$

where $\Delta = (1 - x_1)(1 - x_2)(1 - x_3)$. The \mathcal{E} correspond to helicity amplitudes (indexed by $\lambda_1 \lambda_2 \lambda_3$), whose arguments ijk are short-hand for x_i, x_j, x_k , and also $a = 4m^2/M^2$. This expression must be summed over all polarization states $\lambda_1 \lambda_2 \lambda_3$. Because of numerous identities among the helicity amplitudes, the modulus squared of the amplitude can be expressed in terms of only four of them. Conventionally, we choose

$$E_{\pm\pm\pm}^{(1)}(x_1, x_2, x_3; a) = \frac{1}{2M^2} \mathcal{E}_{\pm\pm\pm}^{(1)}(123), \quad E_{\pm\pm\pm}^{(2)}(x_1, x_2, x_3; a) = \frac{1}{4} \mathcal{E}_{\pm\pm\pm}^{(2)}(123)$$

The dimensionless $E^{(i)}$ are given in the next subsection. In term of these, the modulus squared of the current is

$$\sum_{\lambda_1 \lambda_2 \lambda_3} (G_\alpha^{\lambda_1 \lambda_2 \lambda_3} G^{*\lambda_1 \lambda_2 \lambda_3, \alpha}) = -2^6 \alpha^4 [R(123) + R(213) + R(312)] \quad (\text{A.27})$$

with

$$\begin{aligned}
R(123) &= \frac{1}{3} \left| E_{-+-}^{(2)}(123) \right|^2 + \left| E_{+++}^{(2)}(123) \right|^2 + \frac{1}{x_1^2} \left| E_{+++}^{(1)}(123) + E_{+++}^{(1)}(132) \right|^2 \\
&\quad + \frac{x_1}{x_2 x_3 (1 - x_1)} \left| E_{-+-}^{(1)}(213) \right|^2 + \frac{(1 - x_2)(1 - x_3)}{x_1^2 (1 - x_1)} \left| \frac{1}{1 - x_2} E_{+++}^{(1)}(123) - \frac{1}{1 - x_3} E_{+++}^{(1)}(132) \right|^2
\end{aligned}$$

The R 's for other arguments are obtained by permutation of the x_i . Note that there is no restriction in the contraction (A.27) since current conservation (Ward identity) implies

$$\sum_{\lambda_1 \lambda_2 \lambda_3} \left(G_\alpha^{\lambda_1 \lambda_2 \lambda_3} G_\beta^{* \lambda_1 \lambda_2 \lambda_3} \right) = \frac{1}{3} \left(g_{\alpha\beta} - \frac{P_\alpha P_\beta}{M^2} \right) \left(\sum_{\lambda_1 \lambda_2 \lambda_3} G^{\lambda_1 \lambda_2 \lambda_3} G^{* \lambda_1 \lambda_2 \lambda_3} \right)$$

where the last factor is a scalar function, and where $P = k_1 + k_2 + k_3$. Therefore, the longitudinal part of the vector boson polarization sum never contributes.

The amplitude is then simply

$$\Gamma(V \rightarrow \gamma\gamma\gamma) = \frac{1}{2M} \frac{1}{3!} \int d\Phi_3 \frac{1}{3} \sum_{\lambda_1 \lambda_2 \lambda_3} \left(G_\alpha^{\lambda_1 \lambda_2 \lambda_3} G^{* \lambda_1 \lambda_2 \lambda_3, \alpha} \right)$$

The three-body phase space is

$$d\Phi_3 = M^2 \frac{dx_1 dx_2}{16(2\pi)^3}$$

and therefore

$$\begin{aligned} \Gamma(V \rightarrow \gamma\gamma\gamma) &= -\frac{1}{2^9 \pi^3} \frac{1}{9} M \int dx_1 dx_2 \sum_{\lambda_1 \lambda_2 \lambda_3} \left(G_\alpha^{\lambda_1 \lambda_2 \lambda_3} G^{* \lambda_1 \lambda_2 \lambda_3, \alpha} \right) \\ &= \frac{1}{9} \frac{\alpha^3 g_\psi^2}{2^5 \pi^4} M \int dx_1 dx_2 [R(123) + R(213) + R(312)] \end{aligned}$$

Helicity Amplitudes

The amplitude and squared amplitude can be expressed using helicity amplitudes. Let us note

$$r = 1 - x_1, s = 1 - x_2, t = 1 - x_3$$

Then, we have the four independent amplitudes ($E_{\pm\pm\pm}^{(1,2)} \equiv E_{\pm\pm\pm}^{(1,2)}(x_1, x_2, x_3)$):

$$\begin{aligned}
E_{++++}^{(1)} &= \frac{2t}{1-s} + \left[\frac{4st}{r(1-s)} + \frac{4t}{(1-s)^2} - \frac{2s}{1-s} \right] (B[s/a] - B[1/a]) \\
&+ \left[\frac{4t}{r} + \frac{2t}{1-t} \right] (B[t/a] - B[1/a]) + \left[\frac{a}{r} - \frac{a}{t} \right] T[r/a] \\
&+ \left[-\frac{2(s-t)}{r} + \frac{4st}{r^2} - \frac{3a}{1-s} + \frac{a}{1-t} + \frac{2at}{(1-s)^2} + \frac{a}{r} + \frac{a}{t} \right] T[1/a] \\
&+ \left[\frac{2(s-t)}{r} - \frac{4st}{r^2} + \frac{3a}{1-s} - \frac{2at}{(1-s)^2} - \frac{a}{r} - \frac{a}{s} - \frac{a}{t} \right] T[s/a] \\
&+ \left[\frac{2(s-t)}{r} - \frac{4st}{r^2} - \frac{a}{1-t} - \frac{a}{r} \right] T[t/a] \\
&+ \frac{a(1-r)(r-t)}{rst} I_0[r/a, s/a, 1/a] - \frac{a(1-r)}{rt} I_0[r/a, t/a, 1/a] \\
&+ \left[-\frac{2(s-t)}{r} + \frac{4st}{r^2} - \frac{a}{t} + \frac{3a}{r} + \frac{2a}{s} \right] I_0[s/a, t/a, 1/a] \\
E_{-+++}^{(1)} &= \left[\frac{a}{r} - \frac{a}{t} \right] (T[r/a] + T[s/a] + T[t/a] - T[1/a]) - \frac{a(1-r)}{st} I_0[r/a, s/a, 1/a] \\
&+ \frac{a(1-t)}{sr} I_0[s/a, t/a, 1/a]
\end{aligned}$$

for the first type, and

$$\begin{aligned}
E_{++++}^{(2)} &= \left[\frac{4s}{r} - \frac{2s}{1-s} \right] (B[s/a] - B[1/a]) + \left[\frac{4t}{r} - \frac{2t}{1-t} \right] (B[t/a] - B[1/a]) - \left[\frac{a}{r} + \frac{a}{s} + \frac{a}{t} \right] T[r/a] \\
&+ \left[-\frac{4st}{r^2} - \frac{2(1-r)}{r} - \frac{ar}{t(1-s)} - \frac{3a}{r} \right] T[s/a] + \left[-\frac{4st}{r^2} - \frac{2(1-r)}{r} - \frac{ar}{s(1-t)} - \frac{3a}{r} \right] T[t/a] \\
&+ \left[\frac{4st}{r^2} + \frac{2(1-r)}{r} + \frac{a(1-r)}{st} - \frac{a}{1-s} - \frac{a}{1-t} + \frac{3a}{r} \right] T[1/a] \\
&+ \left[\frac{at}{rs} + \frac{a(1-s)}{rt} + \frac{a^2}{rs} \right] I_0[r/a, s/a, 1/a] + \left[\frac{as}{rt} + \frac{a(1-t)}{rs} + \frac{a^2}{rt} \right] I_0[r/a, t/a, 1/a] \\
&+ \left[\frac{4st}{r^2} + \frac{2(1-r)}{r} + \frac{a(1-r)}{st} + \frac{5a}{r} + \frac{a^2}{st} \right] I_0[s/a, t/a, 1/a] \\
E_{-+++}^{(2)} &= -2 - \left[\frac{a}{r} + \frac{a}{s} + \frac{a}{t} \right] (T[r/a] + T[s/a] + T[t/a] - T[1/a]) \\
&+ \left[\frac{a}{t} + \frac{a^2}{rs} \right] I_0[r/a, s/a, 1/a] + \left[\frac{a}{s} + \frac{a^2}{rt} \right] I_0[r/a, t/a, 1/a] + \left[\frac{a}{r} + \frac{a^2}{st} \right] I_0[s/a, t/a, 1/a]
\end{aligned}$$

for the second type. The form factors appearing in the amplitudes are

$$\begin{aligned}
B[z] &= \frac{1}{2} \int_0^1 dx \ln [1 - i\varepsilon - z(1-x^2)] = \begin{cases} z < 1 : -1 + \sqrt{\frac{1}{z} - 1} \arcsin \sqrt{z} \\ z > 1 : -1 + \sqrt{1 - \frac{1}{z}} \left(\ln [\sqrt{z} + \sqrt{z-1}] - i\frac{\pi}{2} \right) \end{cases} \\
T[z] &= \int_0^1 dx \frac{\ln [1 - i\varepsilon - z(1-x^2)]}{1-x^2} = \begin{cases} z < 1 : -\arcsin^2 \sqrt{z} \\ z > 1 : \left(\ln [\sqrt{z} + \sqrt{z-1}] - i\frac{\pi}{2} \right)^2 \end{cases}
\end{aligned}$$

The constant ε (with a limit $\varepsilon \rightarrow 0$ understood) appearing in the argument of the logarithm is necessary to unambiguously select the correct sheet, i.e. to give a sign to the imaginary part. The result for $z > 1$ is then obtained by analytical continuation, with the convention $-i\varepsilon$ transcribing as a lower half complex plane continuation (a $+i\varepsilon$ would lead to an upper half plane continuation). Note well that both form factor have to be defined with the *same* conventions. The last form factor is more complicated:

$$I_0 [r/a, s/a, 1/a] = F [r/a, \gamma_{rs}] + F [s/a, \gamma_{rs}] - F [1/a, \gamma_{rs}]$$

where

$$\gamma_{rs} = \sqrt{1 + \frac{at}{rs}}, \quad F [z, \gamma_{rs}] = \int_0^1 dx \frac{\ln [1 - i\varepsilon - z(1 - x^2)]}{\gamma_{rs}^2 - x^2}$$

As for B and T , an explicit form for F can be given above and below threshold. For $u/a < 1$,

$$F \left[\frac{u}{a}, \gamma_{rs} \right] = \frac{1}{2\gamma} \left\{ \ln \left[\frac{ut + rs}{rs} \right] \ln \left[\frac{\gamma + 1}{\gamma - 1} \right] - Li_2 \left[\frac{ut}{ut + rs} \right] + 4 \operatorname{Re} Li_2 \left[\left(1 - \frac{1}{\gamma} \right) \cos \theta e^{i\theta} \right] - 2 \left(\frac{\pi}{2} - \theta \right)^2 \right\}$$

where the angle θ is

$$\theta = \arccos \sqrt{\frac{u rs + at}{a rs + ut}}$$

Denoting $b \equiv \sqrt{1 - \frac{a}{u}}$, the analytic continuation to $u/a > 1$ is

$$F \left[\frac{u}{a}, \gamma_{rs} \right] = \frac{1}{2\gamma} \left\{ \begin{aligned} & \ln \left[\frac{ut + rs}{rs} \right] \ln \left[\frac{\gamma + 1}{\gamma - 1} \right] - \frac{2\pi^2}{3} + i\pi \ln \left[\frac{\gamma - b}{\gamma + b} \right] \\ & + \frac{1}{2} \ln^2 \left[\frac{\gamma + 1}{\gamma + b} \right] + \frac{1}{2} \ln^2 \left[\frac{\gamma + 1}{\gamma - b} \right] \\ & + Li_2 \left[\frac{\gamma + b}{\gamma + 1} \right] + Li_2 \left[\frac{\gamma - 1}{\gamma + b} \right] + Li_2 \left[\frac{\gamma - b}{\gamma + 1} \right] + Li_2 \left[\frac{\gamma - 1}{\gamma - b} \right] \end{aligned} \right\}$$

A.2.5 The Ansatz

Here we collect the expressions for the differential rate and total rate using the ansatz (2.28).

The differential rate can be expressed as

$$\frac{d\Gamma (B \rightarrow \gamma\gamma\gamma)}{dx_1} = \frac{2}{9\pi} \alpha^6 m \left(\frac{4m^2}{M^2} \right) F \left(x_1, \frac{2\gamma^2}{M^2} \right)$$

with

$$F (x_1, A) = \frac{2}{(A + x_1)^2} \left(-P_1 + 2P_2 \log \left[\frac{1 + A - x_1}{1 + A} \right] \right)$$

where

$$\begin{aligned} P_1 &= \frac{2(4 + 13A + 10A^2)}{1 + A} + \frac{(1 + 5A)x_1}{1 + A} + \frac{2x_1^2}{1 + A} + \frac{2(10 + 34A + 27A^2)}{x_1 - 2A - 2} \\ &+ \frac{2A^2}{x_1 - A - 1} + \frac{4(1 + A)(2 + 8A + 9A^2)}{(x_1 - 2A - 2)^2} \\ P_2 &= 5 + 6A + \frac{13 + 36A + 24A^2}{x_1 - 2A - 2} + \frac{6(1 + A)(1 + 2A)(1 + 3A)}{(x_1 - 2A - 2)^2} + \frac{2(1 + A)^2(2 + 8A + 9A^2)}{(x_1 - 2A - 2)^3} \end{aligned}$$

The total rate is given by

$$\Gamma(B \rightarrow \gamma\gamma\gamma) = \frac{2}{9\pi} \alpha^6 m \left(\frac{4m^2}{M^2} \right) G \left(\frac{2\gamma^2}{M^2} \right) \quad (\text{A.29})$$

with

$$\begin{aligned} G(A) = & \left(\frac{2}{9} + \frac{11+12A}{27(2+3A)^2} + \frac{4}{27(2+3A)^4} \right) \pi^2 - \frac{6}{1+A} - \frac{6}{1+2A} + \frac{12}{(2+3A)^2} \\ & + \left(\frac{10-27A}{2+3A} + \frac{8(4+3A)}{(2+3A)^3} - \frac{3(3+4A)}{(1+2A)^2} \right) \log \left[\frac{A}{1+A} \right] \\ & + \left(\frac{16(1+A)(1+3A+3A^2)}{(2+3A)^4} + \frac{4(3+8A+6A^2)}{(2+3A)^2} \right) \times \\ & \left(Li_2 \left[-\frac{A}{1+A} \right] - Li_2 \left[\frac{A}{1+2A} \right] + Li_2 \left[\frac{1+A}{1+2A} \right] - 2 \log \left[\frac{A}{1+A} \right] \log \left[\frac{1+A}{1+2A} \right] \right) \end{aligned}$$

Appendix B

Resources for QCD Bound States

B.1 Running of the Strong Coupling Constant

In this section, we will shortly review the basic formulas for the running of the strong coupling constant α_S . It is based on [11], [209], [210], [213], [222], [223]. The basic formula is the renormalization group evolution equation

$$\mu \frac{\partial \alpha_S(\mu)}{\partial \mu} = \beta(\alpha_S(\mu)) \quad (\text{B.1})$$

In perturbation theory, the β function can be calculated from loop corrections as

$$\beta(\alpha_S(\mu)) = -\frac{\beta_0}{2\pi} \alpha_S^2(\mu) - \frac{\beta_1}{4\pi^2} \alpha_S^3(\mu) - \frac{\beta_2}{64\pi^3} \alpha_S^4(\mu) - \dots$$

with

$$\begin{aligned} \beta_0 &= 11 - \frac{2}{3}n_f \\ \beta_1 &= 51 - \frac{19}{3}n_f \\ \beta_2 &= 2857 - \frac{5033}{9}n_f + \frac{325}{27}n_f^2 \end{aligned}$$

The next term β_3 is also known, but too complicated to be given here. Note that only β_0 and β_1 are scheme independent.

B.1.1 One-Loop Running

To compare the values of α_S obtained in various processes, one has to use the renormalization group equation to "run" $\alpha_S(q^2)$ up to M_Z , which is the conventional comparison point. The world average for $\alpha_S(M_Z)$ is

$$\alpha_S(M_Z) = 0.1181 \pm 0.002$$

To lowest order, the coupling constant running is

$$\mu \frac{\partial \alpha_S(\mu)}{\partial \mu} = -\frac{\beta_0}{2\pi} \alpha_S^2(\mu) \rightarrow \alpha_S(\mu) = \frac{4\pi}{\beta_0 \ln \left[\mu^2 / \Lambda_{QCD}^2 \right]} \quad (\text{B.2})$$

where Λ_{QCD}^2 is an integration constant. For specific runnings, we may cast this formula in several useful forms.

1– Taking the difference at two scales, we get

$$\alpha_S^{-1}(m) = \alpha_S^{-1}(\mu) + \frac{\beta_0}{4\pi} \ln \left[\frac{m^2}{\mu^2} \right] \rightarrow \alpha_S(m) = \frac{\alpha_S(\mu)}{1 + \alpha_S(\mu) \frac{\beta_0}{4\pi} \ln \left[\frac{m^2}{\mu^2} \right]} \quad (\text{B.3})$$

Since $\beta_0 > 0$, the coupling constant decreases as the energy increases, a phenomenon called asymptotic freedom.

2– To lowest order in α_S , one sometimes uses

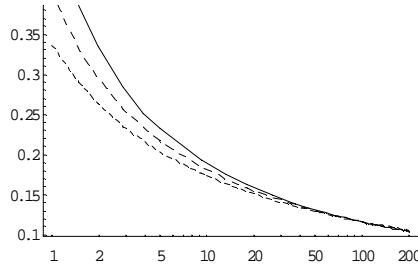
$$\alpha_S(m) = \alpha_S(\mu) \left(1 - \alpha_S(\mu) \frac{\beta_0}{2\pi} \ln \left[\frac{m}{\mu} \right] + O(\alpha_S^2(\mu)) \right) \quad (\text{B.4})$$

3– Forgetting about μ , we can transcribe the running as an equation in terms of Λ_{QCD} :

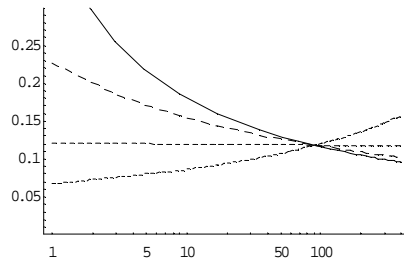
$$\alpha_S(m) = \frac{4\pi}{\beta_0 \ln \left[m^2 / \Lambda_{QCD}^2 \right]} \quad \text{with } \Lambda_{QCD} = \mu \exp \left(-\frac{2\pi}{\beta_0 \alpha_S(\mu)} \right) \quad (\text{B.5})$$

Hence once Λ_{QCD} is known, so is $\alpha_S(m)$ at any scale m .

The quantity β_0 is a function of n_f . This dependence comes about through vacuum polarization diagrams with n_f quark flavors in the loop. Quarks much heavier than the typical energy in the process must decouple, and at a given energy scale E , only n_f with m_f lighter than E must be considered. The running is therefore a function of the number of quark flavors used. For example, taking $\alpha_S(M_Z) = 0.118$,



with $n_f = 3$ (plain), 4, 5 from top to bottom. This running is an illustration of asymptotic freedom since $\alpha_S(q^2) \rightarrow 0$ as $q^2 \rightarrow \infty$. This is true as long as $n_f \leq 16$ (i.e. $\beta_0 > 0$):



for $n_f = 3, 8, 16$ and 30.

Running Down to Beauty, Charm Scales from the Weak Scale (I)

As an example, we will take the running of α_S down to the charmed quark mass, which we take at $m_c = 1.3 \text{ GeV}$. This example is interesting since one has to define how to treat the b quark threshold, $n_f = 5$ between M_Z and $m_b \approx 4.2 \text{ GeV}$, and $n_f = 4$ between m_b and m_c . Of course, the threshold is not a step function, and

the detailed evolution close to it is mass-dependent. Anyway, as a first approximation, such dependences are ignored.

1– The exact running using either (B.3) or integrating numerically the differential RG equation (B.2), gives a strong coupling at m_c of

$$\alpha_S(M_Z) = 0.118 \xrightarrow{n_f=5} \alpha_S(m_b) \approx 0.2119 \xrightarrow{n_f=4} \alpha_S(m_c) \approx 0.3161 \quad (\text{B.6})$$

(note that we are taking too many significative numbers for the purpose of comparison). Ignoring the threshold gives the values

$$\alpha_S(M_Z) = 0.118 \quad \begin{array}{l} \xrightarrow{n_f=3} \alpha_S(m_c) \approx 0.419 \\ \xrightarrow{n_f=4} \alpha_S(m_c) \approx 0.352 \\ \xrightarrow{n_f=5} \alpha_S(m_c) \approx 0.304 \end{array}$$

2– The approximate formula (B.4) gives

$$\alpha_S(M_Z) = 0.118 \xrightarrow{n_f=5} \alpha_S(m_b) \approx 0.170 \xrightarrow{n_f=4} \alpha_S(m_c) \approx 0.215$$

which is quite far from the exact one-loop running (B.6). The reason why this approximation is so poor is because

$$\ln \frac{M_Z^2}{m_b^2} \approx 6.2$$

The formula (B.4) neglects terms of order

$$\alpha_S^3(M_Z) \ln^2 \left[\frac{M_Z^2}{m_b^2} \right] \sim 0.06$$

(in case we would use (B.4) to go upwards $\alpha_S(m_b) \rightarrow \alpha(M_Z)$, this becomes ~ 0.35 , really bad indeed). For the last step

$$\alpha_S^3(m_b) \ln^2 \left[\frac{m_b^2}{m_c^2} \right] \sim 0.05$$

In conclusion, the approximate running formula should be used only to run between closely related scales, which are not too low (i.e. $> 1 \text{ GeV}$).

3– For the last scheme, we take the value of Λ_{QCD} according to

$$\Lambda_{QCD}(M_Z^2) = M_Z \exp \left(-\frac{2\pi}{\beta_0 \alpha_S(M_Z)} \right) \stackrel{n_f=5}{=} 0.088 \text{ GeV}$$

Then, the value of $\alpha_S(m_b)$ is B.5

$$\alpha_S(m_b) = \frac{4\pi}{\beta_0 \ln \left[m_b^2 / \Lambda_{QCD}^2 \right]} \stackrel{n_f=5}{=} 0.2119$$

As before. To continue down to m_c , we have to change Λ_{QCD} as

$$\Lambda'_{QCD}(m_b^2) = m_b \exp \left(-\frac{2\pi}{\beta_0 \alpha_S(m_b)} \right) \stackrel{n_f=4}{=} 0.120 \text{ GeV}$$

and $\alpha_S(m_c) = 0.3161$, exactly the same result as before.

B.1.2 Running Beyond One-Loop

The general RG equation (B.1) is integrated as

$$\int \frac{d\mu}{\mu} = \int \frac{d\alpha}{\beta(\alpha)}$$

If we expand $\beta(\alpha)$ up to β_3 , we have

$$\begin{aligned} \frac{1}{2} \log \frac{\mu^2}{\Lambda^2} &= \int^{\alpha_S(\mu)} \frac{d\alpha}{-\frac{\beta_0}{2\pi}\alpha^2 - \frac{\beta_1}{4\pi^2}\alpha^3 - \frac{\beta_2}{64\pi^3}\alpha^4 - \frac{\beta_3}{128\pi^4}\alpha^5} \\ &= \frac{1}{\beta_0} \left[\frac{2\pi}{\alpha} + \frac{\beta_1 \log \alpha}{\beta_0} + \frac{\beta_0 \beta_2 - 8\beta_1^2}{16\pi\beta_0^2} \alpha + \frac{8\beta_1^3 - 2\beta_0\beta_1\beta_2 + \beta_0^2\beta_3}{64\pi^2\beta_0^4} \alpha^2 \right]_{\alpha=\alpha_S(\mu)} + C \end{aligned}$$

To go from the first to the second line, we have integrated, then Taylor expanded the result around $\alpha = 0$ and finally moved constant terms into C . This expression must now be inverted to get $\alpha_S(\mu)$ as a function of $\log \mu^2/\Lambda^2$. This is not an easy task in general, and we proceed iteratively. Let us introduce the convenient notations

$$L \equiv \frac{1}{\log \frac{\mu^2}{\Lambda^2}} \equiv \frac{1}{\log \chi}$$

The first order is simply

$$\frac{1}{2L} = \frac{2\pi}{\alpha_S(\mu)\beta_0} \rightarrow \alpha_S(\mu) = \frac{4\pi}{\beta_0 L}$$

as before. The next order is found from

$$\begin{aligned} \frac{\beta_0}{2L} &= \left[\frac{2\pi}{\alpha} + \frac{\beta_1 \log \alpha}{\beta_0} - \frac{\beta_1^2}{2\pi\beta_0^2} \alpha + C \right]_{\alpha_S(\mu) \rightarrow \frac{4\pi}{\beta_0 L} + \delta\alpha_S(\mu)} \\ &= \left(C + \frac{\beta_0}{2L} - \frac{2L\beta_1^2}{\beta_0^4} + \frac{\beta_1}{\beta_0} \log \frac{4L\pi}{\beta_0} \right) - \left(\frac{\beta_0^5 - 2L\beta_0^3\beta_1 + 4L^2\beta_1^2}{8L\pi\beta_0^3} \right) \delta\alpha_S(\mu) + \mathcal{O}(\delta\alpha_S(\mu)^2) \end{aligned}$$

The constant C is chosen as

$$C = -\frac{\beta_1}{\beta_0} \log \frac{4\pi}{\beta_0}$$

so as to eliminate the constants in the logarithm. Then, solving for $\delta\alpha_S$ and expanding the result around $L = 0$:

$$\delta\alpha_S = \frac{8\pi\beta_1}{\beta_0^2} L^2 \log L$$

i.e.

$$\alpha_S(\mu) = \frac{4\pi}{\beta_0 \ln \frac{\mu^2}{\Lambda_{QCD}^2}} \left(1 - \frac{2\beta_1 \ln \ln \frac{\mu^2}{\Lambda_{QCD}^2}}{\beta_0^2 \ln \frac{\mu^2}{\Lambda_{QCD}^2}} \right) + \mathcal{O} \left[\ln^{-3} \frac{\mu^2}{\Lambda_{QCD}^2} \right] \quad (\text{B.7})$$

Note that the integration constant Λ is now interpreted as Λ_{QCD} (i.e., Λ_{QCD} is defined by this expression).

Obviously, this method can be pursued to higher order. The result to three loops usually quoted is

$$\alpha_S(\mu) = \frac{4\pi}{\beta_0 \ln \chi} \left(1 - \frac{2\beta_1 \ln \ln \chi}{\beta_0^2 \ln \chi} + \frac{4\beta_1^2}{\beta_0^4 \ln^2 \chi} \left(\left(\ln \ln \chi - \frac{1}{2} \right)^2 + \frac{\beta_0\beta_2}{8\beta_1^2} - \frac{5}{4} \right) \right) + \mathcal{O}[\ln^{-4} \chi] \quad (\text{B.8})$$

Let us emphasize that contrary to the one-loop result, this expression for the running is not exact, since we have made an expansion in $\ln^{-1} \chi$. Anyway, in general, Λ_{QCD} is estimated to be a few hundreds of MeV , so that the expansion parameter is getting better as the scale increases. Around $1 GeV$, we can estimate $\ln^{-1} \chi \approx 0.3$, $\beta_0 (n_f = 3) = 9$, so that the above formula should be quite precise (at least in the perturbative

regime, remember the initial α expansion of the integrated RG equation, and that the value of β is calculated in perturbation theory).

Using the world average value of $\alpha_S(M_Z)$, we can get the value of $\Lambda_{QCD}^{(n_f)}$ using 1, 2- and 3-loop running:

	1 loop	2 loops	3 loops
$\Lambda_{QCD}^{(3)}$	246^{+25}_{-24}	738^{+71}_{-67}	638^{+61}_{-58}
$\Lambda_{QCD}^{(4)}$	153^{+17}_{-16}	436^{+46}_{-43}	387^{+41}_{-38}
$\Lambda_{QCD}^{(5)}$	88^{+11}_{-10}	226^{+27}_{-24}	208^{+25}_{-23}

The rather imprecise determination comes from the logarithmic dependence of α_S on Λ_{QCD} . Note that we have given $\Lambda_{QCD}^{(3)}, \Lambda_{QCD}^{(4)}$ just for the purpose of illustration, since one usually considers $n_f = 5$ close to M_Z .

Running Down to Beauty, Charm Scales from the Weak Scale (II)

Now that the two and three loop running formulas have been presented, we can use them to get the value of the strong coupling at the m_b and m_c mass scales.

As a first exercise, it is instructive to compare the exact running (i.e. integrating numerically the differential equation) to the approximate formula (B.7) and (B.8)

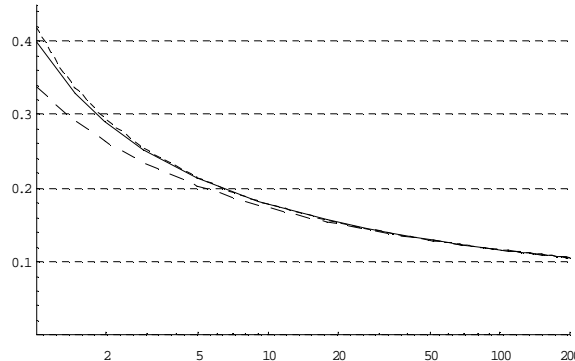
$(n_f = 5)$	2-Loop		3-Loop	
	(B.7)	(B.1)	(B.8)	(B.1)
$\alpha_S(m_b)$	0.2248	0.2233	0.2236	0.2241

The convergence is manifest (with one loop, we obtained $\alpha_S(m_b) \approx 0.2119$).

Integrating first with $n_f = 5$ to m_b , and then with $n_f = 4$ to m_c , we get

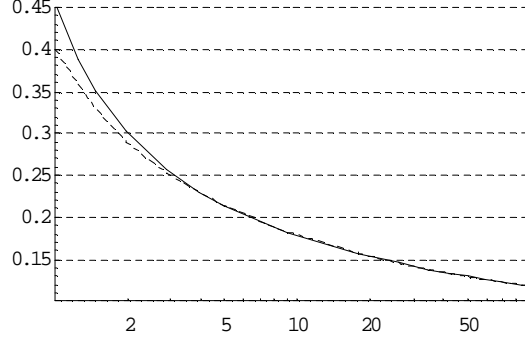
	1-Loop	2-Loop	3-Loop
$\alpha_S(m_c)$	0.316	0.380	0.378

To compare the result with one, two and three loops, we draw the plot of $\alpha_S(q^2)$ (note $n_f = 5$ was kept throughout the plot range)



The plain line is the 3-loop result. One can see that in the low energy range, the 1-loop (bottom line) is down by more than 20%. Since the series is alternating, we can expect the exact curve to lie between the 2-loop and 3-loop results (in fact, the 4-loop result would be indistinguishable from the 3-loop one).

Finally, to illustrate the effect of the quark threshold, let us plot the running with n_f fixed at 5 and with n_f changing to 4 at m_b



One can see that the two curves are identical down to m_b , and then, the exact curve (plain) with $n_f = 4$ is accelerating upwards.

B.2 Standard Annihilation Rate Computations

This appendix contains the computation of quarkonium decay rates in the static limit, i.e. assuming $M = 2m$.

B.2.1 Pseudoscalar Quarkonium Decays

Pseudoscalar Quarkonium Electromagnetic Decays

The transcription of positronium results is straightforward. The two-photon decay is given by

$$\Gamma(^1S(Q\bar{Q}) \rightarrow \gamma\gamma) = \frac{1}{2} \frac{N}{M^2} \int d\Phi_A |\phi_0|^2 \sum_{spins} |\mathcal{M}(q\bar{q} \rightarrow \gamma\gamma)|^2 = 16\pi\alpha^2 (Ne_Q^4) \frac{|\phi_0|^2}{M^2} \quad (\text{B.9})$$

If we ignore the binding energy and express M as $2m_Q$ (as is required in the present approach), we arrive at

$$\Gamma(^1S(Q\bar{Q}) \rightarrow \gamma\gamma) = 12\pi \frac{e_Q^4 \alpha^2}{m_Q^2} |\phi_0|^2$$

The rate into $\gamma e^+ e^-$ (or any pair of light leptons) is equally straightforward to obtain

$$\frac{d\Gamma(^1S(Q\bar{Q}) \rightarrow \gamma e^+ e^-)}{dx} = \frac{16}{3} \alpha^3 (Ne_Q^4) \frac{|\phi_0|^2}{M^2} \frac{\rho(x, a)}{x^2} \quad (\text{B.10})$$

where $a = 4m_e^2/M^2 = m_e^2/m_Q^2$ and the phase space spectrum is

$$\rho(x, a) = \sqrt{1 - \frac{a}{1-x}} [a + 2(1-x)] \frac{x^3}{(1-x)^2}$$

The total width (x ranges from 0 to $1 - a$):

$$\Gamma(^1S(Q\bar{Q}) \rightarrow \gamma e^+ e^-) = \frac{16}{3} \alpha^3 (N e_Q^4) \frac{|\phi_0|^2}{M^2} F(a) \quad (\text{B.11})$$

with

$$F(a) = \frac{4}{3} \sqrt{1-a} (a-4) + 2 \ln \left(\frac{1 + \sqrt{1-a}}{1 - \sqrt{1-a}} \right)$$

The ratio of the two electromagnetic modes is

$$\frac{d\Gamma(^1S(Q\bar{Q}) \rightarrow \gamma e^+ e^-) / dx}{\Gamma(^1S(Q\bar{Q}) \rightarrow \gamma\gamma)} = \frac{\alpha}{3\pi} \frac{\rho(x, a)}{x^2}$$

Except for the x^2 , this is standard. Integrated, we get

$$\frac{\Gamma(^1S(Q\bar{Q}) \rightarrow \gamma e^+ e^-)}{\Gamma(^1S(Q\bar{Q}) \rightarrow \gamma\gamma)} = \frac{\alpha}{3\pi} F(a)$$

Pseudoscalar Quarkonium Decays into Two Gluons

Let us calculate the amplitude

$$\mathcal{M} (^1S(Q\bar{Q}) \rightarrow gg) = \frac{1}{\sqrt{N}} \text{Tr} [P_{J=0} \Gamma(Q\bar{Q} \rightarrow gg)]$$

The scattering amplitude $\Gamma(Q\bar{Q} \rightarrow gg)$ has three contributions: the t and u channel (intermediate virtual quark) and the s channel (virtual gluon, with three-gluon vertex).

$$\begin{aligned} \Gamma_{t+u}(Q\bar{Q} \rightarrow gg) &= ig^2 \left\{ \frac{2k^\mu \gamma^\nu - \gamma^\nu \not{k}_1 \gamma^\mu}{2(k \cdot l_1)} t^j t^i + \frac{\gamma^\mu \not{k}_1 \gamma^\nu - 2k^\mu \gamma^\nu}{2(k \cdot l_1)} t^i t^j \right\}_{ba} \varepsilon_\mu^i(l_1) \varepsilon_\nu^j(l_2) \\ \Gamma_s(Q\bar{Q} \rightarrow gg) &= \frac{g^2}{q^2} \{ \gamma^\alpha (f^{ijk} t^k) \}_{ba} [g^{\mu\nu} (l_2 - l_1)^\alpha - g^{\nu\alpha} (l_2 + q)^\mu + g^{\alpha\mu} (q + l_1)^\nu] \varepsilon_\mu^i(l_1) \varepsilon_\nu^j(l_2) \end{aligned}$$

where $q = l_2 + l_1 = k + k'$ and $k^2 = k'^2 = m^2$. However, the s -channel amplitude vanishes in the trace, because only one (traceless) Gell-Mann matrix $(t^k)_{ba}$ is inserted in the quark current. The color trace for the other contributing amplitude gives

$$\text{Tr} \{ t^j t^i \} = \text{Tr} \{ t^i t^j \} = C(r) \delta^{ij} = \frac{1}{2} \delta^{ij} \quad (\text{B.12})$$

Then the two-gluon amplitude can be written as (external projectors have been used)

$$\Gamma(Q\bar{Q} \rightarrow gg) = \delta^{ij} \frac{ig^2}{2} \left[\frac{\gamma^\mu \not{k}_1 \gamma^\nu - \gamma^\nu \not{k}_1 \gamma^\mu}{2(k \cdot l_1)} \right] \varepsilon_\mu^i(l_1) \varepsilon_\nu^j(l_2)$$

Now that the color structure is factored out, we recover the QED amplitude, which is gauge invariant when $k = k'$. Contrary to the scattering case, the three gluon vertex is not needed to ensure gauge invariance. Then, using known results

$$|\mathcal{M} (^1S(Q\bar{Q}) \rightarrow gg)|^2 = \frac{2}{N} \frac{g^4}{(k \cdot l_1)^2} 2(k \cdot l_1)^2 \delta^{ij} \delta^{ij} = \frac{32}{N} 16\pi^2 \alpha_s^2$$

Note that in the gluon polarization sum, we simply use $g^{\mu\nu}$, since transverse states do not couple to the quark current.

The decay width is

$$\Gamma(^1S(Q\bar{Q}) \rightarrow gg) = \frac{1}{2} \frac{1}{4m_Q^2} \int d\Phi_2 |\mathcal{M}(^1S(q\bar{q}) \rightarrow gg)|^2 |\phi_0|^2 = \frac{8\pi\alpha_S^2}{3m_Q^2} |\phi_0|^2 \quad (\text{B.13})$$

Pseudoscalar Quarkonium Decay into Gluon-Quark-Antiquark

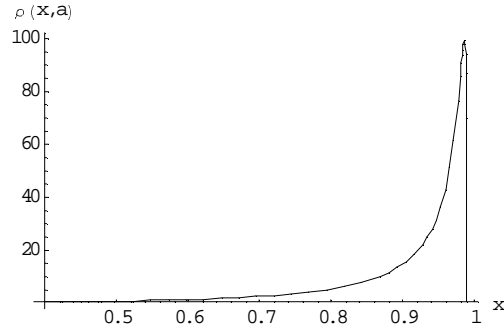
This is the analog of the decay into a photon and an electron-positron pair. The color structure of the amplitude is seen to factorize, and

$$|\mathcal{M}(^1S(Q\bar{Q}) \rightarrow gq\bar{q})|^2 = \frac{\alpha_S^3}{\alpha^3 \epsilon_Q^4} \frac{\delta^{ij} \delta_{ij}}{2N^2} |\mathcal{M}(^1S(Q\bar{Q}) \rightarrow \gamma e^+ e^-)|^2$$

The final formula is then

$$\frac{d\Gamma(^1S(Q\bar{Q}) \rightarrow gq\bar{q})}{dx} = \frac{64}{9} \alpha_S^3 \frac{|\phi_0|^2}{M^2} \frac{\rho(x, a)}{x^2}$$

where $a = 4m_q^2/M^2$ with m_q the final quark mass. Typically, the spectrum function $\rho(x, a)$ is (for $a = 0.01$)



The total width

$$\Gamma(^1S(Q\bar{Q}) \rightarrow gq\bar{q}) = \frac{64}{9} \alpha_S^3 \frac{|\phi_0|^2}{M^2} F(a) \quad (\text{B.14})$$

For example, with $M_{\eta_c} = 2976$ MeV, the function $F(a)$ is

m_q (MeV)	$F(4m_q^2/M^2)$
$m_u \sim 5$	20.2
$m_d \sim 12$	16.7
$m_s \sim 180$	5.93

Pseudoscalar Quarkonium Decay into Three Gluons

There are two topologically distinct contributions to this decay. One is obtained with the three gluon coming from the quark line, and the other from the two-gluon decay amplitude, with one of the gluon going into two gluon by way of the three-gluon vertex. All these amplitude are of order α_S^3 . As discussed in the text, the inclusive rate $^1S(Q\bar{Q}) \rightarrow$ light hadrons is related via duality to the rate into all possible gluonic states. To leading order, it is the two-gluon rate. To order α_S^3 , one has to consider the rate into ggg , $gq\bar{q}$ and strong radiative corrections to the rate into gg . Such a computation is not very complicated, but rather lengthy, and will not be pursued further.

B.2.2 Vector Quarkonium Decays

Vector Quarkonium Electromagnetic Decays

As for the para-state, we just have to include a color factor $N (=3)$ and substitute $\alpha \rightarrow e_Q^2 \alpha$. This gives for three photon decays:

$$\Gamma(^3S(Q\bar{Q}) \rightarrow \gamma\gamma\gamma) = \frac{64 e_Q^6 \alpha^3}{3 M^2} (\pi^2 - 9) |\phi_0|^2 \quad (\text{B.15})$$

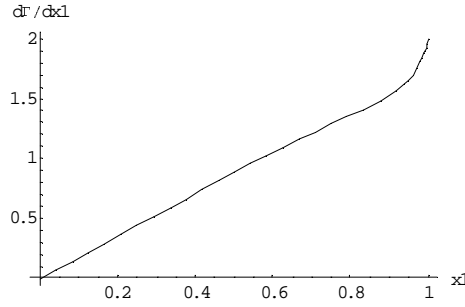
with the differential width

$$\frac{d\Gamma(^3S(Q\bar{Q}) \rightarrow \gamma\gamma\gamma)}{dx} = \frac{64 e_Q^6 \alpha^3}{3 M^2} |\phi_0|^2 \Omega(x_1) \quad (\text{B.16})$$

and the usual three-photon positronium decay spectrum (note that contrary to $\rho(x, a)$, $\Omega(x_1)$ is not the pure phase space, which is $2x_1$ here)

$$\Omega(x_1) = \frac{2(2-x_1)}{x_1} + \frac{2(1-x_1)x_1}{(2-x_1)^2} + 4(1-x_1) \left[\frac{1}{x_1^2} - \frac{(1-x_1)}{(2-x_1)^3} \right] \log(1-x_1) \quad (\text{B.17})$$

Plotted, this is



and $\int_0^1 dx_1 \Omega(x_1) = \pi^2 - 9$.

For lepton pair production, we find

$$\Gamma(^3S(Q\bar{Q}) \rightarrow e^+e^-) = 8\pi e_Q^2 \alpha^2 \frac{|\phi_0|^2}{M^2} \left(2 + \frac{m_e^2}{m_Q^2} \right) \sqrt{1 - \frac{4m_e^2}{M^2}}$$

where m_Q originates from the amplitude and M from phase space. Since we are assuming $M = 2m_Q$:

$$\Gamma(^3S(Q\bar{Q}) \rightarrow e^+e^-) = 2\pi e_Q^2 \alpha^2 \frac{|\phi_0|^2}{m_Q^2} \left(2 + \frac{m_e^2}{m_Q^2} \right) \sqrt{1 - \frac{m_e^2}{m_Q^2}}$$

and when $m_e \ll m_Q$

$$\Gamma(^3S(Q\bar{Q}) \rightarrow e^+e^-) = 4\pi e_Q^2 \alpha^2 \frac{|\phi_0|^2}{m_Q^2} \quad (\text{B.18})$$

Vector Quarkonium Decay into Three Gluons

Now we turn to the amplitude

$$\mathcal{M}(^3S(Q\bar{Q}) \rightarrow ggg) = \frac{1}{\sqrt{N}} g^6 \text{Tr} [P_{J=3} \Gamma_{abc}^{\mu\nu\rho} (Q\bar{Q} \rightarrow ggg)] \varepsilon_\mu^a(l_1) \varepsilon_\nu^b(l_2) \varepsilon_\rho^c(l_3) \quad (\text{B.19})$$

with

$$\begin{aligned}\Gamma_{abc}^{\mu\nu\rho} = & \gamma^\mu \frac{1}{\not{l}_1 - \not{k} - m} \gamma^\nu \frac{1}{\not{k} - \not{l}_3 - m} \gamma^\rho (t_a t_b t_c) + \gamma^\rho \frac{1}{\not{l}_3 - \not{k} - m} \gamma^\nu \frac{1}{\not{k} - \not{l}_1 - m} \gamma^\mu (t_c t_b t_a) \\ & + \gamma^\mu \frac{1}{\not{l}_1 - \not{k} - m} \gamma^\rho \frac{1}{\not{k} - \not{l}_2 - m} \gamma^\nu (t_a t_c t_b) + \gamma^\nu \frac{1}{\not{l}_2 - \not{k} - m} \gamma^\rho \frac{1}{\not{k} - \not{l}_1 - m} \gamma^\mu (t_b t_c t_a) \\ & + \gamma^\nu \frac{1}{\not{l}_2 - \not{k} - m} \gamma^\mu \frac{1}{\not{k} - \not{l}_3 - m} \gamma^\rho (t_b t_a t_c) + \gamma^\rho \frac{1}{\not{l}_3 - \not{k} - m} \gamma^\mu \frac{1}{\not{k} - \not{l}_2 - m} \gamma^\nu (t_c t_a t_b)\end{aligned}$$

where $q = l_1 + l_2 + l_3 = k + k'$ and $k^2 = k'^2 = m^2$. There is no three gluon vertex since we must have three gluon vertex insertions into the quark current to get a non-vanishing trace in (B.19) (also, a diagram $q\bar{q} \rightarrow g \rightarrow gg \rightarrow ggg$, of the same order, does not contribute because of the tracelessness of Gell-Mann matrices). Since all gluons emerge from the quark current, no ghost amplitude need to be considered and gluon polarization sums can be taken as $g^{\mu\nu}$.

This amplitude is again expressible in terms of the three photon decay amplitude. There is two non equivalent permutations of color matrices to be traced : $Tr(t_a t_b t_c)$ and $Tr(t_b t_a t_c)$. For this, we use the identities (B.12) and

$$[t_a t_b] = i f_{abc} t_c \quad \{t_a t_b\} = \frac{1}{3} \delta_{ab} + d_{abc} t_c$$

We can then work out the traces as

$$\begin{aligned}Tr(t_a t_b t_c) &= \frac{1}{4} (i f_{abc} - d_{abc}) \\ Tr(t_b t_a t_c) &= \frac{1}{4} (-i f_{abc} - d_{abc})\end{aligned}$$

Let us consider the first pair of amplitudes:

$$\Gamma_{I,abc}^{\mu\nu\rho} = Tr \left[\gamma^\mu \frac{1}{\not{l}_1 - \not{k} - m} \gamma^\nu \frac{1}{\not{k} - \not{l}_3 - m} \gamma^\rho (t_a t_b t_c) + \gamma^\rho \frac{1}{\not{l}_3 - \not{k} - m} \gamma^\nu \frac{1}{\not{k} - \not{l}_1 - m} \gamma^\mu (t_c t_b t_a) \right]$$

The Dirac trace will be the same for both terms, hence we arrive at

$$\begin{aligned}\Gamma_{I,abc}^{\mu\nu\rho} &= Tr [t_a t_b t_c + t_c t_b t_a] Tr \left[\gamma^\mu \frac{1}{\not{l}_1 - \not{k} - m} \gamma^\nu \frac{1}{\not{k} - \not{l}_3 - m} \gamma^\rho \right] \\ &= \left[\frac{1}{2} d_{abc} \right] Tr \left[\gamma^\mu \frac{1}{\not{l}_1 - \not{k} - m} \gamma^\nu \frac{1}{\not{k} - \not{l}_3 - m} \gamma^\rho \right]\end{aligned}$$

The same manipulations apply for the two other pairings, and we are left with the three-photon amplitude multiplied by the color factor $d_{abc}/4$. This can be understood since the final gluons should be symmetrized, hence only the symmetric tensor d_{abc} , and not f_{abc} , contributes. We thus arrive at

$$|\mathcal{M}(^3S(Q\bar{Q}) \rightarrow ggg)|^2 = \frac{d_{abc} d^{abc}}{16N} \frac{64g^6}{m^2} \left(\frac{(1-x_1)^2}{x_2^2 x_3^2} + \frac{(1-x_2)^2}{x_1^2 x_3^2} + \frac{(1-x_3)^2}{x_1^2 x_2^2} \right)$$

which equals, up to a color factor, the modulus squared of the three-photon decay amplitude. Using

$$d_{abc} d^{abc} = \frac{40}{3}$$

and integrating over phase space, we arrive at

$$\Gamma(^3S(Q\bar{Q}) \rightarrow ggg) = \frac{1}{3} \frac{1}{3!} \frac{|\phi_0|^2}{M^2} \int d\Phi_3 |\mathcal{M}(^3S(Q\bar{Q}) \rightarrow ggg)|^2 = \frac{160(\pi^2 - 9)}{81} \alpha_3^3 \frac{|\phi_0|^2}{M^2} \quad (\text{B.20})$$

with the differential rate given by

$$\frac{d\Gamma(^3S(Q\bar{Q}) \rightarrow ggg)}{dx} = \frac{160}{81} \alpha_S^3 \frac{|\phi_0|^2}{M^2} \Omega(x_1) \quad (\text{B.21})$$

Vector Quarkonium Decay into Two Gluons and a Photon

This time the amplitude is

$$\mathcal{M}(^3S(Q\bar{Q}) \rightarrow gg\gamma) = \frac{e_Q e g^2}{\sqrt{N}} \text{Tr} [P_{J=3} \Gamma_{ab}^{\mu\nu\rho}(Q\bar{Q} \rightarrow \gamma gg)] \varepsilon_\mu^a(l_1) \varepsilon_\nu^b(l_2) \varepsilon_\rho(l_3)$$

with

$$\begin{aligned} \Gamma_{ab}^{\mu\nu\rho} = & \gamma^\mu \frac{1}{\not{l}_1 - \not{k} - m} \gamma^\nu \frac{1}{\not{k} - \not{l}_3 - m} \gamma^\rho (t_a t_b) + \gamma^\rho \frac{1}{\not{l}_3 - \not{k} - m} \gamma^\nu \frac{1}{\not{k} - \not{l}_1 - m} \gamma^\mu (t_b t_a) \\ & + \gamma^\mu \frac{1}{\not{l}_1 - \not{k} - m} \gamma^\rho \frac{1}{\not{k} - \not{l}_2 - m} \gamma^\nu (t_a t_b) + \gamma^\nu \frac{1}{\not{l}_2 - \not{k} - m} \gamma^\rho \frac{1}{\not{k} - \not{l}_1 - m} \gamma^\mu (t_b t_a) \\ & + \gamma^\nu \frac{1}{\not{l}_2 - \not{k} - m} \gamma^\mu \frac{1}{\not{k} - \not{l}_3 - m} \gamma^\rho (t_b t_a) + \gamma^\rho \frac{1}{\not{l}_3 - \not{k} - m} \gamma^\mu \frac{1}{\not{k} - \not{l}_2 - m} \gamma^\nu (t_a t_b) \end{aligned}$$

where $q = l_1 + l_2 + l_3 = k + k'$ and $k^2 = k'^2 = m^2$. The color trace is just yielding a delta function (B.12) and there is no subtlety associated with symmetrization. We thus recover again the three-photon amplitude, with the result

$$|\mathcal{M}(^3S(Q\bar{Q}) \rightarrow gg\gamma)|^2 = \frac{\delta_{ab} \delta^{ab} 64 g^4 e_Q^2 e^2}{4N m^2} \left(\frac{(1-x_1)^2}{x_2^2 x_3^2} + \frac{(1-x_2)^2}{x_1^2 x_3^2} + \frac{(1-x_3)^2}{x_1^2 x_2^2} \right)$$

and then

$$\Gamma(^3S(Q\bar{Q}) \rightarrow gg\gamma) = \frac{1}{3} \frac{1}{2!} \frac{|\phi_0|^2}{M^2} \int d\Phi_3 |\mathcal{M}(^3S(Q\bar{Q}) \rightarrow gg\gamma)|^2 = \frac{128(\pi^2 - 9)}{9} e_Q^2 \alpha_S^2 \frac{|\phi_0|^2}{M^2}$$

with again the photon spectrum

$$\frac{d\Gamma(^3S(Q\bar{Q}) \rightarrow gg\gamma)}{dx} = \frac{128}{9} e_Q^2 \alpha_S^2 \frac{|\phi_0|^2}{M^2} \Omega(x)$$

Other Vector Quarkonium Decay Channels

Following the same line of reasoning as in the pseudoscalar case, any other decay channel into gluons and quarks will be considered as radiative corrections to the inclusive decay rate to hadrons. Other exclusive and semi-inclusive decay channels therefore necessarily involve photons and lepton pairs. For example:

$$\begin{aligned} \Gamma(^3S(Q\bar{Q}) \rightarrow g\gamma\gamma) &= \Gamma(^3S(Q\bar{Q}) \rightarrow g\gamma l^+ l^-) = 0 \quad (\text{due to color}) \\ \Gamma(^3S(Q\bar{Q}) \rightarrow ggl^+ l^-) &: \text{ see [152]} \\ \Gamma(^3S(Q\bar{Q}) \rightarrow \gamma\gamma l^+ l^-) &: \text{ should be obtainable from the above} \end{aligned}$$

Other electromagnetic modes are strongly suppressed (recall that the 2001 upper limit on the branching ratio for $^3S(Q\bar{Q}) \rightarrow \gamma\gamma\gamma$ is 5.5×10^{-5}).

Appendix C

Useful formulae

C.1 Wavefunction for Hydrogen-like Atoms

The complete wave function for the hydrogen atom can be written

$$\psi_{nlm}(\mathbf{r}, t) \rightarrow \phi_{nlm}(r, \theta, \varphi) e^{\frac{i}{\hbar} E_n t}$$

The corresponding energy spectrum is degenerate for l and m , with

$$E_n = \frac{E_I}{n^2} = -\frac{1}{n^2} \frac{\mu}{2\hbar^2} \left(\frac{e^2}{4\pi\epsilon_0} \right)^2 = -\frac{\mu\alpha^2}{2n^2}$$

This is the well-know Balmer series. The time-independent part is

$$\phi_{nlm}(r, \theta, \varphi) = R_{n,l}(r) Y_l^m(\theta, \varphi)$$

The radial wavefunction is expressible in terms of Laguerre polynomials

$$R_{n,l}(r) = \frac{2^{l+1}}{n^{l+2}} \sqrt{\frac{(n-l-1)!}{(n+l)! a_0^{2l+3}}} e^{-\frac{r}{na_0}} r^l L_{n-l-1}^{2l+1} \left(\frac{2r}{na_0} \right)$$

while the Y_l^m are standard spherical harmonics. The complete wave functions can also be written in terms of the hypergeometric functions representation of the Laguerre polynomials

$$\phi_{nlm}(r, \theta, \varphi) = \frac{2^{l+1}}{n^{l+2} a_0^{l+3/2}} \frac{(l+n)!}{(2l+2)!(n-l)!} \sqrt{\frac{(n-l-1)!}{(l+n)!}} Y_l^m(\theta, \varphi) e^{-\frac{r}{na_0}} r^l {}_1F_1 \left(l-n+1; 2l+2; \frac{2r}{a_0 n} \right)$$

Explicitly, the first wavefunctions are

Shell	l	m	$n(l)_{m_l}$	$\phi_{nlm}(r, \theta, \phi)$
$K, n = 1$	0	0	1s	$\frac{1}{\sqrt{\pi a_0^3}} e^{-\frac{r}{a_0}}$
$L, n = 2$	0	0	2s	$\frac{1}{\sqrt{8\pi a_0^3}} e^{-\frac{r}{2a_0}} \left(1 - \frac{r}{2a_0} \right)$
	1	0	2p ₀	$\frac{1}{4\sqrt{2\pi a_0^5}} e^{-\frac{r}{2a_0}} r \cos \theta$
	1	± 1	2p _{± 1}	$\mp \frac{1}{8\sqrt{\pi a_0^5}} e^{-\frac{r}{2a_0} + i\phi} r \sin \theta$
$M, n = 3$	0	0	3s	$\frac{1}{3\sqrt{3\pi a_0^3}} e^{-\frac{r}{3a_0}} \left(1 - \frac{2r}{3a_0} + \frac{2r^2}{27a_0^2} \right)$
	1	0	3p ₀	$\frac{4}{27\sqrt{2\pi a_0^5}} e^{-\frac{r}{3a_0}} \left(1 - \frac{r}{6a_0} \right) r \cos \theta$
	1	± 1	3p _{± 1}	$\mp \frac{2}{27\sqrt{\pi a_0^5}} e^{-\frac{r}{3a_0} + i\phi} \left(1 - \frac{r}{6a_0} \right) r \sin \theta$
	2	0	3d ₀	$\frac{81\sqrt{6\pi a_0^7}}{81\sqrt{6\pi a_0^7}} e^{-\frac{r}{3a_0}} r^2 (3 \cos^2 \theta - 1)$
	2	± 1	3d _{± 1}	$\mp \frac{1}{81\sqrt{\pi a_0^7}} e^{-\frac{r}{3a_0} + i\phi} r^2 \cos \theta \sin \theta$
	2	± 2	3d _{± 2}	$\frac{1}{162\sqrt{\pi a_0^7}} e^{-\frac{r}{3a_0} + 2i\phi} r^2 \sin^2 \theta$

with

$$a_0 = \frac{4\pi\varepsilon_0\hbar^2}{\mu e^2} = \frac{1}{\mu\alpha}$$

The wave function at the origin can also be calculated. Only for s states are the values non vanishing

$$|\psi_{n00}(0, t)|^2 = |R_{n0}(0) Y_0^0(\theta, \varphi)|^2 = \frac{1}{4\pi} |R_{n0}(0)|^2 = \frac{1}{\pi a_0^3 n^3} = \frac{\mu^3 \alpha^3}{\pi n^3}$$

since $L_{n-1}^1(0) = n$ and

$$R_{n,0}(r) = \left[\frac{2}{n^2} \sqrt{\frac{1}{na_0^3}} \right] L_{n-1}^1(0) = 2 \sqrt{\frac{1}{n^3 a_0^3}}$$

C.1.1 Momentum Space Wavefunctions

The general expression of the momentum space wavefunction was found by Podolsky and Pauling [58]

$$\begin{aligned} \Upsilon_{nlm}(p, \Theta, \Phi) &= \left\{ \frac{e^{\pm im\Phi}}{\sqrt{2\pi}} \right\} \left\{ \sqrt{\frac{(2l+1)(l-m)!}{2(l+m)!}} P_l^m(\cos \Theta) \right\} \\ &\times \left\{ \frac{2^{2l+3}\gamma^{l+3}}{\sqrt{2\pi}\gamma} l! \sqrt{\frac{n(n-l-1)!}{(n+l)!}} \frac{p^l}{(p^2+\gamma^2)^{l+2}} C_{n-l-1}^{l+1} \left(\frac{p^2-\gamma^2}{p^2+\gamma^2} \right) \right\} \end{aligned}$$

It is found by taking the Fourier transform of the configuration space wavefunctions (the integration is not straightforward though). The P_l^m are Legendre polynomials, the C_n^l are Gegenbauer functions, and

$$\gamma = \frac{1}{na_0} = \frac{\mu\alpha}{n}$$

The first few are

Shell	l	m	${}^n(l)_{m_i}$	$\Upsilon_{nlm}(p, \Theta, \Phi)$
$K, n=1$	0	0	$1s$	$N \frac{8\pi\gamma}{(p^2+\gamma^2)^2}$
$L, n=2$	0	0	$2s$	$N \frac{16\pi\gamma(p^2-\gamma^2)}{(p^2+\gamma^2)^3}$
	1	0	$2p_0$	$N \frac{32\pi\gamma^2}{(p^2+\gamma^2)^3} p \cos \Theta$
	1	± 1	$2p_{\pm 1}$	$\mp N \frac{16\sqrt{2}\pi\gamma^2}{(p^2+\gamma^2)^3} e^{\pm i\Phi} p \sin \Theta$
$M, n=3$	0	0	$3s$	$N \frac{8\pi\gamma(p^2-3\gamma^2)(3p^2-\gamma^2)}{(p^2+\gamma^2)^4}$
	1	0	$3p_0$	$N \frac{32\sqrt{6}\pi\gamma^2(p^2-\gamma^2)}{(p^2+\gamma^2)^4} p \cos \Theta$
	1	± 1	$3p_{\pm 1}$	$\mp N \frac{32\sqrt{3}\pi\gamma^2(p^2-\gamma^2)}{(p^2+\gamma^2)^4} e^{\pm i\Phi} p \sin \Theta$
	2	0	$3d_0$	$N \frac{16\sqrt{2}\pi\gamma^3}{(p^2+\gamma^2)^4} p^2 (3 \cos 2\Theta + 1)$
	2	± 1	$3d_{\pm 1}$	$\mp N \frac{32\sqrt{3}\pi\gamma^3(p^2-\gamma^2)}{(p^2+\gamma^2)^4} e^{\pm i\Phi} p^2 \sin 2\Theta$
	2	± 2	$3d_{\pm 2}$	$N \frac{32\sqrt{3}\pi\gamma^3(p^2-\gamma^2)}{(p^2+\gamma^2)^4} e^{\pm 2i\Phi} p^2 \sin^2 \Theta$

with $N = (2\pi)^{3/2} \sqrt{\pi/\gamma^3}$.

C.2 Loop Integrals, Gamma Functions and Related

C.2.1 Dirac Matrix Algebra

$$\begin{aligned}
 \gamma^\mu \gamma_\mu &= d \\
 \gamma^\mu \gamma^\nu \gamma_\mu &= (2-d)\gamma^\nu \\
 \gamma^\mu \gamma^\nu \gamma^\rho \gamma_\mu &= 4g^{\nu\rho} + (d-4)\gamma^\nu \gamma^\rho \\
 \gamma^\mu \gamma^\nu \gamma^\rho \gamma^\sigma \gamma_\mu &= -2\gamma^\sigma \gamma^\rho \gamma^\nu + (4-d)\gamma^\nu \gamma^\rho \gamma^\sigma
 \end{aligned}$$

C.2.2 Feynman Parameters

To combine denominators :

$$\frac{1}{A_1 \dots A_n} = \int_0^1 dx_1 \dots dx_n \delta\left(\sum x_i - 1\right) \frac{(n-1)!}{[x_1 A_1 + \dots + x_n A_n]^n}$$

Note that derivatives like for example

$$\frac{1}{AB^2} = \int dx \frac{2(1-x)}{(xA + (1-x)B)^3}$$

are easily obtained from the general equation. We will only quote, since it is used in the text, the formula

$$\frac{1}{A^n B^m} = \frac{\Gamma(m+n)}{\Gamma(m)\Gamma(n)} \int_0^1 dx \frac{x^{n-1} (1-x)^{m-1}}{(xA + (1-x)B)^{m+n}}$$

C.2.3 Complex logarithms

The convention for the logarithm cut is along the negative real axis. The rules for the logarithm of a product are then

$$\begin{aligned}
 \ln(ab) &= \ln(a) + \ln(b) + \eta(a, b) \\
 \eta(a, b) &= 2\pi i \{ \theta(-\operatorname{Im} a) \theta(-\operatorname{Im} b) \theta(\operatorname{Im} ab) - \theta(\operatorname{Im} a) \theta(\operatorname{Im} b) \theta(-\operatorname{Im} ab) \}
 \end{aligned}$$

Important consequences are

$$\begin{aligned}
 \ln(ab) &= \ln(a) + \ln(b) && \text{If } \operatorname{Im} a \operatorname{Im} b < 0 \\
 \ln\left(\frac{a}{b}\right) &= \ln(a) - \ln(b) && \text{If } \operatorname{Im} a \operatorname{Im} b > 0
 \end{aligned}$$

Also, with A, B real :

$$\ln(AB - i\varepsilon) = \ln(A - i\varepsilon) + \ln(B - i\varepsilon/A)$$

C.2.4 D-Dimensional Integrals

All the formulas we need are

$$\begin{aligned} \int \frac{d^d l}{(2\pi)^d} \frac{1}{(l^2 - \Delta)^n} &= \frac{(-1)^n i \Gamma(n - d/2)}{(4\pi)^{d/2} \Gamma(n)} \left(\frac{1}{\Delta}\right)^{n-d/2} \\ \int \frac{d^d l}{(2\pi)^d} \frac{l^2}{(l^2 - \Delta)^n} &= \frac{(-1)^{n-1} i}{(4\pi)^{d/2}} \left[\frac{d}{2}\right] \frac{\Gamma(n - d/2 - 1)}{\Gamma(n)} \left(\frac{1}{\Delta}\right)^{n-d/2-1} \\ \int \frac{d^d l}{(2\pi)^d} \frac{l^\mu l^\nu}{(l^2 - \Delta)^n} &= \frac{(-1)^{n-1} i}{(4\pi)^{d/2}} \left[\frac{g^{\mu\nu}}{2}\right] \frac{\Gamma(n - d/2 - 1)}{\Gamma(n)} \left(\frac{1}{\Delta}\right)^{n-d/2-1} \\ \int \frac{d^d l}{(2\pi)^d} \frac{(l^2)^2}{(l^2 - \Delta)^n} &= \frac{(-1)^n i}{(4\pi)^{d/2}} \left[\frac{d(d+2)}{4}\right] \frac{\Gamma(n - d/2 - 2)}{\Gamma(n)} \left(\frac{1}{\Delta}\right)^{n-d/2-2} \\ \int \frac{d^d l}{(2\pi)^d} \frac{l^\mu l^\nu l^\rho l^\sigma}{(l^2 - \Delta)^n} &= \frac{(-1)^n i}{(4\pi)^{d/2}} \left[\frac{g^{\mu\nu} g^{\rho\sigma} + g^{\mu\rho} g^{\nu\sigma} + g^{\mu\sigma} g^{\nu\rho}}{4}\right] \frac{\Gamma(n - d/2 - 2)}{\Gamma(n)} \left(\frac{1}{\Delta}\right)^{n-d/2-2} \end{aligned}$$

Coherence among integrals can be checked using the fact that for symmetric integration :

$$\begin{aligned} l^\mu l^\nu &\rightarrow \frac{1}{d} l^2 g^{\mu\nu} \\ l^\mu l^\nu l^\rho l^\sigma &\rightarrow \frac{1}{d(d+2)} (l^2)^2 (g^{\mu\nu} g^{\rho\sigma} + g^{\mu\rho} g^{\nu\sigma} + g^{\mu\sigma} g^{\nu\rho}) \end{aligned}$$

To correct for the change of dimension in the measure, one usually introduces an arbitrary mass scale as

$$\int \frac{d^4 q}{(2\pi)^4} \rightarrow \int \frac{\omega^{4-d} d^d q}{(2\pi)^d}$$

Of special interest are expansions near $d = 4$. Using :

$$a^x = \sum \frac{1}{n!} x^n \log^n a = 1 + x \log a + \frac{1}{2} x^2 \log^2 a + \dots$$

and :

$$\Gamma(x) = \frac{1}{x} - \gamma + \frac{x}{2} \left(\gamma^2 + \frac{\pi^2}{6}\right) + \mathcal{O}(x^2)$$

one gets, with $\varepsilon = 4 - d$:

$$\begin{aligned} \omega^\varepsilon \frac{\Gamma(2 - d/2)}{(4\pi)^{d/2}} \left(\frac{1}{\Delta}\right)^{2-d/2} &= \frac{1}{(4\pi)^2} (4\pi\omega^2)^{\varepsilon/2} \Gamma(\varepsilon/2) \left(\frac{1}{\Delta}\right)^{\varepsilon/2} \\ &= \frac{1}{(4\pi)^2} \left(\frac{2}{\varepsilon} - \gamma\right) \left(1 + \frac{\varepsilon}{2} \log 4\pi\right) \left(1 - \frac{\varepsilon}{2} \log \Delta\right) \left(1 + \frac{\varepsilon}{2} \log \omega^2\right) + \mathcal{O}(\varepsilon) \\ &= \frac{1}{(4\pi)^2} \left(\frac{2}{\varepsilon} - \gamma + \log \frac{4\pi\omega^2}{m^2} - \log \frac{\Delta}{m^2} + \mathcal{O}(\varepsilon)\right) \end{aligned}$$

Note that in this last formula, we have introduced another arbitrary scale m^2 . This is a common procedure. The usual divergent quantity is defined as

$$D = \frac{2}{\varepsilon} - \gamma + \log \frac{4\pi\omega^2}{m^2} \quad (\text{C.1})$$

where it is customary to take m as the electron mass in QED. Therefore,

$$\omega^\varepsilon \frac{\Gamma(2-d/2)}{(4\pi)^{d/2}} \left(\frac{1}{\Delta}\right)^{2-d/2} = \frac{1}{(4\pi)^2} \left(D - \log \frac{\Delta}{m^2} + \mathcal{O}(\varepsilon)\right) \quad (\text{C.2})$$

C.2.5 Digamma, Polylogarithms and Riemann Functions

The digamma function is defined as the logarithmic derivative of the gamma function

$$\psi(z) = \frac{\Gamma'(z)}{\Gamma(z)}$$

Generalizing, the n -th digamma function is

$$\psi^{(n)}(z) = \frac{d\psi^{(n)}(z)}{dz^n}$$

Special values are

$$\begin{aligned} \psi(1) &= -\gamma \\ \psi^{(1)}(1) &= \frac{\pi^2}{6} \end{aligned}$$

Note that the Euler constant can also be written as the limit of the series

$$\gamma = \lim_{n \rightarrow \infty} \left(\sum_{i=1}^n \frac{1}{i} - \log n \right)$$

The Riemann zeta function is defined from the series

$$\zeta(k) = \sum_{n=1}^{\infty} n^{-k}$$

This function may be related to digamma function as

$$\zeta(n+1) = \frac{(-1)^{n+1}}{n!} \psi^{(n)}(1)$$

The definition of the polylogarithms is

$$Li_n(z) = \sum_{k=1}^{\infty} \frac{z^k}{k^n}$$

Of special interest in Feynman parameter integration is the Spence function or dilogarithms $Li_2(z)$, to which we now turn.

Spence Functions

These functions are defined through the above series, or through the integral

$$Li_2(z) \equiv Sp(z) = \int_z^0 \frac{\ln(1-t)}{t} dt = - \int_0^1 \frac{\ln(1-zt)}{t} dt = \int_0^{-\ln(1-z)} \frac{u}{e^u - 1} du$$

A useful representation is obtained with the change of variable $t = 1 - e^{-u}$

$$\begin{aligned} Li_2(z) &= \int_0^{-\ln(1-z)} \frac{u}{e^u - 1} du \\ &= \int_0^{-\ln(1-z)} \sum_{n=0}^{\infty} B_n \frac{u^n}{n!} du = \sum_{n=0}^{\infty} B_n \frac{u^{n+1}}{(n+1)!} \Big|_{u=-\ln(1-z)} \end{aligned}$$

with the coefficient B_n being the Bernouilly numbers,

$B_0 = 1$	$B_{10} = -\frac{5}{66}$
$B_1 = -\frac{1}{2}$	$B_{12} = -\frac{691}{2730}$
$B_2 = \frac{1}{6}$	$B_{14} = \frac{7}{6}$
$B_4 = -\frac{1}{30}$	$B_{16} = -\frac{3617}{510}$
$B_6 = -\frac{1}{42}$	$B_{18} = \frac{43867}{798}$
$B_8 = -\frac{1}{30}$

The numbers not appearing in the table are also absent in the series expansion. Some basic properties are : (Euler, 1768)

$$\begin{aligned} Li_2(z) + Li_2(1-z) &= \frac{\pi^2}{6} - \ln(z) \ln(1-z) \\ Li_2(z) + Li_2(1/z) &= -\frac{\pi^2}{6} - \frac{1}{2} \ln^2(-z) \\ Li_2(z) + Li_2(-z) &= \frac{1}{2} Li_2(z^2) \end{aligned}$$

with $z, -z, 1/z, z^2$ not on the logarithm cuts. Also

$$\begin{aligned} Li_2\left(\frac{x}{1-x} \frac{y}{1-y}\right) &= Li_2\left(\frac{x}{1-y}\right) + Li_2\left(\frac{y}{1-x}\right) - Li_2(x) - Li_2(y) - \log(1-x) \log(1-y) \\ Li_2(y) - Li_2(x) &= Li_2\left(\frac{y}{x}\right) + Li_2\left(\frac{1-x}{1-y}\right) - Li_2\left(\frac{y(1-x)}{x(1-y)}\right) - \frac{\pi^2}{6} + \ln(x) \ln\left(\frac{1-x}{1-y}\right) \\ Li_2\left(\frac{x(1-y)^2}{y(1-x)^2}\right) &= Li_2\left(-x \frac{1-y}{1-x}\right) + Li_2\left(-\frac{1}{y} \frac{1-y}{1-x}\right) + Li_2\left(\frac{x(1-y)}{y(1-x)}\right) + Li_2\left(\frac{1-y}{1-x}\right) + \frac{1}{2} \log^2(y) \end{aligned}$$

due respectively to Spence (1809), Schaeffer (1846) and Kummer (1840). The second identity becomes, for complex arguments :

$$\begin{aligned} Li_2(y) - Li_2(x) &= Li_2\left(\frac{y}{x}\right) + Li_2\left(\frac{1-x}{1-y}\right) - Li_2\left(\frac{y(1-x)}{x(1-y)}\right) - \frac{\pi^2}{6} \\ &\quad + \ln(x) [\ln(1-x) - \ln(1-y)] \\ &\quad + \ln\left(\frac{1-x}{1-y}\right) \left[\ln\left(\frac{x-y}{1-y}\right) - \ln(x) - \ln\left(\frac{x-y}{x}\right) + \ln(1-y) \right] \\ &\quad - \ln\left(\frac{y(1-x)}{x(1-y)}\right) \left[\ln\left(\frac{x-y}{x(1-y)}\right) - \ln\left(\frac{x-y}{x}\right) + \ln(1-y) \right] \end{aligned}$$

The discontinuity of the dilogarithm function is the same as the discontinuity of $\ln(1 - zt)$ for $t \in [0, 1]$, hence for $z \in \mathbf{R}, z > 1$ the argument of $\ln(1 - zt)$ becomes negative. The discontinuity property is expressed along the cut as

$$\lim_{\varepsilon \downarrow 0} [Li_2(z + i\varepsilon) - Li_2(z - i\varepsilon)] = 2\pi i \ln(z)$$

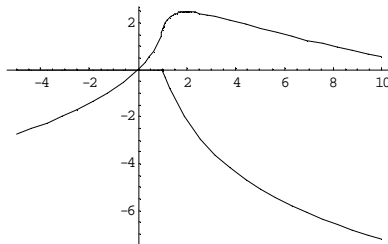
for $z \in \mathbf{R}$ and $z > 1$. Put differently, we may write

$$\text{Im} Li_2(z) = i\pi \ln(z)$$

as can be seen from the defining integral. Finally, some values of the function are

$$\begin{aligned} Li_2(-1) &= -\frac{\pi^2}{12} \\ Li_2(0) &= 0 \\ Li_2(1) &= \frac{\pi^2}{6} \\ Li_2(2) &= \frac{\pi^2}{4} - i\pi \log(2) \end{aligned}$$

and graphically, the real and imaginary parts are



Note that the real part becomes < 0 at around $12.5 \rightarrow +\infty$.

C.2.6 Hypergeometric Functions

The hypergeometric function $F(a, b, c, \xi) \equiv {}_2F_1(a, b, c, \xi)$ is defined as

$${}_2F_1(a, b, c, \xi) = \frac{\Gamma(c)}{\Gamma(b)\Gamma(b-c)} \int_0^1 dx x^{b-1} (1-x)^{c-b-1} (1-x\xi)^{-a}$$

This function is a solution to the differential equation

$$\xi(1-\xi)y'' + [c - (a+b+1)\xi]y' - aby = 0$$

and it has the series expansion

$${}_2F_1(a, b, c, \xi) = 1 + \frac{ab}{c}\xi + \frac{a(a+1)b(b+1)}{c(c+1)}\frac{\xi^2}{2} + \dots = \sum_{k=0}^{\infty} \frac{(a)_k (b)_k}{(c)_k} \frac{\xi^k}{k!}$$

with $(x)_k = x(x+1)\dots(x+k-1)$. From this series, it appear that

$${}_2F_1(a, b, c, \xi) = {}_2F_1(b, a, c, \xi)$$

Some evaluation properties are

$$\begin{aligned} {}_2F_1(a, b, c, 1) &= \frac{\Gamma(c) \Gamma(c-a-b)}{\Gamma(c-a) \Gamma(c-b)} \\ \frac{\partial}{\partial \xi} {}_2F_1(a, b, c, \xi) &= \frac{ab}{c} {}_2F_1(a+1, b+1, c+1, \xi) \end{aligned}$$

Shifting relations are often useful:

$$\begin{aligned} c {}_2F_1(a, b, c, x) - (c-b) {}_2F_1(a, b, c+1, x) - b {}_2F_1(a, b+1, c+1, x) &= 0 \\ c {}_2F_1(a, b, c, x) - (c-a) {}_2F_1(a, b, c+1, x) - a {}_2F_1(a+1, b, c+1, x) &= 0 \end{aligned}$$

and especially

$$c {}_2F_1(a, b, c, x) - (c-a) {}_2F_1(a, b+1, c+1, x) - a(1-x) {}_2F_1(a+1, b+1, c+1, x) = 0$$

Finally, one has sometimes to consider definite integrals involving hypergeometric function. Those can be done with

$${}_2F_1(a, b, c, x) = \frac{\Gamma(c)}{\Gamma(\lambda) \Gamma(c-\lambda)} \int_0^1 dx x^{\lambda-1} (1-x)^{c-\lambda-1} {}_2F_1(a, b, \lambda, xz)$$

All Hypergeometric functions with definite values for a, b, c may be expressed in terms of simple functions of ξ . Some trivial cases are

$$\begin{aligned} {}_2F_1(a, b, c, \xi) &= 1 \text{ if } a = 0 \text{ or } b = 0 \\ {}_2F_1(a, b, 0, \xi) &= \infty \\ {}_2F_1(a, 1, 1, \xi) &= {}_2F_1(1, a, 1, \xi) = \frac{1}{(1-\xi)^a} \end{aligned}$$

With b or a less than zero, Hypergeometric functions are often simple polynomials in ξ

$${}_2F_1(a, -2, 1, \xi) = 1 - 2a\xi + \frac{1}{2}a(1+a)\xi^2$$

since obviously, the series expansion will terminate at the order k such that $b+k=0$ or $a+k=0$. Up to now, all the functions are purely real. Some more complicated cases, which may develop imaginary parts, are

$$\begin{aligned} {}_2F_1(1, 1, 1/2, \xi) &= \frac{1}{1-\xi} + \frac{\sqrt{\xi} \arcsin \sqrt{\xi}}{(1-\xi)^{3/2}} \\ {}_2F_1(1, 1, 2, \xi) &= -\frac{1}{\xi} \log[1-\xi] \\ {}_2F_1(1, 2, 3, \xi) &= -\frac{2}{\xi^2} (\xi + \log[1-\xi]) \end{aligned}$$

To have logarithms, it is necessary that $a, b < c$. Derivatives can also be obtained. For example

$$\frac{\partial}{\partial a} {}_2F_1(a, 1, 1, \xi) = \frac{\partial}{\partial a} {}_2F_1(1, a, 1, \xi) = -\frac{1}{(1-\xi)^a} \log[1-\xi]$$

Finally, some hypergeometric functions with half-integer argument give elliptic functions. In general, orthogonal polynomials can also be expressed in terms of ${}_2F_1$.

C.3 Cross Section, Phase Space

The two-body to n -body cross section is expressed as

$$d\sigma(A+B \rightarrow f_1, f_2, \dots) = \frac{\sum_{spins} |\mathcal{M}(A+B \rightarrow f_1, f_2, \dots)|^2 d\Phi}{4\sqrt{(p_A \cdot p_B)^2 - m_A^2 m_B^2}}$$

with

$$d\Phi_n(p_A + p_B; p_1, \dots, p_n) = (2\pi)^4 \delta^4(p_A + p_B - p_1 - \dots - p_n) \left(\prod_{i=1}^n \frac{d^3 \mathbf{p}_i}{(2\pi)^3 2E_i} \right)$$

(this section is based on [23], [223])

C.3.1 Two-Body Phase Space

The invariant two-body phase space integral is

$$\begin{aligned} d\Phi_2(P; p_1, p_2) &= (2\pi)^4 \delta^4(P - p_1 - p_2) \frac{d^3 \mathbf{p}_1}{(2\pi)^3 2E_1} \frac{d^3 \mathbf{p}_2}{(2\pi)^3 2E_2} \\ &= (2\pi) \delta^0(P_0 - E_1 - E_2) \frac{d^3 \mathbf{p}_1}{(2\pi)^3 2E_1 2E_2} \end{aligned}$$

in the center-of-mass frame, where $\mathbf{P} = 0$, with $\mathbf{P} - \mathbf{p}_1 = \mathbf{p}_2$ hence $\mathbf{p}_2 = -\mathbf{p}_1$. The remaining delta can be converted to a constraint over the energy E_2 as

$$|\mathbf{p}_2| = |\mathbf{p}_1| \rightarrow E_2^2 = E_1^2 - m_1^2 + m_2^2$$

hence

$$d\Phi_2(P; p_1, p_2) = (2\pi) \delta^0\left(P_0 - E_1 - \sqrt{E_1^2 - m_1^2 + m_2^2}\right) \frac{\sqrt{E_1^2 - m_1^2} dE_1 d\Omega_1}{4(2\pi)^3 E_2}$$

Since $\mathbf{p}_1^2 = E_1^2 - m_1^2$, $|\mathbf{p}_1| d|\mathbf{p}_1| = E_1 dE_1$ and $d^3 \mathbf{p}_1 = |\mathbf{p}_1|^2 d|\mathbf{p}_1| d\Omega_1$. Now let us integrate over E_1 . The delta function gives $E_1 = (P_0^2 + m_1^2 - m_2^2)/2P_0$ and since we are using the relation $\delta(f(x)) = \delta(x - x_0)/|f'(x_0)|$, the correction to the measure is

$$\frac{\partial}{\partial E_1} \left(P_0 - E_1 - \sqrt{E_1^2 - m_1^2 + m_2^2} \right) = -\frac{P_0}{E_2}$$

Hence

$$d\Phi_2(P; p_1, p_2) = \frac{\sqrt{E_1^2 - m_1^2} d\Omega_1}{4(2\pi)^2 (E_2 + E_1)}$$

which can be written in terms of invariants as

$$d\Phi_2(P; p_1, p_2) = \frac{d\Omega_1}{32\pi^2} \sqrt{1 + \frac{(m_1^2 - m_2^2)^2}{s^2} - 2\frac{(m_1^2 + m_2^2)}{s}}$$

with $s \equiv P^2 = (p_1 + p_2)^2$. As a special case of interest, if $m_1 = m_2$,

$$d\Phi_2(P; p_1, p_2) = \frac{d\Omega_1}{32\pi^2} \sqrt{1 - \frac{4m^2}{s}}$$

C.3.2 Three-Body Phase Space

The invariant two-body phase space integral is

$$\begin{aligned} d\Phi_2(P; p_1, p_2, p_3) &= (2\pi)^4 \delta^4(P - p_1 - p_2 - p_3) \frac{d^3\mathbf{p}_1}{(2\pi)^3 2E_1} \frac{d^3\mathbf{p}_2}{(2\pi)^3 2E_2} \frac{d^3\mathbf{p}_3}{(2\pi)^3 2E_3} \\ &= (2\pi) \delta(P_0 - E_1 - E_2 - E_3) \frac{d^3\mathbf{p}_1}{(2\pi)^3 2E_1} \frac{d^3\mathbf{p}_2}{(2\pi)^3 2E_2} \frac{1}{2E_3} \end{aligned}$$

with E_3 constrained as $E_3^2 - m_3^2 = \mathbf{p}_3^2$ and $\mathbf{p}_3 = \mathbf{P} - \mathbf{p}_1 - \mathbf{p}_2$. Then, in the center-of-mass frame,

$$\mathbf{p}_3 = -(\mathbf{p}_1 + \mathbf{p}_2) \rightarrow E_3^2 = m_3^2 + |\mathbf{p}_1 + \mathbf{p}_2|^2 = m_3^2 + \mathbf{p}_1^2 + \mathbf{p}_2^2 - 2|\mathbf{p}_1||\mathbf{p}_2|\cos\theta$$

Now the integral can be written

$$d\Phi_3 = \frac{1}{(2\pi)^5} \delta(P_0 - E_1 - E_2 - E_3) \frac{\mathbf{p}_1^2 d|\mathbf{p}_1| d\Omega_1 \mathbf{p}_2^2 d|\mathbf{p}_2| d\Omega_2}{2E_1 2E_2 2E_3}$$

In the case of an unpolarized cross section, the amplitude squared is invariant under global rotations in the c.m. frame. So only one out of the four angular variables is non-trivial, which we choose to be the angle between \mathbf{p}_1 and \mathbf{p}_2 . Also, since $|\mathbf{p}_i| d|\mathbf{p}_i| = E_i dE_i$ and $d^3\mathbf{p}_i = |\mathbf{p}_i|^2 d|\mathbf{p}_i| d\Omega_i$, we arrive at

$$d\Phi_3 = \frac{2}{(2\pi)^3} \delta\left(P_0 - E_1 - E_2 - \sqrt{m_3^2 + \mathbf{p}_1^2 + \mathbf{p}_2^2 - 2|\mathbf{p}_1||\mathbf{p}_2|\cos\theta}\right) \frac{|\mathbf{p}_1| dE_1 |\mathbf{p}_2| dE_2 d\cos\theta}{8E_3}$$

and integrating over $\cos\theta$ with the delta function :

$$\cos\theta = \frac{m_1^2 + m_2^2 - m_3^2 + P_0^2 - 2P_0 E_1 - 2P_0 E_2 + 2E_1 E_2}{-2|\mathbf{p}_1||\mathbf{p}_2|}$$

The correction to the measure is

$$\frac{\partial}{\partial \cos\theta} \left(P_0 - E_1 - E_2 - \sqrt{m_3^2 + \mathbf{p}_1^2 + \mathbf{p}_2^2 - 2|\mathbf{p}_1||\mathbf{p}_2|\cos\theta} \right) = -\frac{\partial}{\partial \cos\theta} E_3 = \frac{|\mathbf{p}_1||\mathbf{p}_2|}{E_3}$$

Hence

$$\boxed{d\Phi_3 = \frac{dE_1 dE_2}{4(2\pi)^3}} \quad (\text{C.3})$$

The bounds for the two last integrals can be found by constraining, for a given value of E_1 say, the value of E_2 such that the $\cos\theta$ exists.

C.3.3 Recursive Calculation of Phase-Space

In some case, we will compute the phase space integrals recursively, using

$$d\Phi_n = d\Phi_j(q; p_1, \dots, p_j) d\Phi_{n-j+1}(p_A + p_B; q, p_{j+1}, \dots, p_n) \frac{dq^2}{(2\pi)}$$

with $q = p_1 + \dots + p_j$.

Bibliography

Standard Books on Quantum Field Theory

- [1] P. A. M. Dirac, "The Principles of Quantum Mechanics", Oxford.
- [2] N. Bogolioubov and D. Chirkov, "Introduction à la Théorie Quantique des Champs", 1960, Dunod.
- [3] E. Merzbacher, "Quantum Mechanics", 1961, Wiley.
- [4] J. D. Jackson, "Classical Electrodynamics", 1962, Wiley.
- [5] J. Bjorken, S. Drell, "Relativistic Quantum Mechanics", "Relativistic Quantum Fields", 1964, McGraw-Hill.
- [6] K. Nishijima, "Fields and Particles : Field Theory and Dispersion Relations", 1969, Benjamin N.Y.
- [7] J. Schwinger, "Particles, Sources, and Fields" Volume I, II and III, 1973, Perseus Books.
- [8] C. Cohen-Tannoudji, B. Diu, F. Laloë, "Mécanique Quantique", Volume I and II, 1973, Hermann.
- [9] J. Jauch and F. Röhrlich, "The Theory of Photons and Electrons", 1980, Springer.
- [10] C. Itzykson, J.-B. Zuber, "Quantum Field Theory", 1980, McGraw-Hill.
- [11] F.J. Yndurain, "The Theory of Quark and Gluon Interactions", 1983, Springer.
- [12] T.-P. Cheng and L.-F. Li, "Gauge Theory of Elementary Particle Physics", 1984, Oxford.
- [13] R. Rivers, "Path Integral Methods in Quantum Field Theory", 1987, Cambridge.
- [14] G. Jones, D. Singerman, "Complex Functions: an Algebraic and Geometric Viewpoint", 1987, Cambridge.
- [15] W. Greiner, A. Schäfer, "Quantum Chromodynamics", 1989, Springer.
- [16] T. Kinoshita (*Editor*), "Quantum Electrodynamics", 1990, World Scientific.
- [17] O. Nachtmann, "Elementary Particle Physics : Concepts and Phenomena", 1990, Springer-Verlag.
- [18] J. Donoghue, E. Golowich, B. Holstein, "Dynamics of the Standard Model", 1992, Cambridge.
- [19] F. Gross, "Relativistic Quantum Mechanics and Field Theory", 1993, Wiley.
- [20] M. Kaku, "Quantum Field Theory", 1993, Oxford University Press.
- [21] W. Greiner, J. Reinhardt, "Field Quantization", 1993, Springer.
- [22] W. Greiner, J. Reinhardt, "Quantum Electrodynamics", 1994, Springer.
- [23] A. Di Giacomo, G. Paffuti, P. Rossi, "Selected Problems in Theoretical Physics", 1994, World Scientific.
- [24] M. Peskin and D. Schoeder, "An Introduction to Quantum Field Theory", 1995, Addison-Wesley.
- [25] S. Weinberg, "The Quantum Theory of Fields (I, II and III)", 1996, Cambridge.
- [26] F.J. Yndurain, "Relativistic Quantum Mechanics and Introduction to Field Theory", 1996, Springer.
- [27] J. Zinn-Justin, "Quantum Field Theory and Critical Phenomena", 1996, Clarendon Press - Oxford.
- [28] A. Dobado, A. Gomez-Nicola, A. Maroto, J. Pelaez, "Effective Lagrangian for the Standard Model", 1997, Springer.

Thesis

- [29] G. Lopez Castro, J. Pestieau and C. Smith, *hep-ph/0004209*, G. Lopez Castro, J. Pestieau, C. Smith and S. Trine, *hep-ph/0006016* and *hep-ph/0006018*.
- [30] J. Pestieau, C. Smith and S. Trine, *hep-ph/0105034*, Int. J. Mod. Phys. **A17**, 1355 (2002).
- [31] J. Pestieau and C. Smith, *hep-ph/0111264*, Phys. Lett. **B524**, 395 (2002).
- [32] J. Pestieau and C. Smith, *hep-ph/0111380*, submitted to Eur. Phys. J. C.

Positronium Experiments

- [33] A.E. Ruark, Phys. Rev. **68**, 278 (1945).
- [34] M. Deutsch, Phys. Rev. **82**, 455 (1951); M. Deutsch, Phys. Rev. **84**, 866 (1951); M. Deutsch, E. Dulit, Phys. Rev. **84**, 601 (1952); M. Deutsch, S. Brown, Phys. Rev. **85**, 1047 (1952).
- [35] V. W. Hughes, S. Marder, C. S. Wu, Phys. Rev. **106**, 934 (1957).
- [36] E. Theriot, R. Beers, V. Hughes, Phys. Rev. Lett. **18**, 767 (1967).
- [37] V. W. Hughes, "Physics of One- and Two-electrons Atoms", North-Holland (1969), pp 407-429.
- [38] E. Theriot, R. Beers, V. Hughes, K. Ziock, Phys. Rev. **A2**, 707 (1970).
- [39] A.P. Mills, G.H. Bearman, Phys. Rev. Lett. **34**, 246 (1974).
- [40] A. P. Mills, Jr., S. Berko, and K. F. Canter, Phys. Rev. Lett. **34**, 1541 (1975).
- [41] T.C. Griffith, G.R. Heyland, K.S. Lines, T.R. Twomey, J. Phys. **B11**, L743 (1978).
- [42] D. Gidley, A. Rich, E. Sweetman, D. West, Phys. Rev. Lett. **49**, 525 (1982).
- [43] M.W. Ritter, P.O. Egan, V.W. Hughes, K.A. Woodle, Phys. Rev. **A30**, 1331 (1984).
- [44] R.S. Conti, S. Hatamian, A. Rich, Phys. Rev. **A33**, 3495 (1986).
- [45] S. Hatamian, R. S. Conti, and A. Rich, Phys. Rev. Lett. **58**, 1833 (1987).
- [46] P. Hasbach, G. Hilkert, E. Klempt, G. Werth, Nuovo Cim. **A97**, 419 (1987).
- [47] C. Westbrook, D. Gidley, R. Conti, A. Rich, Phys. Rev. Lett. **58**, 1328 (1987).
- [48] K. Danzmann, M. S. Fee, and S. Chu, Phys. Rev. **A39**, 6072 (1989).
- [49] C. Westbrook, D. Gidley, R. Conti, A. Rich, Phys. Rev. **A40**, 5489 (1989).
- [50] J. Nico, D. Gidley, A. Rich, P. Zitzewitz, Phys. Rev. Lett. **65**, 1344 (1990).
- [51] D. Gidley, J. Nico, M. Skalsey, Phys. Rev. Lett. **66**, 1302 (1991).
- [52] M. S. Fee, A. P. Mills, Jr., S. Chu, E. D. Shaw, K. Danzmann, R. J. Chicherster, and D. M. Zuckerman, Phys. Rev. Lett. **70**, 1397 (1993); M. S. Fee, S. Chu, A. P. Mills, Jr., R. J. Chicherster, D. M. Zuckerman, and E. D. Shaw, Phys. Rev. **A48**, 192 (1993).
- [53] E. W. Hagen, R. Ley, D. Weil, G. Werth, W. Arnold, and H. Schneider, Phys. Rev. Lett. **71**, 2887 (1993).
- [54] R. S. Conti, S. Hatamian, L. Lapidus, A. Rich, and M. Skalsey, Phys. Lett. **A177**, 43 (1993).
- [55] R. Ley, D. Hagen, D. Weil, G. Werth, W. Arnold, and H. Schneider, Hyperfine Interact. **89**, 327 (1994).
- [56] A. Al-Ramadhan, D. Gidley, Phys. Rev. Lett. **72**, 1632 (1994).
- [57] S. Asai, S. Orito, N. Shinohara, Phys. Lett. **B357**, 475 (1995); O. Jinnouchi, S. Asai, T. Kobayashi, *hep-ex/0011011*.

Positronium Theory

- [58] B. Podolsky, L. Pauling, Phys. Rev. **34**, 109 (1929).
- [59] S. Mohorovicic, Astron. Nachr., 94 (1934).
- [60] J. A. Wheeler, Ann. N. Y. Acad. Sci. **48**, 219 (1946).
- [61] J. Pirenne, Arch. Sci. Phys. Nat. **28**, 233 (1946); **29**, 121, 207 & 265 (1947).
- [62] V.B. Berestetski, L.D. Landau, Zhur. Exsptl. i Teort. Fiz. **19**, 673 (1949); V.B. Berestetski, Zhur. Exsptl. i Teort. Fiz. **19**, 1130 (1949).
- [63] A. Ore and J. L. Powell, Phys. Rev. **75**, 1696 (1949).
- [64] R. Ferrel, Phys. Rev. **84**, 858 (1951).
- [65] L. M. Brown, R. P. Feynman, Phys. Rev. **85**, 231 (1952).
- [66] L. Wolfenstein, D. G. Ravenhall, Phys. Rev. **88**, 279 (1952).
- [67] R. Karplus, A. Klein, Phys. Rev. **87**, 848 (1952).
- [68] T. Fulton, P. Martin, Phys. Rev. **95**, 811 (1954).
- [69] I. Harris and L. Brown, Phys. Rev. **105**, 1656 (1957).

- [70] R. Barbieri, P. Christillin, E. Remiddi, Phys. Rev. **A8**, 2266 (1973).
- [71] M. Stroschio, Phys. Rept. **C22**, 215 (1975).
- [72] A. Barut, J. Kraus, Phys. Lett. **A58**, 361 (1976).
- [73] R. Barbieri, E. Remiddi, Phys. Lett. **B65**, 258 (1976).
- [74] G. P. Lepage, Phys.Rev. **A16**, 863 (1977).
- [75] W. E. Caswell, G. P. Lepage, J. Sapirstein, Phys. Rev. Lett. **38**, 488 (1977).
- [76] W. E. Caswell and G.P. Lepage, Phys. Rev. **A18**, 810 (1978).
- [77] W. E. Caswell and G.P. Lepage, Phys. Rev. Lett. **41**, 1092 (1978).
- [78] G. Bodwin and D. Yennie, Phys. Rept. **43**, 267 (1978).
- [79] R. Barbieri and E. Remiddi, Nucl. Phys. **B141**, 413 (1978).
- [80] W. E. Caswell and G. P. Lepage, Phys. Rev. **A20**, 36 (1979).
- [81] D. Yennie, CLNS-79/436, 1979 (1979 Cargèse Summer School).
- [82] M.I. Vysotsky, Yad.Fiz. **29**, 845 (1979).
- [83] W. Buchmüller, E. Remiddi, Nuovo Cim. **A60**, 109 (1980); Nucl. Phys. **B162**, 250 (1980).
- [84] Y. Tomozawa, Ann. Phys. **128**, 463 (1980).
- [85] A. Rich, Rev. Mod. Phys. **53**, 126 (1981).
- [86] M. Stroschio, Phys. Rev. Lett. **48**, 571 (1982).
- [87] G. Adkins, Ann. Phys. **146**, 78 (1983).
- [88] G. Adkins, F. Brown, Phys. Rev. **A28**, 1164 (1983).
- [89] G. Lepage, P. Mackenzie, K. Streng, P. Zerwas, Phys. Rev. **A28**, 3090 (1983).
- [90] J.R. Sapirstein, E.A. Terray, D.R. Yennie, Phys. Rev. **D29**, 2290 (1984).
- [91] G. Adkins, Phys. Rev. **A31**, 1250 (1985).
- [92] G.T. Bodwin, D.R. Yennie, M.A. Gregorio, Rev. Mod. Phys. **57**, 723 (1985).
- [93] W. E. Caswell and G.P. Lepage, Phys. Lett. **B167**, 437 (1986).
- [94] H. Olsen, Phys. Rev. **D33**, 2033 (1986).
- [95] J. Malenfant, Phys. Rev. **D36**, 863 (1987).
- [96] G. Adkins, M. Bui, D. Zhu, Phys. Rev. **A37**, 4071 (1988).
- [97] I.B. Khriplovich, A.S. Yelkhovskiy, Phys. Lett. **B246**, 520 (1990).
- [98] L.G. Afanasev *et al*, Phys. Lett. **B236**, 116 (1990).
- [99] E.A. Kuraev, T.V. Kukhto, Z.K. Silagadze, Sov. J. Nucl. Phys. **51**, 1036 (1990).
- [100] P. Labelle, *MRST Meeting 92* (CLNS-92-1161).
- [101] V. Dvoeglazov, R. Faustov, Y. Tyukhtyaev, Mod. Phys. Lett. **A8**, 3263 (1993).
- [102] A. Pivovarov, Phys.Rev. **D47**, 5183 (1993).
- [103] V. Dvoeglazov, R. Faustov, Y. Tyukhtyaev, Mod. Phys. Lett. **A8**, 3263 (1993).
- [104] P. Labelle, G. Lepage, U. Magnea, Phys. Rev. Lett. **72**, 2006 (1994).
- [105] P. Labelle, *hep-ph/9407233*.
- [106] I.B. Khriplovich, A.I. Milstein, J. Exp. Theor. Phys. **79**, 379 (1994); I.B. Khriplovich, A.I. Milstein, *hep-ph/9607374*.
- [107] R.N. Faustov, A.P. Martynenko, V.A. Saleev, Phys. Rev. **A51**, 4520 (1995).
- [108] J. Govaerts and M. Van Caillie, Phys. Lett. **B381**, 451 (1996).
- [109] T. Kinoshita, M. Nio, Phys. Rev. **D53**, 4909 (1996); Phys. Rev. **D55**, 767 (1997).
- [110] P. Labelle, S.M. Zebarjad, C.P. Burgess, Phys. Rev. **56**, 8053 (1997).
- [111] U. Jentschura, G. Soff, V. Ivanov and S. Karshenboim, Phys. Rev. **A56**, 4483 (1997); U. Jentschura, G. Soff, V. Ivanov, S. Karshenboim, *hep-ph/9706401*; I.F. Ginzburg, U. Jentschura, S. Karshenboim, F. Krauss, V.G. Serbo, G. Soff, Phys. Rev. **C58**, 3565 (1998).
- [112] T. Kinoshita, *Int. Work. on Hadronic Atoms and Positronium in the Standard Model*, Dubna, Russia, 26-31 May 1998.

- [113] V. Antonelli, V. Ivanchenko, E. Kuraev, V. Laliena, Eur. Phys. J. **C5**, 535 (1998), V. Antonelli, *Int. Work. on Hadronic Atoms and Positronium in the S.M.*, Dubna, 26-31 May 1998.
- [114] A. Vairo, Found. Phys **28**, 829 (1998).
- [115] A. Czarnecki, Acta Phys. Polon. **B30**, 3837 (1999).
- [116] A. Czarnecki and G. Kardhenboim, *14th Int. Work. on HEP and QFT*, Moscow 1999, *hep-ph/9911410*.
- [117] A. Czarnecki, K. Melnikov, A. Yelkhovsky, Phys. Rev. **A59**, 4316 (1999); Phys. Rev. Lett. **82**, 311 (1999).
- [118] G. Adkins, K. Melnikov and A. Yelkhovsky, *hep-ph/9905553*.
- [119] K. Melnikov, A. Yelkhovsky, Phys. Lett. **B458**, 143 (1999).
- [120] A. Pineda, J. Soto, Phys. Rev. **D59**, 016005 (1999).
- [121] A. Czarneski, K. Melnikov, A. Yelkhovsky, Phys. Rev. Lett. **83**, 1135 (1999); *hep-ph/9910488*; Phys. Rev. **A61**, 052502 (2000).
- [122] R. Faustov, A. Martynenko, *hep-ph/0002281*.
- [123] R. Hill, *MRST Meeting*, Rochester, May 2000.
- [124] G. Adkins, R. Fell, J. Sapirstein, Phys. Rev. Lett. **84**, 5086 (2000).
- [125] A.H. Hoang, P. Labelle, S.M. Zebarjad, Phys. Rev. **A62**, 012109 (2000).
- [126] A. Burichenko, *hep-ph/0004063*.
- [127] R. Hill, G. P. Lepage, Phys. Rev. **D62**, 111301 (2000).
- [128] A. Manohar, I. Stewart, Phys. Rev. Lett. **85**, 2248 (2000).
- [129] By R. Foot, S. Gninenko, Phys. Lett. **B480**, 171 (2000).
- [130] B. Kniehl, A. Penin, Phys. Rev. Lett. **85**, 1210 (2000); *ibid.* 5094 (2000).
- [131] K. Melnikov, A. Yelkhovsky, Phys. Rev. **D62**, 116003 (2000); Phys. Rev. Lett. **86**, 1498 (2001).
- [132] S. Karshenboim, *hep-ph/0201241*.
- [133] By S.N. Gninenko, N.V. Krasnikov, A. Rubbia, *hep-ph/0205056*.

Quarkonium Experiment

- [134] G. Abrams *et al*, Phys. Rev. Lett. **44**, 114 (1980).
- [135] D.Sharre *et al*, Phys. Rev. **D23**, 43 (1981).
- [136] Crystal Ball Collaboration (DESY), Phys. Lett. **B267**, 286 (1991).
- [137] F. Harris, *American Physical Society (APS) Meeting of the Division of Particles and Fields (DPF 99)*, Los Angeles, CA, 5-9 Jan. 1999.
- [138] CLEO Collaboration (G. Brandenburg *et al*), Phys. Rev. Lett. **85**, 3095 (2000).
- [139] Xu Guofa (for the BES Collaboration), *31st International Symposium on Multiparticle Dynamics (ISMD 2001)*, Datong, China, 1-7 Sep. 2001
- [140] CLEO Collaboration (B. Nemati *et al.*), Phys. Rev. **D55**, 5273 (1997).
- [141] BES Collaboration, (J.Z. Bai *et al.*), Phys. Rev. **D62**, 072001 (2000).
- [142] M. Stancari (for the E835 Collaboration), Nucl. Phys. (Proc. Suppl.) **B82**, 306 (2000).
- [143] CLEO Collaboration (B. Eisenstein *et al*), Phys. Rev. Lett. **87**, 061801 (2001).

Quarkonium Theory

- [144] T. Appelquist, H. Politzer, Phys. Rev. Lett. **34**, 43 (1975).
- [145] A. De Rujula, S.L. Glashow, Phys. Rev. Lett. **34**, 46 (1975).
- [146] P. Freund, Y. Nambu, Phys. Rev. Lett. **34**, 1645 (1975).
- [147] V. Novikov, L.B. Okun, M. Shifman, A. Vainshtein, M. Voloshin, V. Zakharov, Phys. Rept. **C41**, 1 (1978).
- [148] K. Koller and T. Walsh, Nucl. Phys. **B140**, 449 (1978).

- [149] S. Brodsky, D. Coyne, T. DeGrand and R. Horgan, Phys. Lett. **B73**, 203 (1978).
- [150] C. Quigg, FERMILAB-Conf-78/82-THY (1978); C. Quigg, FERMILAB-Conf-79/74-THY (1979).
- [151] R. Barbieri, E. d'Emilio, G. Curci, E. Remiddi, Nucl. Phys. **B154**, 535 (1979).
- [152] J.P. Leveille and D.M. Scott, Phys. Lett. **B95**, 96 (1980).
- [153] I.I.Y. Bigi, Nucl. Phys. **B164**, 239 (1980).
- [154] W. Buchmüller, S.-H. Tye, Phys. Rev. **D24**, 132 (1981).
- [155] W. Kwong, P. Mackenzie, R. Rosenfeld and J. Rosner, Phys. Rev. **D37**, 3210 (1981).
- [156] P. Mackenzie, G. Lepage, Phys. Rev. Lett. **47**, 1244 (1981).
- [157] G. Grunberg, Phys. Lett. **B114**, 271 (1982).
- [158] J. Körner and J. Kühn, M. Krammer, H. Schneider, Nucl. Phys. **B229**, 115 (1983).
- [159] P. Moxhay, J. Rosner, Phys. Rev. **D28**, 1132 (1983).
- [160] W. S. Hou and A. Soni, Phys. Rev. Lett. **50**, 569 (1983).
- [161] R.D. Field, Phys. Lett. **B133**, 248 (1983).
- [162] W. Kwong, J. Rosner, C. Quigg, Ann. Rev. Nucl. Part. Sci **37**, 325 (1987).
- [163] S. Brodsky, P. Lepage and S.F. Tuan, Phys. Rev. Lett. **59**, 621 (1987).
- [164] A. Bizzeti (Crystal Ball Collaboration), Proc. XXIV Int. Conf. on HEP (1989).
- [165] S. Pinsky, Phys. Lett. **B236**, 479 (1990).
- [166] E. Sima'an Ackleh, *thesis* (University of Tennessee), 1992.
- [167] G. Schuler, (*thesis*) CERN-TH.7170/94.
- [168] S. Catani and F. Hautmann, Nucl. Phys. Proc. Suppl. **39BC**, 359 (1995).
- [169] G. Lopez Castro, J.L. Lucio, J. Pestieau, AIP Conf. Proc. **342**, 441 (1995).
- [170] E. Eichten, C. Quigg, Phys. Rev. **D52**, 1726 (1995).
- [171] G. Bodwin, E. Braaten, G. Lepage, Phys. Rev. **D51**, 1125 (1995).
- [172] T. Barnes, F.E. Close, P.R. Page, E.S. Swanson, Phys. Rev. **D55**, 4157 (1997).
- [173] W.S. Hou, Phys. Rev. **D55**, 6952 (1997).
- [174] K. Chao, H. Huang, J. Liu, J. Tang, Phys. Rev. **D56**, 368 (1997).
- [175] S. Olsen, J. Mod. Phys. **A256**, 4069 (1997).
- [176] E. Braaten, *Third Int. Work. on Particle Physics Phenomenology*, Taipei, November 1997.
- [177] S. Brodsky and M. Karliner, Phys. Rev. Lett. **78**, 4682 (1997).
- [178] A. Manohar, Phys. Rev. **D56**, 230 (1997).
- [179] P. Ko, *PPPP Workshop*, Seoul, Korea, October 1997.
- [180] F. Hautmann, *proceedings of "International Conference on the Structure and the Interactions of the Photon (Photon 97)"* Netherlands, 10-15 May 1997 (*hep-ph/9708496*).
- [181] Y.-Q. Chen and E. Braaten, Phys. Rev. Lett. **80**, 5060 (1998).
- [182] A. Petrelli, M. Cacciari, M. Greco, F. Maltoni, M. Mangano, Nucl. Phys. **B514**, 245 (1998).
- [183] M. Suzuki, Phys. Rev. **D57**, 5717 (1998).
- [184] M. Suzuki, Phys. Rev. **D57**, 5717 (1998); Phys. Rev. **D60**, 051501 (1999).
- [185] M. Krämer, *proceedings of "4th International Symposium on Radiative Corrections (RADCOR 98)"*, Barcelona, 8-12 Sep 1998 (*hep-ph/9901448*).
- [186] J.-M. Gérard, J. Weyers, Phys. Lett. **B462**, 324 (1999).
- [187] A.M. Badalian, V.L. Morgunov, Phys. Rev. **D60**, 116008 (1999).
- [188] B. Grinstein, Int. J. Mod. Phys. **A15**, 461 (2000)
- [189] N. Brambilla, *XXIII Int. Work. on the Fundamental Problems of High Energy Physics*, Protvino (Russia), June 2000.
- [190] I. Stewart, *7th Conf. on the Intersections of Particle and Nuclear Physics*, Quebec City, Canada, May 2000.
- [191] Y.G. Gu and S.F. Tuan, Nucl. Phys. **A675**, 404c (2000).

- [192] M.E. Like, A.V. Manohar, I.Z. Rothstein, Phys. Rev. **D61**, 074025 (2000).
- [193] S. F. Tuan, Commun. Theor. Phys. **33**, 285 (2000).
- [194] Y. F. Gu and X. H. Li, Phys. Rev. **D63**, 114019 (2001).
- [195] F.J. Yndurain, Nucl. Phys. Proc. Suppl. **93**, 196 (2001).
- [196] A. Penin, Nucl. Phys. Proc. Suppl. **96**, 418 (2001).
- [197] S. Wolf, Phys. Rev. **D63**, 074020 (2001).
- [198] A. Leibovich, Nucl. Phys. Proc. Suppl. **93**, 182 (2001).
- [199] W.Q. Chao, C.S. Ju, *hep-ph/0111325*.
- [200] Y.F. Gu, X.H. Li, Phys. Rev. **D63**, 114019 (2001).

General Field Theory

- [201] H. Euler, W. Heisenberg, Z. Phys. **98**, 714 (1936).
- [202] C. Yang, Phys. Rev. **77**, 242 (1950).
- [203] J. Schwinger, Phys. Rev. **82**, 664 (1951).
- [204] F. E. Low, Phys. Rev. **110**, 974 (1958).
- [205] B. De Tollis, Nuovo Cim. **32**, 757 (1964), *ibid.* **35**, 1182 (1965); V. Constantini, B. De Tollis, G. Pistoni, Nuovo Cim. 2A, 733 (1971); M. Laursen, M. Samuel, G. Tupper, A. Sen, Phys. Rev. **D27**, 196 (1983).
- [206] H. Chew, Phys. Rev. **123**, 377 (1961); J. Pestieau, Phys. Rev. **160**, 1555 (1967).
- [207] S. Coleman, R. Jackiw, Annals Phys. **67**, 552 (1971); M. Chanowitz, J. Ellis, Phys. Rev. **D7**, 2490 (1973); S. Adler, J. Collins, A. Duncan, Phys. Rev. **D15**, 1712 (1977).
- [208] L.M. Sehgal, Phys. Rev. **D7**, 3303 (1973).
- [209] W. Caswell, Phys. Rev. Lett. **33**, 244 (1974).
- [210] E. Egorian, O. Tarasov, Theor. Math. Phys. **41**, 863 (1979).
- [211] S. Brodsky, G. Lepage, P. Mackenzie, Phys. Rev. **D28**, 228 (1983).
- [212] L. Bergström, G. Hulth, Nucl. Phys. **B259**, 137 (1985).
- [213] D.W. Duke, R.G. Roberts, Phys. Rept. **120**, 275 (1985).
- [214] L. L. Chau, H. Y. Cheng, Phys. Lett. **B195**, 275 (1987).
- [215] G. Ecker, A. Pich, E. de Rafael, Nucl. Phys. **B303**, 665 (1988).
- [216] J. L. Lucio M., J. Pestieau, Phys. Rev. **D42**, 3253 (1990).
- [217] D.J. Broadhurst, J. Fleischer, O.V. Tarasov, Z. Phys. **C60**, 287 (1993).
- [218] J. Bijnens, G. Ecker and J. Gasser, Nucl. Phys. **B396**, 81 (1993); G. D'Ambrosio, G. Ecker, G. Isidori, H. Neufeld, 2nd DAPHNE Physics Handbook:253-313 (*hep-ph/9411439*).
- [219] B. Kniehl, Acta Phys. Polon. **B27**, 3631 (1996).
- [220] J. Horejsi, M. Schnabl, Z. Phys. **C76**, 561 (1997).
- [221] J.A. Oller, Phys. Lett. **B426**, 7 (1998).
- [222] S. Bethke, J. Phys. **G26**, R27 (2000).
- [223] D.E. Groom *et al*, Eur. Phys. J. **C15**, 1 (2000).